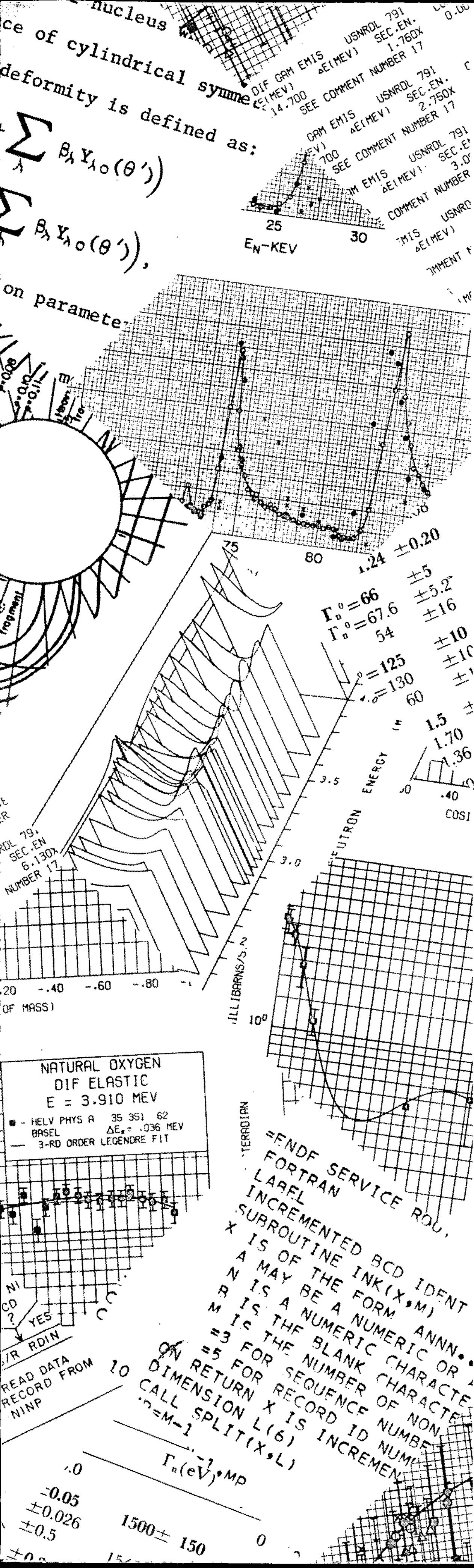

4
m.c.

BNL-NCS-21501
ERDA/NDC-3/U
NEANDC(US)-198/U
INDC(USA)-75/U
Informal Report
Limited Distribution

REPORTS TO THE ERDA NUCLEAR DATA COMMITTEE

Edited by
NATIONAL NEUTRON CROSS SECTION CENTER
for the
U.S. Energy Research and Development Administration
Nuclear Data Committee

May 1976

BROOKHAVEN NATIONAL LABORATORY
ASSOCIATED UNIVERSITIES, INC.
UPTON, NEW YORK 11973

National
Neutron
Cross
Section
Center

BNL-NCS-21501
ERDA/NDC-3/U

REPORTS TO
THE ERDA NUCLEAR DATA COMMITTEE

May 1976

Edited by
NATIONAL NEUTRON CROSS SECTION CENTER
for the
U.S. Energy Research and Development Administration
Nuclear Data Committee

NATIONAL NEUTRON CROSS SECTION CENTER

BROOKHAVEN NATIONAL LABORATORY

ASSOCIATED UNIVERSITIES, INC.

UNDER CONTRACT NO. E(30-1)-16 WITH THE

UNITED STATES ENERGY RESEARCH AND DEVELOPMENT ADMINISTRATION

PREFACE

The reports in this document were submitted to the Energy Research and Development Administration Nuclear Data Committee (ERDA-NDC) in May 1976. The reporting laboratories are those having a substantial effort in measuring neutron and nuclear cross sections of relevance to the U.S. applied nuclear energy program. The material contained in these reports is to be regarded as comprised of informal statements of recent developments and preliminary data. Persons wishing to make use of these data should contact the individual experimenter for further details. <u>The data which appear in this document should be quoted only by permission of the contributor and should be referenced as private communication, and not by this document number</u>. Appropriate subjects are listed as follows:

1. Microscopic neutron cross sections relevant to the nuclear energy program, including shielding. Inverse reactions where pertinent are included.

2. Charged particle cross sections, where they are relevant to 1) above, and where relevant to developing and testing nuclear models.

3. Gamma-ray production, radioactive decay, and theoretical developments in nuclear structure which are applicable to nuclear energy programs.

4. Proton and alpha-particle cross sections, at energies of up to 1 GeV, which are of interest to the space program.

These reports cannot be regarded as a complete summary of the nuclear research efforts in the U.S. A number of laboratories, whose research is less programmatically oriented do not submit reports; neither do the submitted reports reflect all the work related to nuclear data in progress at the submitting laboratory.

This compilation has been produced almost completely from master copies prepared by the individual contributors listed in the Table of Contents.

TABLE OF CONTENTS

The CINDA-type index which follows was prepared by Gail Waite, National Neutron Cross Section Center, Brookhaven National Laboratory, Upton, New York.

ELEMENT S	A	QUANTITY	TYPE	ENERGY MIN	MAX	DOCUMENTATION REF VOL	PAGE	DATE	LAB	COMMENTS
H	001	TOTAL XSECT	EXPT-PROG	50+4	50+6	ERDA-NDC-3	82	576	LRL	PHILLIPS+STANDARD FOR TRITIUM MEAS,
H	001	TOTAL XSECT	EXPT-PROG	50+4	50+7	ERDA-NDC-3	89	576	LAS	SEAGRAVE+LINAC,STANDARD FOR H003,NDG
H	001	DIFF ELASTIC	EXPT-PROG	23+7	29+7	ERDA-NDC-3	101	576	LAS	DROSG,5ES,180DEG CS,CFD PREDICTION,
H	001	DIFF ELASTIC	EXPT-PROG	11+7	25+7	ERDA-NDC-3	101	576	LAS	DROSG,2ES,180DEG CS,CFD PREDICTION,
H	001	ABSORPTION	EXPT-PROG	NDG		ERDA-NDC-3	15	576	ANC	SMITH+RATIO OF H/MN ABS CS,
H	WTR	NONEL GAMMAS	EXPT-PROG	10+6	20+7	ERDA-NDC-3	206	576	ORL	MORGAN,SECONDARY G SPEC,H2O NDG
H	WTR	NEUT EMISSN	EXPT-PROG	10+6	20+7	ERDA-NDC-3	206	576	ORL	MORGAN,SECONDARY N SPEC,H2O NDG
D	002	GAMMA,N	EXPT-PROG		70+5	ERDA-NDC-3	31	576	ANL	JACKSON+ANG DIST OF PHOTO-NEUTS,TBC
D	002	GAMMA,N	EXPT-PROG	NDG		ERDA-NDC-3	303	576	YAL	CROOKS+PHOTONEUT POL MEAS,NDG,
T	003	TOTAL XSECT	EXPT-PROG	50+4	50+6	ERDA-NDC-3	82	576	LRL	PHILLIPS+LINAC,TRNS,CFD,NDG
T	003	TOTAL XSECT	EXPT-PROG	50+4	50+7	ERDA-NDC-3	89	576	LAS	SEAGRAVE+LINAC,TRNS,CS DRVD,NDG,
HE	004	TOTAL XSECT	EXPT-PROG	22+7		ERDA-NDC-3	152	576	NBS	HEATON+STUDY D,T CS VIA INV REAC,NDG
HE	004	TOTAL XSECT	EXPT-PROG		15+7	ERDA-NDC-3	303	576	YAL	FIRK+MEAS TBD
HE	004	POLARIZATION	EXPT-PROG	15+6	60+6	ERDA-NDC-3	303	576	YAL	FIRK+R FN ANAL UP TO 15 MEV TBD,
LI	006	EVALUATION	EVAL-PROG	10+4	10+6	ERDA-NDC-3	115	576	LAS	HALE+CS FOR ENDF4,GRPH,CFD OTH,
LI	006	EVALUATION	EVAL-PROG	10+6		ERDA-NDC-3	117	576	LAS	STEWART+CS FOR ENDF4,GRPH,CFD OTH
LI	006	ELASTIC SCAT	EXPT-PROG	NDG		ERDA-NDC-3	29	576	ANL	SMITH+NDG,TOF,EL,INEL SCAT,ANAL TBD,
LI	006	DIFF ELASTIC	EXPT-PROG	40+6	75+6	ERDA-NDC-3	251	576	OHO	KNOX+VDG,TOF,LITTLE RES STRUCT,NDG
LI	006	DIFF ELASTIC	EXPT-PROG	40+6	80+6	ERDA-NDC-3	252	576	OHO	LANE+STRUCT STUDY,LEG COEFS,NDG
LI	006	DIFF ELASTIC	EXPT-PROG	20+6	60+6	ERDA-NDC-3	253	576	OHO	KNOX+EXPT TBD,NDG
LI	006	DIFF ELASTIC	EXPT-PROG	10+6	50+6	ERDA-NDC-3	303	576	YAL	FIRK+IMPROVES PREVIOUS DATA ANAL,NDG
LI	006	DIFF ELASTIC	EXPT-PROG	75+6	14+7	ERDA-NDC-3	176	576	DKE	PURSER+TOF,6ANG DISTR,ANAL TBD,
LI	006	DIFF ELASTIC	EXPT-PROG	NDG		ERDA-NDC-3	29	576	ANL	SMITH+NDG,TOF,EL,INEL SCAT,ANAL TBD,
LI	006	POLARIZATION	EXPT-PROG	20+6	60+6	ERDA-NDC-3	253	576	OHO	KNOX+EXPT TBD,NDG
LI	006	POLARIZATION	EXPT-PROG	10+6	50+6	ERDA-NDC-3	303	576	YAL	FIRK+IMPROVES PREVIOUS DATA ANAL,NDG
LI	006	DIFF INELAST	EXPT-PROG	75+6	14+7	ERDA-NDC-3	176	576	DKE	PURSER+TOF,6ANG DISTR,ANAL TBD,
LI	006	DIFF INELAST	EXPT-PROG	NDG		ERDA-NDC-3	29	576	ANL	SMITH+NDG,TOF,EL,INEL SCAT,ANAL TBD,
LI	006	N, TRITON	EXPT-PROG	96+5		ERDA-NDC-3	143	576	MHG	ENGDAHL+NEW IMPROVED MEAS TBD,NDG
LI	006	N, TRITON	EXPT-PROG	10+4	50+5	ERDA-NDC-3	148	576	NBS	LAMAZE+TOF,LINAC,CS MEAS,ENDF,NDG,
LI	006	N, TRITON	EXPT-PROG	NDG		ERDA-NDC-3	28	576	ANL	POENITZ+EVAL OF U235NF/LI6NT TBD,NDG
LI	006	N, TRITON	EXPT-PROG	50-5	25+4	ERDA-NDC-3	181	576	ORL	HARVEY+ANGULAR ANISOTROPY STUDY
LI	006	N, TRITON	EVAL-PROG	10+4	10+6	ERDA-NDC-3	115	576	LAS	HALE+CS FOR ENDF4,GRPH,CFD OTH,
LI	006	N,ALPHA REAC	EXPT-PROG	NDG		ERDA-NDC-3	28	576	ANL	POENITZ,EVAL OF U235NF/LI6NA TBD,NDG
LI	007	ELASTIC SCAT	EXPT-PROG	70+6	15+7	ERDA-NDC-3	278	576	DKE	PURSER+SEL DRVD FROM (N,G),NDG,
LI	007	ELASTIC SCAT	EXPT-PROG	NDG		ERDA-NDC-3	29	576	ANL	SMITH+NDG,TOF,EL,INEL SCAT,ANAL TBD,

ELEMENT S	A	QUANTITY	TYPE	ENERGY MIN	MAX	DOCUMENTATION REF	VOL	PAGE	DATE	LAB	COMMENTS
LI	007	DIFF ELASTIC	EXPT-PROG	40+6	75+6	ERDA-NDC-3		251	576	OHO	KNOX+VDG,TOF,LITTLE RES STRUCT,NDG
LI	007	DIFF ELASTIC	EXPT-PROG	40+6	80+6	ERDA-NDC-3		252	576	OHO	LANE+STRUCT STUDY,LEG COEFS,NDG
LI	007	DIFF ELASTIC	EXPT-PROG	20+6	60+6	ERDA-NDC-3		253	576	OHO	KNOX+EXPT TBD,NDG
LI	007	DIFF ELASTIC	EXPT-PROG	70+6	15+7	ERDA-NDC-3		278	576	DKE	PURSER+TOF,7ANG DISTR,ANAL TBD,TBC,
LI	007	DIFF ELASTIC	EXPT-PROG	NDG		ERDA-NDC-3		29	576	ANL	SMITH+NDG,TOF,EL,INEL SCAT,ANAL TBD,
LI	007	POLARIZATION	EXPT-PROG	20+6	60+6	ERDA-NDC-3		253	576	OHO	KNOX+EXPT TBD,NDG
LI	007	DIFF INELAST	EXPT-PROG	70+6	15+7	ERDA-NDC-3		278	576	DKE	PURSER+TOF,7ANG DISTR,ANAL TBD,TBC,
LI	007	DIFF INELAST	EXPT-PROG	NDG		ERDA-NDC-3		29	576	ANL	SMITH+NDG,TOF,EL,INEL SCAT,ANAL TBD,
LI	007	INELST GAMMA	EXPT-PROG		40+6	ERDA-NDC-3		26	576	ANL	SMITH+TBP IN NSE,NDG
BE	009	DIFF ELASTIC	EXPT-PROG	70+6	15+7	ERDA-NDC-3		278	576	DKE	PURSER+TOF,9ES,NDG,DATA AT NNCSC,
BE	009	DIFF ELASTIC	EXPT-PROG	70+6	15+7	ERDA-NDC-3		279	576	DKE	PURSER+INSTRM FOR MEASANGS ,5TO150DEG
BE	009	DIFF ELASTIC	EXPT-PROG	90+6	15+7	ERDA-NDC-3		281	576	DKE	PURSER+DATA CFD OPTMDL,GRPHS,TBL
BE	009	DIFF ELASTIC	EXPT-PROG	59+6	14+7	ERDA-NDC-3		90	576	LAS	DRAKE+3ES,11 ANGS,TBL
BE	009	DIFF INELAST	EXPT-PROG	70+6	15+7	ERDA-NDC-3		278	576	DKE	PURSER+TOF,9ES,NDG,DATA AT NNCSC,
BE	009	DIFF INELAST	EXPT-PROG	70+6	15+7	ERDA-NDC-3		279	576	DKE	PURSER+INSTRM FOR MEASANGS ,5TO150DEG
BE	009	DIFF INELAST	EXPT-PROG	90+6	15+7	ERDA-NDC-3		281	576	DKE	PURSER+DATA CFD COUPL CHANL,GRPH,TBL
BE	009	DIFF INELAST	EXPT-PROG	59+6	14+7	ERDA-NDC-3		90	576	LAS	DRAKE+3ES,11 ANGS,TBL
BE	009	N2N REACTION	EXPT-PROG	14+7	24+7	ERDA-NDC-3		98	576	LAS	VEESER+LIQ SCINT,GRPHS,CFD OTH EXPT
BE	009	NXN REACTION	EXPT-PROG	14+7	24+7	ERDA-NDC-3		98	576	LAS	VEESER+N3N,LIQ SCINT,GRPHS,CFD OTH
BE	009	NEUT EMISSN	EXPT-PROG	59+6	14+7	ERDA-NDC-3		90	576	LAS	DRAKE+E SPEC CFD ENDF,NDG
B	010	EVALUATION	EVAL-PROG	10+3	10+6	ERDA-NDC-3		115	576	LAS	HALE+CS FOR ENDF4,GRPH,CFD OTH
B	010	DIFF ELASTIC	EXPT-PROG	40+6	80+6	ERDA-NDC-3		251	576	OHO	WHITE+VDG,TOF,LITTLE RES STRUCT,NDG
B	010	DIFF ELASTIC	EXPT-PROG	40+6	80+6	ERDA-NDC-3		252	576	OHO	LANE+STRUCT STUDY,LEG COEFS,NDG
B	010	DIFF ELASTIC	EXPT-PROG	20+6	60+6	ERDA-NDC-3		253	576	OHO	KNOX+EXPT TBD,NDG
B	010	POLARIZATION	EXPT-PROG	20+6	60+6	ERDA-NDC-3		253	576	OHO	KNOX+EXPT TBD,NDG
B	010	N,ALPHA REAC	EXPT-PROG	50+3	70+5	ERDA-NDC-3		148	576	NBS	SCHRACK+TOF,(N,ALF G)CS,478KEV G,NDG
B	010	N,ALPHA REAC	EXPT-PROG	10+3	10+6	ERDA-NDC-3		115	576	LAS	HALE+CS FOR ENDF4,CFD OTH,GRPH,
B	011	DIFF ELASTIC	EXPT-PROG	40+6	80+6	ERDA-NDC-3		251	576	OHO	WHITE+VDG,TOF,SOME RES STRUCT,NDG,
B	011	DIFF ELASTIC	EXPT-PROG	40+6	80+6	ERDA-NDC-3		252	576	OHO	LANE+STRUCT STUDY,LEG COEFS,NDG
B	011	DIFF ELASTIC	EXPT-PROG	20+6	60+6	ERDA-NDC-3		253	576	OHO	KNOX+EXPT TBD,NDG
B	011	POLARIZATION	EXPT-PROG	20+6	60+6	ERDA-NDC-3		253	576	OHO	KNOX+EXPT TBD,NDG
C	012	ELASTIC SCAT	EXPT-PROG	NDG		ERDA-NDC-3		29	576	ANL	SMITH+NDG,TOF,EL,INEL SCAT,ANAL TBD,
C	012	DIFF ELASTIC	EXPT-PROG	90+6	15+7	ERDA-NDC-3		276	576	DKE	PURSER+25 TO,165 DEG,GRPHS,14ES,
C	012	DIFF ELASTIC	EXPT-PROG	90+6	15+7	ERDA-NDC-3		279	576	DKE	PURSER+INSTRM FOR MEASANGS ,5TO150DEG
C	012	DIFF ELASTIC	EXPT-PROG	90+6	15+7	ERDA-NDC-3		281	576	DKE	PURSER+DATA CFD OPT MDL,NDG

ELEMENT S	A	QUANTITY	TYPE	ENERGY MIN	MAX	DOCUMENTATION REF VOL	PAGE	DATE	LAB	COMMENTS
C	012	DIFF ELASTIC	EXPT-PROG	NDG		ERDA-NDC-3	29	576	ANL	SMITH+NDG,TOF,EL,INEL SCAT,ANAL TBD.
C	012	DIFF INELAST	EXPT-PROG	90+6	15+7	ERDA-NDC-3	276	576	DKE	PURSER+25 TO 165 DEG,GRPHS,14ES
C	012	DIFF INELAST	EXPT-PROG	90+6	15+7	ERDA-NDC-3	279	576	DKE	PURSER+INSTRM FOR MEASANGS .5TO15DEG
C	012	DIFF INELAST	EXPT-PROG	90+6	15+7	ERDA-NDC-3	281	576	DKE	PURSER+DATA CFD COUPL CHANL,GRPH,TBL
C	012	DIFF INELAST	EXPT-PROG	NDG		ERDA-NDC-3	29	576	ANL	SMITH+NDG,TOF,EL,INEL SCAT,ANAL TBD.
C	013	GAMMA,N	EXPT-PROG	75+6	42+7	ERDA-NDC-3	83	576	LRL	MEYER+CS MEAS FOR (G,N),(G,2N),NDG
N	014	NONEL GAMMAS	EXPT-PROG	14+7		ERDA-NDC-3	74	576	LRL	HANSEN+DET RESPONSE RECALC,AIR CORRC
N	014	NONEL GAMMAS	EXPT-PROG	10+6	20+7	ERDA-NDC-3	205	576	ORL	MORGAN,SPEC OF SECONDARY GS,4ANG,NDG
N	014	NEUT EMISSN	EXPT-PROG	10+6	20+7	ERDA-NDC-3	205	576	ORL	MORGAN,SPEC OF SECONDARY NS,4ANG,NDG
O	016	DIFF ELASTIC	EXPT-PROG	11+7		ERDA-NDC-3	236	576	OHO	BAINUM+CS MEAS TO CORRC MO96 CS,
O	016	NONEL GAMMAS	EXPT-PROG	10+6	20+7	ERDA-NDC-3	205	576	ORL	MORGAN,SPEC OF SECONDARY GS,4ANG,NDG
O	016	NEUT EMISSN	EXPT-PROG	10+6	20+7	ERDA-NDC-3	205	576	ORL	MORGAN,SPEC OF SECONDARY NS,4ANG,NDG
O	017	GAMMA,N	EXPT-PROG	43+6	62+6	ERDA-NDC-3	31	576	ANL	HOLT+THRS PHOTO-NEUT SPEC,2 ANGS,TBC
O	017	GAMMA,N	EXPT-PROG	76+6	30+7	ERDA-NDC-3	85	576	LRL	MEYER+CS MEAS FOR (G,N),(G,2N),NDG
O	CMP	NONEL GAMMAS	EXPT-PROG	10+6	20+7	ERDA-NDC-3	206	576	ORL	MORGAN,SECONDARY G SPEC SIO2,NDG
O	CMP	NEUT EMISSN	EXPT-PROG	10+6	20+7	ERDA-NDC-3	206	576	ORL	MORGAN,SECONDARY N SPEC SIO2,NDG
F	019	NONEL GAMMAS	EXPT-PROG	10+5	20+7	ERDA-NDC-3	168	576	ORL	MORGAN+LINAC,DIFF CS FOR G PROD,NDG.
NA	023	TOTAL XSECT	EXPT-PROG	30+5	30+6	ERDA-NDC-3	259	576	RPI	BLOCK+CS AT MINIMA,TBL,GRPH,CFD ENDF
NA	023	TOTAL XSECT	EXPT-PROG	40+4	20+7	ERDA-NDC-3	178	576	ORL	LARSON+TRNS,NDG ABST 76LOWELL CONF
NA	023	DIFF ELASTIC	EXPT-PROG	50+5	30+6	ERDA-NDC-3	182	576	ORL	KINNEY+8ANGS,25 TO 155 DEG,REL C,NDG
NA	023	INELST GAMMA	EXPT-PROG	50+5	30+6	ERDA-NDC-3	182	576	ORL	KINNEY+30,90,125DEG,REL LI7.G,NDG
NA	023	INELST GAMMA	EXPT-PROG	50+5	30+6	ERDA-NDC-3	182	576	ORL	KINNEY+30PCT 4M GEOM REL LI7.G,NDG
NA	023	RESON PARAMS	EXPT-PROG	40+4	20+7	ERDA-NDC-3	178	576	ORL	LARSON+NEW RES ES ABST 76LOWELL CONF
MG		DIFF ELASTIC	EXPT-PROG	11+7		ERDA-NDC-3	221	576	OHO	BAINUM+TOF,OPT MDL ANAL,CFD(P,P)DATA
MG		POLARIZATION	EXPT-PROG	NDG		ERDA-NDC-3	32	576	ANL	HOLT+N DOUBLE SCT METHOD,TBC.
MG	024	TOTAL XSECT	EXPT-PROG		+6	ERDA-NDC-3	171	576	ORL	WEIGMANN+TOF,TRNS,TBP PR/C,NDG
MG	024	N, GAMMA	EXPT-PROG		+6	ERDA-NDC-3	171	576	ORL	WEIGMANN+ANAL TO 850KEV NDG TBP PR/C
MG	024	RESON PARAMS	EXPT-PROG	NDG		ERDA-NDC-3	171	576	ORL	WEIGMANN+I AND PI ASSIGNNDG TBP PR/C
MG	025	TOTAL XSECT	EXPT-PROG		+6	ERDA-NDC-3	171	576	ORL	WEIGMANN+TOF,TRNS,TBP PR/C,NDG
MG	025	N, GAMMA	EXPT-PROG		+6	ERDA-NDC-3	171	576	ORL	WEIGMANN+ANAL TO 265KEV NDG TBP PR/C
MG	026	TOTAL XSECT	EXPT-PROG		+6	ERDA-NDC-3	171	576	ORL	WEIGMANN+TOF,TRNS,TBP PR/C,NDG
MG	026	N, GAMMA	EXPT-PROG		+6	ERDA-NDC-3	171	576	ORL	WEIGMANN+ANAL TO 440KEV NDG TBP PR/C
AL	027	DIFF ELASTIC	EXPT-PROG	11+7		ERDA-NDC-3	221	576	OHO	BAINUM+TOF,OPT MDL ANAL,CFD(P,P)DATA
AL	027	DIFF ELASTIC	EXPT-PROG	26+7		ERDA-NDC-3	232	576	OHO	BAINUM+ANAL TBD,NDG.
AL	027	INELST GAMMA	EXPT-PROG	50+5	30+6	ERDA-NDC-3	182	576	ORL	KINNEY+30PCT 4M GEOM REL LI7.6,NDG

ELEMENT S A	QUANTITY	TYPE	ENERGY MIN	MAX	DOCUMENTATION REF	VOL	PAGE	DATE	LAB	COMMENTS
AL 027	NONEL GAMMAS	EXPT-PROG	10+6	20+7	ERDA-NDC-3		182	576	ORL	MORGAN+LINAC,TOF,127DEG,TBP NSE
AL 027	NONEL GAMMAS	EXPT-PROG	10+6	20+7	ERDA-NDC-3		206	576	ORL	MORGAN,SPEC OF SECONDARY NS,4ANG,NDG
AL 027	NEUT EMISSN	THEO-PROG	14+7		ERDA-NDC-3		69	576	LRL	HANSON+3 NUCL-MDL NEM SPEC CALC,NDG
AL 027	NEUT EMISSN	EXPT-PROG	10+6	20+7	ERDA-NDC-3		182	576	ORL	MORGAN+LINAC,TOF,127DEG,TBP NSE
AL 027	NEUT EMISSN	EXPT-PROG	10+6	20+7	ERDA-NDC-3		206	576	ORL	MORGAN,SPEC OF SECONDARY NS,4ANG,NDG
AL 027	N, PROTON	EXPT-PROG	14+7		ERDA-NDC-3		74	576	LRL	GRIMES+ (N,XP)CS MEAS,NDG,
AL 027	N, PROTON	EXPT-PROG	NDG		ERDA-NDC-3		26	576	ANL	SMITH+INTEG RESPONSE FN DETERMINED,
AL 027	N, DEUTERON	EXPT-PROG	14+7		ERDA-NDC-3		74	576	LRL	GRIMES+ (N,XD)CS MEAS,NDG
AL 027	N,ALPHA REAC	EXPT-PROG	14+7		ERDA-NDC-3		74	576	LRL	GRIMES+ (N,XA)CS MEAS,NDG
SI	DIFF ELASTIC	EXPT-PROG	11+7		ERDA-NDC-3		221	576	OHO	BAINUM+TOF,OPT MDL ANAL,CFD(P,P)DATA
SI	DIFF ELASTIC	EXPT-PROG	20+7		ERDA-NDC-3		225	576	OHO	BAINUM+ANAL TBD,NDG,
SI	DIFF ELASTIC	EXPT-PROG	26+7		ERDA-NDC-3		232	576	OHO	BAINUM+ANAL TBD,NDG,
SI	DIFF ELASTIC	EXPT-PROG	50+5	30+6	ERDA-NDC-3		182	576	ORL	KINNEY+8ANGS,25 TO 155 DEG,REL C,NDG
SI	N, GAMMA	EXPT-PROG		15+6	ERDA-NDC-3		171	576	ORL	BOLDEMAN+CS MEAS,NDG,ABST NP/A 252,
SI	INELST GAMMA	EXPT-PROG	50+5	30+6	ERDA-NDC-3		182	576	ORL	KINNEY+30PCT 4M GEOM REL LI7.6,NDG
SI 028	TOTAL XSECT	EXPT-PROG		45+6	ERDA-NDC-3		284	576	DKE	CLEMENT+R-MTX ANAL,RES STRUC NDG,TBP
SI 028	DIFF INELAST	EXPT-PROG	NDG		ERDA-NDC-3		246	576	OHO	BAINUM+T=0 NUCLEI,SEVERAL ES,NDG
SI 028	RESON PARAMS	EXPT-PROG		15+6	ERDA-NDC-3		171	576	ORL	BOLDEMAN+DRVD RES DATA,ABST NP/A252,
SI CMP	NONEL GAMMAS	EXPT-PROG	10+6	20+7	ERDA-NDC-3		206	576	ORL	MORGAN,SECONDARY G SPEC SIO2,NDG
SI CMP	NEUT EMISSN	EXPT-PROG	10+6	20+7	ERDA-NDC-3		206	576	ORL	MORGAN,SECONDARY N SPEC SIO2,NDG
S	DIFF ELASTIC	EXPT-PROG	11+7		ERDA-NDC-3		221	576	OHO	BAINUM+TOF,OPT MDL ANAL,CFD(P,P)DATA
S	DIFF ELASTIC	EXPT-PROG	20+7		ERDA-NDC-3		225	576	OHO	BAINUM+ANAL TBD,NDG,
S	DIFF ELASTIC	EXPT-PROG	26+7		ERDA-NDC-3		232	576	OHO	BAINUM+ANAL TBD,NDG,
S 032	TOTAL XSECT	EXPT-PROG	NDG		ERDA-NDC-3		180	576	ORL	JOHNSON+TRNS,RES PARS DRVD,NDG,
S 032	DIFF INELAST	EXPT-PROG	NDG		ERDA-NDC-3		246	576	OHO	BAINUM+T=0 NUCLEI,SEVERAL ES,NDG
S 032	RESON PARAMS	EXPT-PROG	NDG		ERDA-NDC-3		180	576	ORL	JOHNSON+WN,WG,PI 15 RES,VAL MDL,NDG
S 033	N, GAMMA	EXPT-PROG	10+3	70+5	ERDA-NDC-3		172	576	ORL	AUCHAMPAUGH+CS MEAS,MAX DIST AVG,NDG
S 033	N,ALPHA REAC	EXPT-PROG	10+3	70+5	ERDA-NDC-3		172	576	ORL	AUCHAMPAUGH+CS MEAS,MAX DIST AVG,NDG
S 033	RESON PARAMS	EXPT-PROG	10+3	70+5	ERDA-NDC-3		172	576	ORL	AUCHAMPAUGH+RES PARS,LVL SPACING,
CL 035	SPECT N,GAMM	EXPT-PROG	40+2	25+4	ERDA-NDC-3		52	576	BNL	KOPECKY+INT MEAS,CFD,THR SPECT,NDG
CA	DIFF ELASTIC	EXPT-PROG	11+7		ERDA-NDC-3		221	576	OHO	BAINUM+TOF,OPT MDL ANAL,CFD(P,P)DATA
CA	DIFF ELASTIC	EXPT-PROG	20+7		ERDA-NDC-3		225	576	OHO	BAINUM+ANAL TBD,NDG,
CA	DIFF ELASTIC	EXPT-PROG	26+7		ERDA-NDC-3		232	576	OHO	BAINUM+ANAL TBD,NDG,
CA 040	DIFF INELAST	EXPT-PROG	11+7		ERDA-NDC-3		246	576	OHO	BAINUM+2ES,ANAL TBD,NDG
CA 040	N, GAMMA	EXPT-PROG		30+5	ERDA-NDC-3		172	576	ORL	MUSGROVE+CS MEAS,,2 PCT RESOL,TBP NP

ELEMENT S A	QUANTITY	TYPE	ENERGY MIN	ENERGY MAX	DOCUMENTATION REF VOL	PAGE	DATE	LAB	COMMENTS
CA 040	SPECT N,GAMM	EXPT-PROG	80+6	12+7	ERDA-NDC-3	279	576	OKE	PURSER+E2 STRENGTH OBS,NDG,TBC
CA 040	SPECT N,GAMM	EXPT-PROG		30+5	ERDA-NDC-3	172	576	ORL	MUSGROVE+G SPECTRA,TBP IN NP
CA 040	NONEL GAMMAS	EVAL-PROG	10+6	20+7	ERDA-NDC-3	209	576	ORL	FU+ NEUT,G RAY PROD CS CALCS,CFD EXP
CA 040	RESON PARAMS	EXPT-PROG		30+5	ERDA-NDC-3	172	576	ORL	MUSGROVE+LVL SPACING,AVG WIDS,TBP NP
CA 040	RESON PARAMS	THEO-PROG	NDG		ERDA-NDC-3	286	576	OKE	DIVADEENAM+DOORWAY CALC,TBP ZP/A,NDG
CA 040	STRNGTH FUNC	EXPT-PROG		30+5	ERDA-NDC-3	172	576	ORL	MUSGROVE+P,D WAVE VALS GVN,TBP IN,NP
SC 045	N2N REACTION	EXPT-PROG	14+7	24+7	ERDA-NDC-3	98	576	LAS	VEESER+LIQ SCINT,GRPHS,CFD OTH EXPT
SC 045	NXN REACTION	EXPT-PROG	14+7	24+7	ERDA-NDC-3	98	576	LAS	VEESER+N3N,LIQ SCINT,GRPHS,CFD OTH
TI	EVALUATION	EXPT-PROG	NDG		ERDA-NDC-3	27	576	ANL	GUENTHER+NDG,TBD
TI 046	N, PROTON	EXPT-PROG	14+7		ERDA-NDC-3	74	576	LRL	GRIMES+ (N,XP)CS MEAS,NDG,
TI 046	N, PROTON	EXPT-PROG	NDG		ERDA-NDC-3	26	576	ANL	SMITH+INTEG RESPONSE FN DETERMINED,
TI 046	N, DEUTERON	EXPT-PROG	14+7		ERDA-NDC-3	74	576	LRL	GRIMES+ (N,XD)CS MEAS,NDG
TI 046	N,ALPHA REAC	EXPT-PROG	14+7		ERDA-NDC-3	74	576	LRL	GRIMES+ (N,XA)CS MEAS,NDG
TI 047	N, PROTON	EXPT-PROG	NDG		ERDA-NDC-3	26	576	ANL	SMITH+INTEG RESPONSE FN DETERMINED,
TI 048	N, PROTON	EXPT-PROG	14+7		ERDA-NDC-3	74	576	LRL	GRIMES+ (N,XP)CS MEAS,NDG,
TI 048	N, PROTON	EXPT-PROG	NDG		ERDA-NDC-3	26	576	ANL	SMITH+INTEG RESPONSE FN DETERMINED,
TI 048	N, DEUTERON	EXPT-PROG	14+7		ERDA-NDC-3	74	576	LRL	GRIMES+ (N,XD)CS MEAS,NDG
TI 048	N,ALPHA REAC	EXPT-PROG	14+7		ERDA-NDC-3	74	576	LRL	GRIMES+ (N,XA)CS MEAS,NDG
V 051	EVALUATION	EXPT-PROG	NDG		ERDA-NDC-3	27	576	ANL	GUENTHER+NDG,TBD
V 051	TOTAL XSECT	EXPT-PROG	46+5	54+6	ERDA-NDC-3	27	576	ANL	WHALEN+TOF,TRNS,30 KEV STEPS,NDG,TBP
V 051	ELASTIC SCAT	EXPT-PROG	NDG		ERDA-NDC-3	29	576	ANL	SMITH+NDG,TOF,EL,INEL SCAT,ANAL TBD,
V 051	DIFF ELASTIC	EXPT-PROG	11+7		ERDA-NDC-3	221	576	OHO	BAINUM+TOF,OPT MDL ANAL,CFD(P,P)DATA
V 051	DIFF ELASTIC	EXPT-PROG	NDG		ERDA-NDC-3	29	576	ANL	SMITH+NDG,TOF,EL,INEL SCAT,ANAL TBD,
V 051	DIFF INELAST	EXPT-PROG	NDG		ERDA-NDC-3	29	576	ANL	SMITH+NDG,TOF,EL,INEL SCAT,ANAL TBD,
V 051	INELST GAMMA	EXPT-PROG	50+5	30+6	ERDA-NDC-3	182	576	ORL	KINNEY+30PCT 4M GEOM REL LI7,6,NDG
V 051	NONEL GAMMAS	EXPT-PROG	20+5	20+7	ERDA-NDC-3	168	576	ORL	NEWMAN+CS MEAS,NDG,ORNL-TM-5299 ABST
CR	NONEL GAMMAS	EXPT-PROG	20+5	20+7	ERDA-NDC-3	169	576	ORL	MORGAN+LINAC,DIFF CS FOR G PROD,NDG,
MN 055	DIFF ELASTIC	EXPT-PROG	11+7		ERDA-NDC-3	221	576	OHO	BAINUM+TOF,OPT MDL ANAL,CFD(P,P)DATA
MN 055	ABSORPTION	EXPT-PROG	NDG		ERDA-NDC-3	15	576	ANC	SMITH+RATIO OF H/MN ABS CS,
FE	ELASTIC SCAT	EXPT-PROG	NDG		ERDA-NDC-3	29	576	ANL	SMITH+NDG,TOF,EL,INEL SCAT,ANAL TBD,
FE	DIFF ELASTIC	EXPT-PROG	11+7		ERDA-NDC-3	221	576	OHO	BAINUM+TOF,OPT MDL ANAL,CFD(P,P)DATA
FE	DIFF ELASTIC	EXPT-PROG	20+7		ERDA-NDC-3	225	576	OHO	BAINUM+ANAL TBD,NDG,
FE	DIFF ELASTIC	EXPT-PROG	11+7	26+7	ERDA-NDC-3	232	576	OHO	BAINUM+ANAL TBD,GRPH,
FE	DIFF ELASTIC	EXPT-PROG	50+5	30+6	ERDA-NDC-3	182	576	ORL	KINNEY+BANGS,25 TO 155 DEG,REL C,NDG
FE	DIFF ELASTIC	EXPT-PROG	NDG		ERDA-NDC-3	29	576	ANL	SMITH+NDG,TOF,EL,INEL SCAT,ANAL TBD,

ELEMENT S	A	QUANTITY	TYPE	ENERGY MIN	MAX	DOCUMENTATION REF VOL	PAGE	DATE	LAB	COMMENTS
FE		DIFF INELAST	EXPT-PROG	NDG		ERDA-NDC-3	29	576	ANL	SMITH+NDG,TOF,EL,INEL SCAT,ANAL TBD.
FE		INELST GAMMA	EXPT-PROG	5Ø+5	3Ø+6	ERDA-NDC-3	182	576	ORL	KINNEY+3Ø,9Ø,125DEG,REL LI7,G,NDG
FE		INELST GAMMA	EXPT-PROG	5Ø+5	3Ø+6	ERDA-NDC-3	182	576	ORL	KINNEY+3ØPCT 4H GEOM REL LI7,G,NDG
FE		INELST GAMMA	EXPT-PROG		2Ø+6	ERDA-NDC-3	26	576	ANL	SMITH+NDG,REPORT TBP.
FE		NEUT EMISSN	THEO-PROG	14+7		ERDA-NDC-3	69	576	LRL	HANSON+3 NUCL-MDL NEM SPEC CALC,NDG
FE	Ø54	N, PROTON	EXPT-PROG	NDG		ERDA-NDC-3	26	576	ANL	SMITH+INTEG RESPONSE FN DETERMINED.
FE	Ø56	DIFF ELASTIC	EXPT-PROG	11+7		ERDA-NDC-3	23Ø	576	OHO	BAINUM+OPTMOL FIT,PARS DRVD,ANAL TBD
FE	Ø56	DIFF INELAST	EXPT-PROG	11+7	2Ø+7	ERDA-NDC-3	232	576	OHO	BAINUM+EXCTD STATE RESOLVED.
FE	Ø56	N, PROTON	EXPT-PROG	NDG		ERDA-NDC-3	26	576	ANL	SMITH+INTEG RESPONSE FN DETERMINED.
CO	Ø59	DIFF ELASTIC	EXPT-PROG	11+7		ERDA-NDC-3	221	576	OHO	BAINUM+TOF,OPT MDL ANAL,CFD(P,P)DATA
CO	Ø59	N, GAMMA	EXPT-PROG	25+3	1Ø+6	ERDA-NDC-3	173	576	ORL	SPENCER+CS,AREA MEAS,NDG,TBP NSE
CO	Ø59	N2N REACTION	EXPT-PROG	NDG		ERDA-NDC-3	98	576	LAS	VEESER+NDG,ANAL TBD
CO	Ø59	NXN REACTION	EXPT-PROG	NDG		ERDA-NDC-3	98	576	LAS	VEESER+NDG,ANAL TBD N3N
CO	Ø59	N, PROTON	EXPT-PROG	NDG		ERDA-NDC-3	26	576	ANL	SMITH+INTEG RESPONSE FN DETERMINED.
CO	Ø59	N, PROTON	EXPT-PROG	THR		ERDA-NDC-3	26	576	ANL	SMITH+TBP IN NSE,NDG.
CO	Ø59	RESON PARAMS	EXPT-PROG	25+3	1Ø+6	ERDA-NDC-3	173	576	ORL	SPENCER+S WAV,WG,WN,NDG,TBP NSE
NI		EVALUATION	EXPT-PROG	1Ø+5	2Ø+7	ERDA-NDC-3	27	576	ANL	GUENTHER+REPORTED IN ANL-NDM-11.
NI		DIFF ELASTIC	EXPT-PROG	11+7		ERDA-NDC-3	221	576	OHO	BAINUM+TOF,OPT MDL ANAL,CFD(P,P)DATA
NI		NEUT EMISSN	THEO-PROG	14+7		ERDA-NDC-3	69	576	LRL	HANSON+3 NUCL-MDL NEM SPEC CALC,NDG
NI	Ø58	N, PROTON	EXPT-PROG	NDG		ERDA-NDC-3	26	576	ANL	SMITH+INTEG RESPONSE FN DETERMINED.
NI	Ø59	TOTAL XSECT	EXPT-PROG	1Ø+2	12+4	ERDA-NDC-3	183	576	ORL	HARVEY+CFD WITH EARLIER RESULT
NI	Ø59	ABSORPTION	EXPT-PROG	THR		ERDA-NDC-3	183	576	ORL	HARVEY+ABS CS=87+-6B CFD PREV WORK
NI	Ø59	N, GAMMA	EXPT-PROG	1Ø+2	12+4	ERDA-NDC-3	183	576	ORL	HARVEY+THR CS=7Ø+-5B CFD PREV WORK
NI	Ø59	N, PROTON	EXPT-PROG	1Ø-2	2Ø+4	ERDA-NDC-3	183	576	ORL	HARVEY+THR CS=2,Ø+-,5B CFD PREV WORK
NI	Ø59	N,ALPHA REAC	EXPT-PROG	1Ø-2	2Ø+4	ERDA-NDC-3	183	576	ORL	HARVEY+THR CS=12+-1B,CFD PREV WORK
NI	Ø59	RESON PARAMS	EXPT-PROG	2Ø+2		ERDA-NDC-3	183	576	ORL	HARVEY+WT,WN,WG,A-WID,P-WID AT 203EV
CU		TOTAL XSECT	THEO-PROG	14+7		ERDA-NDC-3	2Ø8	576	ORL	FU+CS FOR N INTERACTION CALC,NDG
CU		NONEL GAMMAS	EXPT-PROG	2Ø+5	2Ø+7	ERDA-NDC-3	169	576	ORL	CHAPMAN+LINAC,DIFF CS FOR G PROD,NDG
CU		NEUT EMISSN	THEO-PROG	14+7		ERDA-NDC-3	69	576	LRL	HANSON+3 NUCL-MDL NEM SPEC CALC,NDG
CU	Ø63	TOTAL XSECT	EXPT-PROG	NDG		ERDA-NDC-3	18Ø	576	ORL	PANDEY+TRNS,RESPARS DRVD,NDG,TBP PR
CU	Ø63	N, GAMMA	EXPT-PROG	+3	+5	ERDA-NDC-3	173	576	ORL	PANDEY+CS,CAPT YLDS,NDG,TBP PHYS REV
CU	Ø63	N,ALPHA REAC	THEO-PROG		2Ø+7	ERDA-NDC-3	2Ø8	576	ORL	FU+HELIUM PROD CS CALC VIA H-F.
CU	Ø63	RESON PARAMS	EXPT-PROG	+3	+5	ERDA-NDC-3	173	576	ORL	PANDEY+WG,N-WID,LVL SPACING,TBP PR.
CU	Ø63	RESON PARAMS	EXPT-PROG	1Ø+4	15+4	ERDA-NDC-3	18Ø	576	ORL	PANDEY+WN,PI,LVL SPACING,TBP PR
CU	Ø63	STRNGTH FUNC	EXPT-PROG	+3	+5	ERDA-NDC-3	173	576	ORL	PANDEY+S,=(,44+-,07)-4

ELEMENT S A	QUANTITY	TYPE	ENERGY MIN	MAX	DOCUMENTATION REF	VOL PAGE	DATE	LAB	COMMENTS
CU 063	STRNGTH FUNC	EXPT-PROG	10+4	15+4	ERDA-NDC-3	180	576	ORL	PANDEY+S WAVE STF,VALS GVN, TBP PR
CU 065	TOTAL XSECT	EXPT-PROG	NDG		ERDA-NDC-3	180	576	ORL	PANDEY+TRNS,RES PARS DRVD,NDG,TBP PR
CU 065	N, GAMMA	EXPT-PROG	+3	+5	ERDA-NDC-3	173	576	ORL	PANDEY+CS,CAPT YLDS,NDG,TBP PHYS REV
CU 065	RESON PARAMS	EXPT-PROG	+3	+5	ERDA-NDC-3	173	576	ORL	PANDEY+LVL SPACING S WAV,TBP PHY REV
CU 065	RESON PARAMS	EXPT-PROG	10+4	15+4	ERDA-NDC-3	180	576	ORL	PANDEY+WN,PI,LVL SPACING,TBP PR
CU 065	STRNGTH FUNC	EXPT-PROG	10+4	15+4	ERDA-NDC-3	180	576	ORL	PANDEY+ S WAVE STF, VALS GVN,TBP PR,
ZN 064	N, PROTON	EXPT-PROG	NDG		ERDA-NDC-3	26	576	ANL	SMITH+INTEG RESPONSE FN DETERMINED,
ZN 066	N, PROTON	EXPT-PROG		10+7	ERDA-NDC-3	26	576	ANL	SMITH+NDG,RESULTS IN ANL-NDM-14,
SR 088	DIFF INELAST	EXPT-PROG	11+7		ERDA-NDC-3	246	576	OHO	BAINUM+TBD,NDG
SR 088	N, GAMMA	EXPT-PROG	25+3	40+5	ERDA-NDC-3	173	576	ORL	BOLDEMAN+CS MEAS,NDG,VAL MDL,TBP NP
SR 088	SPECT N,GAMM	EXPT-PROG	20+3	24+4	ERDA-NDC-3	50	576	BNL	CHRIEN+ES,INT,PARTICLE HOLE STATES,
SR 088	RESON PARAMS	EXPT-PROG	20+3	24+4	ERDA-NDC-3	50	576	BNL	CHRIEN+SPIN-PI VALS,
SR 088	RESON PARAMS	EXPT-PROG	25+3	40+5	ERDA-NDC-3	173	576	ORL	BOLDEMAN+WG,WN CORR,VAL MDL,TBP NP,
Y 089	TOTAL XSECT	THEO-PROG	30+5	12+6	ERDA-NDC-3	286	576	DKE	DIVADEENAM+RES STRUCT OBS,TBP AP,NDG
Y 089	DIFF INELAST	EXPT-PROG	11+7		ERDA-NDC-3	246	576	OHO	BAINUM+TBD,NDG
Y 089	N2N REACTION	EXPT-PROG	14+7	24+7	ERDA-NDC-3	98	576	LAS	VEESER+LIQ SCINT,GRPHS,CFD OTH EXPT
Y 089	NXN REACTION	EXPT-PROG	14+7	24+7	ERDA-NDC-3	98	576	LAS	VEESER+N3N,LIQ SCINT,GRPHS,CFD OTH
Y 089	RESON PARAMS	THEO-PROG	30+5	12+6	ERDA-NDC-3	286	576	DKE	DIVADEENAM+SHELL MDL CALC,TBP AP,NDG
ZR 090	DIFF INELAST	EXPT-PROG	11+7		ERDA-NDC-3	246	576	OHO	BAINUM+ANAL TBD,NDG
ZR 090	DIFF INELAST	EXPT-PROG	NDG		ERDA-NDC-3	246	576	OHO	BAINUM+2+,3- STATES CS,ANAL TBD,NDG
ZR 090	N, GAMMA	EXPT-PROG	30+3	20+5	ERDA-NDC-3	174	576	ORL	BOLDEMAN+CS MEAS,NDG,ABST NP/A 246
ZR 090	RESON PARAMS	EXPT-PROG	30+3	20+5	ERDA-NDC-3	174	576	ORL	BOLDEMAN+WG,WN CORR,VAL MDL,ABST NP,
ZR 090	STRNGTH FUNC	EXPT-PROG	30+3	20+5	ERDA-NDC-3	174	576	ORL	BOLDEMAN+S,P WAVE,ABST NP/A 246,
ZR 092	DIFF INELAST	EXPT-PROG	NDG		ERDA-NDC-3	246	576	OHO	BAINUM+2+,3- STATES CS,ANAL TBD,NDG
NB 093	TOTAL XSECT	THEO-PROG	14+7		ERDA-NDC-3	208	576	ORL	FU+CS FOR N INTERACTION CALC,NDG
NB 093	DIFF ELASTIC	EXPT-PROG	11+7		ERDA-NDC-3	221	576	OHO	BAINUM+TOF,OPT MDL ANAL,CFD(P,P)DATA
NB 093	DIFF ELASTIC	EXPT-PROG	26+7		ERDA-NDC-3	232	576	OHO	BAINUM+ANAL TBD,NDG,
NB 093	N, GAMMA	EXPT-PROG	26+3	70+5	ERDA-NDC-3	174	576	ORL	MACKLIN,AVG CS 3TO5PCT ACC, NDG,
NB 093	NONEL GAMMAS	EXPT-PROG	65+5	20+7	ERDA-NDC-3	169	576	ORL	DICKENS+LINAC,DIFF CS FOR G PROD,NDG
NB 093	N2N REACTION	EXPT-PROG	NDG		ERDA-NDC-3	98	576	LAS	VEESER+NDG,ANAL TBD
NB 093	NXN REACTION	EXPT-PROG	NDG		ERDA-NDC-3	98	576	LAS	VEESER+NDG,ANAL TBD N3N
NB 093	NEUT EMISSN	THEO-PROG	14+7		ERDA-NDC-3	69	576	LRL	HANSON+3 NUCL-MDL NEM SPEC CALC,NDG
NB 094	N, GAMMA	EXPT-PROG	70+5		ERDA-NDC-3	17	576	ANC	TURK+MEAS BY NON-LINEAR LEAST SQ,2CS
MO	NONEL GAMMAS	EXPT-PROG	20+5	20+7	ERDA-NDC-3	170	576	ORL	MORGAN+ LINAC,DIFF CS FOR G PROD,NDG
MO 092	DIFF ELASTIC	EXPT-PROG	11+7		ERDA-NDC-3	221	576	OHO	BAINUM+TOF,OPT MDL ANAL,CFD(P,P)DATA

ELEMENT S A	QUANTITY	TYPE	ENERGY MIN	MAX	DOCUMENTATION REF	VOL	PAGE	DATE	LAB	COMMENTS
MO Ø92	DIFF ELASTIC	EXPT-PROG	7Ø+6	11+7	ERDA-NDC-3		225	576	OHO	BAINUM+3ES,7,9,11MEV.ANAL TBD,NDG
MO Ø92	DIFF ELASTIC	EXPT-PROG	2Ø+7		ERDA-NDC-3		225	576	OHO	BAINUM+ANAL TBD,NDG,
MO Ø92	DIFF ELASTIC	EXPT-PROG	26+7		ERDA-NDC-3		232	576	OHO	BAINUM+ANAL TBD,NDG,
MO Ø92	DIFF INELAST	EXPT-PROG	11+7		ERDA-NDC-3		246	576	OHO	BAINUM+ANAL TBD,NDG
MO Ø92	DIFF INELAST	EXPT-PROG	NDG		ERDA-NDC-3		246	576	OHO	BAINUM+2+,3- STATES CS,ANAL TBD,NDG
MO Ø92	N, GAMMA	EXPT-PROG	3Ø+3	9Ø+4	ERDA-NDC-3		175	576	ORL	MUSGROVE+CS MEAS.NDG,TBP IN NUC PHYS
MO Ø92	RESON PARAMS	EXPT-PROG	3Ø+3	9Ø+4	ERDA-NDC-3		175	576	ORL	MUSGROVE+S,P WAVE WIDS,NDG TBP NP
MO Ø92	STRNGTH FUNC	EXPT-PROG	3Ø+3	9Ø+4	ERDA-NDC-3		175	576	ORL	MUSGROVE+S,P WAVE,VAL MDL,TBP NP.
MO Ø95	TOTAL XSECT	EXPT-PROG	+3		ERDA-NDC-3		255	576	RPI	HOCKENBURY+TRNS,NDG,ANAL TBD
MO Ø95	N, GAMMA	EXPT-PROG	+3		ERDA-NDC-3		255	576	RPI	HOCKENBURY+B1Ø-NAI DET,CAPT CS,NDG
MO Ø95	RESON PARAMS	EXPT-PROG	+3		ERDA-NDC-3		255	576	RPI	HOCKENBURY+RES PARS TO NORM CS,NDG
MO Ø96	DIFF ELASTIC	EXPT-PROG	11+7		ERDA-NDC-3		221	576	OHO	BAINUM+TOF,OPT MDL ANAL,CFD(P,P)DATA
MO Ø96	DIFF ELASTIC	EXPT-PROG	7Ø+6	11+7	ERDA-NDC-3		225	576	OHO	BAINUM+3ES,7,9,11MEV.ANAL TBD,NDG
MO Ø96	DIFF ELASTIC	EXPT-PROG	2Ø+7		ERDA-NDC-3		225	576	OHO	BAINUM+ANAL TBD,NDG,
MO Ø96	DIFF ELASTIC	EXPT-PROG	26+7		ERDA-NDC-3		232	576	OHO	BAINUM+ANAL TBD,NDG,
MO Ø96	DIFF ELASTIC	EXPT-PROG	11+7		ERDA-NDC-3		236	576	OHO	BAINUM+OPTMDL FIT,PARS DRVD,GRPHS,
MO Ø96	DIFF INELAST	EXPT-PROG	NDG		ERDA-NDC-3		246	576	OHO	BAINUM+2+,3- STATES CS,ANAL TBD,NDG
MO Ø97	TOTAL XSECT	EXPT-PROG	+3		ERDA-NDC-3		255	576	RPI	HOCKENBURY+TRNS,NDG,ANAL TBD
MO Ø97	N, GAMMA	EXPT-PROG	+3		ERDA-NDC-3		255	576	RPI	HOCKENBURY+B1Ø-NAI DET,CAPT CS,NDG
MO Ø97	RESON PARAMS	EXPT-PROG	+3		ERDA-NDC-3		255	576	RPI	HOCKENBURY+RES PARS TO NORM CS,NDG
MO Ø98	DIFF ELASTIC	EXPT-PROG	11+7		ERDA-NDC-3		221	576	OHO	BAINUM+TOF,OPT MDL ANAL,CFD(P,P)DATA
MO Ø98	DIFF ELASTIC	EXPT-PROG	7Ø+6	11+7	ERDA-NDC-3		225	576	OHO	BAINUM+3ES,7,9,11MEV.ANAL TBD,NDG
MO Ø98	DIFF ELASTIC	EXPT-PROG	2Ø+7		ERDA-NDC-3		225	576	OHO	BAINUM+ANAL TBD,NDG,
MO Ø98	DIFF ELASTIC	EXPT-PROG	26+7		ERDA-NDC-3		232	576	OHO	BAINUM+ANAL TBD,NDG,
MO Ø98	DIFF INELAST	EXPT-PROG	NDG		ERDA-NDC-3		246	576	OHO	BAINUM+2+,3- STATES CS,ANAL TBD,NDG
MO Ø98	N, GAMMA	EXPT-PROG	3Ø+3	9Ø+4	ERDA-NDC-3		175	576	ORL	MUSGROVE+CS MEAS.NDG,TBP IN NUC PHYS
MO Ø98	SPECT N,GAMM	EXPT-PROG	12+1	56+3	ERDA-NDC-3		184	576	ORL	MUGHABGHAB+CAPT G GIVE I AND PI,
MO Ø98	RESON PARAMS	EXPT-PROG	3Ø+3	9Ø+4	ERDA-NDC-3		175	576	ORL	MUSGROVE+S,P WAVE WIDS,NDG TBP NP
MO Ø98	RESON PARAMS	EXPT-PROG	12+1	56+3	ERDA-NDC-3		184	576	ORL	MUGHABGHAB+I AND PI OF N RES
MO Ø98	STRNGTH FUNC	EXPT-PROG	3Ø+3	9Ø+4	ERDA-NDC-3		175	576	ORL	MUSGROVE+S,P WAVE,VAL MDL,TBP NP.
MO Ø99	N, GAMMA	EXPT-PROG	NDG		ERDA-NDC-3		175	576	ORL	MUSGROVE+FROM RES PARS,NDG,TBP NP.
MO 1ØØ	TOTAL XSECT	EXPT-PROG	NDG		ERDA-NDC-3		185	576	ORL	WEIGMANN+NEEDED TO DRV WN,CFD ENDF
MO 1ØØ	DIFF ELASTIC	EXPT-PROG	11+7		ERDA-NDC-3		221	576	OHO	BAINUM+TOF,OPT MDL ANAL,CFD(P,P)DATA
MO 1ØØ	DIFF ELASTIC	EXPT-PROG	7Ø+6	11+7	ERDA-NDC-3		225	576	OHO	BAINUM+3ES,7,9,11MEV.ANAL TBD,NDG
MO 1ØØ	DIFF ELASTIC	EXPT-PROG	2Ø+7		ERDA-NDC-3		225	576	OHO	BAINUM+ANAL TBD,NDG,

ELEMENT S A	QUANTITY	TYPE	ENERGY MIN	MAX	DOCUMENTATION REF VOL	PAGE	DATE	LAB	COMMENTS
MO 100	DIFF ELASTIC	EXPT-PROG	26+7		ERDA-NDC-3	232	576	OHO	BAINUM+ANAL TBD,NDG,
MO 100	DIFF INELAST	EXPT-PROG	NDG		ERDA-NDC-3	246	576	OHO	BAINUM+2+,3+ STATES CS,ANAL TBD,NDG
MO 100	SPECT N,GAMM	EXPT-PROG		50+3	ERDA-NDC-3	184	576	ORL	WEIGMANN+TOF,G SPEC,ANAL TBC,VAL MDL
MO 100	RESON PARAMS	EXPT-PROG		25+4	ERDA-NDC-3	185	576	ORL	WEIGMANN+WN DRVD,CFD ENDF
RU 101	TOTAL XSECT	EXPT-PROG	20+1	20+5	ERDA-NDC-3	255	576	RPI	HOCKENBURY+TRNS MEAS,NDG
RU 101	N, GAMMA	EXPT-PROG	20+1	20+5	ERDA-NDC-3	255	576	RPI	HOCKENBURY+CAPT CS MEAS,NDG,
RU 101	RESON PARAMS	EXPT-PROG	+3		ERDA-NDC-3	255	576	RPI	HOCKENBURY+RES PARS DRVD,NDG
RU 102	TOTAL XSECT	EXPT-PROG	20+1	20+5	ERDA-NDC-3	255	576	RPI	HOCKENBURY+TRNS MEAS,NDG
RU 102	N, GAMMA	EXPT-PROG	20+1	20+5	ERDA-NDC-3	255	576	RPI	HOCKENBURY+CAPT CS MEAS,NDG,
RU 102	RESON PARAMS	EXPT-PROG	+3		ERDA-NDC-3	255	576	RPI	HOCKENBURY+RES PARS DRVD,NDG
RU 104	TOTAL XSECT	EXPT-PROG	20+1	20+5	ERDA-NDC-3	255	576	RPI	HOCKENBURY+TRNS MEAS,NDG
RU 104	N, GAMMA	EXPT-PROG	20+1	20+5	ERDA-NDC-3	255	576	RPI	HOCKENBURY+CAPT CS MEAS,NDG,
RU 104	RESON PARAMS	EXPT-PROG	+3		ERDA-NDC-3	255	576	RPI	HOCKENBURY+RES PARS DRVD,NDG
RH 103	N2N REACTION	EXPT-PROG	NDG		ERDA-NDC-3	98	576	LAS	VEESER+NDG,ANAL TBD
RH 103	NXN REACTION	EXPT-PROG	NDG		ERDA-NDC-3	98	576	LAS	VEESER+NDG,ANAL TBD N3N
PD 108	SPECT N,GAMM	EXPT-PROG	25-2	30+2	ERDA-NDC-3	52	576	BNL	CASTEN+REVISED I AND SPECT FACTORS,
PD 108	SPECT N,GAMM	EXPT-PROG	25-2	30+2	ERDA-NDC-3	52	576	BNL	CASTEN+PARTIAL WG MEAS,REVISED I,
AG	NONEL GAMMAS	EXPT-PROG	30+5	20+7	ERDA-NDC-3	170	576	ORL	DICKENS+LINAC,DIFF CS FOR G PROD,NDG
CD 110	N, GAMMA	EXPT-PROG	NDG		ERDA-NDC-3	26	576	ANL	SMITH+TBD,CONTRIB TO CD111 ISOM REAC
CD 111	TOT INELASTI	EXPT-PROG	NDG		ERDA-NDC-3	26	576	ANL	SMITH+TBD,CD110 DNG CONTRIB,
IN	DIFF ELASTIC	EXPT-PROG	11+7		ERDA-NDC-3	221	576	OHO	BAINUM+TOF,OPT MDL ANAL,CFD(P,P)DATA
IN 113	TOT INELASTI	EXPT-PROG		10+7	ERDA-NDC-3	26	576	ANL	SMITH+NDG,RESULTS IN ANL-NDM-14,
IN 115	TOT INELASTI	EXPT-PROG		10+7	ERDA-NDC-3	26	576	ANL	SMITH+NDG,RESULTS IN ANL-NDM-14,
IN 115	N, GAMMA	EXPT-PROG	96+5		ERDA-NDC-3	143	576	MHG	ROBERTSON+NA-BE SOURCE,TBD,NDG,
SN 115	SPECT N,GAMM	EXPT-PROG	NDG		ERDA-NDC-3	185	576	ORL	RAMAN+G SPEC,LVL STRUCT STUDY,TBD
SN 115	RESON PARAMS	EXPT-PROG	NDG		ERDA-NDC-3	185	576	ORL	RAMAN+I AND PI ASSIGNMENTS TBD,NDG
SN 117	SPECT N,GAMM	EXPT-PROG	NDG		ERDA-NDC-3	185	576	ORL	RAMAN+G SPEC,LVL STRUCT STUDY,TBD
SN 117	RESON PARAMS	EXPT-PROG	NDG		ERDA-NDC-3	185	576	ORL	RAMAN+I AND PI ASSIGNMENTS TBD,NDG
SN 119	SPECT N,GAMM	EXPT-PROG	NDG		ERDA-NDC-3	185	576	ORL	RAMAN+G SPEC,LVL STRUC STUDY,NDG,TBC
SN 119	RESON PARAMS	EXPT-PROG	NDG		ERDA-NDC-3	185	576	ORL	RAMAN+I AND PI ASSIGNMENTS TBD,NDG
SN 120	TOTAL XSECT	EXPT-PROG	NDG		ERDA-NDC-3	186	576	ORL	CARLTON+TRNS,RESPARS DRVD,NDG,TBP,PR
SN 120	DIFF ELASTIC	EXPT-PROG	11+7		ERDA-NDC-3	221	576	OHO	BAINUM+TOF,OPT MDL ANAL,CFD(P,P)DATA
SN 120	DIFF ELASTIC	EXPT-PROG	26+7		ERDA-NDC-3	232	576	OHO	BAINUM+ANAL TBD,NDG,
SN 120	DIFF ELASTIC	EXPT-PROG	94+6	23+7	ERDA-NDC-3	232	576	OHO	BAINUM+2ES,CFD OPT MDL PREDICT,CURVS
SN 120	SPECT N,GAMM	EXPT-PROG	NDG		ERDA-NDC-3	186	576	ORL	CARLTON+G SPEC,RES PARS,NDG,TBP PR,

ELEMENT S A	QUANTITY	TYPE	ENERGY MIN	ENERGY MAX	DOCUMENTATION REF	VOL	PAGE	DATE	LAB	COMMENTS
SN 120	RESON PARAMS	EXPT-PROG		98+4	ERDA-NDC	3	186	576	ORL	CARLTON+LVL SPACING,PI,I,NDG,TBP PR,
SN 121	SPECT N,GAMM	EXPT-PROG		70+3	ERDA-NDC	3	185	576	ORL	RAMAN+G SPEC,LVL STRUC STUDY,NDG,TBC
SN 121	RESON PARAMS	EXPT-PROG		70+3	ERDA-NDC	3	185	576	ORL	RAMAN+I AND PI ASSIGNMENTS TBD,NDG,
SN 125	SPECT N,GAMM	EXPT-PROG	NDG		ERDA-NDC	3	185	576	ORL	RAMAN+G SPEC,LVL STRUC STUDY,NDG,TBC
SN 125	RESON PARAMS	EXPT-PROG	NDG		ERDA-NDC	3	185	576	ORL	RAMAN+I AND PI ASSIGNMENTS TBD,NDG,
TE 125	N, GAMMA	EXPT-PROG	20+3	24+4	ERDA-NDC	3	49	576	BNL	GREENWOOD+TEST FOR TRIPLET MEMBERS,
TE 125	RESON PARAMS	EXPT-PROG	20+3	24+4	ERDA-NDC	3	49	576	BNL	GREENWOOD+TE126 PI INFORMATION,
XE 124	N, GAMMA	EXPT-PROG	52+0	99+0	ERDA-NDC	3	47	576	BNL	KANE+CS ESTABLISHED THR TO 50EV,NDG
XE 124	RESON PARAMS	EXPT-PROG	52+0	99+0	ERDA-NDC	3	47	576	BNL	KANE+5,16,9,88EV RES PARS TBD,
CS 133	TOTAL XSECT	EXPT-PROG	+3		ERDA-NDC	3	255	576	RPI	HOCKENBURY+TRNS,NDG,ANAL TBD
CS 133	N, GAMMA	EXPT-PROG	+3		ERDA-NDC	3	255	576	RPI	HOCKENBURY+B10-NAI DET,CAPT CS,NDG
CS 133	RESON PARAMS	EXPT-PROG	+3		ERDA-NDC	3	255	576	RPI	HOCKENBURY+RES PARS TO NORM CS,NDG
BA 134	N, GAMMA	EXPT-PROG	30+3	10+5	ERDA-NDC	3	175	576	ORL	MUSGROVE+30KEV AVG CS,ABST NP/A 256
BA 134	RESON PARAMS	EXPT-PROG	30+3	11+4	ERDA-NDC	3	175	576	ORL	MUSGROVE+LVL SPACING,WG,ABST NP/A256
BA 134	STRNGTH FUNC	EXPT-PROG	30+3	11+4	ERDA-NDC	3	175	576	ORL	MUSGROVE+S,P WAVE STF,ABST NP/A 256
BA 135	N, GAMMA	EXPT-PROG	30+3	10+5	ERDA-NDC	3	176	576	ORL	MUSGROVE+CS MEAS,NDG,
BA 135	RESON PARAMS	EXPT-PROG	30+3	60+3	ERDA-NDC	3	176	576	ORL	MUSGROVE+AVG WG,
BA 135	STRNGTH FUNC	EXPT-PROG	30+3	60+3	ERDA-NDC	3	176	576	ORL	MUSGROVE+P WAVE, VAL GVN
BA 136	N, GAMMA	EXPT-PROG	30+3	10+5	ERDA-NDC	3	175	576	ORL	MUSGROVE+30KEV AVG CS ABST NP/A 256
BA 136	RESON PARAMS	EXPT-PROG	30+3	35+4	ERDA-NDC	3	175	576	ORL	MUSGROVE+WG,ABST NP/A 256
BA 138	N, GAMMA	EXPT-PROG		10+5	ERDA-NDC	3	176	576	ORL	MUSGROVE+CS MEAS,NDG,TBP IN NP,
BA 138	RESON PARAMS	EXPT-PROG		10+5	ERDA-NDC	3	176	576	ORL	MUSGROVE+S,P AVG PARS,WG,WN,TBP NP,
BA 138	STRNGTH FUNC	EXPT-PROG		10+5	ERDA-NDC	3	176	576	ORL	MUSGROVE+S,P WAVE STF,
ND 143	TOTAL XSECT	EXPT-PROG	+3		ERDA-NDC	3	255	576	RPI	HOCKENBURY+TRNS,NDG,ANAL TBD
ND 143	N, GAMMA	EXPT-PROG	+3		ERDA-NDC	3	255	576	RPI	HOCKENBURY+B10-NAI DET,CAPT CS,NDG
ND 143	RESON PARAMS	EXPT-PROG	+3		ERDA-NDC	3	255	576	RPI	HOCKENBURY+RES PARS TO NORM CS,NDG
ND 145	TOTAL XSECT	EXPT-PROG	20+1	20+5	ERDA-NDC	3	255	576	RPI	HOCKENBURY+TRNS MEAS,NDG
ND 145	N, GAMMA	EXPT-PROG	20+1	20+5	ERDA-NDC	3	255	576	RPI	HOCKENBURY+CAPT CS MEAS,NDG,
ND 145	RESON PARAMS	EXPT-PROG	+3		ERDA-NDC	3	255	576	RPI	HOCKENBURY+RES PARS DRVD,NDG
SM 149	TOTAL XSECT	EXPT-PROG	20+1	20+5	ERDA-NDC	3	255	576	RPI	HOCKENBURY+TRNS MEAS,NDG
SM 149	N, GAMMA	EXPT-PROG	20+1	20+5	ERDA-NDC	3	255	576	RPI	HOCKENBURY+CAPT CS MEAS,NDG,
SM 149	RESON PARAMS	EXPT-PROG	+3		ERDA-NDC	3	255	576	RPI	HOCKENBURY+RES PARS DRVD,NDG
HO 165	DIFF ELASTIC	EXPT-PROG	11+7		ERDA-NDC	3	221	576	OHO	BAINUM+TOF,OPT MDL ANAL,CFD(P,P)DATA
HO 165	N, GAMMA	EXPT-PROG	30+3	45+5	ERDA-NDC	3	176	576	ORL	MACKLIN,TOF,NDG,
HO 165	N, GAMMA	EXPT-PROG	30+5	40+6	ERDA-NDC	3	28	576	ANL	POENITZ,TOF,CS MEAS,H-F CALC,NDG,

ELEMENT S	A	QUANTITY	TYPE	ENERGY MIN	MAX	DOCUMENTATION REF	VOL	PAGE	DATE	LAB	COMMENTS
HO	165	RESON PARAMS	EXPT-PROG	30+3	45+5	ERDA-NDC	3	176	576	ORL	MACKLIN,BELOW 3KEV,RESPARS,NDG.
HO	165	STRNGTH FUNC	EXPT-PROG	30+3	45+5	ERDA-NDC	3	176	576	ORL	MACKLIN,S,P,D WAVE STF
ER	164	SPECT N,GAMM	EXPT-PROG	20+3	24+4	ERDA-NDC	3	51	576	BNL	KOENE+9 RES ES,UP TO 2MEV EXCIT,NDG
ER	164	RESON PARAMS	EXPT-PROG	20+3	24+4	ERDA-NDC	3	51	576	BNL	KOENE+PARTIAL WG REL AU197,PI, NDG
TM	169	N2N REACTION	EXPT-PROG	14+7	24+7	ERDA-NDC	3	98	576	LAS	VEESER+LIQ SCINT,GRPHS,CFD OTH EXPT
TM	169	NXN REACTION	EXPT-PROG	14+7	24+7	ERDA-NDC	3	98	576	LAS	VEESER+N3N,LIQ SCINT,GRPHS,CFD OTH
YB	173	SPECT N,GAMM	EXPT-PROG	NDG		ERDA-NDC	3	187	576	ORL	MUGHABGHAB+GE-LI,G SPEC,NDG
YB	173	RESON PARAMS	EXPT-PROG	NDG		ERDA-NDC	3	187	576	ORL	MUGHABGHAB+CORR COEF WG,WN,I,NDG.
LU	175	N2N REACTION	EXPT-PROG	14+7	24+7	ERDA-NDC	3	98	576	LAS	VEESER+LIQ SCINT,GRPHS,CFD OTH EXPT
LU	175	NXN REACTION	EXPT-PROG	14+7	24+7	ERDA-NDC	3	98	576	LAS	VEESER+N3N,LIQ SCINT,GRPHS,CFD OTH
TA	181	DIFF ELASTIC	EXPT-PROG	11+7		ERDA-NDE	3	221	576	OHO	BAINUM+TOF,OPT MDL ANAL,CFD(P,P)DATA
TA	181	N, GAMMA	EXPT-PROG	30+5	40+6	ERDA-NDC	3	28	576	ANL	POENITZ,TOF,CS MEAS,H-F CALC,NDG.
TA	181	SPECT N,GAMM	EXPT-PROG	20+0	90+4	ERDA-NDE	3	69	576	LRL	STELTS+GE-LI,LINAC,G SPEC GRPHS.
TA	181	N2N REACTION	EXPT-PROG	NDG		ERDA-NDC	3	98	576	LAS	VEESER+NDG,ANAL TBD
TA	181	NXN REACTION	EXPT-PROG	NDG		ERDA-NDC	3	98	576	LAS	VEESER+NDG,ANAL TBD N3N
W	182	TOTAL XSECT	EXPT-PROG	46+5	54+6	ERDA-NDC	3	27	576	ANL	WHALEN+TOF,TRNS,30 KEV STEPS,NDG,TBP
W	182	ELASTIC SCAT	EXPT-PROG	NDG		ERDA-NDC	3	29	576	ANL	SMITH+NDG,TOF,EL,INEL SCAT,ANAL TBD.
W	182	DIFF ELASTIC	EXPT-PROG	NDG		ERDA-NDC	3	29	576	ANL	SMITH+NDG,TOF,EL,INEL SCAT,ANAL TBD.
W	182	DIFF INELAST	EXPT-PROG	NDG		ERDA-NDE	3	29	576	ANL	SMITH+NDG,TOF,EL,INEL SCAT,ANAL TBD.
W	184	TOTAL XSECT	EXPT-PROG	46+5	54+6	ERDA-NDE	3	27	576	ANL	WHALEN+TOF,TRNS,30 KEV STEPS,NDG,TBP
W	184	ELASTIC SCAT	EXPT-PROG	NDG		ERDA-NDE	3	29	576	ANL	SMITH+NDG,TOF,EL,INEL SCAT,ANAL TBD.
W	184	DIFF ELASTIC	EXPT-PROG	NDG		ERDA-NDE	3	29	576	ANL	SMITH+NDG,TOF,EL,INEL SCAT,ANAL TBD.
W	184	DIFF INELAST	EXPT-PROG	NDG		ERDA-NDE	3	29	576	ANL	SMITH+NDG,TOF,EL,INEL SCAT,ANAL TBD.
W	186	TOTAL XSECT	EXPT-PROG	46+5	54+6	ERDA-NDC	3	27	576	ANL	WHALEN+TOF,TRNS,30 KEV STEPS,NDG,TBP
W	186	ELASTIC SCAT	EXPT-PROG	NDG		ERDA-NDE	3	29	576	ANL	SMITH+NDG,TOF,EL,INEL SCAT,ANAL TBD.
W	186	DIFF ELASTIC	EXPT-PROG	NDG		ERDA-NDE	3	29	576	ANL	SMITH+NDG,TOF,EL,INEL SCAT,ANAL TBD.
W	186	DIFF INELAST	EXPT-PROG	NDG		ERDA-NDE	3	29	576	ANL	SMITH+NDG,TOF,EL,INEL SCAT,ANAL TBD.
OS	186	N, GAMMA	EXPT-PROG		15+5	ERDA-NDE	3	80	576	LRL	BROWNE+GRPH,CS VS E,AGE OF UNIVERSE
OS	186	N, GAMMA	EXPT-PROG	25+4		ERDA-NDE	3	149	576	NBS	BROWNE+OS 187 RATIO,UNIVERSE AGE,TBP
OS	187	N, GAMMA	EXPT-PROG		15+5	ERDA-NDC	3	80	576	LRL	BROWNE+GRPH,CS VS E,AGE OF UNIVERSE
OS	187	N, GAMMA	EXPT-PROG	25+4		ERDA-NDE	3	149	576	NBS	BROWNE+OS 186 RATIO,UNIVERSE AGE,TBP
OS	187	SPECT N,GAMM	EXPT-PROG	NDG		ERDA-NDE	3	82	576	LRL	STOLOVY+LINAC,GE-LI,NG SPEC,NDG,TBP
OS	187	RESON PARAMS	EXPT-PROG	NDG		ERDA-NDE	3	82	576	LRL	STOLOVY+I STATES FOR 25 RES,NDG,TBP.
OS	189	SPECT N,GAMM	EXPT-PROG	NDG		ERDA-NDE	3	82	576	LRL	STOLOVY+LINAC,GE-LI,NG SPEC,NDG,TBP
OS	189	RESON PARAMS	EXPT-PROG	NDG		ERDA-NDC	3	82	576	LRL	STOLOVY+I STATES FOR 40 RES,NDG,TBP

ELEMENT S	A	QUANTITY	TYPE	ENERGY MIN	MAX	DOCUMENTATION REF VOL	PAGE	DATE	LAB	COMMENTS
OS	190	SPECT N,GAMM	EXPT-PROG	25-2	20+3	ERDA-NDC-3	53	576	BNL	CASTEN+LVL ES,I-PI,NILSSON MDL,TBC,
PT	195	SPECT N,GAMM	EXPT-PROG	12+1		ERDA-NDC-3	54	576	BNL	CIZEWSKI+PT196 LVL STRUCT,TBC
AU	197	N, GAMMA	EXPT-PROG	30+3	55+5	ERDA-NDC-3	177	576	ORL	MACKLIN+PULSE HEIGHT WEIGHTING,NDG
AU	197	N, GAMMA	EXPT-PROG	10+4	50+4	ERDA-NDC-3	190	576	ORL	GWIN+CS MEAS,CFD ENDF,ABST NSE59,NDG
AU	197	NONEL GAMMAS	EXPT-PROG	20+5	20+7	ERDA-NDC-3	170	576	ORL	MORGAN+LINAC,DIFF CS FOR G PROD,NDG,
AU	197	N2N REACTION	EXPT-PROG	14+7	24+7	ERDA-NDC-3	98	576	LAS	VEESER+LIQ SCINT,GRPHS,CFD OTH EXPT
AU	197	NXN REACTION	EXPT-PROG	14+7	24+7	ERDA-NDC-3	98	576	LAS	VEESER+N3N,LIQ SCINT,GRPHS,CFD OTH
AU	197	RESON PARAMS	EXPT-PROG	26+3	49+3	ERDA-NDC-3	177	576	ORL	MACKLIN+RES PARS DEDUCED,NDG,
TL	203	N, GAMMA	EXPT-PROG	NDG		ERDA-NDC-3	177	576	ORL	MACKLIN+HIGH RESOL DATA,NDG TBP AJ
TL	203	RESON PARAMS	EXPT-PROG	NDG		ERDA-NDC-3	177	576	ORL	MACKLIN+RES PAR DATA,NDG,TBP AJ,
TL	205	TOTAL XSECT	EXPT-PROG	NDG		ERDA-NDC-3	177	576	ORL	WINTERS+NDG,ABST 76 LOWELL CONF
TL	205	N, GAMMA	EXPT-PROG	NDG		ERDA-NDC-3	177	576	ORL	MACKLIN+HIGH RESOL DATA,NDG TBP AJ
TL	205	N, GAMMA	EXPT-PROG	NDG		ERDA-NDC-3	177	576	ORL	WINTERS+NDG,ABST 76 LOWELL CONF
TL	205	RESON PARAMS	EXPT-PROG	NDG		ERDA-NDC-3	177	576	ORL	MACKLIN+RES PAR DATA,NDG,TBP AJ,
TL	205	RESON PARAMS	EXPT-PROG	NDG		ERDA-NDC-3	177	576	ORL	WINTERS+NG,NDG,ABST 76 LOWELL CONF,
TL	205	STRNGTH FUNC	EXPT-PROG		65+4	ERDA-NDC-3	177	576	ORL	WINTERS+S,P WAVE,ABST 76LOWELL CONF
PB		EVALUATION	EVAL-PROG	10-5	20+7	ERDA-NDC-3	209	576	ORL	FU+RECOMMENDED N CS DATA,NDG,
PB		DIFF ELASTIC	EXPT-PROG	11+7		ERDA-NDC-3	221	576	OHO	BAINUM+TOF,OPT MDL ANAL,CFD(P,P)DATA
PB	204	TOT INELASTI	EXPT-PROG	NDG		ERDA-NDC-3	26	576	ANL	SMITH+NDG,PRELIM MEAS FOR ISOM REAC,
PB	206	DIFF ELASTIC	EXPT-PROG	11+7		ERDA-NDC-3	221	576	OHO	BAINUM+TOF,OPT MDL ANAL,CFD(P,P)DATA
PB	206	DIFF ELASTIC	EXPT-PROG	20+7		ERDA-NDC-3	225	576	OHO	BAINUM+ANAL TBD,NDG,
PB	206	DIFF ELASTIC	EXPT-PROG	26+7		ERDA-NDC-3	232	576	OHO	BAINUM+ANAL TBD,NDG,
PB	206	DIFF ELASTIC	EXPT-PROG	60+5	10+6	ERDA-NDC-3	30	576	ANL	SMITH,OPTMDL PARAMS OBTAINED,NDG
PB	206	SPECT N,GAMM	EXPT-PROG		20+5	ERDA-NDC-3	185	576	ORL	RAMAN+G SPEC,TBC,NDG,
PB	207	TOTAL XSECT	EXPT-PROG		+5	ERDA-NDC-3	180	576	ORL	HOREN+TRNS,RES PARS ANAL TBD,NDG,
PB	207	DIFF ELASTIC	EXPT-PROG	60+5	10+6	ERDA-NDC-3	30	576	ANL	SMITH,OPTMDL PARAMS OBTAINED,NDG
PB	207	SPECT N,GAMM	EXPT-PROG		20+5	ERDA-NDC-3	185	576	ORL	RAMAN+G SPEC,TBC,NDG,
PB	207	RESON PARAMS	EXPT-PROG		+5	ERDA-NDC-3	180	576	ORL	HOREN+PARS ANAL TBD,D+S WAVE MIX,NDG
PB	208	TOTAL XSECT	EXPT-PROG	70+5	15+6	ERDA-NDC-3	181	576	ORL	FOWLER+TRNS,TOF,NDG
PB	208	DIFF ELASTIC	EXPT-PROG	11+7		ERDA-NDC-3	221	576	OHO	BAINUM+TOF,OPT MDL ANAL,CFD(P,P)DATA
PB	208	DIFF ELASTIC	EXPT-PROG	20+7		ERDA-NDC-3	225	576	OHO	BAINUM+ANAL TBD,NDG,
PB	208	DIFF ELASTIC	EXPT-PROG	26+7		ERDA-NDC-3	232	576	OHO	BAINUM+ANAL TBD,NDG,
PB	208	DIFF ELASTIC	EXPT-PROG	26+7		ERDA-NDC-3	236	576	OHO	BAINUM+OPTMDL FIT,PARS DRVD,ANAL TBD
PB	208	DIFF ELASTIC	EXPT-PROG	60+5	10+6	ERDA-NDC-3	30	576	ANL	SMITH,OPTMDL PARAMS OBTAINED,NDG
PB	208	DIFF INELAST	EXPT-PROG	11+7	26+7	ERDA-NDC-3	246	576	OHO	BAINUM+2ES,ANAL TBD,NDG

ELEMENT S	A	QUANTITY	TYPE	ENERGY MIN	MAX	DOCUMENTATION REF VOL	PAGE	DATE	LAB	COMMENTS
PB	206	RESON PARAMS	EXPT-PROG	70+5	15+6	ERDA-NDC-3	181	576	ORL	FOWLER+SPIS,PI,RED WIDS TBD,NDG
BI	209	DIFF ELASTIC	EXPT-PROG	11+7		ERDA-NDC-3	221	576	OHO	BAINUM+TOF,OPT MDL ANAL,CFD(P,P)DATA
BI	209	DIFF ELASTIC	EXPT-PROG	26+7		ERDA-NDC-3	232	576	OHO	BAINUM+ANAL TBD,NDG,
BI	209	DIFF ELASTIC	EXPT-PROG	60+5	10+6	ERDA-NDC-3	30	576	ANL	SMITH,OPTMDL PARAMS OBTAINED,NDG
BI	209	N, GAMMA	EXPT-PROG		90+5	ERDA-NDC-3	178	576	ORL	MACKLIN+AVG CS=10,7MBAT30KEV,TBP PRC
BI	209	N2N REACTION	EXPT-PROG	NDG		ERDA-NDC-3	98	576	LAS	VEESER+NDG,ANAL TBD
BI	209	NXN REACTION	EXPT-PROG	NDG		ERDA-NDC-3	98	576	LAS	VEESER+NDG,ANAL TBD N3N
BI	209	RESON PARAMS	EXPT-PROG	26+3	30+5	ERDA-NDC-3	178	576	ORL	MACKLIN+AVG WG,LVL SPACING,TBP PR/C,
TH	229	FISSION	EXPT-PROG	NDG		ERDA-NDC-3	63	576	COL	LUERS+NEW MEAS FOR BETTER STATS,TBC,
TH	229	RESON PARAMS	EXPT-PROG	NDG		ERDA-NDC-3	63	576	COL	LUERS+AVG WG,NDG,D=,3EV,TBC
TH	232	N, GAMMA	EXPT-PROG	THR		ERDA-NDC-3	93	576	LAS	JURNEY+G SPEC,THR CS=7,1+-,6B,GRPH,
TH	232	SPECT N,GAMM	EXPT-PROG	20+3	24+4	ERDA-NDC-3	47	576	BNL	GREENWOOD+TH233 LVL STRUCT,PI,GRPH
TH	232	SPECT N,GAMM	EXPT-PROG	THR		ERDA-NDC-3	93	576	LAS	JURNEY+G SPEC MEAS,GRPHS,
TH	232	FISSION	EXPT-PROG	10+0	10+5	ERDA-NDC-3	256	576	RPI	BLOCK+LINAC,IONIZ CH,GRPH,STRUCT OBS
TH	232	FISSION	EXPT-PROG	72+5		ERDA-NDC-3	93	576	LAS	VEESER+2,7KEV RESOL,SOME STRUCT,NDG
TH	232	F NEUT DELAY	EXPT-PROG	FAST		ERDA-NDC-3	306	576	WAU	ECCLESTON+NEAR EQUILIBRIA SPEC,NDG
TH	232	RESON PARAMS	EXPT-PROG	20+3	24+4	ERDA-NDC-3	47	576	BNL	GREENWOOD+TH233 SPIN,PI ASSIGNED,TBP
TH	232	RESON PARAMS	EXPT-PROG	72+5		ERDA-NDC-3	93	576	LAS	VEESER+I AND PI ANAL TBD,NDG
U	233	FISSION	EXPT-PROG	10+1	70+4	ERDA-NDC-3	66	576	LRL	CZIRR+TOF,CS REL LI6,ANAL TBD,NDG
U	233	FISSION	EXPT-PROG	50+3	20+5	ERDA-NDC-3	190	576	ORL	GWIN+CS MEAS,CFD ENDF,ABST NSE59,NDG
U	233	F NEUT DELAY	EXPT-PROG	FAST		ERDA-NDC-3	306	576	WAU	ECCLESTON+NEAR EQUILIBRIA SPEC,NDG
U	234	FISSION	EXPT-PROG	50+5	40+6	ERDA-NDC-3	27	576	ANL	MEADOWS+REL U235,2,5 MEV VAL GVN,
U	235	EVALUATION	EVAL-PROG	NDG		ERDA-NDC-3	120	576	LAS	FOSTER+TIME DEP SPEC FROM 1NANO SEC
U	235	ABSORPTION	EXPT-PROG	20-2	20+5	ERDA-NDC-3	190	576	ORL	GWIN+CFD ENDF ABST NSE 59,NDG,
U	235	ABSORPTION	EXPT-PROG	20-2	20+5	ERDA-NDC-3	210	576	ORL	GWIN,NSE 59 CFD ENDF,WESCOT G FACTOR
U	235	N, GAMMA	EXPT-PROG	20-2	20+5	ERDA-NDC-3	190	576	ORL	GWIN+CS MEAS,CFD ENDF,ABST NSE59,NDG
U	235	N, GAMMA	EXPT-PROG	20-2	20+5	ERDA-NDC-3	210	576	ORL	GWIN,NSE 59 CFD,ENDF,WESCOT G FACTOR
U	235	SPECT N,GAMM	EXPT-PROG	52+0	49+1	ERDA-NDC-3	51	576	BNL	KOENE+INT MEAS,LVL ES DETERMINED,NDG
U	235	FISSION	EXPT-PROG	14+7	15+7	ERDA-NDC-3	65	576	LRL	CARLSON+MEAS OF CS TBD,NDG,
U	235	FISSION	EXPT-PROG	14+7	15+7	ERDA-NDC-3	65	576	LRL	CARLSON+MEAS OF CS TBD,NDG,
U	235	FISSION	EXPT-PROG	10+3	15+7	ERDA-NDC-3	65	576	LRL	BEHRENS+PU240,PU242 RATIO MEAS,NDG
U	235	FISSION	EXPT-PROG	10+3	15+7	ERDA-NDC-3	65	576	LRL	BEHRENS+PU239/U235 CS RATIO MEAS,NDG
U	235	FISSION	EXPT-PROG	10+3	15+7	ERDA-NDC-3	6	576	LRL	BEHRENS+PU241/U235 CS RATIO MEAS,NDG
U	235	FISSION	EXPT-PROG	14+5	77+5	ERDA-NDC-3	141	576	MHG	DAVIS+CS AT 2ES,ANAL TBD,TBP,NDG,
U	235	FISSION	EXPT-PROG	SPON		ERDA-NDC-3	142	576	MHG	DAVIS+CF252 SPON SPEC,CS MEAS,NDG,

ELEMENT S	A	QUANTITY	TYPE	ENERGY MIN	MAX	DOCUMENTATION REF VOL	PAGE	DATE	LAB	COMMENTS
U	235	FISSION	EXPT-PROG	50+3	80+5	ERDA-NDC-3	149	576	NBS	WASSON,CS SHAPE MEAS,NORM,NDG,
U	235	FISSION	EXPT-PROG	60+0	30+4	ERDA-NDC-3	149	576	NBS	WASSON,KEV DATA NORM BY THIS,NDG,
U	235	FISSION	EXPT-PROG	50+5	+6	ERDA-NDC-3	150	576	NBS	CARLSON+CS SHAPE MEAS,TBD NDG,
U	235	FISSION	EXPT-PROG	SPON		ERDA-NDC-3	152	576	NBS	HEATON+CF252 SOURCE,CFD ENDF,
U	235	FISSION	EXPT-PROG	SPON		ERDA-NDC-3	155	576	NBS	GILLIAM+CF252 SOURCE,RATIOS,TBL
U	235	FISSION	EXPT-PROG	NDG		ERDA-NDC-3	28	576	ANL	POENITZ+EVAL OF U235NF/LI6NT TBD,NDG
U	235	FISSION	EXPT-PROG	20-2	20+5	ERDA-NDC-3	190	576	ORL	GWIN+CS MEAS,CFD ENDF,ABST NSE59,NDG
U	235	FISSION	EXPT-PROG	20-2	20+5	ERDA-NDC-3	210	576	ORL	GWIN,NSE 59 CFD,ENDF,WESCOT G FACTOR
U	235	FISSION	EXPT-PROG	50+5	40+6	ERDA-NDC-3	27	576	ANL	MEADOWS+U234/U235,U236/U235 NF RATIO
U	235	FISSION	EXPT-PROG	NDG		ERDA-NDC-3	28	576	ANL	POENITZ,EVAL OF U235NF/LI6NA TBD,NDG
U	235	NUBAR,(NU)	EXPT-PROG	+6	25+7	ERDA-NDC-3	66	576	LRL	HOWE+PRELIMINARY RESULTS,GRPH,TBC
U	235	NUBAR,(NU)	EXPT-PROG	50-3	-1	ERDA-NDC-3	188	576	ORL	GWIN+NU E DEP,REL CF252,GRPH,CFD,TBC
U	235	F NEUT DELAY	EXPT-PROG	FAST		ERDA-NDC-3	300	576	WAU	ECCLESTON+GRPH NEAR EQUILIB SPEC,CFD
U	235	F NEUT DELAY	EXPT-PROG	FAST		ERDA-NDC-3	90	576	LAS	EVANS+E SPEC OF DELAYED NEUTS,GRPH,
U	235	SPECT FISS N	EVAL-PROG	MAXW		ERDA-NDC-3	159	576	NBS	GRUNDL+UPDATE 75 WASH CONF EVAL,
U	235	FISS PROD GS	EXPT-PROG	MAXW	FISS	ERDA-NDC-3	190	576	ORL	DICKENS+SPEC MEAS,TOT YLDS,CFD ENDF
U	235	FISS PROD GS	EXPT-PROG	MAXW	FISS	ERDA-NDC-3	190	576	ORL	DICKENS+SPEC MEAS,TOT YLDS,CFD ENDF
U	235	FISS YIELD	EXPT-PROG	MAXW	FISS	ERDA-NDC-3	157	576	NBS	GILLIAM+ZR,RU,TE,CS NFYS REL BA,
U	235	FISS YIELD	EXPT-PROG	25-2	14+7	ERDA-NDC-3	94	576	LAS	FORD+NFY COMPILATION,SEE LA-6129,NDG
U	235	FRAG SPECTRA	EXPT-PROG	NDG		ERDA-NDC-3	62	576	COL	LUERS+COINC ES MEAS CLARIFY DATA,TBD
U	235	FRAG SPECTRA	EXPT-PROG	27+5	97+5	ERDA-NDC-3	144	576	MHG	HSUE+2E,FISS FRAG,ANG DISTR,NDG,TBC,
U	235	RESON PARAMS	EXPT-PROG	52+0	49+1	ERDA-NDC-3	51	576	BNL	KOENE+PARITY ASSIGNMENTS PROPOSED,
U	235	RESON PARAMS	EXPT-PROG	11+0	20+2	ERDA-NDC-3	99	576	LAS	KEYWORTH+J ASSIGN TO 90EV,TBL,TBC,
U	236	FISSION	EXPT-PROG	50+5	40+6	ERDA-NDC-3	27	576	ANL	MEADOWS+REL U235,2,5MEV VAL GVN,
U	236	FISS YIELD	EXPT-PROG	25-2	14+7	ERDA-NDC-3	94	576	LAS	FORD+NFY COMPILATION,SEE LA-6129,NDG
U	238	TOTAL XSECT	EXPT-PROG		12+2	ERDA-NDC-3	43	576	BNL	CHRIEN+5 SAMPLES,TRNS,CS VS E GRPHS
U	238	TOTAL XSECT	THEO-PROG	10+4	50+6	ERDA-NDC-3	68	576	LRL	GARDNER+ STAT MDL CALC,CFD ENDF,NDG
U	238	TOTAL XSECT	EXPT-PROG	52-1	40+3	ERDA-NDC-3	202	576	ORL	OLSEN+TRNS,TOF,LINAC,CFD ENDF,NDG
U	238	TOTAL XSECT	EVAL-PROG	40+0	58+3	ERDA-NDC-3	209	576	ORL	DE+SAUSSURE+IMPROVE ENDF4 TOT CS,TBP
U	238	TOTAL XSECT	THEO-PROG	+3	10+7	ERDA-NDC-3	30	576	ANL	SMITH,TOT CS FROM OPTMDL,NDG
U	238	ELASTIC SCAT	THEO-PROG	10+4	50+6	ERDA-NDC-3	68	576	LRL	GARDNER+ STAT MDL CALC,CFD ENDF,NDG
U	238	DIFF ELASTIC	THEO-PROG	10+4	50+6	ERDA-NDC-3	68	576	LRL	GARDNER+ STAT MDL CALC,CFD ENDF,NDG
U	238	DIFF ELASTIC	THEO-PROG		+6	ERDA-NDC-3	30	576	ANL	SMITH,SCT DISTR FROM OPTMDL PARS,NDG
U	238	TOT INELASTI	THEO-PROG	10+4	50+6	ERDA-NDC-3	68	576	LRL	GARDNER+ STAT MDL CALC,CFD ENDF,NDG
U	238	DIFF INELAST	THEO-PROG	10+4	50+6	ERDA-NDC-3	68	576	LRL	GARDNER+ STAT MDL CALC,CFD ENDF,NDG

ELEMENT S A	QUANTITY	TYPE	ENERGY MIN	MAX	DOCUMENTATION REF VOL	PAGE	DATE	LAB	COMMENTS
U 238	DIFF INELAST	EXPT-PROG	10+5	30+6	ERDA-NDC-3	29	576	ANL	GUENTHER+NDG,DIN 3 ES,ENDF SET CS,
U 238	DIFF INELAST	THEO-PROG		+6	ERDA-NDC-3	30	576	ANL	SMITH,SCT DISTR FROM OPTMDL PARS,NDG
U 238	N, GAMMA	EXPT-PROG	40-1	12+2	ERDA-NDC-3	43	576	BNL	CHRIEN+CS GRPH TO 6.7EV,CFD CALC CS,
U 238	N, GAMMA	THEO-PROG	10+4	50+6	ERDA-NDC-3	68	576	LRL	GARDNER+ STAT MDL CALC,CFD ENDF,NDG
U 238	N, GAMMA	EXPT-PROG	24+4	18+5	ERDA-NDC-3	266	576	RPI	QUAN,REL B10,6ES,GRPH,TBL,CFD ENDF,
U 238	N, GAMMA	EXPT-PROG	NDG		ERDA-NDC-3	28	576	ANL	POENITZ,EVAL OF U238 NG CS UNDERWAY,
U 238	NXN REACTION	EXPT-PROG	14+7		ERDA-NDC-3	98	576	LAS	VEESER+EXPT TBD
U 238	FISSION	THEO-PROG	10+4	50+6	ERDA-NDC-3	68	576	LRL	GARDNER+ STAT MDL CALC,CFD ENDF,NDG
U 238	FISSION	EXPT-PROG	SPON		ERDA-NDC-3	155	576	NBS	GILLIAM+CF252 SOURCE,RATIO U235,TBL,
U 238	FISSION	EXPT-PROG	30+0	10+5	ERDA-NDC-3	256	576	RPI	SLOVACEK+GRPH,CALC THR CS=2.7+-,3)-6
U 238	FISSION	EXPT-PROG	60+2	20+6	ERDA-NDC-3	195	576	ORL	DIFILIPPO+SUBTR,AVG CS VAL,TBP ANS
U 238	FISSION	EXPT-PROG	60+2	10+6	ERDA-NDC-3	197	576	ORL	DIFILIPPO+SUBTR,NDG , 76 LOWELL CONF
U 238	RES INT FISS	EXPT-PROG	40-1	30+4	ERDA-NDC-3	256	576	RPI	SLOVACEK+CALC VAL=1,33+-,15MB,
U 238	F NEUT DELAY	EXPT-PROG	FAST		ERDA-NDC-3	306	576	WAU	ECCLESTON+NEAR EQUILIBRIA SPEC NDG
U 238	F NEUT DELAY	EXPT-PROG	FAST		ERDA-NDC-3	90	576	LAS	EVANS+E SPEC OF DELAYED NEUTS,GRPH,
U 238	F NEUT DELAY	EXPT-PROG	25+6	50+6	ERDA-NDC-3	28	576	ANL	MEADOWS,NO E DEP.PU241/U238 AVG GVN,
U 238	FISS YIELD	EXPT-PROG	25-2	14+7	ERDA-NDC-3	94	576	LAS	FORD+NFY COMPILATION,SEE LA-6129,NDG
U 238	RESON PARAMS	EXPT-PROG	67+0	12+2	ERDA-NDC-3	43	576	BNL	CHRIEN+WN,WG FROM AREA,ANAL,TBL,GRPH
U 238	RESON PARAMS	EXPT-PROG	67+0	27+1	ERDA-NDC-3	256	576	RPI	SLOVACEK+FW MEAS AT 4 RES ES,
U 238	RESON PARAMS	EXPT-PROG	+1	30+3	ERDA-NDC-3	268	576	RPI	KOBAYASHI+T DEP SELF INDIC MEAS,NDG
U 238	RESON PARAMS	EXPT-PROG	60+2	20+6	ERDA-NDC-3	195	576	ORL	DIFILIPPO+SUBTR,LVL SPAC,WF, TBP ANS
U 238	RESON PARAMS	EXPT-PROG	60+2	10+6	ERDA-NDC-3	197	576	ORL	DIFILIPPO+SUBTR,NDG , 76 LOWELL CONF
U 238	RESON PARAMS	EXPT-PROG	14+3	27+3	ERDA-NDC-3	202	576	ORL	OLSEN+TRNS,WN FROM AREA ANAL,NDG
U 238	RESON PARAMS	EXPT-PROG	67+0	37+1	ERDA-NDC-3	202	576	ORL	OLSEN+3ES,WN,WG,CFD ENDF,TBL,TBP ANS
NP 237	FISSION	EXPT-PROG	SPON		ERDA-NDC-3	155	576	NBS	GILLIAM+CF252 SOURCE,RATIO U235,TBL,
NP 237	FISS YIELD	EXPT-PROG	25-2	14+7	ERDA-NDC-3	94	576	LAS	FORD+NFY COMPILATION,SEE LA-6129,NDG
PU 239	EVALUATION	EVAL-PROG	NDG		ERDA-NDC-3	120	576	LAS	FOSTER+TIME DEP SPEC FROM 1NANO SEC
PU 239	ABSORPTION	EXPT-PROG	20-2	20+5	ERDA-NDC-3	190	576	ORL	GWIN+CFD ENDF,NDG,ABST NSE 59,
PU 239	ABSORPTION	EXPT-PROG	20-2	20+5	ERDA-NDC-3	210	576	ORL	GWIN,NSE 59 CFD,ENDF,WESCOT G FACTOR
PU 239	N, GAMMA	EXPT-PROG	20-2	20+5	ERDA-NDC-3	190	576	ORL	GWIN+CS MEAS,CFD ENDF,ABST NSE59,NDG
PU 239	N, GAMMA	EXPT-PROG	20-2	20+5	ERDA-NDC-3	210	576	ORL	GWIN,NSE 59 CFD,ENDF,WESCOT G FACTOR
PU 239	FISSION	EXPT-PROG	10+3	30+7	ERDA-NDC-3	65	576	LRL	BEHRENS+PU239/U235 CS RATIO MEAS,NDG
PU 239	FISSION	EXPT-PROG	10+1	70+4	ERDA-NDC-3	66	576	LRL	CZIRR+TOF,CS REL LI6,ANAL TBD,NDG
PU 239	FISSION	EXPT-PROG	14+5	96+5	ERDA-NDC-3	141	576	HHG	DAVIS+RE-EVAL ANS 22+NEW 770KEV DATA
PU 239	FISSION	EXPT-PROG	SPON		ERDA-NDC-3	142	576	HHG	DAVIS+CF252 SPON SPEC,CS MEAS,NDG,

ELEMENT S A	QUANTITY	TYPE	ENERGY MIN	MAX	DOCUMENTATION REF	VOL	PAGE	DATE	LAB	COMMENTS
PU 239	FISSION	EXPT-PROG	SPON		ERDA-NDC	3	155	576	NBS	GILLIAM+CF252 SOURCE,RATIO U235,TBL,
PU 239	FISSION	EXPT-PROG	20-2	20+5	ERDA-NDC	3	190	576	ORL	GWIN+CS MEAS,CFD ENDF,ABST NSE59,NDG
PU 239	FISSION	EXPT-PROG	20-2	20+5	ERDA-NDC	3	210	576	ORL	GWIN,NSE 59 CFD,ENDF,WESCOT G FACTOR
PU 239	ALPHA	EXPT-PROG	20-2	20+5	ERDA-NDC	3	190	576	ORL	GWIN+CFD,ENDF,NDG,ABST NSE 59,
PU 239	NUBAR,(NU)	EXPT-PROG	50-3	-1	ERDA-NDC	3	188	576	ORL	GWIN+NU E DEP,REL CF252,GRPH,CFD TBC
PU 239	NUBAR,(NU)	EXPT-PROG		80+6	ERDA-NDC	3	188	576	ORL	GWIN+NU E DEP,REL CF252,GRPH,TBC
PU 239	F NEUT DELAY	EXPT-PROG	FAST		ERDA-NDC	3	406	576	WAU	ECCLESTON+NEAR EQUILIBRIA SPEC NDG
PU 239	F NEUT DELAY	EXPT-PROG	FAST		ERDA-NDC	3	90	576	LAS	EVANS+E SPEC OF DELAYED NEUTS,GRPH,
PU 239	FISS YIELD	EXPT-PROG	25-2	14+7	ERDA-NDC	3	94	576	LAS	FORD+NEY COMPILATION,SEE LA-6129,NDG
PU 239	FRAG SPECTRA	EXPT-PROG	27+5	97+5	ERDA-NDC	3	144	576	MHG	HSUE+2E,FISS FRAG,ANG DISTR,NDG,TBC,
PU 240	SPECT N,GAMM	EXPT-PROG	10+2	24+4	ERDA-NDC	3	51	576	BNL	BLOCK+EXCITATION ES DET
PU 240	FISSION	EXPT-PROG	10+3	30+7	ERDA-NDC	3	65	576	LRL	BEHRENS+PU240/U235 CS RATIO MEAS,NDG
PU 240	FISSION	EXPT-PROG	50+2	10+4	ERDA-NDC	3	194	576	ORL	AUCHAMPAUGH+SUBTR FISS,NDG,TBP PR/C
PU 240	RESON PARAMS	EXPT-PROG	10+2	24+4	ERDA-NDC	3	51	576	BNL	BLOCK+WG DET REL TO AU197 WID,NDG
PU 240	RESON PARAMS	EXPT-PROG	50+2	10+4	ERDA-NDC	3	194	576	ORL	AUCHAMPAUGH+SUBTR FISS,WF,LVL SPAC,
PU 241	FISSION	EXPT-PROG	10+3	30+7	ERDA-NDC	3	65	576	LRL	BEHRENS+PU241/U235 CS RATIO MEAS,NDG
PU 241	FISSION	EXPT-PROG	10+1	70+4	ERDA-NDC	3	66	576	LRL	CZIRR+TOF,CS REL LI6,ANAL TBD,NDG
PU 241	F NEUT DELAY	EXPT-PROG	15+5	50+6	ERDA-NDC	3	28	576	ANL	MEADOWS,NO E DEP,PU241/U238 AVG GVN,
PU 242	SPECT N,GAMM	EXPT-PROG	NDG		ERDA-NDC	3	54	576	BNL	CASTEN+PU243 LVLS FROM NG,DP,DT,NDG
PU 242	FISSION	EXPT-PROG	10+3	30+7	ERDA-NDC	3	65	576	LRL	BEHRENS+PU242/U235 CS RATIO MEAS,NDG
AM 241	ABSORPTION	EXPT-PROG	10-2	37+5	ERDA-NDC	3	198	576	ORL	WESTON+GRPHS,AVG CS VS E,CFD ENDF,
AM 241	RESON PARAMS	EXPT-PROG		50+1	ERDA-NDC	3	198	576	ORL	WESTON+RES PARS DRVD,NDG,TBP NSE,
CM 243	FISSION	EXPT-PROG	NDG		ERDA-NDC	3	201	576	ORL	DABBS+CS MEAS TBD,ABST 76LOWELL CONF
CM 243	FISSION	EXPT-PROG	15+1	30+6	ERDA-NDC	3	95	576	LAS	SILBERT,TOF,MEV CS GVN,SEE LA-6239
CM 243	RESON PARAMS	EXPT-PROG	15+0	80+1	ERDA-NDC	3	95	576	LAS	SILBERT,WF=225MEV,D=.85+-.09EV,TBC
CM 243	STRNGTH FUNC	EXPT-PROG	15+0	80+1	ERDA-NDC	3	95	576	LAS	SILBERT,S0=(1.04+-.30)-4,ANAL TBC,
CM 245	FISSION	EXPT-PROG	60-3	20+1	ERDA-NDC	3	66	576	LRL	BROWNE+CS DATA,ANAL TBD,NDG
CM 245	FISSION	EXPT-PROG	NDG		ERDA-NDC	3	201	576	ORL	DABBS+CS MEAS TBD,ABST 76LOWELL CONF
BK 249	TOTAL XSECT	EXPT-PROG	50-3	10+5	ERDA-NDC	3	201	576	ORL	HARVEY+CS MEAS,TO DRV ABS CS,NDG
BK 249	ABSORPTION	EXPT-PROG	NDG		ERDA-NDC	3	201	576	ORL	HARVEY+ABS CS DRVD FROM TOT MEAS,NDG
BK 249	RESON PARAMS	EXPT-PROG	50-3	10+5	ERDA-NDC	3	201	576	ORL	HARVEY+LVL SPACING TO 20EV,PARS,TBD,
CF 249	ABSORPTION	EXPT-PROG	NDG		ERDA-NDC	3	201	576	ORL	HARVEY+NDG,THR VAL TBD,
CF 249	RESON PARAMS	EXPT-PROG	NDG		ERDA-NDC	3	201	576	ORL	HARVEY+NDG,RES PARS TBD,
CF 250	NUBAR,(NU)	EXPT-PROG	SPON		ERDA-NDC	3	93	576	LAS	VEESER+LIQ SCINT,NU MEAS,NDG
CF 252	ETA	EXPT-PROG	NDG		ERDA-NDC	3	15	576	ANC	SMITH+SUGGEST RAISE NU BY .2PC,

ELEMENT S A	QUANTITY	TYPE	ENERGY MIN MAX	DOCUMENTATION REF VOL PAGE DATE	LAB	COMMENTS
CF 252	NUBAR,(NU)	EXPT-PROG	SPON	ERDA-NDC-3 144 576	MHG	BOZORGMANES+ANAL TBD.NDG,
CF 252	NUBAR,(NU)	EXPT-PROG	SPON	ERDA-NDC-3 187 576	ORL	SPENCER,MEAS OF NU TBD,NDG,
CF 252	NUBAR,(NU)	EXPT-PROG	SPON	ERDA-NDC-3 93 576	LAS	VEESER+LIQ SCINT.NU MEAS,NDG
CF 252	NUBAR,(NU)	EXPT-PROG	NDG	ERDA-NDC-3 15 576	ANC	SMITH+SUGGEST RAISE NU BY .2PC,
CF 252	SPECT FISS N	EVAL-PROG	SPON	ERDA-NDC-3 159 576	NBS	GRUNDL+UPDATE 75 WASH CONF EVAL,
FM 256	NUBAR,(NU)	EXPT-PROG	SPON	ERDA-NDC-3 93 576	LAS	VEESER+LIQ SCINT.NU MEAS,NDG
FM 257	NUBAR,(NU)	EXPT-PROG	SPON	ERDA-NDC-3 93 576	LAS	VEESER+LIQ SCINT,TBD

IDAHO NATIONAL ENGINEERING LABORATORY
IDAHO FALLS, IDAHO

A. DATA COMPILATION AND EVALUATION ACTIVITIES

1. Re-evaluation of Precise Gamma-Ray Energies for Energy-Calibration Standards for Ge(Li) Spectrometers: (R. G. Helmer, R. C. Greenwood, R. J. Gehrke)

A set of previously reported gamma-ray energies, from 45 to 1300 keV, that are useful for calibration of Ge(Li) spectrometers has been re-evaluated. These results have been re-evaluated so that they correspond to the 1973 adjusted values of the fundamental constants of Cohen and Taylor[3] instead of the 1969 set of Taylor *et al*.[4] used previously. In addition, we have included in the re-evaluation the results of several recent curved-crystal diffraction spectrometer measurements. These measurements[5-9] provide energies of gamma rays from the decay of ^{51}Cr, ^{57}Co, ^{137}Cs, ^{170}Tm, ^{182}Ta, ^{183}Ta, ^{192}Ir, ^{198}Au and ^{203}Hg.

The results of this re-evaluation provide the energies of 138 gamma rays from 38 isotopes. All of these energies are traceable either to the energy scale based on the energy of the W K_{α_1} x-ray or to that based on the rest mass of the electron, m_0c^2. The[1] uncertainty in the energy of a 1-MeV gamma ray is typically 18 eV. Of this error, 17 ppm comes from the uncertainty in the energy of the 411-keV line from the decay of ^{198}Au which is, in practice, the basis for the m_0c^2 energy scale. Relative to the energy of this 411-keV line, many 1-MeV energies are now known with an error of only 4 eV compared to the 14 eV in our previous evaluation[2].

---

[1] R. C. Greenwood, R. G. Helmer and R. J. Gehrke, Nucl. Instr. and Meth 77 (1970) 141.

[2] R. G. Helmer, R. C. Greenwood and R. J. Gehrke, Nucl. Instr. and Meth. 96 (1971) 173.

[3] E. R. Cohen and B. N. Taylor, J. Phys. Chem. Ref. Data 2 (1973) 663.

[4] B. N. Taylor, W. H. Parker and D. N. Langenberg, Rev. Mod. Phys. 41 (1969) 375.

[5] O. Piller, W. Beer and J. Kern, Nucl. Instr. and Meth. 107 (1973) 61.

[7] G. L. Borchert, W. Scheck and O. W. B. Schult, Nucl. Instr. and Meth. 124 (1975) 107.

[8] G. L. Borchert, W. Scheck and K. P. Wieder, Z. Naturforsch. 30a (1975) 274.

[9] G. L. Borchert, Priv. com. (1975).

2. Evaluated Decay Scheme Data for Use in the ILRR Program (R. G. Helmer)

The decay scheme parameters of a number of radioactive nuclides have been evaluated to provide an up-to-date set of "best" values. The isotopes involved include a number of interest for neutron dosimetry as well as a number of fission products. These decay-scheme parameters have been evaluated specifically for use in the ILRR (Interlaboratory LMFBR Reaction Rate) program, although they will be incorporated into other special purpose data files as well. In the ILRR program the absolute gamma-ray intensities (or branching ratios) and half-lives of these isotopes are used to determine the rates of various (n,2n),(n,p), (n,n$^{\prime}$) and (n, fission) reactions.

Table A-2-1 gives the evaluated results for the half-lives and for the energies and absolute intensities of one or two prominent gamma rays for each isotope. Although the intensities of the other gamma rays (and the beta rays) in a decay scheme are not needed for most applications, they have been evaluated and will be included in our laboratory decay-data file. This evaluation includes the references that were available through about June 1975. Except for the gamma-ray energies, these results represent an evaluation in the sense of averaging the available results and do not represent simply a selection of a single "best" value from among several measurements.

TABLE A-2-1

SUMMARY OF ILRR DECAY-SCHEME PARAMETERS

Isotope	Half-life	E_γ (keV)	I_γ (%)
^{24}Na	15.00(2) h	1368.599(29) 2753.965(56)	99.993(2) 99.873(6)
^{27}Mg	9.462(12) m	843.75(3) 1014.44(4)	71.7(5) 28.3(5)
^{46}Sc	83.9(3) d	889.253(16) 1120.521(19)	99.984(6) 99.987(6)
^{47}Sc	3.40(3) d	159.381(15)	69.0(25)
^{48}Sc	43.8(1) h	983.4(2) 1037.4(2) 1311.8(4)	99.987(2) 97.5(3) 99.992(2)
^{51}Cr	27.700(10) d	320.076(5)	9.83(14)
^{54}Mn	312.5(5) d	834.827(21)	99.97(2)
^{58}Co	70.85(15) d	810.753(20)	99.44(1)
^{59}Fe	44.6(1) d	1099.228(19) 1291.568(23)	56.1(10) 43.6(10)
^{60}Co	5.271(2) y	1173.208(20) 1332.464(28)	99.86(2) 99.980(3)
^{64}Cu	12.702(4) h	511.00 [a]	38.(2)
^{95}Zr	64.1(3) d	724.179(13) 756.710(18)	44.1(5) 54.6(5)
^{97}Zr	16.88(6) h	743.3(1)	92.9(3)
^{103}Ru	39.43(10) d	497.08(1)	89.(1)
^{106}Ru	368.2(12) d		
^{106}Rh	30.0(2) s [d]	511.8(2)	20.5(2) [b]

TABLE A-2-1 (Cont'd)

SUMMARY OF ILRR DECAY-SCHEME PARAMETERS

Isotope	Half-life	E_γ (keV)	I_γ (%)
^{115m}In	4.486(4) h	336.23(5)	45.9(1)
^{116m}In	54.2(1) m	1293.54(15)	84.8(5)
^{132}Te	77.9(5) h	228.16(6)	89.(5)
^{137}Cs	30.03(15) y	661.647(12)	85.3(4)
^{140}Ba	12.789(6) d	537.35(5)	24.4(3)
^{140}La	40.26(2) h [c,d]	1596.18(5)	95.40(8)
^{141}Ce	32.50(7) d	145.440(3)	49.(2)
^{143}Ce	33.0(2) h	293.26(2)	47.(4)
^{144}Ce	284.4(4) d	133.53(3)	11.0(2)
^{144}Pr	17.28(5) m [d]	696.49(2) 1489.15(5) 3185.70(6)	1.342(13) 0.279(3) 0.700(10)
^{196}Au	6.1(1) d	355.73(5)	87.7(20)
^{198}Au	2.6956(10) d	411.794(7)	95.52(5)
^{239}Np	2.355(4) d	277.60(3)	14.3(2)

---

[a] This is the value of the electron rest mass, m_0c^2. The observed annihilation photon energy may be lower.

[b] There may be some experimental problems due to the presence of 511.0-keV photons from positron annihilation.

[c] In equilibrium the ratio of the ^{140}La to ^{140}Ba activities is $T_{\frac{1}{2}}(Ba)/\left[T_{\frac{1}{2}}(Ba) - T_{\frac{1}{2}}(La)\right] = 1.15097(12)$.

[d] These isotopes will normally occur with the parent half-life.

B. NUCLEAR LEVEL-SCHEMES STUDIES

1. Gamma-Ray Emission from ^{134}Ce and the Level Scheme of ^{134}La. (R. C. Greenwood, R. J. Gehrke, R. G. Helmer, C. W. Reich and J. D. Baker)

Prior to the present investigation, no information existed concerning excited states in ^{134}La. Although ^{134}Ce ($T_{1/2}$ = 75.9 h) decays to ^{134}La, no γ radiation had previously been reported to be associated with its decay. Furthermore, values of 120^{+60}_{-20} and 110^{+90}_{-30} keV, respectively, have been reported[1,2] for the decay energy of ^{134}Ce. The study of the ^{134}Ce decay is made difficult by the short half-life (6.67 min), large decay energy (3720 keV) and the resulting complexity of the ^{134}La γ-ray spectrum. In view of the short half-life of ^{134}La, it has generally proven convenient to study the ^{134}La decay scheme by using as a source the ^{134}La in equilibrium with its ^{134}Ce parent. This procedure, together with the reported low Q-value for the ^{134}Ce decay and the reported absence of γ radiation in the ^{134}Ce decay, has led to the assignment of several low-energy ($\lesssim$ 0.3 MeV) γ rays to the ^{134}La decay in the recent A = 134 mass-chain evaluation[3]. However, in the present study we have been able to associate for the first time a number of γ-ray transitions, ranging in energy up to $\sim$ 355 keV, with the ^{134}Ce decay. This result indicates that the previously reported values[1,2] for the ^{134}Ce decay energy are incorrect and that the three low-energy (< 0.3 MeV) γ rays reported[3] in the ^{134}La decay in fact are associated with the decay of ^{134}Ce.

The ^{134}Ce-^{134}La activities were produced by 800-MeV proton bombardment of Pr-metal foils in LAMPF. Typical bombardments involved an integrated beam current of $\sim$ 10-15 μA-h. Following the bombardment, the irradiated Pr was shipped to the INEL, where the Ce fraction was extracted and isotope separation was performed to obtain the mass-134 fraction. The resultant ^{134}Ce-^{134}La source material was loaded onto a HDEHP column and the ^{134}La daughter was continuously eluted from the ^{134}Ce. Removal of the ^{134}La daughter provided increased sensitivity for the detection of low-energy ($\lesssim$ 0.5 MeV) γ rays.

A typical γ-ray spectrum of the ^{134}Ce "column" source is given in Fig. B-1-1. The presence of these γ rays in the "Ce-enhanced" γ-ray spectra and their absence (at least for the stronger transitions) in spectra from ^{134}La (with the ^{134}Ce removed) establish that they are in fact associated with the Ce decay rather than with the ^{134}La decay. Analysis of this and similar spectra has established the existence of some 32 γ rays in the decay of ^{134}Ce. Extensive γ-γ coincidence measurements have been made on the Ce-enhanced sources. These results have been analyzed to prepare an energy-level scheme for the ^{134}La levels excited in the ^{134}Ce decay. The ^{134}Ce decay scheme proposed from these data is shown in Fig. B-1-2.

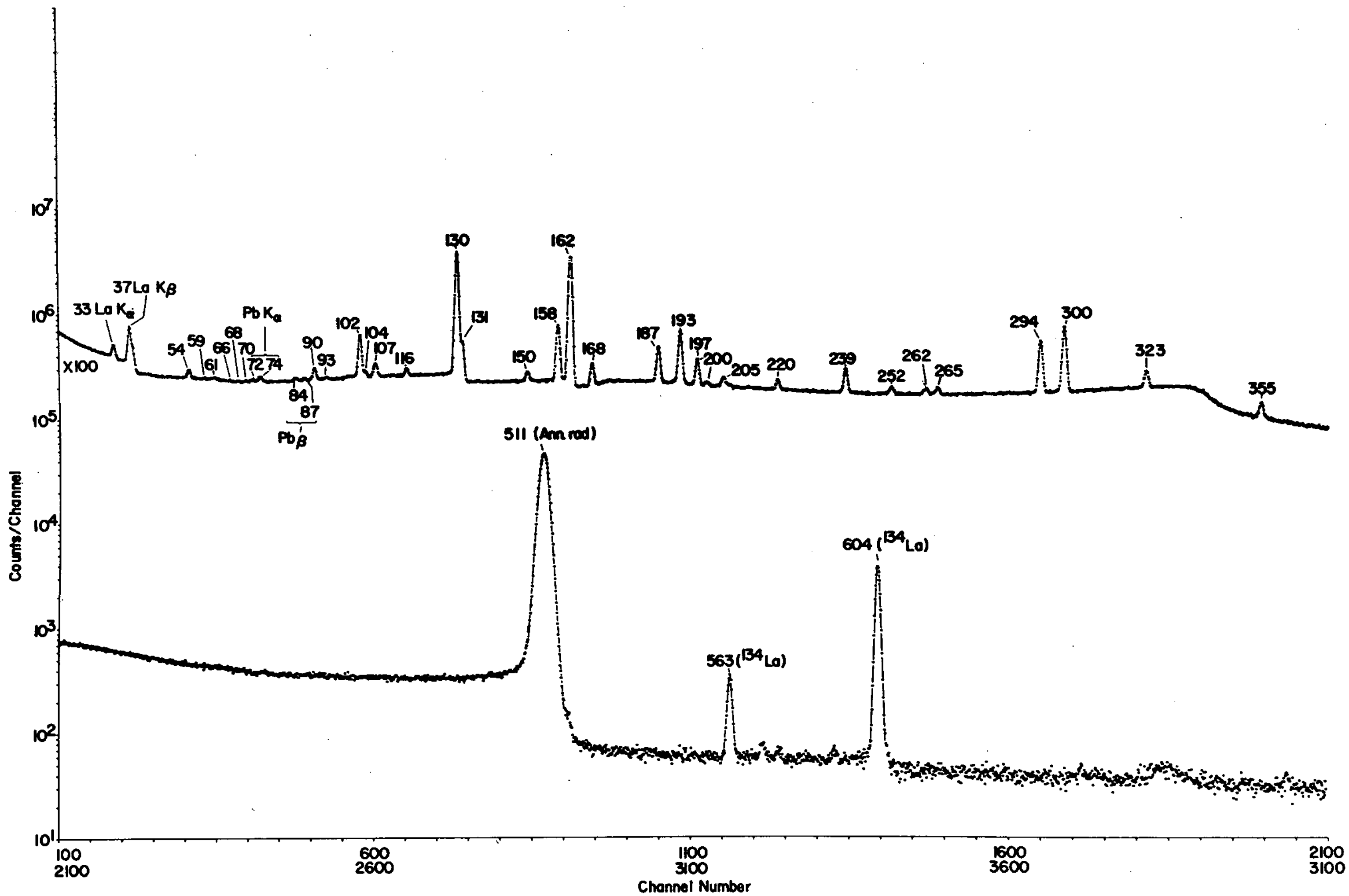

Fig. B-1-1. Gamma-ray spectrum of the ^{134}Ce activity in the separation column measured with a 42-cm^3 coaxial Ge(Li) detector. The ^{134}Ce-to-^{134}La enhancement, relative to the equilibrium source condition, is $\sim$ 41 in this spectrum.

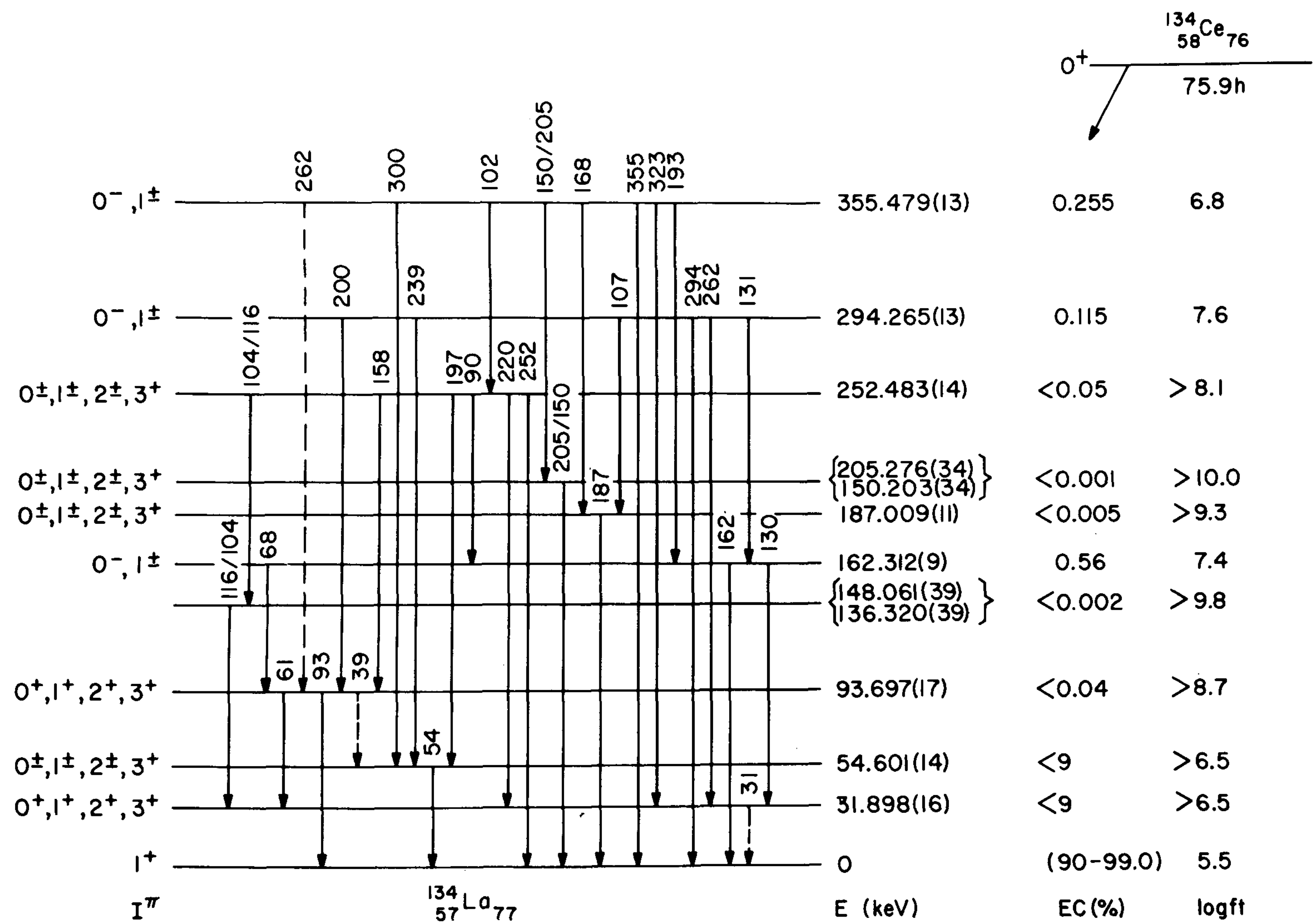

Fig. B-1-2. Proposed decay scheme for ^{134}Ce.

[1] E. I. Biryukov, V. T. Novikov and N. S. Shimanskaya, Izv. Akad. Nauk SSSR, Ser. Fiz. 29 (1965) 151; Bull. Acad. Sci. USSR, Phys. Ser. 29 (1966) 148.

[2] V. S. Aleksandrov, V. S. Buttsev, T. Vylov, K. Ya Gromov and V. G. Kalinnikov, Izv. Akad.Sci. SSSR, Ser. Fiz. 37 (1973) 948; Bull. Acad. Sci. USSR, Phys. Ser. 37, No. 5 (1974) 34.

[3] E. A. Henry, Nuclear Data Sheets 15, No. 2 (1975) 203.

2. Decay of ^{131}Ba
(R. J. Gehrke, R. G. Helmer, C. W. Reich, R. C. Greenwood, R. A. Anderl).

The decay of 11.7-d ^{131}Ba has been studied with Ge(Li) spectrometers. The ^{131}Ba activity was produced by bombarding Pr-metal foils with ∿ 800-MeV protons in LAMPF. Following bombardment, the irradiated Pr foils were shipped to INEL, were chemical and isotope separations were carried out to produce carrier-free samples of ^{131}Ba. Gamma-ray singles and extensive gamma-gamma coincidence measurements were carried out using a variety of Ge(Li) spectrometer systems. The decay scheme for ^{131}Ba proposed from our studies is shown in Fig. B-2-1.

As a result of the present investigation previously unreported levels in ^{131}Cs have been identified at 919, 1170 and 1341 keV. These levels are based on the placement of previously unreported γ rays of 128, 546, 703, 795, 919, 1046, 1126, 1170, 1208 and 1341 keV and on previously reported[1] but unplaced γ rays at 797 and 954 keV. The γ-ray spectra in coincidence with the 216-keV and 373-keV gates indicate that the 546- and 954-keV γ rays decay from the 919-keV level, the 797- and 954-keV γ rays come from a 1170-keV level and the 1126-keV γ ray decays from the 1341-keV level. A newly reported γ ray at 369 keV feeding the 216-keV level from the 585-keV level has been placed in the decay scheme on the basis of coincidence information and its energy. Gamma rays at 128, 550, 795, 1170, 1208 and 1341 keV were placed in the level scheme on the basis of their energy. Possible peaks at 334 and 585 keV were observed in the γ-ray spectrum in coincidence with the 585-keV gate and are tentatively placed feeding the 585-keV level. The γ ray at 563 keV which was previously reported by Kučarova et al.[2] but not placed by them has been confirmed and placed in the proposed decay scheme on the basis of coincidence information. The existence of reported γ rays at 323[3] and 508[2] keV could not be verified. The results of the coincidence measurements of the present experiment are indicated in the level scheme by dots at the heads of the γ-ray transition symbols. These dots indicate the γ rays entering the level which are in coincidence with the ground-state transition.

The intensities of the electron-capture branches were determined from the intensity balances of the transitions populating and depopulating each of the ^{131}Cs levels. The multipolarities were taken from Horen et al.[4] and were used to determine the conversion coeffiecients. Where no definitive multipolarity assignments were reported by them, we used their relative electron intensities and our relative γ-ray intensities to determine the conversion coefficients. The sum of the relative electron intensities of the $K + L_1 + L_2 + L_3$ shells[2] associated with the 123-keV γ ray were normalized to a 95% E2 + 5% M1 multipolarity.

The only reported measurement of the Q-value of the ^{131}Ba decay is 1165±15 keV[5]. However, in their 1971 Atomic Mass Evaluation, Wapstra and Gove[6] point out that this value is ∿ 200 keV lower than that computed from the other mass-related information. Our observation of the 1341-keV state clearly indicates that the Q-value must be at least this large and thus sets a lower limit on it. To obtain a value for this decay energy, we have measured the electron-capture to positron intensity to the 216-keV level, this ratio being quite sensitive to transition energy in this energy region. This was done by looking for 511-keV annihilation radiation in the spectrum of γ radiation in coincidence with the 216-keV γ ray. From the intensity of the 511-keV photons in this spectrum, we deduce a value of $(4.7\pm2.3) \times 10^4$ for the e.c./β^+ ratio for this transition. From the tables of Gove and Martin[7], this corresponds to a β^+ endpoint energy (for an allowed transition) of 134^{+10}_{-20} keV. This gives a Q-value for the ^{131}Ba decay of 1372^{+10}_{-20} keV.* This value was used in computing the log ft values given in the decay scheme.

At present, the features of the ^{131}Cs level scheme deduced from these data are being compared with the predictions of a quasiparticle-phonon coupling model. These model calculations have been carried out by G. J. Mathews[8] of the University of Maryland.

---

* Recent work by Firestone et al. [Phys. Rev. Letters 35 (1975) 713] suggests that in some cases the theoretical and experimental e.c./β^+ ratios disagree and hence that, in these cases, the deduced Q-values may be in error.

1 L. Hasselgren, S. Antman, H. S. Sahota and J. E. Thun, Nucl. Phys. A153 (1970) 625.

2 T. Kučarova, B. Kracik and V. Zvolska, Soviet Journal of Nuclear Physics (a translation of Yadernaya Fizika) 7 (1968) 433.

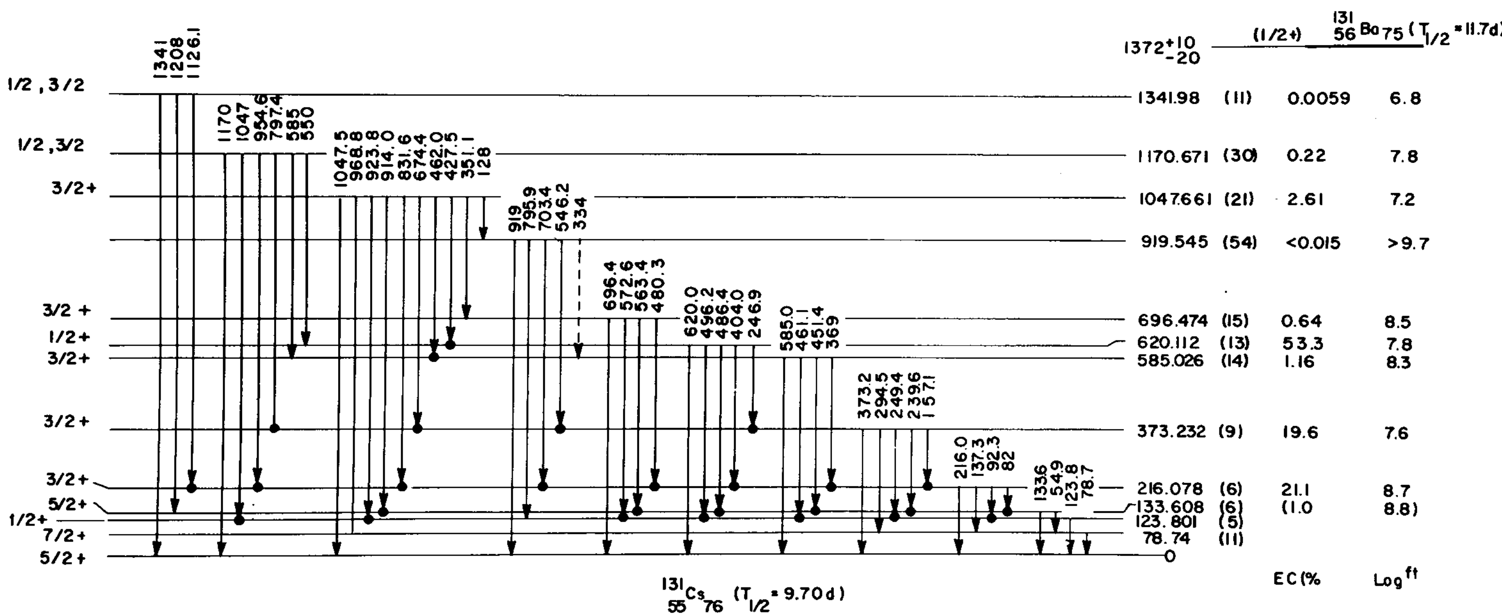

Fig. B-2-1. Decay scheme of ^{131}Ba.

[3] K. Karlsson, Arkiv För Fysik 33 (1966) 47.

[4] D. J. Horen, J. M. Hollander and R. L. Graham, Phys. Rev 135 (1964)B301.

[5] B. L. Robinson, Bull. Am. Phys. Soc. 7 (1962) 541.

[6] A. H. Wapstra and N. B. Gove, Nuclear Data Tables A9 (1971) Nos. 4 and 5.

[7] N. B. Gove and M. J. Martin, Nucl. Data Tables A10 (1971).

[8] G. J. Mathews, private communication.

3. Decay of ^{128}Ba
(R. G. Helmer, R. J. Gehrke, R. C. Greenwood, C. W. Reich, L. D. McIsaac)

The following is the abstract of a paper which has been accepted for publication in Nuclear Physics A. The decay scheme which has been proposed from this study is shown in Fig. B-3-1.

Samples of ^{128}Ba have been produced by $\approx$ 800 MeV proton-induced spallation in praseodymium metal foils at LAMPF. Chemical purification and isotope separation have been performed to produce pure samples of ^{128}Ba(2.4 d)-^{128}Cs(3.9 min). Some of the γ-ray and γ-γ coincidence measurements were made during continuous Ba-Cs separations which increased the Ba/Cs ratio by factors of between two and six from that at secular equilibrium. These measurements improved the sensitivity for detecting weak transitions from the ^{128}Ba decay and allowed isotopic assignment of several γ rays. From the experimental results, twelve γ-ray transitions have been assigned to the ^{128}Ba decay, compared to only one previously, and they have all been placed in a level scheme with excited states in ^{128}Cs at 187, 215, 229, 273, 317, 359 and 374 keV. By comparison with the daughter decay, absolute γ-ray intensities are determined.

4. Features of the Low-Energy Level Scheme of ^{229}Th as Observed in the α-Decay of ^{233}U: (L. A. Kroger, C. W. Reich)

The following is the abstract of a paper which has been accepted for publication in Nuclear Physics A. This paper describes work carried out by Dr. Kroger in partial fulfillment of the requirements for the Ph.D. degree at the University of Wyoming, Laramie, Wyoming. The decay scheme proposed from this work is shown in fig. B-4-1.

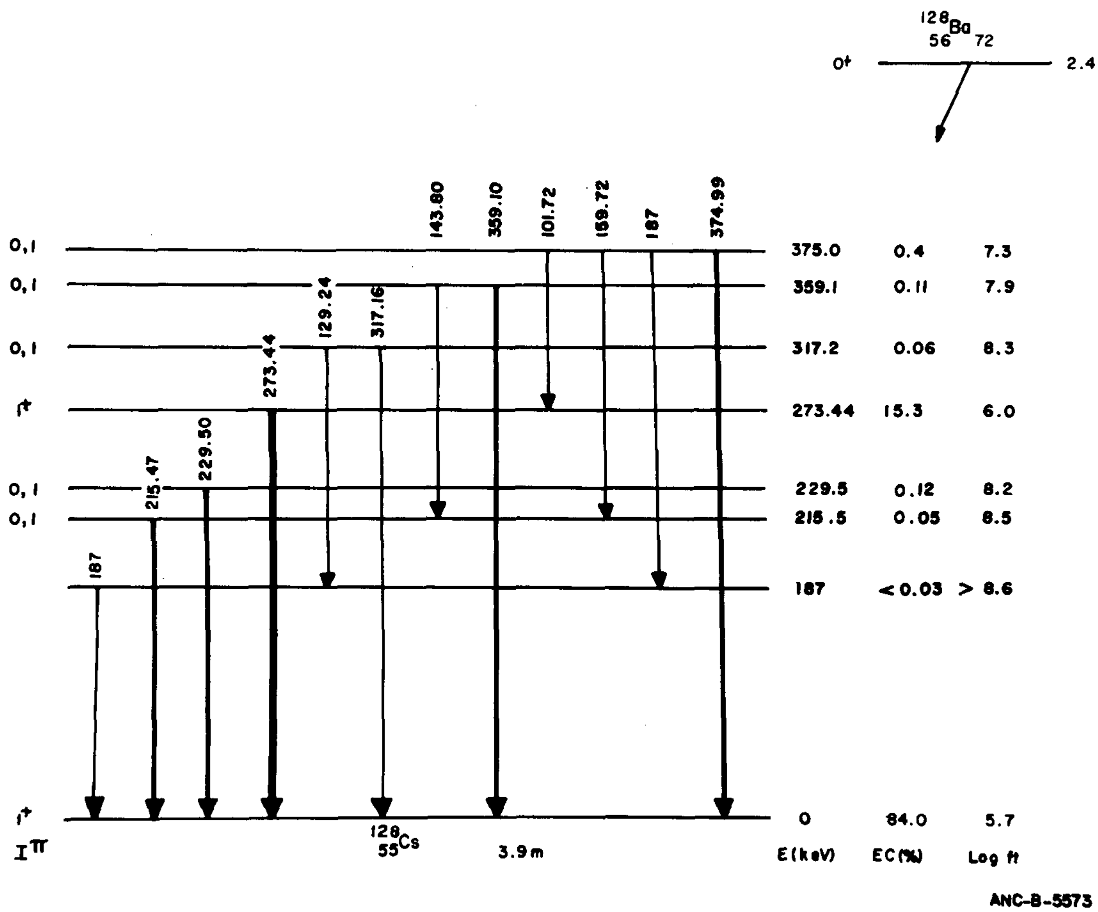

Fig. B-3-1 Proposed decay scheme of ^{128}Ba. The electron-capture intensities have been computed assuming the γ transitions all have M1 character. The log ft values are for a decay energy of 700 keV.

The γ radiation emitted following the α-particle decay of ^{233}U has been studied using a variety of Ge(Li) spectrometers and a Si(Li) spectrometer system. Analysis of γ-singles and γ-γ coincidence measurements has established the existence of 91 γ rays which can be definitely established as representing transitions in ^{229}Th. From these data, a level scheme consisting of 28 excited states below $\approx$ 0.53 MeV in ^{229}Th is proposed. The well known state at 29.16 keV is shown to have $I^{\pi} = 5/2^{+}$, in contrast with several previous proposals. Additional states which are shown to be members of the rotational band associated with this state are the following (with the assigned I^{π} values in parentheses): 71.82($7/2^{+}$); 125.45($9/2^{+}$); and 195.76 keV ($11/2^{+}$). Evidence is presented which indicates that these four states are members of a $K^{\pi} = 3/2^{+}$ rotational band, built on the Nilsson orbital $3/2^{+}$[631]. The $I^{\pi} = 3/2^{+}$ band head is shown from indirect evidence to lie within $\approx$ 0.1 keV of the $5/2^{+}$[633] ground state of ^{229}Th. Seven negative-parity states are proposed to lie between $\approx$ 146 keV and $\approx$ 237 keV; and their energies can be well described in terms of Coriolis coupling among the j15/2-related Nilsson states 3/2-[761], 5/2-[752], 1/2-[770]and 7/2-[743]. Evidence is presented which strongly suggests that a signficant component of the K^{π} = 3/2- octupole-vibrational state {$3/2^{+}$ [631], 0-}is present in these low-lying negative-parity states.

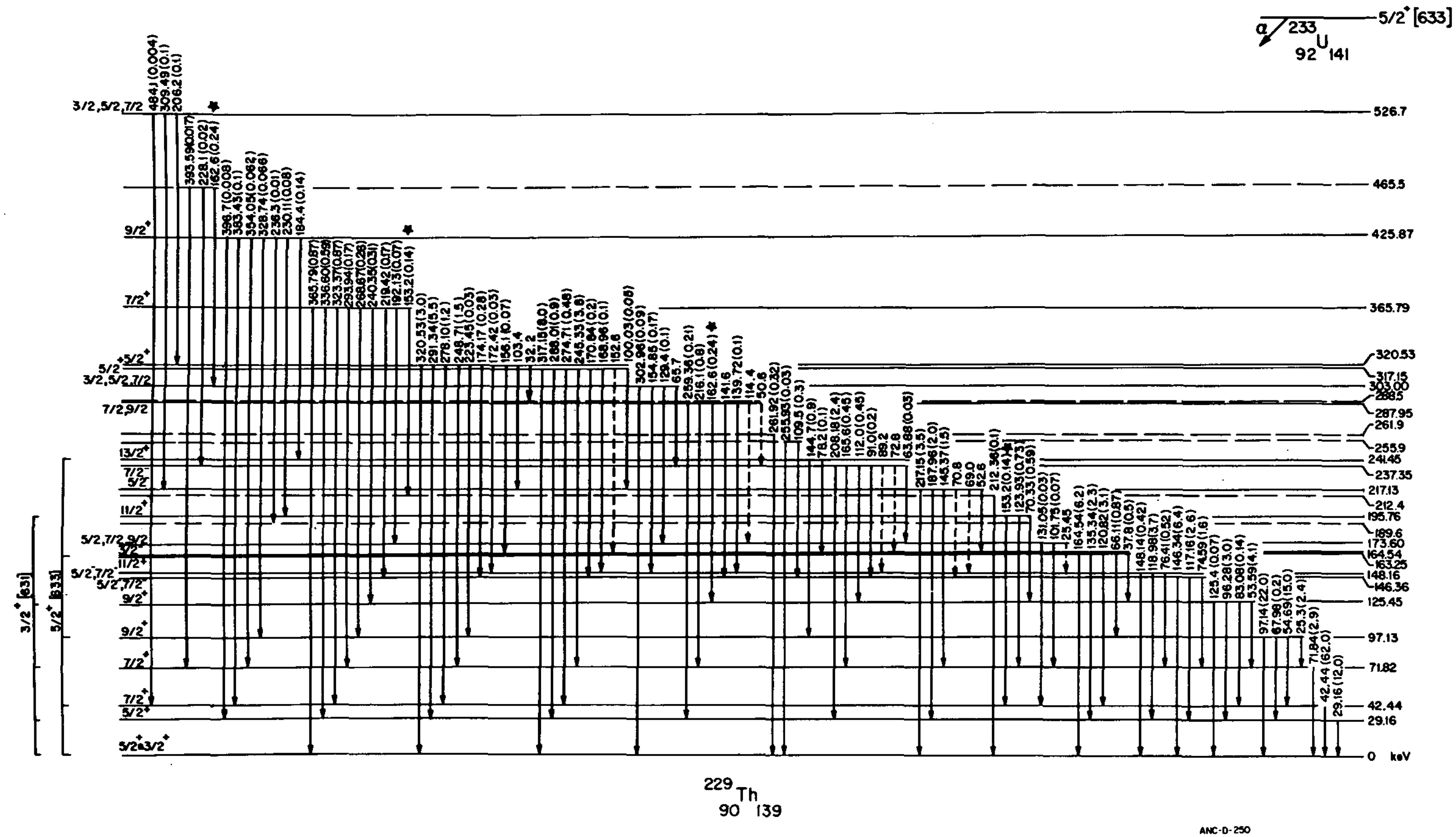

Fig. B-4-1. Proposed level scheme for ^{229}Th. The γ-ray intensities are listed in parentheses in units of γ rays/10^5 decays.

C. RATIO OF THE HYDROGEN AND MANGANESE ABSORPTION CROSS SECTIONS (J. R. Smith, S. D. Reeder,* B. M. Coursey,** V. Spiegel**)

As part of a series of studies aimed at resolving a discrepancy that exists between measured values of $\bar{\nu}$ (average number of neutrons per fission) for ^{252}Cf and η (average number of neutron per absorption) for the fissile nuclides, the MTR η measurements[1] were reanalyzed. The results of this analysis were reported at the 1975 Cross Section Conference in Washington,[2] and reconfirmed both the values and the errors from the previous analysis.

In the second phase of this investigation, the ratio of the absorption cross sections of hydrogen and manganese was measured. This measurement was chosen as a point of investigation not only because it is an important systematic factor in the derivation of neutron source strengths from manganese bath activation measurements, but also because the two prior measurements of Axton[3] and DeVolpi[4] differ by 1.4% in spite of claimed accuracies of 0.2%.

The σ_H/σ_{Mn} measurement consists of determining the activity induced in a manganese bath by a neutron source as a function of concentration of $MnSO_4$ in the bath. In order to obviate the necessity of corrections for manganese resonance absorption, leakage, and losses to $^{16}O(n,\alpha)^{13}C$ and $^{32}S(n,p)^{32}P$, the experiment was performed using a 0.02 eV Bragg beam from a pyrolytic graphite crystal at the National Bureau of Standards Reactor. A manganese-aluminum monitor foil was used to normalize the solution activity to beam intensity, as in the η measurements.[1]

Concentration was measured three ways: (1) volumetrically, by titration with EDTA; (2) gravimetrically, by evaporation of samples and

---

* Allied Chemical Co., INEL

** National Bureau of Standards, Gaithersburg, Md.

[1] J. R. Smith et. al., IDO-17083 (1966).

[2] J. R. Smith, Nuclear Cross Sections and Technology, NBS Spec. Publ. Vol. 1, p. 262 (1975).

[3] E. J. Axton, P. Cross, and J. C. Robertsen, J. Nucl. Energy, Vol. 19, p. 409 (1965).

[4] A. DeVolpi and K. G. Porges, Metrologia, Vol. 5, No. 4, p. 128 (1969).

weighing of the residue, and (3) densimetrically, by measuring solution density and comparing with density-concentration curves.[5] The solutions were analyzed for impurities, searching particularly for neutron absorbers and impurities that would titrate along with manganese. No neutron absorbers were found in significant quantities. The absence also of titratable impurities confirmed the validity of the volumetric methods as a specifically manganese analysis, and allowed use of the volumetric-gravimetric difference as a measure of solution impurities present. Impurity levels, as indicated by both the grav-vol differences and the analyses, were about 0.2% of the $MnSO_4$ concentration for concentrated solutions (to 530 grams/liter) rising to about 0.4% for the dilute solutions (to 30 grams/liter), due to a 50 ppm contaminant level in the NBS demineralized water supply.

The σ_H/σ_{Mn} ratio was found to be 0.02506 ± 0.35%, using contaminant-corrected concentrations. The densimetric and gravimetric results, uncorrected for contaminant effect upon concentration; gave values about 0.7% higher. The latter result suggests that DeVolpi's higher value for σ_H/σ_{Mn} may have been caused by concentration problems. The 0.35% error is nearly twice Axton's quoted error. However, a reexamination of his published data[3] indicates that his errors are underestimated. Refitting his data by either weighted or unweighted least squares techniques indicates errors of 0.5% for Axton's source strength determination, and 0.65% for his value of σ_H/σ_{Mn}, which at 0.024965 is 0.38% lower than our value.

Impact of the present results upon DeVolpi's value of $\bar{\nu}$ for ^{252}Cf is uncertain. Any estimate would require speculation as to the linearity of the impurity level in his solution, and the interaction between this nonlinearity and the adjustments made to give DeVolpi's derived values for high energy neutron absorption. Impact on Axton's $\bar{\nu}$ value is also uncertain, because of a lack of published details concerning the actual experiment. On the basis of published information about Axton's neutron source measurement techniques, however, the current information suggests that it might be appropriate to raise the $\bar{\nu}$ value by about 0.2% and expand the error estimate to about 0.7%.

---

[5] A. DeVolpi, R. J. Armani, and K. G. Porges, J. Nucl. Energy, Vol. 19, p. 597 (1965), and J. Nucl. Energy, Vol. 21, p. 521 (1967).

D. INTEGRAL CAPTURE CROSS SECTION OF ^{94}Nb (E. H. Turk and Y. D. Harker)

The need for experimental data for the ^{94}Nb(n,γ)^{95}Nb,^{95m}Nb cross sections in the high-energy neutron region ($\sim$ 1 MeV) is discussed in a paper presented in the Proceedings of a Conference on Nuclear Cross Sections and Technology held in Washington, D.C. in March 1975.[1] These cross sections are important in evaluating the near term (days, weeks) afterheat problem associated with niobium which is a possible structural material for the controlled thermonuclear reactor. Experimental neutron cross section data in the high-energy neutron region has been non-existent so a measurement program was undertaken at Aerojet to measure the integral capture cross section of ^{94}Nb using the CFRMF which has a mean neutron energy of 700 keV as the fast neutron irradiation facility and a sample of ^{94}Nb produced in the Materials Testing Reactor.

A powdered Nb metal sample which had been irradiated in the Materials Testing Reactor (MTR) to produce ^{94}Nb by neutron capture in ^{93}Nb was used for the ^{94}Nb(n,γ) cross section measurements. Mass spectrometric analysis of this sample after the MTR irradiation gave a mass 94 content of 0.813%.

The Nb metal sample was divided into four approximately equal aliquots which were sealed in quartz ampoules 7 mm O.D. and $\sim$ 2.5 cm long. The ^{94}Nb content of each sample was measured by a determination of the ^{94}Nb disintegration rate using the 702.5 keV and 871.1 keV γ-ray lines and a calibrated Ge(Li) detector. A half-life of 2.0×10^4 years[2] was used in the conversion from absolute disintegration rate to ^{94}Nb content. Two of the four samples were selected for irradiation in the CFRMF, the other two were saved for a future irradiation in the Argonne Fast Source Reactor (AFSR). The two samples selected for CFRMF irradiation contained 70.3 μg and 63.3 μg ^{94}Nb, respectively.

The two quartz ampoules were irradiated at the center-line of the CFRMF for 76.67 hours with the reactor operated at a 10 kilowatt power level. Two 5 mil thick gold neutron flux monitors were irradiated at the same time as the ^{94}Nb samples. One gold foil was directly above the ^{94}Nb samples and the other one below.

For the gold foils a half-life of 64.7 hours[3] was used for decay corrections. A branching ratio of 95.48%[4] was used for the 411 keV ^{198}Au gamma. The ^{198}Au activity averaged for the two monitor foils gave a neutron flux of 1.18×10^{11} n/cm^2/sec for this irradiation.

Because of the small amount of ^{95}Nb and ^{95m}Nb produced it was necessary to count the two samples together and treat them as one sample. The samples were counted at a distance of 20 cm from the face of a calibrated Ge(Li) detector for 40,000 second counting time. The counting distance of of 20 cm was necessary in order to reduce the dead time of the detector to $\sim$ 20%.

Analysis of the counting data was done by two different methods to determine the cross section for the $^{94}Nb(n,\gamma)^{95m}Nb$ reaction.

One method was a non-linear least squares fit of a two mode decay to the ^{95}Nb 765 keV gamma activity versus decay time.

The second method was to determine the ^{95m}Nb 234.7 keV gamma activity directly by subtracting the background contribution of the ^{94}Nb from the ^{95m}Nb photopeak. Only the first four sets of decay data covering the following decay times were used for this analysis: 72.80 h, 93.75 h, 113.47 h, 140.27 h.

For the ^{95m}Nb decay a half-life of 86.6 h[5] was used and a branching ratio of 26%.

The cross section for the $^{94}Nb(n,\gamma)^{95m}Nb$ reaction measured by the background subtraction technique for the four sets of decay data are shown in Table D-1.

Table D-1

$^{94}Nb(n,\gamma)^{95m}Nb$ CROSS SECTION

Measured by the background subtraction method.

Decay (hours)	237.5 keV Area (counts)	σ (millibarns)
72.80	1993	9 ± 8
93.75	136	1 ± 12
113.47	1003	6 ± 10
140.27	563	4 ± 12
	Average	5 ± 6

The cross section for the $^{94}Nb(n,\gamma)^{95m}Nb$ and $^{94}Nb(n,\gamma)^{95}Nb$ reactions as measured by the non-linear least squares fit of a two mode decay to the ^{95}Nb 765 keV gamma activity are shown in Table II

Table D-2

$^{94}Nb(n,\gamma)^{95m}Nb$ AND $^{94}Nb(n,\gamma)^{95}Nb$ CROSS SECTIONS

Measured by non-linear least squares treatment of decay data of the ^{95}Nb 765 keV gamma

Reaction	σ (millibarns)
$^{94}Nb(n,\gamma)^{95m}Nb$	5 ± 16
$^{94}Nb(n,\gamma)^{95}Nb$	236 ± 18

For the $^{94}Nb(n,\gamma)^{95m}Nb$ reaction in the CFRMF (mean neutron energy 700 keV) the experimental cross section is 5 ± 16 millibarns. This small value should remove any concern about its contribution to the afterheat problem using Nb as a structural material for a CTR.

The cross section for the $^{94}Nb(n,\gamma)^{95}Nb$ reaction is 236 ± 18 millibarns.

---

[1] Persiani, Pennington, Harker, Heath, Proceddings of a Conference on Nuclear Cross Sections and Technology, Washington, D.C., March 3-7, 1975, (NBS Special Publication 425), Vol. 2, 708.

[2] Lederer, Hollander, Perlman, Tables of Isotopes, Sixth Edition, 43.

[3] Ibid, 119.

[4] R. G. Helmer, R. C. Greenwood, "Evaluated Decay Scheme Data," Nuclear Technology 25 258 (1975).

[5] Nuclear Data Tables, Vol. 8, Numbers 1-2, October, 1970.

This Page Intentionally Blank

ARGONNE NATIONAL LABORATORY

A. CHARGED PARTICLE REACTIONS RELEVANT TO CONTROLLED THERMONUCLEAR RESEARCH

1. Cross Sections for Charged Particles from ^{6}Li + d Reactions at Low Energies (A. J. Elwyn, R. E. Holland, C. N. Davids, L. Meyer-Schützmeister, F. P. Mooring, and F. J. Lynch)

We have measured the differential and total cross sections for the outgoing protons and alpha particles in the bombardment of ^{6}Li by ~0.1 to 1.0 MeV deuterons accelerated in the ANL Dynamitron. These experiments along with recently completed measurements[1] of similar quantities for the outgoing neutrons in ^{6}Li + d reactions provide nuclear cross sections of importance to the evaluation of ^{6}Li-D as a possible fusion fuel.[2] At the same time, such studies can contribute to the understanding of the nuclear structure of light nuclei and of the relative importance of various reaction mechanisms. Differential and total cross sections of the protons in the ^{6}Li(d,p) reaction, both to the ground and first excited state in ^{7}Li, and the energetic alpha particles in the ^{6}Li(d,α)α reaction have been obtained by use of silicon surface barrier detectors and a 30" scattering chamber. Targets of ^{6}LiF have been utilized, and target thickness and total integrated charge have been determined with sufficient accuracy to allow absolute cross-section measurements to 13—14%. Figure A-1 shows a comparison of the ^{6}Li(d,p) cross sections with previously measured ^{6}Li(d,n) values. Charged particles that arise in the breakup of ^{7}Li and ^{7}Be in the ^{6}Li + d reactions have been investigated by time-of-flight techniques using the post-acceleration pulsed beam from the Dynamitron. From two-dimensional analysis of both the energy and time-of-flight of low-energy charged particles over 20-cm flight paths, the spectra associated with the continuum protons can be extracted, and absolute cross sections for the ^{7}Li breakup process may be determined.

---

[1] Elwyn, Holland, Lynch, Monahan, and Mooring, Proc. Conf. on Nucl. Cross Sections and Tech., NBS Special Pub. 425 (Washington, D.C., 1975) p. 692.

[2] See, e.g., J. R. McNally, Jr., Proc. Conf. on Nucl. Cross Sections and Tech., NBS Special Pub. 425 (Washington, D.C., 1975) p. 683.

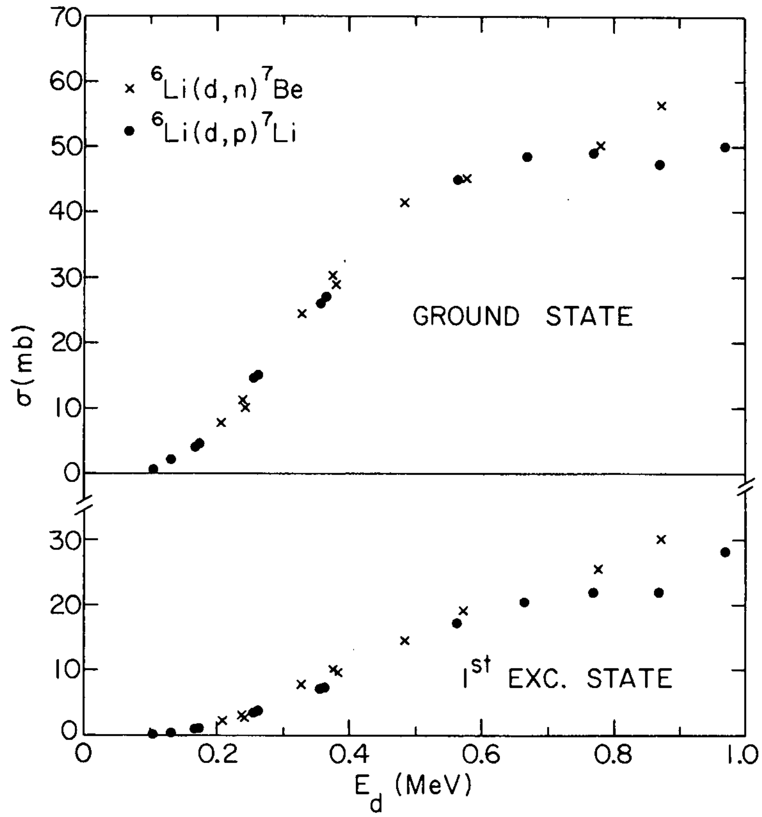

Figure A-1. Cross sections for the $^6Li(d,p)^7Li$ and $^6Li(d,n)^7Be$ reactions to the ground and first excited states as a function of incident deuteron energy.

Analysis of the raw data (both discrete and continuous energy groups) and attempts to interpret the observed angular distributions in terms of various reaction mechanisms are currently in progress. Future measurements that involve the study of the interaction of some of the outgoing particles in ^{6}Li + d reactions with ^{6}Li [e. g., ^{6}Li(p, ^{3}He)α reaction] are planned.

2. Three-Body Breakup in ^{6}Li + d Reactions (A. J. Elwyn, J. E. Monahan, and R. E. Holland)

The interaction between particles in the final-state modifies the cross sections and energy spectra in three-body breakup reactions. The interpretation of the continuous energy spectrum of the outgoing particles in, for example, ^{6}Li + d reactions may lead to an understanding of the reaction mechanisms that can produce a particle in the final state as well as the structure of the various light nuclei involved. The energy dependence of the neutron continuum distributions that arise from the breakup of ^{7}Be (based on ^{6}Li + d reactions recently measured at Argonne) have been compared with calculations based on the factored-wave-function method of treating final-state interactions. Preliminary results suggest that the 0^{o} spectra at neutron energies between 750 keV and ~2.5 MeV can be interpreted in terms of an s-wave Coulomb interaction between the ^{3}He and α particles in the final state. (See Fig. A-2). This interaction, furthermore, predicts phase shifts in good agreement with those previously obtained at other laboratories[1] for ^{3}He-α scattering. Attempts at a more complete interpretation of the neutron continuum distributions particularly at neutron energies below 750 keV, as well as a study of the outgoing protons in the three-body breakup of ^{7}Li, are now in progress.

3. Thermonuclear Reaction Rates for ^{6}Li + d Reactions (A. J. Elwyn, J. E. Monahan, and F. J. D. Serduke)

The reaction-rate parameter associated with interacting ions in a hot plasma is the product of the reaction cross section and the relative velocity between the ions averaged over the distribution, usually assumed to be Maxwellian, of their relative velocities.

[1]See, e.g., L. S. Chuang, Nucl. Phys. A174, 399 (1971).

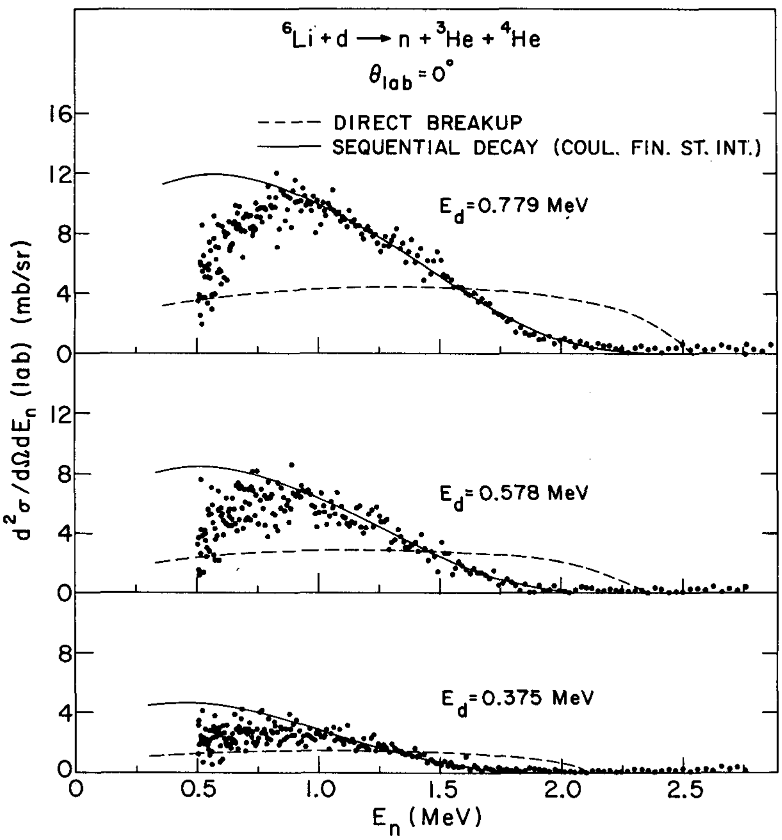

Figure A-2. Lab. differential cross sections per MeV as a function of E_n at $\theta = 0°$ for various deuteron energies compared to calculations for direct ^7Be breakup (dashed curve) and for sequential decay with a Coulomb final state interaction between ^3He and α (solid curve). The calculations were normalized to the data at neutron energies greater than 0.9 MeV.

Since the power released by nuclear reactions in such a plasma is proportional to these reaction rates, the feasibility of utilizing a particular fuel, such as e. g. ^{6}Li-D, in thermonuclear applications will depend in part on the values of the associated reaction rates and thus on the absolute reaction cross sections. Reaction-rate parameters for ^{6}Li + d reactions based on reaction cross sections recently measured at Argonne have been calculated, by numerical integration techniques, for temperatures that correspond to relative ion energies between 1 and 1000 keV. For ion energies below the range of the measurements, extrapolated cross sections were obtained by use of an expression that has been shown to be an adequate representation of the cross section for all energies up to several hundred keV. Calculations of the power released into a heated plasma in ^{6}Li + d processes have been compared to similar quantities for the more usual d + t and d + d fusion reactions. The value for ^{6}Li + d surpasses that for the d + d reactions near relative ion energies of 100 keV, and is comparable to the d + t value at temperatures above 500 keV.

4. Extrapolation of Low-Energy Reaction Cross Sections
(J. E. Monahan, A. J. Elwyn, and F. J. D. Serduke)

Many applications in astrophysical and controlled-fusion research require values of nuclear-reaction cross sections at interaction energies considerably below the range in which absolute measurements are practical. Measured cross sections must be extrapolated to the energies of interest. The extrapolation formulas that are used for this purpose are empirical and thus introduce uncertainty in the extrapolation procedure. For exoergic reactions, which are not dominated by resonances in the range of measurement, a physically meaningful extrapolation formula can be derived from the R-matrix theory. For energies such that only incident s-waves contribute to the reaction, the resulting formula contains two "free" parameters. This procedure has been used to extrapolate cross sections for various d + ^{6}Li reactions, measured at energies above $\sim$100 keV, to energies in the range of one keV. The resulting fits are consistent with the assigned "relative error" (i. e., the error obtained by neglecting uncertainties in overall normalization) of $\sim$5% for the measured cross sections and a relative error of $\sim$15% at the extremity of the extrapolation range.

B. FAST NEUTRON PHYSICS

1. Fast-Neutron Activation Cross Section Studies (D. L. Smith and J. W. Meadows)

Previously reported data on (n, p) data for ^{27}Al, ^{46,47,48}Ti, ^{54,56}Fe, ^{58}Ni, ^{59}Co and ^{64}Zn were further analyzed to determine the integral response functions for these reactions in fast-neutron spectra resulting from ^{235}U thermal fission and ^{252}Cf spontaneous fission.[1,2] Data on the ^{66}Zn(n, p)^{66}Cu and ^{113,115}In(n, n')^{113m,115m}In reactions at energies up to 10 MeV have been analyzed and the results reported.[3] Recently obtained data on the ^{59}Co(n, p)^{59}Fe reaction near threshold have been processed and a paper on the results has been submitted for publication.[4] Additional measurements have been made on fast-neutron excitation of the 49 min isomer in ^{111}Cd to determine the contribution from the ^{110}Cd(n, γ')^{111m}Cd reaction at energies below threshold for the ^{111}Cd(n,n')^{111m}Cd reaction. These data are being analyzed. Preliminary measurements have been made on the ^{204}Pb(n,n')^{204m}Pb reaction using a sample enriched in ^{204}Pb.

2. Gamma-Ray Production Cross Section Studies (D. L. Smith)

Two reports have been prepared which describe a facility used for (n,n'γ) studies and discuss various aspects of the data processing in detail.[5,6] Data from studies of the ^{7}Li(n,n'γ)^{7}Li reaction at energies below 4 MeV have been processed and a paper has been submitted for publication.[7] Data on Fe(n,n'γ)Fe reactions at energies below 2 MeV have been processed and a report is being prepared on the results of this work.

---

[1] D. L. Smith and J. W. Meadows, ANL/NDM-10, Argonne National Laboratory (1975).

[2] D. L. Smith and J. W. Meadows, ANL/NDM-13, Argonne National Laboratory (1975).

[3] D. L. Smith and J. W. Meadows, ANL/NDM-14, Argonne National Laboratory (1975).

[4] D. L. Smith and J. W. Meadows, Nucl. Sci. Eng. (to be published).

[5] D. L. Smith, ANL/NDM-12, Argonne National Laboratory (1975).

[6] D. L. Smith, ANL/NDM-17, Argonne National Laboratory (1975).

[7] D. L. Smith, manuscript submitted to Nucl. Sci. & Eng.

3. Total Cross Sections of ^{182}W, ^{184}W, ^{186}W, and ^{51}V (J. F. Whalen)

Total cross sections of the separated isotopes ^{182}W, ^{184}W, ^{186}W and natural V were measured from 0.460 MeV to 5.4 MeV in approximately 30-keV steps. The measurements used the transmission method with time-of-flight instrumentation. The data will be published at a later date as part of a more comprehensive study.

4. Cross Section Evaluations (P. T. Guenther, A. B. Smith, (D. L. Smith, J. F. Whalen, and R. Howerton*)

A comprehensive evaluation of neutron-induced reactions for nickel in the range 0.1—20 MeV has been completed and the results reported.[1] A corresponding project for vanadium and titanium is underway.

5. Improved Calibration Method for the Fast-Neutron Time-of-Flight Facility (A. B. Smith and P. T. Guenther)

A new method for calibration of the scintillation detectors in the FNG time-of-flight facility has been put into routine application. This involves use of neutrons emitted in the spontaneous fission of ^{252}Cf. The approach permits calibration of the facility for measurements over a wider energy range with greater accuracy than was previously the case. A report on this method is in preparation.

6. The ^{234}U and ^{236}U Fission Cross Sections Relative to ^{235}U (J. W. Meadows)

Measurements of the $^{234}U/^{235}U$ and $^{236}U/^{235}U$ fission cross section ratios have been completed over the energy range 0.5 to 4 MeV. Preliminary values for the relative sample weights are based on the relative alpha activities of the uranium deposits. At 2.5 MeV the ratios are:

$$^{234}U/^{235}U = 1.165$$
$$^{236}U/^{235}U = 0.679.$$

---

*Lawrence Livermore Laboratory, Livermore, California.

[1] Guenther, Smith, A., Smith, D., Whalen, and Howerton, ANL/NDM-11, Argonne National Laboratory (1975).

7. The Delayed Neutron Yield of ^{238}U and ^{241}Pu
(J. W. Meadows)

The total delayed neutron yield for ^{238}U and ^{241}Pu were observed as a function of energy. The measurements extend from 2.5 to 5 MeV for ^{238}U and from 0.15 to 5 MeV for ^{241}Pu. No significant energy dependence was observed. If ENDF/B-IV fission cross sections are used the average ratio of the ^{241}Pu delayed neutron yield to that of ^{238}U is $0.292 \pm .022$.

8. Studies on Cross Section Standards (W. P. Poenitz)

An evaluation of the ratio U-235(n,f)/Li-6(n,α) has been undertaken. The evaluation effort is being complimented by measurements now in progress at the FNG laboratory. Concurrently, a detailed and internally consistent evaluation of fast neutron standard processes is underway including $Li^6(n,\alpha)$, U-235 fission and U-238 capture.

9. Neutron Capture Cross Section Measurements
(W. P. Poenitz)

Measurements of neutron capture cross sections were made for several different medium-heavy nuclei as part of an on-going program at the FNG laboratory. These measurements were made in the energy range 0.3—4.0 MeV using a 1300 liter large liquid scintillator and time-of-flight techniques. The experimental work has been complimented by statistical calculations which employ Hauser-Feshbach formalism and a gamma cascade model. Completed portions of this work have been reported.[1,2]

---

[1] W. P. Poenitz, ANL/NDM-15, Argonne National Laboratory (1975).

[2] W. P. Poenitz, Bull. Am. Phys. Soc. 20, 172 (1975).

10. Fast-Neutron Excitation of the Ground-State Rotational Band of ^{238}U (P. Guenther, D. Havel and A. Smith)

The differential neutron cross sections for the excitation of the 2+(45 keV), 4+(148 keV) and 6+(308 keV) states of ^{238}U have been measured for scattered neutron energies in the range 0.1 to 3.0 MeV. The observed excitation cross sections vary smoothly with energy with no significant fluctuations. The experimental results were correlated with the predictions of compound-nucleus and direct-reaction models. At lower energies ($\leqslant$0.8 MeV) the observed inelastic scattering cross sections are consistent in shape and magnitude with the predictions of compound-nucleus theory. Above $\approx$ 1.0 MeV comparison of measured and calculated values indicates large direct-reaction contributions. The experimental and computational results were compared with the evaluated nuclear data file, ENDF/B-IV, and significant discrepancies were noted. The results from these measurements and selected values from the literature were used to deduce an evaluated set of ^{238}U inelastic scattering cross sections.

11. Fast-Neutron Elastic and Inelastic Scattering Studies on $Li^{6,7}$, C, V, Fe and $W^{182,184,186}$ (A. Smith and P. Guenther)

Measurements of scattering cross sections for several materials of importance for nuclear energy applications have been made using the time-of-flight spectrometer at the ENG laboratory. Data is available on lithium, carbon, vanadium, iron and tungsten. These data are in various stages of analysis and results will be reported as they become available.

12. Direct Reaction Effects on Compound Cross Sections (P. A. Moldauer)

Two effects of a direct reaction on compound processes have been investigated: the enhancement of the average compound cross section that competes with the direct process and the cross correlations in the fluctuations of cross sections involving the directly coupled channels.[1] For the case of two directly coupled channels it was shown that both effects are maximized at the causality limit of the average S matrix where the penetration matrix P is singular. Computer

---

[1] P. A. Moldauer, "Direct Reaction Effects on Compound Cross Sections," Phys. Rev. C 12, 744 (1975).

experiments demonstrated that both effects fall off sharply when $\overline{S}$ is not near this causality limit and similar reductions in the effects are expected when more than two channels are strongly coupled to one another. A formula based upon the Engelbrecht-Weidenmüller transformation and the M-cancellation principle gives an excellent account of the enhancements obtained from the computer experiments. It also gives a qualitative account of the magnitudes of the cross section cross correlation coefficients. A somewhat more complicated formula due to Hofmann et al. also gives a good account of the enhancements. Both of these formulas agree with that of Kawai et al. in the limit of large width-to-spacing ratios.

13. The Optical Potential Near A = 208 (A. Smith)

Elastic neutron scattering cross sections of ^{206}Pb, ^{207}Pb, ^{208}Pb and ^{209}Bi were measured at incident neutron energy intervals of $\approx$ 25 keV from 0.6 to 1.0 MeV with resolutions of $\approx$ 25 keV. Optical model parameters were obtained from the energy-averaged experimental results for each of the isotopes. The observed elastic neutron scattering distributions and derived parameters for the lead isotopes (doubly magic or neutron holes in the closed shell) tend to differ from those of ^{209}Bi (doubly closed shell plus a proton). These potentials, derived in the approximately spherical region of A $\approx$ 208, are extrapolated for the analysis of total and scattering cross sections of ^{238}U introducing only a small (N-Z)/A dependence and the known deformation of ^{238}U. Good descriptions of ^{238}U total cross sections are obtained from a few hundred keV to 10.0 MeV and the prediction of measured scattering distributions in the few MeV region are as suitable as frequently reported with other potentials.

C. PHOTONUCLEAR PHYSICS

1. Photodisintegration of the Deuteron Near Threshold
(H. E. Jackson, R. J. Holt, R. M. Laszewski, and W. M. Wilson*)

The simplest and most basic threshold measurement is the photodisintgration of the deuteron. This experiment is of particular interest because the deuteron is the one nuclear system for which the effects of meson exchange currents and virtual isobaric states can be calculated accurately. The photomagnetic disintegration amplitude of

*Now at University of Florida, Gainesville, Florida.

the deuteron is particularly sensitive to these phenomena and it is in the threshold region that photomagnetic disintegration is strongest. The only information comes from the inverse reaction, e.g. thermal capture cross section is observed to be enhanced over predicted values by 10%. This enhancement can be explained in terms of mesonic effects.

The experiments are performed by irradiating a deuterium target with pulsed bremsstrahlung. Initial efforts have been focused on determination of the angular distribution of the photoneutrons. To date a precision of about 10% has been achieved, which is adequate for testing the simple effective-range theory. The measured magnetic-to-electric dipole cross-section ratio is shown in Fig. C-1. Future measurements of increased precision should permit a comparison with this theory which will place limits on any final state interaction or momentum-dependent component in the nucleon potential. Such effects would cause spin mixing and lead to an interference term in the photoneutron distribution. Such terms are absent in the predictions of the effective-range theory.

2. Threshold Photoneutron Spectroscopy of ^{17}O

(R. J. Holt and H. E. Jackson)

The ^{17}O nucleus is particularly well suited for the study of single-particle M1 transitions ($1d_{5/2} \rightarrow 1d_{3/2}$) from many points of view. (i) The ^{17}O nucleus is thought to be well represented by an ^{16}O core plus a neutron in in $1d_{5/2}$ orbital. (ii) Most ($\sim$70%) of the $1d_{3/2}$ strength is believed to be concentrated in the 5.08-MeV level. (iii) It is unnecessary to renormalize the single-particle M1 operator since the magnetic moment of ^{17}O is given almost completely by the Schmidt estimate. The primary objective of the present study is to determine the extent to which the $1d_{5/2} \rightarrow 1d_{3/2}$ M1 excitation (5.08 MeV) can be represented by a transition between two single-particle states.

The threshold photoneutron spectra for the $^{17}O(\gamma, n_0)^{16}O$ reaction were observed, for the first time, throughout the excitation energy range 4.3 to 6.2 MeV and at reaction angles of 90° and 135°. A tentative value for the M1 reduced transition probability for the

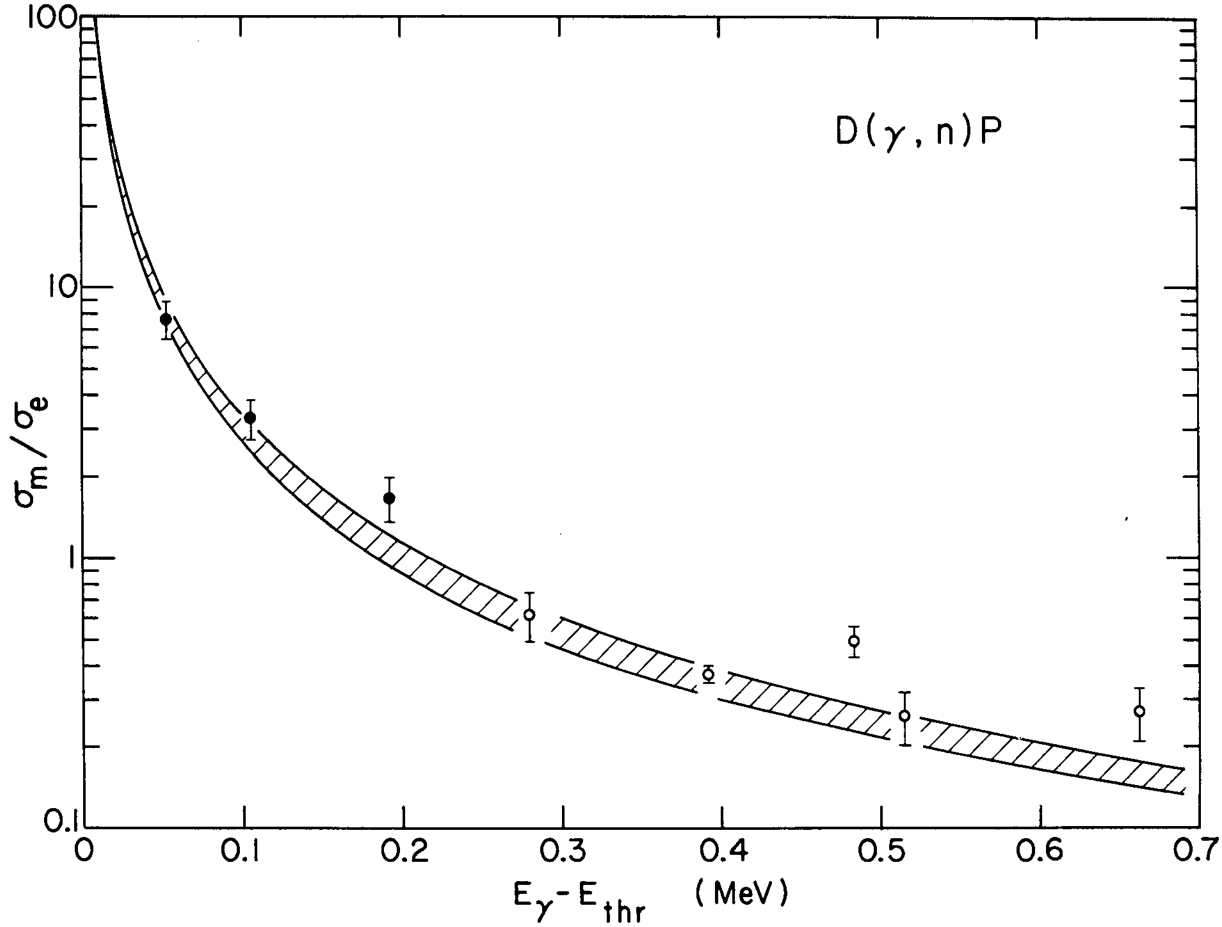

Figure C-1. The solid circles represent the present measurements, while the open circles represent previous photodisintegration studies. The smooth curves indicate the limits of the present uncertainty of the effective range theory.

5.08-MeV resonance was observed to be $B(M1, d_{3/2} \rightarrow d_{5/2}) = 0.9\ \mu_0^2$. A value of $B(M1) = 1.3\ \mu_0^2$ was deduced from the single-particle model. In order to compare in detail the present observation and calculation, it is necessary to determine the proper normalization for the unbound $d_{3/2}$ radial wave function. Further refinements in the experiment and theory are necessary in order to determine the source of the discrepancy.

3. Nonresonant (γ, n) Reactions and Channel Transition in Medium-Weight Nuclei (H. E. Jackson, R. J. Holt, R. M. Laszewski, and W. M. Wilson*)

A particularly striking example of a doorway state common to both the entrance and exit channel has been observed in studies of the (γ, n) reaction for ^{29}Si performed at the ANL threshold photoneutron facility. A preliminary analysis has established complete correlation between photon and neutron partial widths and an unexpectedly large non-resonant background cross section for a group of $3/2^+$ resonances near 750 keV. The strong correlation of partial widths and the "anomalous" background cross section are precisely the features that are associated with dominance of simple single-particle configurations in the initial and final nuclear states. In the case of ^{29}Si, these results can be attributed to the presence of a common doorway state consisting of a $2p_{3/2}$ neutron coupled to a ^{28}Si core.

A similar study has been made for targets in the Cr-Ni region in an effort to determine the magnitude of channel transitions, that is, radiative transitions which involve direct emission of valence nucleons into the continuum. As in the case of ^{29}Si, strong correlations are observed for s-wave resonances in both ^{53}Cr and ^{61}Ni. In addition the strength of non-resonant processes displays a mass dependence in exact agreement with the predictions of the channel-capture theory of radiative transitions. A complete analysis of the data will be used to establish the degree to which the radiative widths can be explained in terms of channel transitions.

---

*Now at University of Florida, Gainesville, Florida.

4. Measurement of Ground State Radiation Widths Near Photoneutron Threshold in ^{140}Ce (R. M. Laszewski, R. J. Holt, and H. E. Jackson)

The ground-state transition strengths of levels near the photoneutron threshold in ^{140}Ce have been studied by means of the ^{140}Ce$(\gamma,n)^{139}$Ce reaction. The angular distribution of photoneutrons was measured at laboratory angles of 90^o and 135^o with high-energy resolution (0.5 ns/m). The time-of-flight spectra are shown in Fig. C-2. The angular distribution enables E1 and M1 transitions to be distinguished. For nuclei with $A \sim 140$, M1 ground state radiation widths are expected to be enhanced because of the possibility of collective spin-flip transitions between the filled $\nu(1h_{11/2})$ shell and the vacant $\nu(1h_{9/2})$ orbital. It is also possible for protons in the $\pi(1g_{9/2})$ orbital to be excited into the vacant $\pi(1g_{7/2})$ orbital by M1 radiation. A total M1 strength of $B(\uparrow M1) = 0.39\ (e\hbar/2Mc)^2$ was observed over the 40-keV interval of excitation centered at 9.08 MeV. This unusually large amount of integrated M1 strength suggests the proximity of a collective M1 resonance. A total E1 strength of $B(\uparrow E1) = 6.6\ e^2fm^2$ was observed over the same excitation interval.

5. Development of Polarimeter and Instrumentation for Threshold Photoneutron Polarization Studies (R. J. Holt, H. E. Jackson, J. R. Specht, and R. M. Laszewski)

a. Polarimeter System

It is well known that photonucleon polarization studies provide a powerful method for determining the existence and magnitude of E1-M1 and E1-E2 admixtures in photoexcitations of nuclei. In order to determine the nature of the giant M1 and isoscalar E2 resonances in nuclei, a photoneutron polarimeter system was developed which is suitable for use with continuous energy spectrum of neutrons in the energy range 170 keV to 2 MeV. The feasibility of measuring the polarization of photoneutrons from resonances near threshold was demonstrated for the first time for the case of the ^{208}Pb$(\gamma,\vec{n}_0)^{207}$Pb reaction.

In order to observe the polarization over this broad energy range Mg, ^{16}O and ^{12}C were used as analyzing targets in separate experiments. A neutron spin-precession solenoid, designed for use with a continuous energy spectrum of neutrons, was developed in order

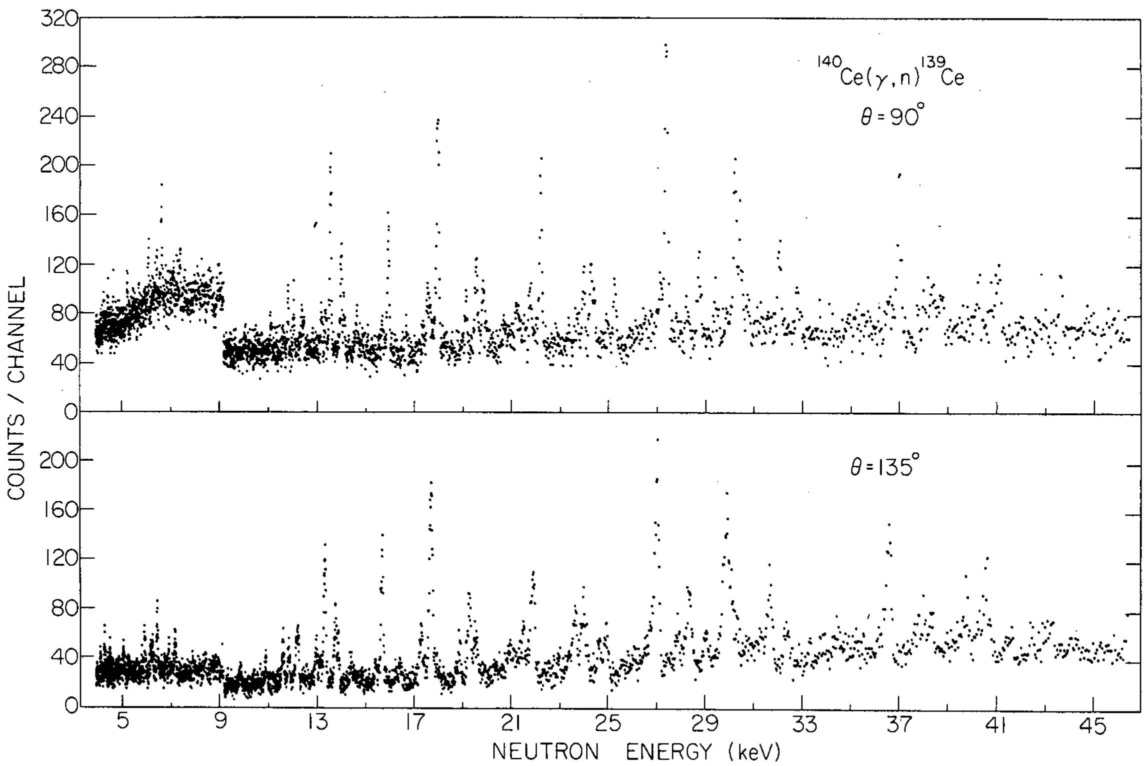

Figure C-2. Photoneutron spectra for the $^{140}Ce(\gamma,n)^{139}Ce$ reaction at reaction angles of 90° and 135°.

to minimize systematic errors.

b. Absolute Calibration of the Polarimeter: Neutron Double Scattering

In order to determine the absolute analyzing power of the polarimeter in the energy range 170 to 320 keV the polarization of neutrons elastically scattered from Mg was measured using a true neutron double-scattering method. The present work represents the first attempt at establishing an absolute calibration standard for neutron polarization studies in this energy region. Intense pulsed beams of unpolarized neutrons were obtained by allowing a 20-MeV electron beam to impinge on a target of natural uranium. These neutrons scatter elastically from the first Mg target at an angle of 45° and become polarized. The amount of polarization is measured by allowing the polarized neutrons to scatter again from a second target, identical to the first, at the same reaction angle, 45°. A preliminary analysis of the data indicates that the observed polarizations are in general agreement with a previous study of the $Mg(n,\vec{n})Mg$ reaction.

6. Threshold Photoneutron Polarization Studies of ^{208}Pb
(R. J. Holt, H. E. Jackson, and R. M. Laszewski)

The ^{208}Pb nucleus should provide an ideal example of the giant M1 resonance since it has more nucleons which are available for spin-flip transitions than any other nucleus. It is widely believed that a collective M1 resonance exists at an excitation energy of 7.9 MeV, is fragmented and spread over 700 keV in ^{208}Pb. Thus far, the large spreading cannot be explained within the framework of current theories. For these reasons, we observed the polarization of photoneutrons emitted from resonances in the expected giant M1 resonance region of ^{208}Pb in order to deduce the multipolarities of these resonances. The photoneutron polarizations were measured at reaction angles of 90° and 135° throughout the excitation energy range 7.56 to 8.40 MeV (E_n = 180 to 1000 keV). Definitive multipolarity assignments for 12 resonances were made on the basis of these polarization observations. The resonances observed at photoneutron energies of 7.56, 7.70, 7.92, 7.98, 8.03, and 8.23 MeV, previously believed to comprise a major part (~75%) of the giant M1 resonance, are shown to be E1 excitations. Only one M1 resonance, located at 7.99 MeV, was found in this energy region. This single resonance accounts for only 28% of the M1 strength expected from calculations based on the collective vibrational model of

Bohr and Mottelson. The search for the giant M1 resonance in ^{208}Pb has been completed above the photoneutron threshold.

7. Discovery of Large sd-Wave Admixtures for 1^- Resonances in the $^{207}Pb + n$ System (R. J. Holt, R. M. Laszewski, and H. E. Jackson)

A recent shell-model calculation of Harvey and Khanna indicates that segments of the $|^{207}Pb \otimes 3d_{3/2}\rangle$ and $|^{207}Pb \otimes 4s_{1/2}\rangle$ basis states in ^{208}Pb are expected to occur in 1^- resonances near the photoneutron threshold. Furthermore, Harvey and Khanna predict that the ratios of d-to-s-wave amplitudes of these basis states should be $\gg 1$. Hence, these shell-model calculations can be tested by searching for abnormally-large ratios of the neutron-reduced widths γ_d^2/γ_s^2. The signature of large sd-wave mixing for 1^- resonances in the $^{207}Pb + n$ system is a large photoneutron polarization for the $^{208}Pb(\gamma, n_0)^{207}Pb$ reaction at a suitable reaction angle, say 135^o.

Photoneutron polarizations were observed at 135^o for the 180- and 254-keV resonances for the $^{208}Pb(\gamma, n_0)^{207}Pb$ reaction. The observed polarizations are shown in Fig. C-3. The lower graphs indicate the raw photoneutron spectra from ^{208}Pb after the emitted neutrons scatter from a Mg analyzer at angles of ±45. A large polarization effect is signified by the difference in the spectra with and without the field of the neutron spin-precession solenoid. On the basis of these measurements and previous angular-distribution studies, the ratios γ_d^2/γ_s^2 were found to be 9 and 21 for the 180- and 254-keV resonances. These results support the shell-model calculations for ^{208}Pb. Although the polarization studies are essential in order to identify resonances with large sd-wave mixing, the exact magnitude of γ_d^2/γ_s^2 was found to be sensitive to angular-distribution measurements. More accurate angular-distribution studies are necessary in order to determine the amount of the $|^{207}Pb \otimes 3d_{3/2}\rangle$ configuration above the photoneutron threshold.

8. Studies of the Distribution of E2 Transition Strength in ^{208}Pb Using Photoneutron Polarization Measurements (R. M. Laszewski and R. J. Holt)

Preliminary measurements of the polarization of neutrons in the energy range 1.4 to 2.0 MeV from the $^{208}Pb(\gamma, \vec{n})^{207}Pb$ reaction have been made in order to examine the distribution of E2 ground-state transition strength in ^{208}Pb. Inelastic electron and proton scattering

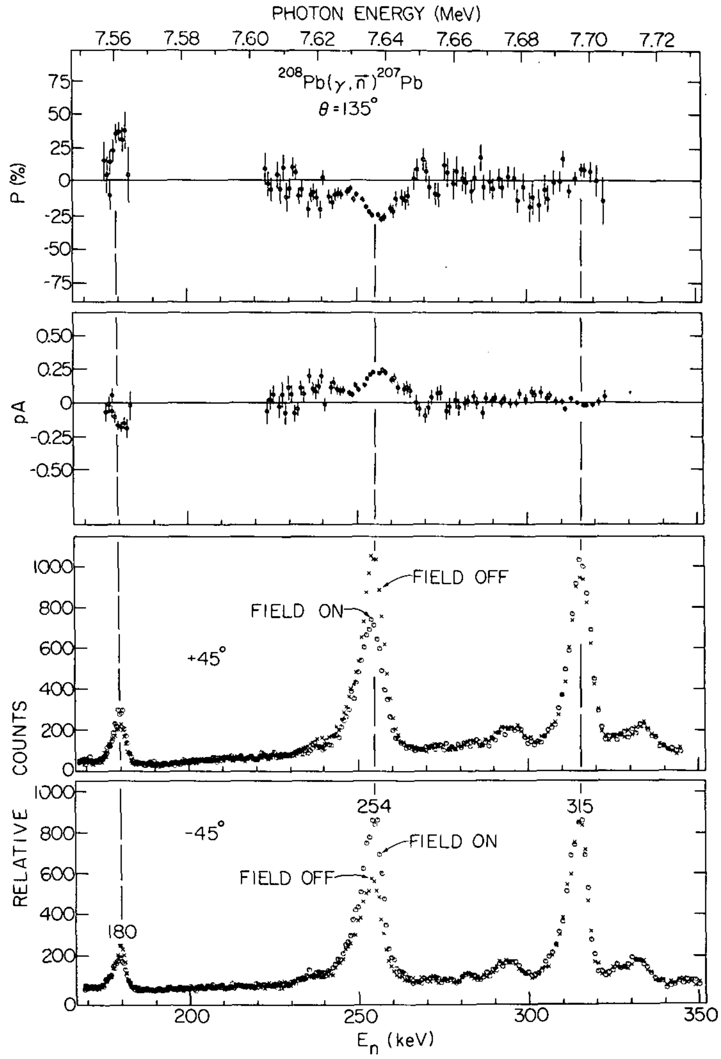

Figure C-3. Upper graphs represent the observations of the photoneutron polarization p and the asymmetry product pA. Lower graphs indicate the photoneutron spectra from ^{208}Pb after scattering from a Mg analyzer at angles of ±45° with and without the field of the neutron spin-precession solenoid.

experiments have shown broad resonances in many nuclei including ^{208}Pb at excitations near that predicted for the isoscalar monopole and quadrupole giant resonances. The photoneutron polarization technique enables the location of the quadrupole excitation to be determined unambiguously and with much greater energy resolution than was previously possible. The preliminary measurements show a significant E2 resonance at an excitation of 9.04 MeV. The measurements are currently being extended to neutron energies above 2.0 MeV.

D. NUCLEAR PROPERTIES

1. Half Lives of ^{239}Pu and ^{238}Pu (A. H. Jaffey, H. Diamond, K. Flynn, and W. Bentley)

We have recently completed some measurements on the half lives of ^{239}Pu and ^{238}Pu, motivated in large part by the large discrepancies between results derived by calorimetry and by specific activity or other counting measurements. Our results have resolved the discrepancies, mostly in the direction of showing that, particularly in the case of ^{239}Pu, the previous specific activity measurements must have had systematic errors much larger than the indicated experimental errors.

a. ^{239}Pu

(The values given represent preliminary calculations). Specific activity measurement. Counting of weighed and analyzed samples in a counter of accurately-known geometry factor.

24130 ± 16 yr

Mass spectrometric measurement. Isotope dilution measurement of the amount of ^{235}U grown into an analyzed ^{239}Pu sample during a known decay period.

24143 ± 10 yr

The results by our two independent methods are consistent with each other and with the Oetting calorimetric result of 24080 ± 50 yr, as well as with some recent preliminary specific activity results by Alexandrov (24060 ± 38) and Glover (24115 + 80).

b. ^{238}Pu

(The value given represents preliminary calculations). Measurement of the growth of ^{238}Pu activity into a sample of measured ^{242}Cm activity, using an isotope dilution method to determine the absolute amount of ^{238}Pu grown within a known time.

87.74 (± 0.03%)

This is in excellent agreement with the calorimetric result: 87.78 (±0.02%).

2. Nuclear Moments and Moment Ratios as Determined by Mössbauer Spectroscopy (J. G. Stevens* and B. D. Dunlap)

An article with the above title has been accepted for publication in the Journal of Physics and Chemistry Reference Data. The abstract follows: Values are given for Mössbauer effect measurements of nuclear magnetic moments, spectroscopic quadrupole moments, ratios of moments between low-lying excited states and the ground state of the same isotope, and ratios of moments between states of different isotopes. Adopted values for moments, obtained by direct selection of specific results or by an averaging process, are presented. The literature has been covered through December 1974.

---

*University of North Carolina, Asheville, N. C.

A. DELAYED NEUTRON STUDIES WITH AN ON-LINE MASS SPECTROMETER (Reeder, Alquist, Wright, Ballou)

1. Half-Lives of Neutron-Rich Rb and Cs Isotopes

Half-lives of $^{92-97}Rb$ and $^{142-145}Cs$ were measured last year by beta counting of the separated isotopes and have been published.[1] This year we have remeasured the half-lives by counting delayed-neutrons. The uncertainties in the half-lives are considerably reduced when measured by neutron counting because the neutron decay curves have fewer components. The half-lives measured by neutron counting tend to be slightly less than the half-lives measured by beta counting. Uncertainties of 1-2% are typical of the recent data.

Table A-1. Half-lives of Rb and Cs Nuclides (in sec.)

Mass	Beta Counting	Neutron Counting
92	4.54 ±.02	
93	6.12 ±.08	5.82 ±.03
94	2.83 ±.03	2.73 ±.01
95	.377±.004	.369±.005
96	.205±.004	.197±.002
97	.182±.007	.167±.002
142	1.70 ±.02	1.70 ±.09
143	1.79 ±.02	1.79 ±.04
144	1.00 ±.04	.99 ±.02
145	.65 ±.03	.577±.006
146		.28 ±.03

2. Delayed-Neutron Emission Probabilities

We have completed our experimental measurements of the delayed-neutron emission probabilities for 16 isotopes of Br, Rb, I, and Cs. We used the on-line mass spectrometer facility SOLAR to provide chemically and mass separated ion beams of the desired nuclide. The total number of atoms deposited on our collector was determined by counting the ions with an electron multiplier detector. The total number of neutrons was determined by simultaneous counting of the neutrons in a high-efficiency neutron counter which surrounded the collector. Corrections were made

[1] P. L. Reeder and J. F. Wright, Phys. Rev. C 12, 718 (1975).

for beta activity on the electron multiplier, the ion counting efficiency, the neutron counting efficiency, and backgrounds. The absolute efficiency of the neutron counter as a function of neutron energy was determined by counting photo-neutron sources calibrated against a primary ^{252}Cf standard source. Our absolute delayed-neutron emission probabilities tend to be somewhat higher than other recent measurements so we are now recalibrating our primary ^{252}Cf source. Most, but not all, of the relative (from mass to mass) delayed-neutron emission probabilities agree with other recent measurements. Our absolute values for $^{87-89}Br$, $^{92-97}Rb$, $^{137-138}I$, and $^{141-146}Cs$ will be ready for publication in May 1976.

3. Mean Energy of Delayed Neutrons

Our neutron detector consisted on 3 concentric rings of ^{3}He tubes embedded in a block of polyethylene. The absolute efficiency of each ring of tubes was determined as a function of neutron energy. The inner ring of 9 counter tubes was undermoderated and thus the efficiency was highly dependent on neutron energy. The middle and outer rings consisting of 33 counter tubes together gave a relatively constant efficiency as a function of neutron energy. Thus the ratios of counts in the 3 rings could be used to determine the "average" energy of the neutron spectrum for each nuclide studied. We have found that the "average" neutron energy is about 400 keV for most of the Rb isotopes whereas for Cs isotopes the "average" energy is about 300 keV. These data will be ready for publication in May 1976.

4. Energy Spectra of Delayed Neutrons

During the coming year we will be measuring the energy spectra of delayed neutrons from mass separated sources. Our neutron energy spectrometer is a ^{3}He ionization chamber built by Shalev in Israel. We have checked the resolution of this detector with monoenergetic neutrons from a Van de Graaff accelerator. It gives a FWHM of <30 keV for 1 MeV neutrons.

BROOKHAVEN NATIONAL LABORATORY

A. NEUTRON-NUCLEAR PHYSICS

1. Neutron Capture in U-238
(R. E. Chrien, H.I. Liou and J. Kopecky†)

Designers of thermal reactors have always had to "adjust" basic nuclear data in order to predict the neutron multiplication in low-enrichment uranium lattices. It has been surmised that the problem lies in the capture cross sections of U-238 below 100 eV. We have checked these cross sections by a series of transmission and self-indication measurements on samples of U-238 ranging from 0.0020 to 0.635 cm thick. The resonance parameters obtained are shown in the table.

Table 1. U-238 Resonance Parameters

Eo(eV)	Γn(meV)	$\Gamma\gamma$(meV)	Eo(eV)	Γn(meV)	$\Gamma\gamma$(meV)
6.67	1.50 ± 0.03	21.8 ± 1.0	80.74	2.16 ± 0.18	23.7 ± 2.5
20.90	9.86 ± 0.50	23.5 ± 1.5	102.47	68. ± 5.	24.3 ± 2.5
36.80	33.3 ± 1.2	23.6 ± 2.0	116.85	30. ± 3.	23.4 ± 2.8
66.15	25.6 ± 1.8	22.2 ± 2.0	10.25	$g\Gamma_n$ = 0.00165 ± 0.00015	

These parameters have been obtained by using a single-level Breit-Wigner level analysis on a series of samples ranging from 0.025 cm to 0.635 cm thick. An example of the quality of the data is shown in Fig. A-1, which illustrates the Γvs.Γn dependence for five transmission samples and the self-indication analysis for the 6.67 eV level.

A check on the data for the region up to 37 eV is obtained by inserting these parameters into a Breit-Wigner many-level formula and comparing the computed and measured total cross sections. Examples of the comparison are shown in Figs. A-2 and A-3. It should be stressed that there is no adjustment in these comparisons, the parameters were fixed from the area measurements; the only exception is a small energy-dependent R_∞ term added to simulate the effect of distant levels.

The main discrepancy with previous data is the case of the 6.67 eV resonance, where we report 22.3 ± 1.0 meV as compared to the 27.2 ± 0.4 meV reported by Jackson and Lynn.* We conclude that the experiment of Jackson and Lynn was relatively insensitive to the value of the resonance width, due to the large correction for Doppler broadening (about 60 meV) necessary near the resonance peak. Hence their quoted errors

---

† Permanent address: Reactor Centrum Nederland, Petten, The Netherlands
* H.E. Jackson and J.E. Lynn, Phys. Rev. 127, 461 (1962).

are not realistic. We have avoided this difficulty by using an area analysis and we observe excellent fits to the measured cross section in the resonance wings, where Doppler effects are negligible.

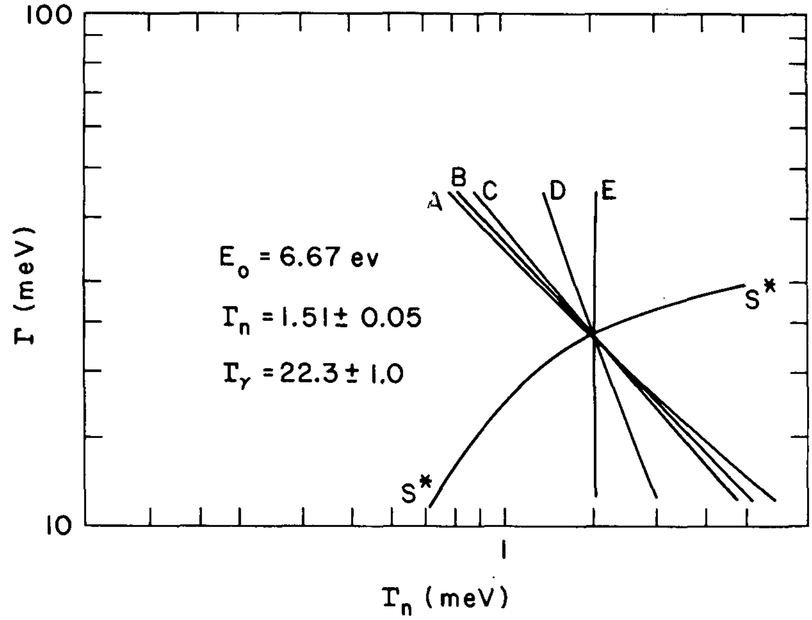

Fig. A-1. The results of transmission area and self-indication measurements on the 6.67 eV resonance in ^{238}U.

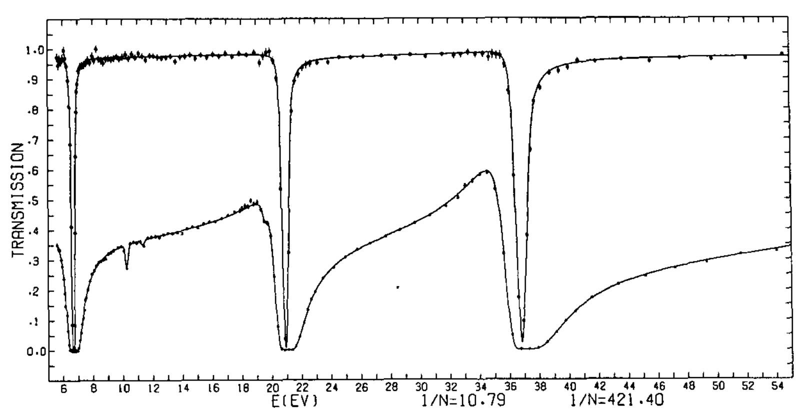

Fig. A-2. Calculated transmission curves for two samples of uranium using parameters derived from single-level area analysis. The transmissions are calculated from a multi-level Breit-Wagner formula with no parameter adjustments.

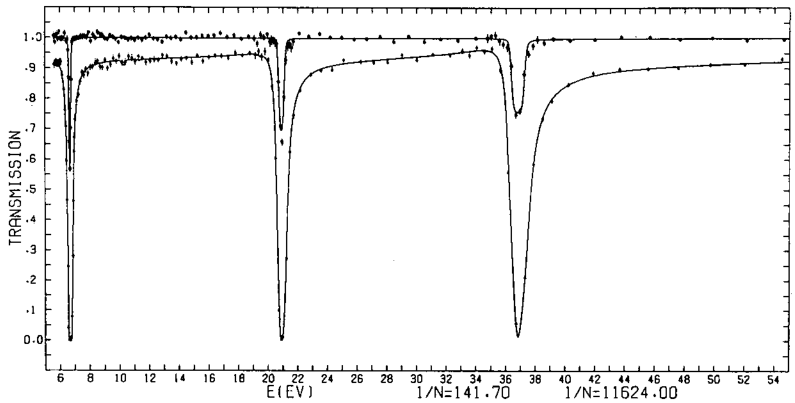

Fig. A-3. Transmission curves as calculated for Fig. A-2 (see caption) for two thinner samples.

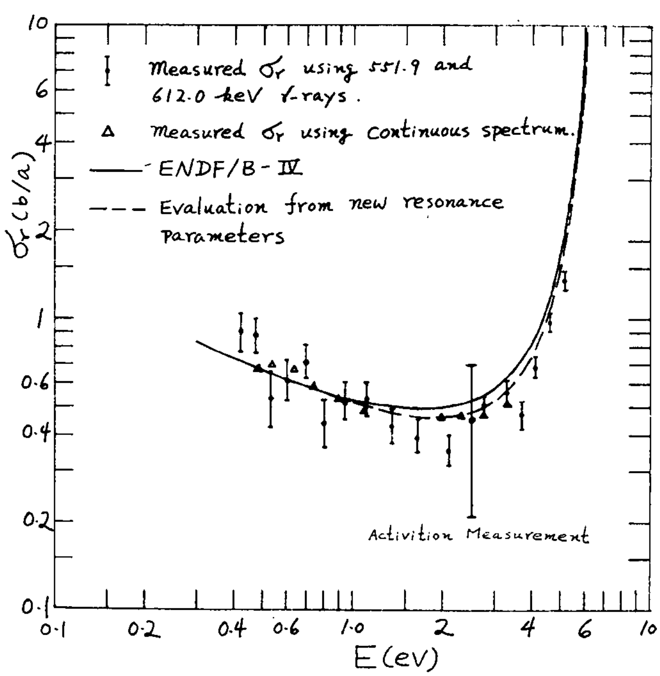

Fig. A-4. Direct measurement of the capture cross sections below 6.67 eV with comparisons to curves derived from total cross section measurements.

These parameters were further confirmed by direct measurements on both the continuum and discrete line fractions of the capture γ-ray spectra. To do this it was necessary to place the low energy lines observed from ~ 0.5 to 1.2 MeV in the level scheme of U-239. The energy behavior of these lines also suggests a reversal of the spins assigned to the first 2 members of the 1/2-[761] band, at 739 and 746 keV, by previous workers. The cross sections above and below the 6.7 eV resonance were inferred from the γ-ray spectra and agree well with the parameters of Table 1.

Figure A-4 shows a portion of the capture cross section below the 6.67 eV energy. The curves describe the capture cross section as derived from ENDF/B IV parameters (———) and the parameters of our transmission experiments (---). The experimental points are measurements based on the observation of discrete lines at 551.9 and 612 keV(•) and from the spectral continuum (Δ). The measurements support the cross section derived from the newer parameters.

As a final check, U-238 samples were activated in a monochromatic beam from our Bragg-diffraction spectrometer at several distinct energies below 10 eV. We count the 74.7 keV γ-ray following the beta decay of U-239. The result as derived in the region of 2.5 eV is fully consistent with the measured value of 0.47 barns obtained from the data of Fig. A-4.

These measurements, when coupled with Monte Carlo calculations of Rothenstein,* on the effective resonance integral remove most of the discrepancy in predicting multiplication in light-water thermal lattices.

---

* W. Rothenstein, private communication.

2. Level Structure of ^{233}Th from the ^{232}Th(n,γ) Reaction Using 2- and 24-keV Neutrons
(R. C. Greenwood† and R. E. Chrien)

Uncertainty still exists regarding the I^{π} assignments, and the structure, of low energy states in ^{233}Th, despite recent studies using the (d,p) and (n,γ) reactions with thermal and resonance neutrons. In order to provide further information on the distribution and I^{π} of the low-spin states in ^{233}Th, we have measured prompt γ-ray spectra resulting from 2- and 24-keV neutron capture in ^{232}Th using the Brookhaven HFBR filtered beam facility. Since these spectra result from averages over many resonance states, fluctuations in the primary γ-ray intensities are averaged out. The 2-keV capture is predominantly s-wave and thus final states with $I^{\pi} = 1/2^-$ and $3/2^-$ are most strongly populated. The p- and s-wave contributions are comparable to the 24-keV capture and hence primary transitions to final states with $I^{\pi} = 1/2^+$, $3/2^+$ and $5/2^+$ are also significant. Figure A-5 shows a plot of reduced transition intensities $I_\gamma E_\gamma^{-3}$ for primary γ-rays resulting from 24-keV neutrons in ^{232}Th; transitions to negative parity states are shown in the upper section, and transitions to positive parity states shown below.

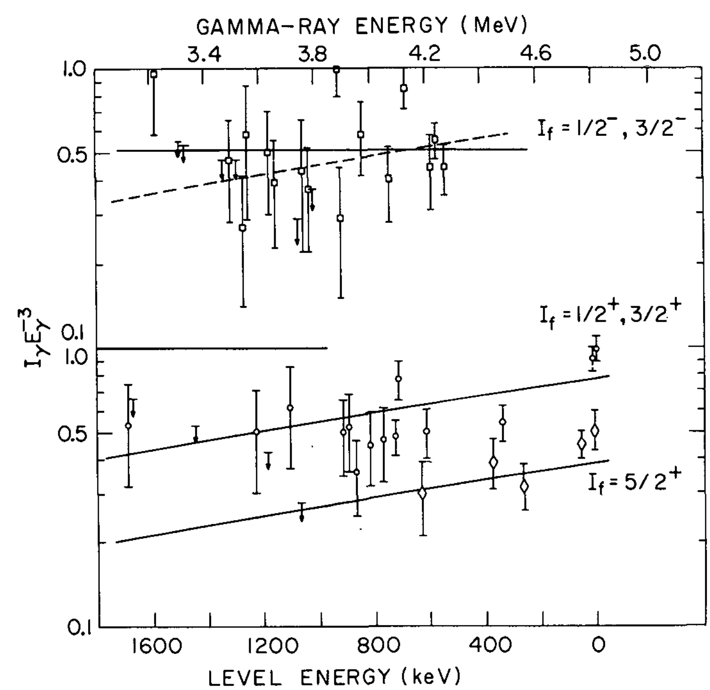

Fig. A.5. Deduced transition intensities for 24-keV capture on ^{232}Th.

† Permanent address: Idaho National Engineering Lab. Idaho Falls, Idaho.

It is seen that transitions to positive parity states are best described as following the shape of the tail of the giant-dipole resonance in this energy region--that is, somewhere between on E^4 and E^5 dependence. This curve is plotted in the lower portion of the figure, along with a curve at 1/2 height for comparison to $5/2^+$ final states. A similar curve is plotted dotted in the upper portion, although here the energy variation expected for M-1's is not known.

Complete lists of transition energies and intensities, and of level energies and spin-parity assignments for ^{233}Th has been prepared and will be published as part of a BNL-Grenoble collaboration.

3. <u>The Low Energy Neutron Capture Cross Section of Xe-124</u>
(W.R. Kane, R.F. Casten, G.J. Smith, J.A. Cizewski, and S.F. Mughabghab)

Because of the low abundance (0.96%) of Xe-124 in natural xenon, its low energy neutron capture cross section is subject to major uncertainties. In particular, the thermal cross section calculated from the parameters of the only resonance assigned to Xe-124, at 5.16 eV, is a factor 2 smaller than the experimentally determined value. The cross section of this isotope is of some interest because of the utility of the light xenon isotopes as tracers in the detection of reactor fuel element failures. This method consists of introducing inside the envelope of each fuel element a different mixture of the nine stable isotopes of xenon. When the presence of fission products in the atmosphere surrounding the reactor core indicates the presence of a leak, the fuel element responsible can immediately be identified by a mass spectrometer analysis of the core atmosphere. Since the heavier isotopes of xenon are produced abundantly as fission products, it is preferable to use mixtures of the lighter xenon isotopes for this purpose. Some change in isotopic composition is inevitable, however, owing to neutron capture in the high flux region of the core. This is particularly important for Xe-124, which has a thermal capture cross section in excess of 100 barns. Reliable values for the low energy neutron capture cross section of Xe-124 are thus essential for this method. In the course of a study of the Xe-124 (n,γ) reaction employing a target of xenon gas highly enriched in Xe-124, an additional, previously unassigned resonance of xenon, at 9.88 eV has been shown unequivocally to originate in Xe-124. This was done by observing the yield of capture gamma rays characteristic of the Xe-124 (n,γ) reaction while the energies of the neutrons provided by the monochromator were varied in the vicinity of 9.88 eV. With the inclusion of the 9.88-eV resonance the thermal neutron cross section is now accounted for satisfactorily and the capture cross section of Xe-124 well established from thermal energy to $\sim$ 50 eV. The thermal cross section of Xe-124 has been remeasured and the parameters of the 5.16- and 9.88-eV resonances are being redetermined.

4. The $^{125}Te(n,\gamma)$ Reaction at 2- and 24-keV
(R. C. Greenwood† and R. E. Chrien)

The experimental information which is available for doubly even neulei in the region Z>50, N<82 has generally tended to indicate that 0^+ member of the two-phonon triplet is not present, or at least is shifted to a significantly higher excitation energy. However for some nuclides, such as ^{126}Te, there is some evidence for the existence of this triplet.[1]

The ^{126}Te nucleus proves to be an ideal case to test this point using the averaged neutron capture technique. The compound states resulting from s-wave neutron capture in ^{125}Te have $I^{\pi} = 0^+$ and 1^+ and hence primary dipole transitions populate final states in ^{126}Te with spin values of 0, 1 and 2. Furthermore, the prompt spectra which result from neutron capture using the 2- and 24-keV neutron beams from Sc and Fe/Aℓ filters at the HFBR represent averages over ~ 25 and ~ 50 s-wave compound nucleus states, respectively. Hence with this degree of averaging we would expect primary transitions to all states of the same parity and spins 0, 1 or 2 to have comparable intensities.

These (n,γ) spectra shows clear evidence of the primary transitions to the 0^+ ground and 1873-keV states and to the 2^+ 666- and 1420-keV states. There is, however, no evidence for a 0^+ state at ~ 1.4 MeV, such as that proposed at 1396 keV.[1] We therefore conclude from this data that the lowest excited 0^+ state in ^{126}Te has an energy of 1873 keV; i.e. ~ 0.5 MeV above the energy of the two-phonon states.

Definitive parity information has also been obtained for higher lying states in ^{126}Te both from the 2-keV neutron capture data (from the relative E1 and M1 transition intensities) and from a comparison of the 2- and 24-keV neutron capture data. The 2-keV neutron capture is predominantly s-wave, and at 24-keV s- and p-wave capture are comparable.

---

† Permanent address: Idaho National Engineering Laboratory, Idaho Falls, Idaho 83401.

[1] Z.T. Zhelev, N.G. Zaitseva, S.S. Sabirov, Izv. Akad. Nauk, SSSR Ser. Fiz. 35, 43 (1971).

5. <u>The Excitation of Particle-Hole States in ^{88}Sr by the (n,γ) Reaction</u>
(R.E. Chrien, J. Kopecky†, R.C. Greenwood‡, and M. Stelts)

Strontium isotopes are of interest because they lie near the closed neutron shell at N=50 and because previous experiments have identifed the importance of direct neutron capture near the 3 p neutron single particle resonance. Charged-particle experiments have identified strong neutron particle and particle-hole states in ^{89}Sr and ^{88}Sr respectively.

Energies and intensities of some 95 transitions have been measured for these isotopes for the 2- and 24-keV neutron beams from HFBR. Resonance neutron capture with the HFBR fast chopper time-of-flight facility was used to supplement the filtered-beam results. Thirteen new primary transitions were found, some of which populate $J^{\pi} = 2^+$ levels not seen in reference 1. Improved values for level energies were obtained. Of special interest are the particle-hole levels of the type $\{(\ell,j)_n(1g9/2)_n^{-1}\}$ in ^{88}Sr.[2] The averaged intensities for p-wave capture show a striking concentration of radiative strength near the $d_{5/2}$ and $s_{1/2}$ levels near 4.5 and 5.5 MeV excitation. The use of the filtered beams, with their admixtures of ℓ=1 and ℓ=0 components, combined with ℓ=0 resonance data, serves to select spin-parity values for many final states.

No transitions from ^{88}Sr(n,γ)^{89}Sr were seen at 2 keV; however at 24.3 keV primary transitions were observed to the $5/2^+$ gs of ^{89}Sr and to the $1/2^+$ first excited state. This observation strongly suggests that capture from a $3/2^-$ resonance is dominant near 24.3 keV.

6. <u>Primary Transitions in ^{235}U from Resonance Capture</u>
(B.K.S. Koene, H.I. Liou, and R.E. Chrien)

Gamma rays from the ^{234}U(n,γ) reaction at the 5.2, 31 and 49 eV resonances have been investigated at the Fast Chopper Facility of the Brookhaven HFBR. States of ^{235}U up to $\sim$ 2 MeV excitation energy were analyzed. Parity assignments are proposed on the basis of the absolute photon intensities in the three resonances.

---

† Permanent address: Reactor Centrum Nederland, The Netherlands.
‡ Permanent address: Idaho National Engineering Laboratory, Idaho Falls, Idaho 83401.

1 H. Lycklama and J.J. Kennett, Nucl. Phys. <u>A139</u>, 625 (1969).
2 E.R. Cosman and D.C. Slater, Phys. Rev. <u>172</u>, 1126 (1968).

About 50 primary transitions have been identifed that populate levels of ^{235}U below 2 MeV excitation energy, including nearly all of the states seen earlier in thermal capture.[1] Level energies were determined with a typical uncertainty of 0.5 keV. Absolute photon intensities were obtained by comparison with the reaction $^{197}Au(n,\gamma)$.

The E1 and M1 primary transitions populate states of ^{235}U that are first or second members of bands of negative and positive parity, respectively. Parities are proposed on the basis of the average values of the reduced intensities $I_\gamma/E_\gamma{}^3$ over the three resonances.

7. Gamma Ray Spectroscopy from $^{240}Pu(n,\gamma)^{241}Pu$ at Resonance and 24-keV Neutron Energies
(R.C. Block†, R.C. Greenwood‡, H.I. Liou, and R.E. Chrien)

Neutron capture γ-ray spectra of $^{240}Pu(n,\gamma)^{241}Pu$ have been measured in resonances below 160 eV with the BNL fast chopper and at 24 keV with the Fe-filtered beam facility. The 24-keV spectrum clearly exhibits the primary transition to the $5/2^+$ ^{241}Pu ground state, and equal strengths to the lowest lying $1/2^+$ and $3/2^+$ states. We determine the excitation energies of the $1/2^+$ and $3/2^+$ states as 162.1 $\pm$ 0.9 keV and 171.8 $\pm$ 0.8 keV, respectively. Resonance capture shows a 5079.5 $\pm$ 0.3 keV γ-ray to the $1/2^+$ state which results in a neutron binding energy of 5241.6 $\pm$ 0.9 keV, when combined with the above. Absolute radiative decay widths have been determined relative to the partial capture widths in the 4.9 eV ^{197}Au resonance.

8. Gamma Ray Spectroscopy from $^{164}Er(n,\gamma)$ at Resonance and keV Neutron Energies
(B.K.S. Koene, R.C. Greenwood‡, H.I. Liou, and R.E. Chrien)

Neutron capture γ-ray spectra of $^{164}Er(n,\gamma)^{165}Er$ have been measured in resonances below 200 eV with the fast chopper and at 2 and 24 keV with the filtered-beam facilities in HFBR. For the nine resonances studied, absolute partial radiation widths have been determined relative to the partial widths in the 4.9 eV ^{197}Au resonance. States of ^{165}Er up to $\sim$ 2 MeV excitation energy were analyzed, with a typical uncertainty in the level energies of 0.5 keV. Restrictions on the spin-parity

---

[1] F.A. Rickey, E.T. Jurney and H.C. Britt, Phys. Rev. C5, 2072 (1972).
† Permanent address: Rensselaer Polytechnic Inst. Troy, New York.
‡ Permanent address: Idaho National Engineering Laboratory, Idaho Falls, Idaho 83401.

assignments of these levels were obtained from the observed systematics of primary γ-ray intensities in the three neutron energy regions.

9. Study of Levels in ^{36}Cl by Neutron Capture
(J. Kopecky†, K. Rimawi‡, H.I. Liou, and R.E. Chrien)

Thermal neutron capture intensities in the mass region near chlorine have recenly received considerable interest because of observed correlations with (d,p) spectroscopic factors. The correlation is observed for M-1 transitions to final ℓ=0 states in ^{36}Cl and is difficult to explain in any direct capture model. We have extended these measurements to higher energies by studying 25 keV neutron interactions, using an iron-filtered beam from HFBR, and by studying the 400 eV p-wave resonance in ^{35}Cl with the HFBR chopper. The data at higher energies are compared to thermal capture. We find a surprising over-all correspondence between radiative intensities at high and low neutron energies, but little evidence for correlations to s states as previously observed. The M-1 transitions are strongly enhanced in the resonance region and are quite comparable to E-1 strengths. The data taken at 25 keV indicate a strong probability that the previously accepted isotopic identifications of chlorine resonances at 25.3 and 26.6 keV are in error.

10. Study of the Filling of Shell Model Orbits in ^{109}Pd
(R.F. Casten, M.R. Macphail, J.A. Cizewski, G.J. Smith, D. Breitig, S.F. Mughabghab, and W.R. Kane)

The experiments on which this work is based consist of studies of the ^{108}Pd(n,γ)^{109} reaction at thermal energy and on the 2.96 eV resonance. The resonance was found to be P-wave with a spin of 3/2. This fact permits the spins of low-lying levels populated by strong primary transitions on resonance to be determined by measuring the gamma-ray angular anisotropy. Coupled with the thermal data (capture state spin-parity $1/2^+$) this has yielded a number of spin assignments for levels up to 1600 keV in ^{109}Pd, and the measurement of the absolute partial radiative widths for the resonance. In earlier reports the comparison of these widths with the predictions of the valence neutron model were discussed. The current emphasis of this work concerns the implications of several new spin assignments. Specifically, two states previously assigned J-π values of $7/2^+$ are now shown to have lower spin. This alters considerably the (d,p) and (d,t) spectroscopic factors for these states and, consequently, the sums of spectroscopic factors are closely related to the effective numbers of neutrons in each j-subshell and their revision provides the key to an existing puzzle known as the

† Permanent address: Reactor Centrum Nederland, Petten, The Netherlands
‡ Permanent address: N.Y. State Dept. of Health, Syracuse, New York.

g-7/2--h-11/2 anomaly. In this anomaly the spectroscopic factors indicated that the g-7/2 orbit was more empty than the h-11/2 orbit in Pd but fuller in the isotonic Sn nuclei while the h-11/2 orbit, a high lying one, was too full in the Pd region. The current data demonstrate that the anomaly for the g-7/2 orbit was due to incorrect spin assignments while that for h-11/2 is probably due to the failure to observe higher lying fragments. These results are important because of attempts to associate the anomaly with major breakdowns in basic stripping theory or with the onset of deformation in the Pd region. These results, particularly the revised spins and spectroscopic factors, have substantial impact on several recent theoretical treatments of the entire mass region.

11. The Level Scheme of ^{191}Os and Fragmentation of Nilsson Model Strength
(R.F. Casten, M.R. Macphail, W.R. Kane, G.J. Smith, and J.A. Cizewski)

As a part of the program on transitional nuclides we are studying two aspects of the level structure of ^{191}Os. First, the (n,γ) reaction at thermal energies was studied. A detailed level scheme including states up to 2 MeV has been developed. From the level energies, the spin-parity assignments made from these and earlier data, and the systematics of gamma-ray transitions, we have made several Nilsson model assignments for the states below $\sim$ 600 keV. The most interesting result is the almost unvarying pattern of intrinsic energies, rotational constants and gamma-ray branching ratios of the 1/2-[510] and 3/2-[512] rotational bands throughout the heavier tungsten nuclei and the osmium isotopes from ^{185}Os to ^{191}Os. This occurs in a mass region in which the even-even isotopes undergo a steady decrease in the deformation of their ground-state bands and in which negative parity high spin states with partially decoupled oblate structure appear. The second aspect of our study of ^{191}Os is an investigation of the fragmentation of Nilsson strength in the intermediate energy region from 1.2-2.5 MeV. The experimental technique in this phase relies on average resonance capture at 2 keV: this approach should disclose primary transitions to all 1/2 and 3/2 states up to some limiting excitation energy. In studying the fragmentation of model excitations it is essential to have this sort of experimental probe capable of disclosing all the fragments. The experimental phase of this work is complete and the results are currently being analyzed.

12. Rotational Band Assignments in ^{184}W Using Population Systematics
(R.F. Casten, M.R. Macphail, and W.R. Kane)

Using the methods of population systematics described in last year's report, we have established that the 1775-keV level in ^{184}W is a K=2 bandhead intrinsic excitation and not 2^+ rotational excitation of a K=1 band. The implications for the fragmentation of Nilsson model strength are pointed out. The result also allows a new assessment of the states of levels between 1600 and 1900 keV in ^{184}W. It has been possible to suggest that the 1/2-[510] x 3/2- [501], K=1,2 configurations occur as important amplitudes of states in this region and to discuss on a firmer footing the unusual rotational spacings that occur and their interpretation in terms of Coriolis mixing.

13. Level Structure in ^{196}Pt
(J.A. Cizewski, R.F. Casten, G.J. Smith, and W.R. Kane)

As part of our continuing study of this region we have studied the reaction ^{195}Pt(n,γ)^{196}Pt on the 11.9 eV resonance. High resolution gamma-ray singles experiments have been carried out on a natural target. Further singles as well as gamma-gamma coincidence experiments using an enriched target are planned. The data are currently being analyzed and a level scheme developed. In the light of our findings concerning 0^+ excitations in ^{188,190}Os, the principal current emphasis is on similar states in ^{196}Pt. Levels known to be 0^+ occur at 1135, 1403, and (possibly) 1824 keV. The analysis so far rather clearly shows that the branching ratios of transitions from these states to lower-lying 2^+ levels differ qualitatively from the corresponding ratios for ^{188,190}Os and, in fact, appear to resemble more closely the nuclei ^{200,202}Hg. Further work is in progress.

14. Levels in ^{243}Pu with the (n,γ), (d,p), and (d,t) Reactions
(R.F. Casten, W.R. Kane, J.R. Erskine (ANL), A.M. Friedman (ANL), and D.S. Gale (East Texas State Univ.))

This nuclide demonstrates the power of combining (n,γ) studies with charged particle data. The resulting level scheme is one of the most extensive in existence for the actinides. One result for ^{243}Pu beyond those earlier is that the 1/2-[501] orbital does not appear to be significantly fragmented in ^{243}Pu, in contrast to ^{241}Pu. Current theoretical efforts are under way by others at Argonne National Laboratory to understand the active degrees of freedom and their couplings that are responsible for this effect. It might be noted that the 1/2-[501] orbital is particularly important since it plays an essential role both in the (p,t) and (t,p) cross sections to excited 0^+ states in the actinide nuclei and in the fragmentation of Nilsson strength in the heavy rare-earth nuclei.

A list of publications by members of the BNL Neutron-Nuclear Group in the period March 1975 through 1976 is as follows:

Bhat, M.R., Chrien, R.E., Cole, G.W., and Wasson, O.A. Neutron capture gamma rays from Sn-116 and Sn-122 and the valence model. Phys. Rev. C12, 1457-1461 (1975).

Block, R.C., Greenwood, R.C., Liou, H.I., and Chrien, R.E. Gamma-ray spectroscopy from 240-Pu(n,γ)241-Pu at resonance and 24 keV neutron energies. Bull. Am. Phys. Soc. II, 20, 1197 (1975).

Casten, R.F., Macphail, M.R., and Kane, W.R. Character of the 1775 keV state in 184-W. Phys. Rev. C12, 821-826 (1975).

Casten, R.F. Nuclear structure studies with the (n,γ) reaction. Bull. Am. Phys. Soc. II, 20, 1186 (1975).

Casten, R.F. Study of complex states in deformed nuclei with the (n,γ) reaction. Presented at 1975 Meeting of the American Physical Society Southeastern Section, Auburn, Ala., November, 1975.

Casten, R.F., Burke, D., and Hansen, O. The 180,182-W(t,p) reactions at 15 MeV. Nucl. Phys. (in press).

Casten, R.F., Kane, W.R., Erskine, J.R., Friedman, A.M., and Gale, D.S. Study of 243-Pu with the (n,γ), (d,p), and (d,t) reactions. Phys. Rev. (submitted).

Casten, R.F., Macphail, M.R., Cizewski, J.A., Smith, G.J., Mughabghab, S.F., Breitig, D., and Kane, W.R. The 108-Pd(n,γ)109-Pd reaction and shell model states in 109-Pd. Nucl. Phys. (submitted).

Chrien, R.E. Neutron capture cross section measurement techniques. NBS Special Publication 425, Vol. I, 139 (1975).

Chrien, R.E., Cole, G.W., Slaughter, G.G., and Harvey, J.A. The failure of the Bohr's compound nucleus hypothesis for the 98-Mo(n,γ) 99-Mo reaction. Phys. Rev. C13, 578-594 (1976).

Chrien, R.E., Kopecky, J., and Liou, H.I. Low energy gamma rays from 238-U(n,γ)239-U. Bull. Am. Phys. Soc. II, 20, 1155 (1975).

Cizewski, J., Casten, R.F., Kane, W.R., and Mughabghab, S.F. Spins of levels in 109-Pd from p-wave resonance neutron capture. Bull. Am. Phys. Soc. II. 20, 1195 (1975).

Flynn, E.R., Hansen, O., Casten, R.F., Garrett, J.D., and Ajzenberg-Selove, F. (t,p) reactions with 36,38,40-Ar. Nucl. Phys. A246, 117-140 (1975).

Garg, J.B., Cole, G.W., Liou, H.I., and Chrien, R.E. Resonance neutron capture gamma rays from 168-Er. Phys. Rev. (in press).

Gelletly, W., Kane, W.R., and Casten, R.F. Thermal neutron capture on 142-Ce. Phys. Rev. (in press).

Greenwood, R.C., Chrien, R.E., and Reich, C.W. keV neutron capture studies in 232-Th. Bull. Am. Phys. Soc. II, 20, 1197 (1975).

Greenwood, R.C., Chrien, R.E., and Rimawi, K. Radiative capture on neutrons in the keV region. NBS Special Publication 425, Vol. I, 912 (1975).

Kopecky, J., Rimawi, K., Liou, H.I., and Chrien, R.E. Study of 35-$C\ell(n,\gamma)$36-$C\ell$ with epithermal neutrons. Bull. Am. Phys. Soc. II, 20, 1195 (1975).

Liou, H.I., and Chrien, R.E. Low energy neutron resonance parameters of 238-U. Presented at Annual Meeting of American Physical Society, New York, February 1976.

Macphail, M.R., Casten, R.F., and Kane, W.R. Systematics of the population of rotational bands in deformed nuclei in the (n,γ) reaction. Phys. Lett. 58B, 39-42 (1975).

Macphail, M.R., Casten, R.F., and Kane, W.R. Study of 191-Os by the (n,γ) reaction. Bull. Am. Phys. Soc. II, 20, 1154 (1975).

Macphail, M.R., Casten, R.F., and Kane, W.R. Gamma-ray de-excitation of 0^+, 2^+ states in 188,190-Os. Phys. Lett. 59B, 435-439 (1975).

Rimawi, K., and Chrien, R.E. Activation cross sections at 24 keV. Bull. Am. Phys. Soc. II, 20, 173,(1975).

Rimawi, K., and Chrien, R.E. Measurement of 24.3 keV activation cross section with the iron filter technique. NBS Special Publication 425, Vol. I, 920 (1975).

Rimawi, K, and Chrien, R.E. Gamma-ray spectra from ℓ=1 neutron capture near 24 keV. NBS Special Publication 425, Vol. I, 926 (1975).

von Egidy, T. Kaiser, W., Mampe, W., Balodis, M.K., Prokofje, P.T., Simonova, L.I., Lanier, R.G., Muhlbauer, K., Schult, O.W., Koch, H.R., Baader, H.A., Mlekodaj, R.L., Sheline, R.K., Shera, E.B., Ungrin, J., Seyfarth, H., Kardon, B., Delang, W., Gottel, P., Breitig, D., Kane, W.R., Casten, R.F., Scheerer, H.J. Glassl, P., Huenges, E., Loffler, M., Rosler, H., Vonach, H.K., Rabenstein, D., Hillenbrand, C., Stoffl, W. The odd-odd nucleus Eu-152. Contribution to the 26th All Union Conference on Nuclear Spectroscopy and Nuclear Structure, Baku, USSR, January 1976.

B. NATIONAL NEUTRON CROSS SECTION CENTER

1. Data Libraries

NNCSC has continued the literature coverage of publications originating in the United States and Canada for the CINDA publication. In addition, during the past year a project to upgrade the contents of CINDA was undertaken. The references for a single experiment have been linked together, obsolete references removed from the book (but not from the computer file) and data index lines to indicate the availability of numerical data at NNCSC for nearly 500 experiments completed since 1970.

Data from approximately 140 experiments performed in the United States and Canada have been compiled and added to the CSISRS experimental data library. This constitutes about 40% of the total new data added to the library in the past year. The remaining 60% of the data was compiled by the other three neutron data compilation centers. In the past year, a special effort was made to complete the conversion of the old BNL data files to the CSISRS format. All data were checked and the sets upgraded to format specifications. Data quoted in the new edition of BNL-325 but missing from the old computerized files were added during this operation.

During the past year the ENDF/B Dosimetry and Fission Product libraries were released for international distribution. Preparation for ENDF/B version V is well under way. The neutron standard reactions cross sections have been evaluated. Computer processing programs have been upgraded to reflect format changes. A library of evaluated data for the actinides is now being constructed for use in fuel burn up, reprocessing and waste management calculations. A preliminary tape will be available in May.

NNCSC continues to provide special services to the neutron community. Statistics for these services provided between January 1, 1975 and December 31, 1975 are attached.

2. Data Evaluation and Data Testing

The evaluation of (n, particle) cross sections of all the stable isotopes of nickel, chromium and manganese from threshold to 20 MeV has been completed. In addition, the resolved resonance region of manganese has been fitted up to 250 keV. These will be used as parts of the evaluations for the elements nickel, chromium and manganese for ENDF/B-V.

The NNCSC Data Testing Group was active in the past year in analyzing a great number of fast, thermal and shielding benchmarks as a means of validating evaluated data files. The NNCSC has been actively involved in the evaluation, development and use of Monte Carlo transport code. We have exhaustively studied the effects of U-238 resonance capture and the validation of this data with regards to thermal integral benchmark experiments of low enrichment uranium lattices. In these studies Monte Carlo was effectively used to calculate the resonance reaction rates.

The NNCSC also sponsored a seminar on the subject in March 1975. The results of this seminar greatly assisted the reactor community to resolve some of the computational and accurate data acquisition problems associated with the analysis of these critical assemblies. The seminar also stimulated new measurements of U-238 resonance parameters.

3. Publications

The new edition of BNL-325 Vol. II is now in press and should be available in the summer 1976. Summary documentation (ENDF-201) and the "book of curves" (ENDF-200) for version IV of ENDF/B are now available. The Codes and Formats Manual (ENDF-102) will be available in April. A new publication of decay schemes for fission product nuclides based on ENDF/B-IV data will be available before the end of 1976.

Table B-1

Request Statistics for Experimental Information

Jan. 1, 1975 to Dec. 31, 1975

1.	Requests	
	a) Number of requests	188
2.	Origin of Requests	
	a) Government Agencies	8
	b) Educational Institutions	34
	c) Industry (includes CSEWG members)	28
	d) Foreign	10
	e) Four-Center Members	30
	f) National Laboratories (includes CSEWG members)	78
3.	Mode of Requests (may be more than one mode per request)	
	a) Magnetic Tapes	70
	b) Computer Listing	131
	c) Cards	1
	d) Plots	33
	e) Documentation	53
	f) Telephone	16
	g) Teletype	0

Table B-2

Request Statistics for
Evaluated Information

Jan. 1, 1975 to Dec. 31, 1975

1.	<u>Requests</u>	
	a) Number of requests	356
2.	<u>Origin of Requests</u>	
	a) Government Agencies	13
	b) Educational Institutions	66
	c) Industry	31
	d) Foreign (includes Four-Center Members)	56
	e) CSEWG Members	190
3.	Mode of Requests (may be more than one mode per request)	
	a) Magnetic Tapes	156
	b) Computer Listings	122
	c) Cards	4
	d) Plots	31
	e) Documentation	196
	f) Telephone	8
	g) Teletype	1

Columbia University
Division of Nuclear Science and Engineering

Studies of the Neutron Interaction with Fissile and Fertile Nuclei

B. Luers, J.P. Felvinci, E. Melkonian and W.W. Havens, Jr.

^{235}U Fission Fragment Kinetic Energies

We have reported during the Nuclear Cross Sections and Technology Conference[1] results on pulse height effects in the resonance energy region of ^{235}U. Subsequently a measurement by Weigmann et al[2] has been reported which did not observe the effects we saw. In order to clarify the situation, we performed another experiment at ORELA in the summer of 1975. We used three larger targets instead of one small one and slightly changed the target-detector configuration. The number of events recorded was 15 times higher than in the 1973 measurement.

The results were indecisive; we did not obtain the clearcut effect, which was expected because of the improvement in statistics. However, the same type of patterns persisted, as were reported earlier. We tried different techniques in analyses, i.e. contingency tables, Kolmogorov-Smirnov statistics and Fourier analysis. All of these showed non-statistical effects but did not produce a unified picture.

These results baffled us to such a degree that we postponed reporting on the results until more conclusive evidence is found which will confirm or refute the earlier results. The evidence points to the existence of pulse height effects but at a more complex level than previously interpreted.

A more informative experiment would be the measurement of the energies of both fragments in coincidence, which yields information on the mass and total kinetic energy distributions. We did try this experiment during the 1975 run and obtained some encouraging results but the statistics were very poor.

We are presently in the process of collecting data at ORELA on the double energy experiment, and some results should be available on the mass distributions of ^{235}U resonances by early fall 1976.

---

1. J.P. Felvinci, E. Melkonian and W.W. Havens, Jr., Proceedings of the Nuclear Cross Sections and Technology Conference, p. 580 (1975)

2. H. Weigmann et al., Physical Review Letters, 35, 1213 (1975)

Fission Cross Sections of ^{229}Th

We have reported earlier[1] on the measurement of cross sections of ^{229}Th. A repetition of this measurement to obtain better statistics is under way at ORELA. Preliminary results indicate that the average level spacing of ^{229}Th is quite small, $\langle D \rangle \sim 0.3$ eV (0 - 30 eV). This figure is similar to the we reported on ^{235}U[2]. In the case of ^{229}Th the average fission width seems to be also smaller than in ^{235}U, so it is much easier to separate the levels. The data which are being collected at present are of good quality and more detailed results should be available by fall 1976.

---

1. J.P. Felvinci et al, BAPS Vol. 16, No. 1, p. 16 (1971)

2. See (1) of first page.

Columbia University
Nevis Labs

Current activities are focussed on completion of data analysis on ^{181}Ta, ^{140}Ce and $^{63,65}Cu$. Journal articles containing tables of resonance parameters E_0, $g\Gamma_n^0$, $\Gamma\gamma$ and including strength functions, level spacings, and cross section information will be prepared for these isotopes. An article on ^{209}Bi appears in Physical Review C, January 1976. A paper on ^{139}La is scheduled for the May 1976 issue of Physical Review C.

Over the past year, our group has continued to be active in communicating our neutron cross section results (stored on magnetic tapes) to the National Neutron Cross Section Center at Brookhaven National Laboratory.

The Nevis Cyclotron, which is used as a source of moderated neutron beam in NVS experiments, is now in the final stages of its improvement program. Prior to the start of modification it produced 1.5μ amps of 350 MeV protons. There is currently an internal beam of ∿9μ amps of 560 MeV protons. It is anticipated that beam intensity will be improved significantly, and that the machine will be available for experimentation in the near future. At that stage NVS data acquisition will begin again, using a far more intense neutron beam than was available in the past. (A complete summary of pre-cyclotron-modification experimental characteristics and of published results through mid-1975 can be found in Ref. 1, which also contains a list of references.)

Ref. 1: G. Hacken, H.I. Liou, J. Rainwater, U.N. Singh, Neutron Resonance Spectroscopy at Nevis Laboratories, in Nuclear Cross Sections and Technology, Proceedings of a Conference, Vol. 2, NBS Special Publication 425, Ed. by R.A. Schrack and C.D. Bowman

A. STANDARDS

1. Fission Cross Sections of ^{235}U and ^{238}U Near 14 MeV. (G. W. Carlson)

Measurements of the fission cross sections of ^{235}U and ^{238}U near 14 MeV are being planned. The goal of the measurements will be to determine the absolute cross sections with an uncertainty less than 2% and to measure the shape of the cross sections versus neutron energy from 13.7 to 15 MeV. The measurements will be made using the LLL Rotating Target Neutron Source (RTNS).

B. NEUTRON DATA APPLICATIONS

1. High Energy Fission Cross Section Ratio Measurements. (J. W. Behrens, G. W. Carlson, and J. C. Browne)

We have completed the neutron-induced fission cross section measurements on a series of plutonium isotopes using ionization fission chambers at the LLL 100-MeV electron linear accelerator. Ratios of the cross sections of ^{239}Pu, ^{240}Pu, ^{241}Pu, and ^{242}Pu relative to ^{235}U have been measured as functions of neutron energy over the range .001 to 30 MeV, except where limited by low cross sections on the threshold isotopes. We normalized the results independent of other measurements by using the threshold cross section method. These ratio measurements[1-3] were obtained in a manner similar to the series of uranium isotopes

[1] G. W. Carlson and J. W. Behrens, Fission Cross Section Ratio of ^{239}Pu to ^{235}U from 0.1 to 30 MeV, Lawrence Livermore Laboratory, Rept. UCID-16981 (1975).

[2] J. W. Behrens and G. W. Carlson, Measurement of the Neutron-Induced Fission Cross Section of ^{241}Pu Relative to ^{235}U from 0.001 to 30 MeV, Lawrence Livermore Laboratory, Rept. UCRL-51925 (1975).

[3] J. W. Behrens, J. C. Browne, and G. W. Carlson, Measurements of the Fission Cross Sections of ^{240}Pu and ^{242}Pu Relative to ^{235}U, Lawrence Livermore Laboratory, Rept. UCID-17047 (1976).

which were presented at the Conference on Nuclear Cross Sections and Technology, March 3-7, 1975[4].

2. Fission Cross Sections of ^{233}U, ^{239}Pu and ^{241}Pu relative to ^{6}Li. (J. B. Czirr, J. W. Behrens, and G. W. Carlson)

We have obtained fission cross section data for ^{241}Pu, ^{239}Pu and ^{233}U in the energy range from 10 eV to 70 keV. The incident neutron spectrum was measured with a thin ^{6}Li-glass scintillator and energies were obtained by time of flight. The cross sections will be normalized to accepted thermal values by using similar data obtained in the thermal to keV range. The results will be separated in broad energy bins to improve the statistical precision.

3. Fission $\bar{\nu}$ Measurements. (R. E. Howe and T. W. Phillips)

Measurement of $\bar{\nu}$ for $^{235}U(n,f)$ in the MeV region ($E_n \leq 25$ MeV) is nearing completion. Preliminary results are shown in Figure B-1. These data were normalized to the recommended prompt $\bar{\nu}$ values of Manero and Konshin[5] in the energy range 0.5 to 1.0 MeV but using a prompt $\bar{\nu}$ for ^{252}Cf (spontaneous fission) = 3.724. Work is currently underway to normalize our results to the thermal energy value of $\bar{\nu}$ for ^{235}U, to calibrate our neutron energy scale, and to investigate the influence of some potential systematic effects on our results. These latter are not expected to exceed the statistical errors in $\bar{\nu}$ shown in the figure.

Current plans are to proceed with prompt $\bar{\nu}$ measurements at MeV energies for other isotopes when the ^{235}U work is completed.

4. Fission Cross Section of ^{245}Cm. (J. C. Browne)

The fission cross section of ^{245}Cm has been measured from 0.006 eV to 20 eV using an isotopically-pure 3-μg sample of ^{245}Cm obtained by Savannah River Laboratory from the decay of ^{249}Bk. These data, which were taken at a 3.5-m flight path at the LLL 100-MeV linac, are presently being analyzed.

---

[4] J. W. Behrens, G. W. Carlson, and R. W. Bauer, "Neutron-Induced Fission Cross Sections of ^{233}U, ^{234}U, and ^{238}U with Respect to ^{235}U, Proc. Conf. Nuclear Cross Sections and Technology, Washington, D.C., March 3-7, 1975, Vol. 2, p. 591.

[5] Manero, Rl, Konshin, V. A., Atomic Energy Review 10, (1972) 637.

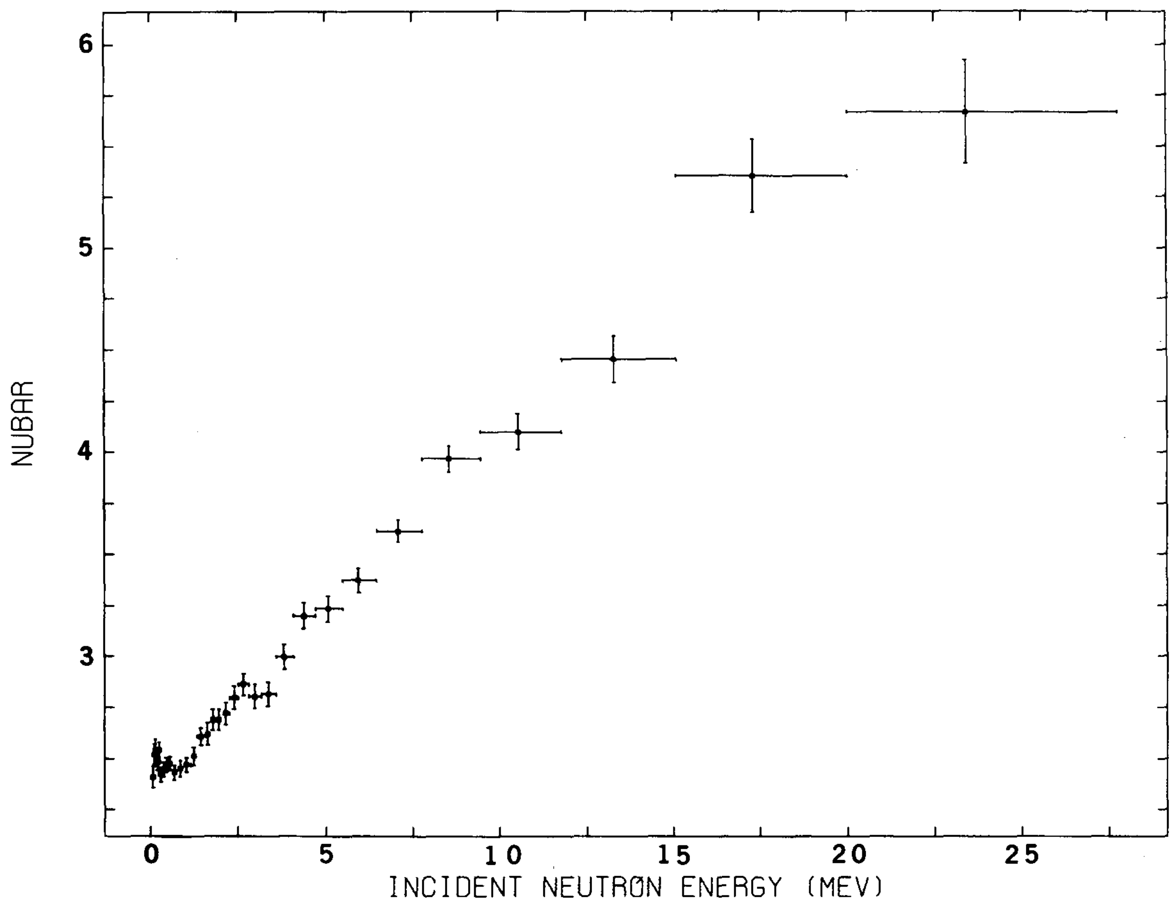

Figure B-1. Prompt $\bar{\nu}$ for ^{235}U (n,f) versus incident neutron energy. Data have been corrected for deadtime losses and background neutrons. Horizontal error bars represent the inclusive neutron energies used in the calculation of each data point.

5. Measurements of the $^7Li(p,n_0)^7Be$ and $^7Li(p,n_1)^7Be^*$ Cross Sections Between 4.2 and 26 MeV. (S. M. Grimes, C. H. Poppe, J. D. Anderson, J. C. Davis and C. Wong)

Cross sections for the $^7Li(p,n_0)^7Be$ and $^7Li(p,n_1)^7Be^*$ reactions have been measured over the energy ranges 4.25 to 12 MeV and 15.1 to 25 MeV in 1-MeV steps. The data span the angular range 3.5 to 159° and were obtained with the LLL cyclograaff and multi-detector TOF spectrometer. Because the thickness of the Li target was known only roughly, the absolute cross sections were fixed by normalizing them to the value measured by Gibbons and Macklin[6] at 5 MeV. This normalization agreed to within 4% with that inferred from a measurement of the $^7Li(p,n_0)$ and $^7Li(p,n_1)$ cross sections at forward angles (where the n_0 and n_1 neutron groups are higher in energy than any neutrons from $^{19}F(p,n)$) with a LiF target of known thickness.

At the highest energies ($E \gtrsim 20$ MeV), the n_0 and n_1 groups were incompletely resolved at a flight path of 10.8 m; the separate cross sections were obtained by using a peak fitting routine. This procedure was tested by performing 0° measurements with a flight path of 30 m; good agreement between the cross sections obtained in the two different measurements was observed. The forward angle ratio of neutrons in the n_1 group to those in the n_0 group is larger than 25% for all energies above 7 MeV, reaching a peak of 55% at 9 MeV. This ratio then falls to about 30% near 17 MeV and is 35% at 26 MeV.

It is concluded that the large n_1 cross section and the large flux of lower energy neutron make the $^7Li(p,n)$ reaction inappropriate as a neutron source for some applications; however, the large forward angle cross section (30 mb/sr at 26 MeV) makes it attractive in situations where large fluxes of lower energy neutrons do not pose a problem.

6. Calculations of Neutron Reactions with ^{238}U. (D. G. Gardner)

The following is an abstract of an LLL Chemistry Department Technical Note No. 75-48.

> "Preliminary calculations are presented for various neutron reactions with ^{238}U over the incident energy range 10 keV to 5 MeV. The statistical model calculations were performed with the COMNUC-CASCADE code, and direct inelastic scattering input was provided by the coupled-channel codes JUPITOR and FOURPLUS. Excitation functions are given for the total, elastic, inelastic, capture and fission reactions as well as inelastic scattering to the first 2+ and 4+ states.

[6] J. H. Gibbons and R. L. Macklin, Phys. Rev. 114, 571 (1959).

Some angular distributions are shown for elastic scattering to the 2+ and 4+ states. Comparisons are provided between the present calculations and the ENDL and ENDF/B-IV evaluated data libraries."

7. An Investigation of the Dependence of γ-Ray Spectral Shape on the Averaging Interval Size for the ^{181}Ta (n,γ) Reaction. (M. L. Stelts* and J. C. Browne)

The γ-ray spectra for the ^{181}Ta(n,γ) reaction were measured from 2 eV to 90 keV neutron energy at the LLL 100-MeV linac using a three-crystal (Ge(Li)-NaI) spectrometer. The γ-ray spectra were unfolded using the measured δ-function response of the spectrometer as described in Report No. UCRL-77467 (accepted for publication in Nuclear Instruments and Methods) and averaged into broad neutron energy bands. The results are shown in Fig. B-2. The spectra are identical (to within experimental error) except in the γ-ray energy region from 5 to 6 MeV where there is a systematic decrease in strength as the neutron energy increases.

8. Calculations of the Neutron Emission Spectra from Materials Bombarded with 14-MeV Neutrons. (L. F. Hansen, S. M. Grimes, R. J. Howerton and J. D. Anderson)

Neutron emission spectra from targets bombarded by 14-MeV neutrons have been calculated using three nuclear models. The elements studied included Al, Fe, Cu, Ni, and Nb and were selected because of their potential importance in fusion reactor design and because measured cross sections and calculated cross section libraries are available for comparison with the calculations.

The main features of the calculation are: 1) Contributions from statistical, preequilibrium and direct reactions are included to achieve a good fit to the data; 2) It does not make use of experimental neutron data to generate the cross sections; 3) It does make use of nuclear reaction systematics and deformation parameters, as inferred from charged particle measurements, to predict the neutron inelastic spectra above 6 MeV. For 14-MeV neutrons incident on a nucleus, the statistical model predicts quite adequately the low energy part of the emitted spectrum, but underestimates the production of higher energy neutrons. These neutrons are the result of pre-equilibrium processes or direct reactions. The pre-equilibrium processes have been calculated using the hybrid model of Blann where it is assumed that the compound nucleus reaches equilibrium through a series of two-body interactions. The

*Now at Brookhaven National Laboratory.

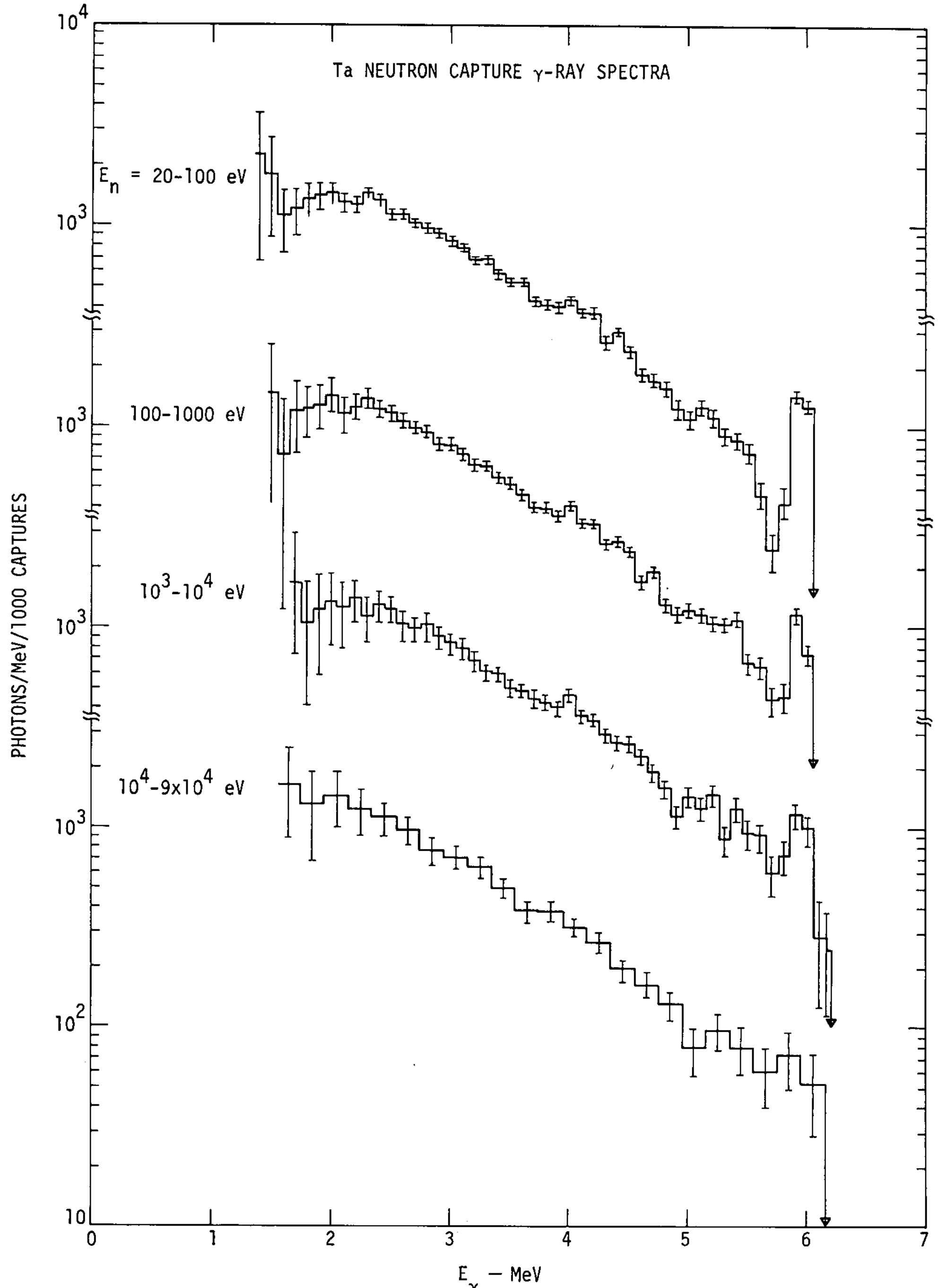

Fig. B-2. Results of unfolding ^{181}Ta(n,γ) spectra for the neutron energy region between 20 eV and 9x10^4 eV. Background has been subtracted, detector efficiency and absolute normalization applied to give absolute intensities in photons/MeV/1000 captures.

direct inelastic (n,n') cross sections to the lower excited levels were calculated using the Oregon State University's Coupled-Channel-Code (C-CH-C) assuming a collective model for the interactions. Contributions to the inelastic neutron spectrum from the (n,2n) cross section were calculated assuming the emission of the second neutron to be statistical. The results of this calculation are shown in Figure B-3.

A complete summary of the results and their comparison with those predicted by the ENDF/B-IV and ENDL neutron evaluated libraries together with experimental measurements available for the above nuclei can be found in UCRL-77778*. The calculations reproduce the experimental results fairly well; since no experimental neutron data were used to generate them and the calculations are based in nuclear models well supported by experiments, this suggests that the predicted secondary spectra from other materials bombarded with 14-MeV neutrons, where no measurements are available, may be equally accurately predicted.

9. Comparison Between Measurements and Calculations Using the ENDF/B-IV Neutron Library for Structural Materials Used in Fusion Reactors. (L. F. Hansen, C. Wong, T, Komoto and J. D. Anderson)

Measurements of the integral neutron energy spectra from C, O, Al, Ti and Fe, obtained using the pulsed sphere and time-of-flight techniques, were compared with the predictions of the most recent version of the ENDF/B-IV library. Spherical assemblies of the above materials ranging from 1 to 5 mean-free-paths were bombarded with a centered 14-MeV (nominal) neutron source. Since these materials have been used by different authors[7] in the design of the CTR fusion blanket structures and their calculations have been carried out with the preceding version III of the ENDF/B library, the above integral measurements were also calculated with this early library.

Table B-1 gives the calculated integrals with versions III and IV for Al, Ti and Fe (the complete results of these measurements can be found in UCRL-77270†). The integrals are given in neutrons per source neutron for three neutron energy intervals: 15 MeV to 10 MeV, 10 to 5 MeV and 5 to 2 MeV. Use of the ENDF/B-IV cross sections resulted in larger calculated total integrals and closer agreement with the measurements. Discrepancies of 10-20% still exist for the 2-10 MeV region for the thicker spheres in Table I, but version IV of the library represents a clear improvement over the ENDF/B-III library, where discrepancies of as much as a factor of 2 existed between measurements and

---

*This work has been accepted for publication by Nuc. Sc. & Eng. (1976).

[7] R. G. Alsmiller, Jr., R. T. Santoro, J. Barish and T. A. Gabriel, Nuc. Sci. and Eng. 57, 122 (1975).

†The paper has been accepted for publication in Nuc. Sci. and Eng. To be published 1976.

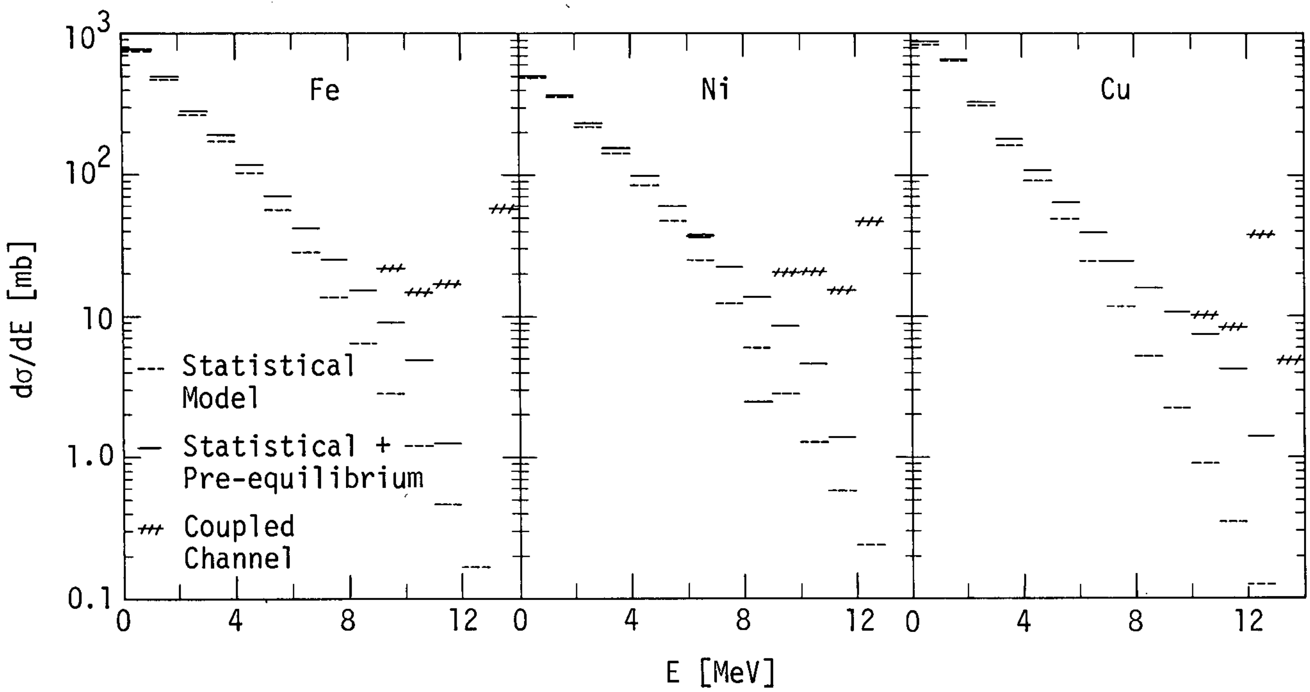

Fig. B-3. Calculations of the compound nucleus cross sections for Fe, Ni, and Cu (---); the respective pre-equilibrium contribution added to each of the above cross sections (-); direct contribution to the inelastic (n,n') cross sections for the lower excited levels in these nuclei (⧻).

Table B-1. Measured and calculated Integrals with Versions III and IV of the ENDF/B Library for the energy intervals 15-10, 10-5 and 5-2 MeV. The integrals are given in neutrons/source neutron.

MATERIAL	mfp	θ	ENERGY INTERVAL	EXPERIMENT ± 7%	TART ENDF/B-IV	TART ENDF/B-III
ALUMINUM	0.9	30°	15-10	4.603-02	4.615-02	4.971-02
			10-5	0.398-02	0.448-02	0.152-02
			5-2	0.785-02	0.693-02	0.554-02
			TOTAL	5.786-02	5.756-02	5.677-02
TITANIUM	1.2	30°	15-10	4.083-02	4.401-02	5.237-02
			10-5	0.319-02	0.233-02	0.088-02
			5-2	1.072-02	0.774-02	0.593-02
			TOTAL	5.474-02	5.408-02	5.918-02
IRON	0.9	30°	15-10	4.854-02	4.915-02	4.970-02
			10-5	0.275-02	0.276-02	0.091-02
			5-2	0.810-02	0.704-02	0.482-02
			TOTAL	5.939-02	5.895-02	5.543-02

calculations. Fig. B-4 shows the measured and calculated energy spectra with library IV for Al, Ti and Fe.

10. Measurements and Calculations of the Gamma Spectra from Nitrogen for a 14-MeV Neutron Source. (L. B. Hansen, T. Komoto, E. F. Plechaty, B. A. Pohl and C. Wong)

In the last USNDC report, UCID-16725 (March 11, 1975), measurements of the gamma spectra from 0.5, 1.0 and 3.0 mfp nitrogen bombarded with 14-MeV neutrons were reported. The measurements were done using the pulsed sphere transmission and time-of-flight techniques using NE213 scintillators at angles of 26° and 120° for flight paths ranging between 7 m and 10 m. At that time calculations with the ENDF/B-IV neutron-photon library were also reported, where the recoil electron response of the detector was calculated with the Monte Carlo Photon Transport code TORTE. The response function of the detector has been recalculated using a Monte Carlo Electron-Photon Transport code TORTE-EP. This code follows electrons and positrons from Compton, and photons from photoelectric and pair interactions until they have either stopped or have left the detector system. In the present calculations, a correction factor for the air absorption of the source neutrons was included which was not used in the original calculations. Also a new measurement for 7.0 mfp nitrogen was carried out.

The integrals of the measured and calculated spectra, corresponding to the total number of electron pulses above bias per source neutron, are given in Table B-2. The values have been normalized to a flight path of 10 m. The measured integrals for the 26° and 120° detectors, normalized to the same flight path of 10 m, show differences smaller than the quoted experimental errors of 7.5% and hence have been averaged for comparison with the calculations. The discrepancies are much less than 20%. A fraction of these discrepancies may be attributed to the use of the calculated detector efficiency which is between 5 and 8.0% too high.

11. Measurement of (n,xp), (n,xd) and (n,xα) Cross Sections for ^{27}Al, ^{46}Ti and ^{48}Ti at 14 MeV. (S. M. Grimes, R. C. Haight and J. D. Anderson)

Cross sections for (n,xp), (n,xd) and (n,xd) reactions induced by 14-MeV neutrons on ^{27}Al, ^{46}Ti and ^{48}Ti have been measured with a quadrupole spectrometer. Particles with energies as low as 0.8 MeV were detected. Large sub-Coulomb barrier peaks are found in the proton spectra from ^{27}Al and ^{46}Ti but not for that of ^{48}Ti; alpha particle and deuteron spectra do not show such a peak. The presence or absence of such a peak is related to the importance of the (n,n'p) reaction for a given isotope. Enhancement of the total charged particle cross section

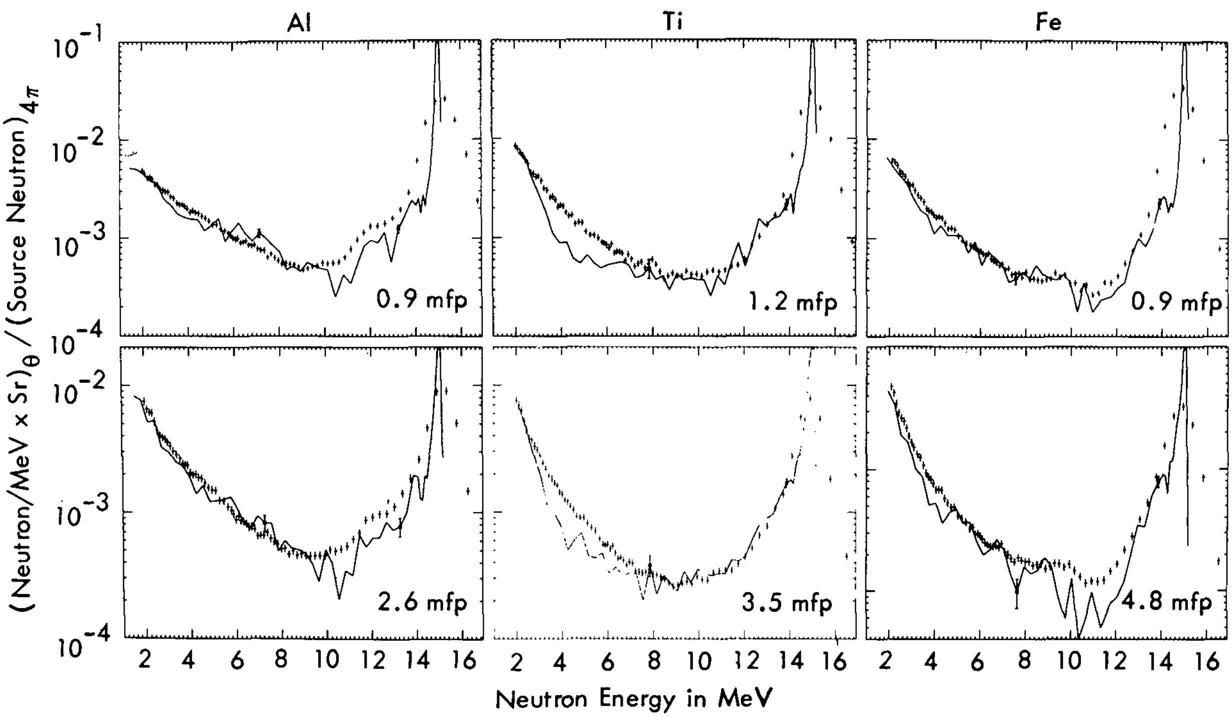

Figure B-4. Measured (+) and calculated (line) energy spectra using ENDF/B-IV for 0.6 and 2.6 mfp aluminum, 1.2 and 3.5 mfp titanium, and 0.9 and 4.8 mfp iron.

Table B-2. Measured integrals of the gamma-ray spectra from nitrogen as a function of mean free path, and calculated integrals using ENDF/B-IV. The integrals correspond to the total number of electron pulses above 340 keV electron bias per source neutron.

θ	mfp	Measured* x 10^{-8} ± 7.5%	Calculated* ENDF/B-IV x 10^{-8}	Discrepancy† (%)
26	0.5	3.947	4.815	19
120	0.5	4.199	4.850	
26	1.0	5.661	6.639	13
120	1.0	6.132	6.743	
30	3.0	7.417	7.867	4.5
120	3.0	7.674	7.908	3.6
26	7.0	2.935	2.833	

*Normalized to 10 m flight path.

†Discrepancy between the calculated and measured integrals. (The ratio was calculated for the respective average values from the two angles.)

by about 65% through such reactions is found for ^{27}Al and ^{46}Ti. Such charged particle cross sections are important in estimating materials damage problems in fusion reactors. Nuclear transmutation and hydrogen and helium accumulation are directly related to charged particle cross sections. It appears that the presence or absence of a large (n,n'p) cross section (because of the (n,2n) Q value) could be an important consideration in the choice of materials for fusion reactor construction.

12. Reaction Rates In A Uranium Pile Surrounding A 14-MeV Neutron Source: Calculations of the Weale Experiment. (R. C. Haight, J. D. Lee and J. A. Maniscalco)

A report (UCRL-77364, Rev. 1) on this subject has been submitted to Nuclear Science and Engineering. Results of the calculation are summarized in Table B-3. The abstract of this paper follows:

> "To validate the neutronics analysis of hybrid fusion-fission reactor blankets, calculations were made of an experiment by Weale *et al.*,[8] where a 14-MeV neutron source was surrounded by a natural uranium metal pile. The evaluated nuclear data libraries, ENDL and ENDF/B, were used. The calculated parameters were found to be in closer agreement for present versions* of these libraries than for preceding versions; however, there were still 15% differences in the ^{235}U(n,f) and ^{238}U(n,f) reaction rates. The present version of ENDL gives results that are the closest to the experimental values for these reactions. For the ^{238}U(n,γ) reaction, the calculations with the ENDF/B libraries are closer to the measured values. Both the ENDL and ENDF/B evaluations, however, fail to calculate correctly the neutron leakage or derived values for the ^{238}U(n,2n) and ^{238}U(n,3n) reaction rates. The spatial variations of the ^{235}U(n,f), ^{238}U(n,γ), ^{238}U(n,f) and ^{239}Pu(n,f) reaction rates show that the penetration of high-energy neutrons in the pile is better described by the calculation with ENDL, which gives a greater penetration. The effects of resonance self-shielding were investigated and found to require a correction much smaller than the differences between calculations with different data libraries."

---

[8] J. W. Weale, H. Godfellow, M. H. McTaggart, and M. L. Mullender, J. Nucl. Energy A/B 14, 91 (1961).

*Present version ENDF/B-IV.

Table B-3. Reactions per 14-MeV Source Neutron Integrated over the Pile

Reaction	Calculation				Experiment[a]
	Historical Libraries		Current Libraries		
	ENDF/B-III	ENDL(old)[b]	ENDF/B-IV	ENDL(new)[c]	
^{235}U(n,f)	0.226	0.287	0.228	0.266	0.281 ± 0.017
^{235}U(n,γ)	0.055	0.064	0.057	0.061	-
^{238}U(n,f)	0.828	1.31	0.949	1.11	1.18 ± 0.06
^{238}U(n,γ)	4.03	4.63	4.27	4.36	4.08 ± 0.24
^{238}U(n,2n)	0.328	0.417	0.358	0.388	0.277 ± 0.008[d]
^{238}U(n,3n)	0.173	0.179	0.176	0.195	0.327 ± 0.052[d]
Leakage	0.284	0.587	0.296	0.504	0.42 ± 0.02

[a] Integrated reaction rates were determined by drawing smooth curves through points measured at various positions in the pile and then integrating. The errors are those assigned in Ref. 8.

[b] ENDL (old) is the version of the LLL Evaluated Nuclear Data Library dated January 25, 1974.

[c] ENDL (new) is the version of ENDL dated February 18, 1975.

[d] Experimental values were actually derived based on the 14-MeV flux as determined by the ^{63}Cu(n,2n) ^{62}Cu results and on an assumed value of the ^{238}U(n,2n) ^{237}U or ^{238}U(n,3n) ^{236}U cross section at 14 MeV.

C. DATA COMPILATION PROGRAM

1. Recent Evaluations for Neutron-Induced Reaction Data. (R. J. Howerton)

At the request of the CSEWG, complete evaluations for ^{236}U, ^{242,243}Pu, ^{241,242m}, ^{243}Am, ^{244,245,246,247,248}Cm, ^{249,250,251,252}Cf were done for inclusion in the ENDF/B-V data file. The low neutron energy (<1 keV) data, for the transplutonium isotopes are based on the Savannah River Laboratory partial evaluation done by Benjamin. At higher energies most of the data are based on nuclear systematics for reaction and energy ranges where no measurements have been reported.

The LLL ENDL data file has been upgraded for all the uranium and plutonium isotopes. ^{231,233}Th have been added as complete evaluations. The fission cross sections have been modified by basing the ^{235}U fission cross sections for neutron energies greater than 800 keV on the Czirr-Sidhu measurements;[9] and for ^{233,234,236,238}U, ^{239,240,241,242}Pu the Behrens-Carlson ratios [1-4] were applied to the adopted ^{235}U fission cross section. Forty-six standard spherical critical assemblies fueled by ^{235}U, ^{233}U and ^{239}Pu and reflected by various materials were calculated using the TART Monte Carlo neutronics code. The resulting mean value for k_{eff} was .99934. To test the high energy (14-15 MeV) data, LLL pulsed spheres were calculated with excellent agreement with experiment.

A new version of the LLL ENDL data file in the ENDF/B format was distributed to LASL, NNCSC, and RSIC. The file is available from either of the latter two facilities.

A revised version of UCRL-50400, Vol. 6, "Tables and Graphs of Photon Interaction Cross Sections from 1.0 keV to 100 MeV Derived from the LLL Evaluated Nuclear Data Library," was distributed. Part A of Vol. 15 of UCRL-50400, "The LLL Evaluated Nuclear Data Library (ENDL): Evaluation Techniques, Graphical Displays and Descriptions of Individual Evaluations," was distributed. Volume 14 of UCRL-50400, "TARTNP: A Coupled Neutron-Photon Monte Carlo Code," was distributed. A revision of Vol. 5 of UCRL-50400, "CLYDE: A Nuclear Data-Processing Computer Program for Producing Calculational Constants," was distributed.

New editions of Volumes 2, 3, 7, 8, 10, and 16 of UCRL-50400 are being prepared. These are respectively the bibiography (Vol. 2), indexes (Vol. 3), graphical data (Vols. 7 and 8), and tabulation of experimental data (Vol. 10) of the Experimental Cross Section Information Library (ECSIL), and tables and graphs of 175 neutron group constants derived from ENDL (Vol. 16).

---

[9] J. B. Czirr and G. S. Sidhu, Nucl. Sci. Eng. 57, 18 (1975); Nucl. Sci. Eng. 58, 371 (1975).

D. BASIC PHYSICS

1. An Upper Limit On A Time-Reversal Non-Invariant Part Of Wigner's Random Matrix Model. (H. S. Camarda)

A report (UCRL-77501) has been accepted for publication in Physical Review C. The following is the abstract for this paper.

"The results of a Monte Carlo investigation and comparison with experimental data of Wigner's random matrix model with differing amounts of a time reversal non-invariant part are presented. With $H_{ij} = R_{ij} + iyI_{ij}$, calculations were performed with y = 0.00, 0.05, 0.10, 0.20, 0.50, and 1.00 using 40 x 40 matrices and y = 0.00, 0.05, an 0.10 with 80 x 80 matrices. After unfolding the density variation of the eigenvalues the behavior of the Dyson-Mehta Δ_3 statistic was examined for different values of y. The behavior of the reduced widths, which has also been examined in a previous calculation by Rosenzweig, Monahan, and Mehta, was found to be considerably more sensitive to small y values than the Δ_3 statistic. Thus the reduced width data can place a much lower limit on y than the level spacing information. A comparison to the calculations performed here with recently collected high quality neutron resonance data gives $y < 0.05$ at the 99.7% confidence level. It is also shown that the same value of the Dyson-Mehta Δ_3 statistic results when the matrix elements of Wigner's model are chosen from a gaussian or flat distribution."

2. Neutron-Capture Cross Sections for ^{186}Os and ^{187}Os and the Age of the Universe. (J. C. Browne and B. L. Berman)

We have measured the neutron-capture cross sections for ^{186}Os and ^{187}Os in the energy range up to 150 keV which corresponds to stellar temperatures up to about 18×10^8 °K. These cross sections (shown in Fig. D-1) enable us to calibrate the $^{187}\text{Re} \rightarrow {}^{187}\text{Os}$ β-decay clock which can be used to determine the age of the universe. These results, which have been submitted to Nature in Report No. UCRL-77967, yield $19.6 \pm 4 \times 10^9$ years for the age of the universe which is larger than results from other dating techniques.

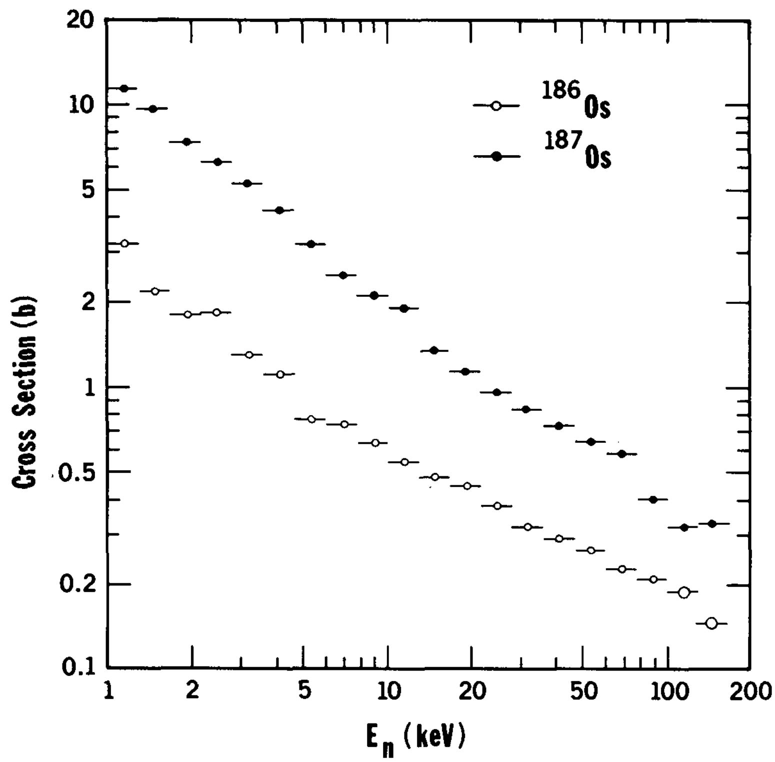

Figure D-1. The neutron-capture cross sections versus laboratory neutron energy for ^{186}Os and ^{187}Os. The horizontal bar represents the size of the energy bin into which the data have been averaged. (The energy resolution of the actual measurement was much better.) The uncertainty for each data point lies within the plotted symbol and typically is 5% at 30 keV.

3. ^{187}Os and ^{189}Os Neutron-Capture Spectra. (A. Stolovy* and B. L. Berman)

The results of this LLL-NRL collaboration will be presented at the 1976 Washington APS Meeting; a paper on this work has been submitted to Phys. Rev. C as well. The APS abstract follows:

> "The Spin states of 25 resonances for ^{187}Os and 40 resonances for ^{189}Os have been determined with probabilities of correctness exceeding 85%. These measurements are far superior to previous data[10] taken with much smaller samples. The spin distribution for the ^{187}Os case is needed for the determination of the age of the universe which makes use of the ^{187}Re-^{187}Os radioactive dating technique. The experiments were performed at the Livermore Linac, using two Ge(Li) detectors and a two-parameter data-collection system. Spin assignments were made on the basis of the ratio of low-energy capture γ-ray intensities depopulating 4^+ states to those of γ rays from 2^+ states. For both isotopes, the spin distribution is consistent with a (2J+1) level-density distribution. The level spacings were found to be in agreement with the theory of Dyson and Mehta,[11] which implies the presence of long-range ordering."

4. Neutron Total Cross Section for Tritium. (T. W. Phillips, B. L. Berman, W. A. Barletta, J. D. Seagrave†)

The results of this LLL-LASL collaboration will be presented at the 1976 Washington APS Meeting. The abstract follows:

---

[10] A. I. Namenson, A. Stolovy, and G. L. Smith, Nucl. Phys. A237, 45 (1975).

[11] F. J. Dyson and M. L. Mehta, J. Math. Phys. 4, 701 (1963).

*Naval Research Laboratory, Washington, D.C.

†Los Alamos Scientific Laboratory, Los Alamos, N.M.

"Using the LLL 100-MeV Linac, we have acquired neutron-transmission data for tritium and hydrogen samples in the neutron energy range from 50 keV to 50 MeV. The 200,000-Ci high-pressure tritium sample, the equivalent hydrogen sample and an evacuated sample container were cycled alternately into the neutron beam along a 250-m flight path. These data have been analyzed to obtain the neutron total cross section for ^{3}H. That part of the present results which lies within the appropriate energy range is in reasonable agreement with the results of the only previous measurement of this cross section.[12]"

5. Photonuclear Reactions.
   (a) Photoneutron Cross Sections for ^{13}C, ^{17}O, and ^{18}O.

A collaborative series of experiments on these cross sections has been performed at the LLL and Toronto linacs. The ground-state photoneutron cross section for ^{17}O was performed at Toronto; ^{13}C, ^{17}O and ^{18}O photoneutron measurements were made at Livermore. Fig. D-2 shows the photoneutron cross sections for ^{18}O. Some of these results were reported at the 1976 New York APS meeting. The abstracts for the work performed at Livermore follow:

"Photoneutron Cross Sections for ^{13}C.† K. G. McNEILL and J. G. WOODWORTH, U. of Toronto, J. W. JURY, Trent U., and P. MEYER, D. D. FAUL, and B. L. BERMAN, Lawrence Livermore Lab.--The (γ,n) and $(\gamma,2n)$ cross sections for ^{13}C have been measured from 7.5 to 42 MeV, using monoenergetic photons from the annihilation in flight of fast positrons from the Livermore Electron-Positron Linac. The photon energy resolution ranged from 300 to 450 keV, and data were acquired at 125-keV intervals below 25 MeV. The photoneutrons were detected in a $\sim$40%-efficient BF_3-tube-plus-paraffin 4π neutron detector. The sample consisted of 46g of pressed elemental carbon enriched to 96% in ^{13}C. Peaks in the (γ,n) cross section occur at 7.8, 8.2, 11.0, 13.6, and 14.9 MeV. The main giant resonance is centered at 23 MeV. The $(\gamma,2n)$ cross section rises slowly from threshold and remains small throughout the energy range measured."

---

†Work supported in part by the U.S. Energy Research and Development Administration and the National Research Council of Canada.

[12] Los Alamos Physics and Cryogenics group, Nucl. Phys. 12, 291 (1959).

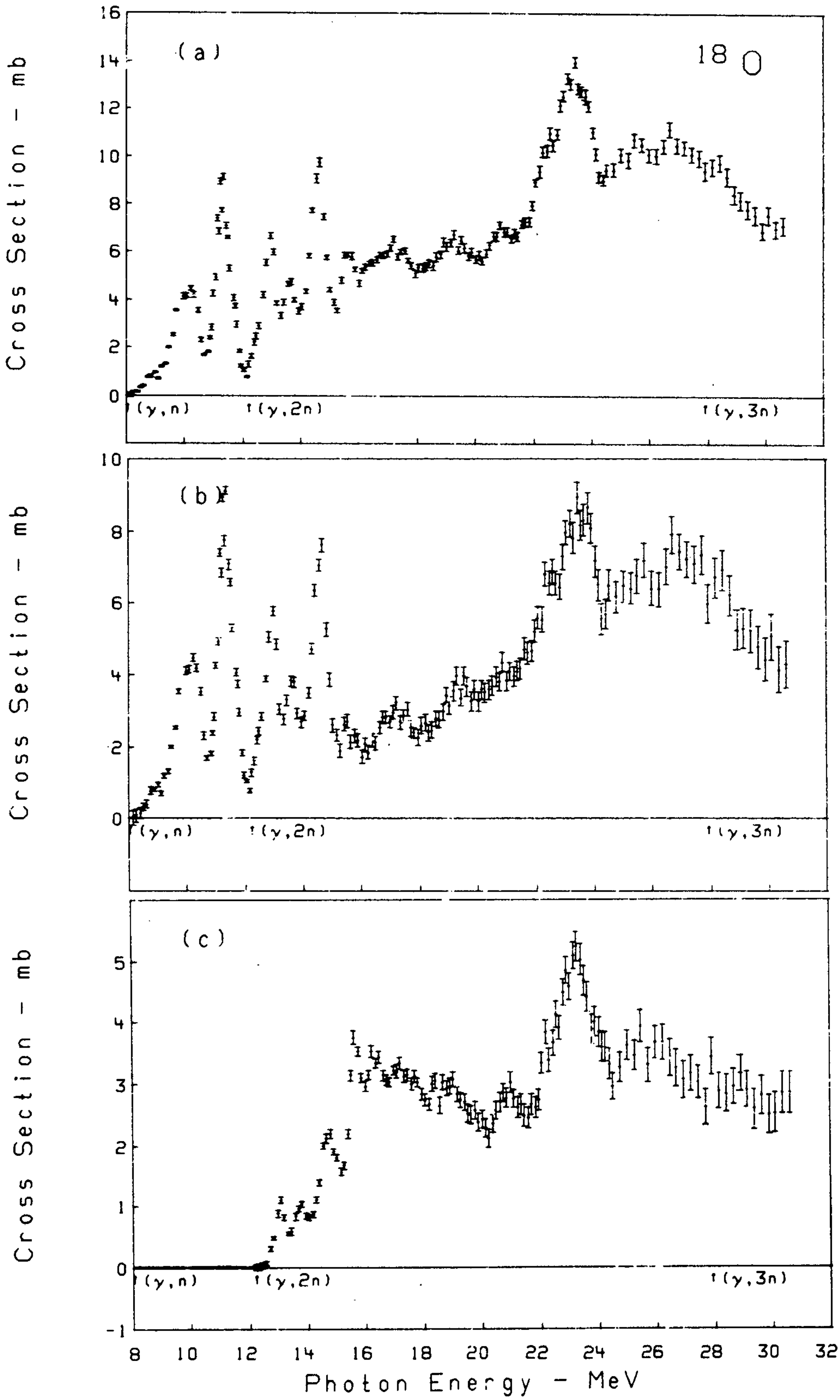

Figure D-2. Photoneutron cross sections for ^{18}O. (a) Total photoneutron cross section $\sigma[(\gamma,n)+(\gamma,pn)+(\gamma,2n)]$. (b) Single photoneutron cross section $\sigma[(\gamma,n)+(\gamma,pn)]$. (c) $\sigma(\gamma,2n)$, "Photoneutron Cross Section for ^{17}O. P. MEYER, D. D. FAUL, and B. L. BERMAN, Lawrence Livermore Lab., J. W. JURY, Trent U., and J. G. WOODWORTH and K. G. McNEILL, U. of Toronto--The (γ,n) cross section for ^{17}O has been measured from 7.6 to 30 MeV at the Livermore Electron-Positron Linac (under the same conditions as the work on ^{13}C, above.). The sample consisted of 102g of H_2O enriched to 30% in ^{17}O, with most of the balance of the oxygen as ^{18}O. Sequential measurements using a sample of $H_2{}^{18}O$ (96.5% pure) allowed the subtraction of the neutron counts from the ^{18}O impurity. Additional sequential measurements with samples of $H_2{}^{16}O$ and $D_2{}^{16}O$ (at somewhat larger energy intervals) served as a check on the experimental normalization. A broad giant resonance centered at about 23 MeV dominates the $^{17}O(\gamma,n)$ cross section. The $^{17}O(\gamma,2n)$ cross section is very small and difficult to measure in the face of the large (γ,2n) cross section for ^{18}O (see next abstract)."

"Photoneutron Cross Sections for ^{18}O. D. D. FAUL, B. L. BERMAN, P. MEYER, and R. A. ALVAREZ, Lawrence Livermore Lab. and J. G. WOODWORTH, U. of Toronto--The (γ,n) and (γ,2n) cross sections for ^{18}O have been measured from threshold to 42 MeV at the Livermore Electron-Positron Linac (under similar conditions to those for the work on ^{13}C, above). The samples used consisted of 34- and 120-g quantities of H_2O enriched to 96.5% in ^{18}O. Many peaks appear in both the (γ,n) and (γ,2n) cross sections; the most prominent of these occur at 10.1, 11.3, 12.9, 13.7, 14.6, and 15.6 MeV. The main giant resonance is centered at 23.4 MeV. The (γ,2n) cross section rises sharply from threshold, contains prominent structure, and remains large throughout the energy range measured."

(b) Photoproton Cross Sections for ^{18}O: A Measure of the Effect of the Valence Neutrons on the ^{16}O Core.

A report of this work also was given at the 1976 New York A.P.S. meeting, and a paper has been prepared for submittal to Phys. Rev. Letters. Fig. D-3 shows the striking similarities and differences between the ^{18}O and ^{16}O cross sections. The A.P.S. abstract follows:

"Photoproton Cross Section for ^{18}O. B. L. BERMAN, D. D. FAUL, R. A. ALVAREZ, and P. MEYER, Lawrence Livermore Lab.--The (γ,p) cross section for ^{18}O has been measured from threshold to 42 MeV, at the Livermore Electron-Positron Linac, simultaneously with the photoneutron cross sections by detecting (between beam bursts) the delayed

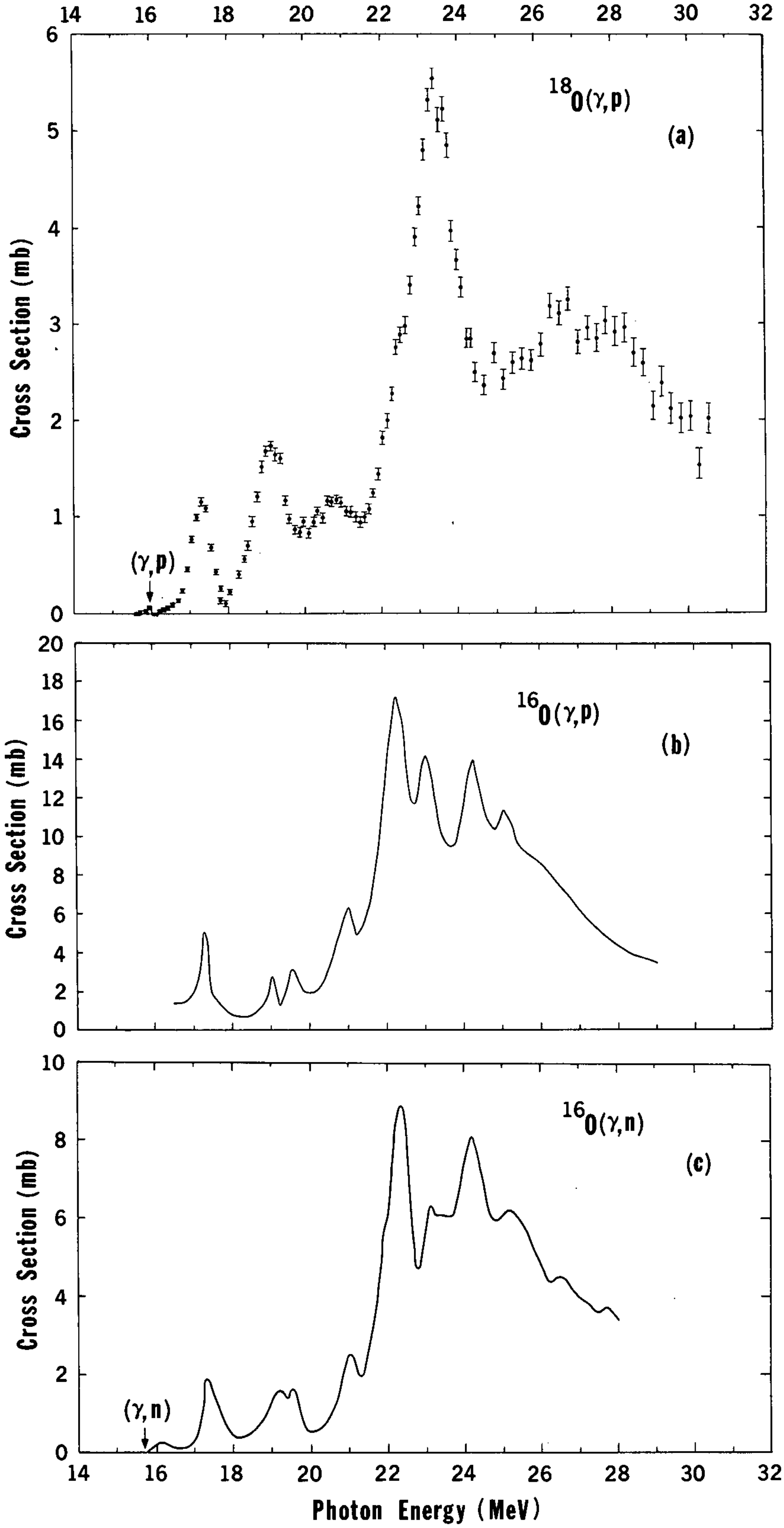

Fig. D-3. (a) Photoproton cross section for ^{18}O measured in this experiment. (b) and (c) Photoproton and photoneutron cross sections for ^{16}O taken from the literature.

neutrons from the β-decay of the residual ^{17}N nuclei to neutron-unstable states in ^{17}O. The $^{18}O(\gamma,p)$ cross section contains prominent peaks at 17.3, 19.2, 20.8, and 23.4 MeV, as well as a broad peak centered at ∿27 MeV. This cross section will be compared and contrasted with the $^{16}O(\gamma,p)$ cross section (synthesized from published data) in order to demonstrate the dramatic effect of the two valence neutrons in ^{18}O upon the ^{16}O core."

(c) Isospin Shift of the Giant-Resonance Energy.

The results of this LLL-LASL-NBS collaboration will be presented at the 1976 Washington A.P.S. meeting. The abstract follows:

"Isospin Shift of Giant-Resonance Energy. B. L. BERMAN, Lawrence Livermore Laboratory, B. F. GIBSON, Los Alamos Laboratory, and J. S. O'CONNELL, National Bureau of Standards and ERDA.--An examination of the giant-resonance energy derived from Lorentz-curve fits[13] to photoabsorption cross sections of spherical nuclei ($A \gtrsim 90$) reveals an isotope shift larger in magnitude than the general A-dependence of the resonance energy. These data imply an isospin dependence of the giant-resonance energy. Theoretical models of the electric dipole resonance and isospin sum rules are examined to account for this phenomenon."

(d) Photoneutron Cross Sections for Osmium Isotopes.

The results of these measurements will be presented at the 1976 Quebec A.P.S. meeting. The abstract follows:

"Photoneutron Cross Sections for Osmium Isotopes. (B. L. BERMAN, R. A. ALVAREZ, D. D. FAUL, and P. MEYER, Lawrence Livermore Lab.--We have measured the photoneutron cross sections for $^{188,189,190,192}Os$ from the (γ,n) threshold to 30 MeV and for ^{186}Os from 11 to 19 MeV, using monoenergetic photons from the annihilation in flight of fast positrons from the LLL Electron-Positron Linac. The photon energy resolution ranged from 300 to 400 keV over the energy range of the experiment. Isotopically enriched powdered-metal osmium samples were used. The objective of this experiment was to test the recent theoretical prediction[14] of a nuclear phase transition, from

---

[13] B. L. Berman, Atomic Data and Nuclear Data Tables 15, 319 (1975).

[14] R. Sedlmayr, M. Sedlmayr, and W. Greiner, Nucl. Phys. A232, 465 (1974).

prolate deformed to γ-unstable between the ^{188}Os and ^{190}Os nuclei. Values for integrated cross sections and branching ratios for multiple-neutron-emission cross sections were obtained as well."

E. FACILITIES

1. Photoneutron Angular Distribution Facility. (T. W. Phillips)

A facility for the study of the angular distribution and energy spectra of photoneutrons has been installed at the LLL 100 MeV electron linear accelerator. Five angles have been instrumented with neutron detectors. The angles are 22.5°, 67.5°, 90°, 112.5°, and 135°. Neutron spectra are obtained by measuring their time of flight along a 10 m flight path at each angle. Using these flight paths and a 5 nsec electron beam burst width gives an energy resolution of 400 keV for 10 MeV neutrons and 14 keV for 1 MeV neutrons.

As a test of the facility, the angular distribution of photoneutrons from ^{16}O leaving ^{15}O in its ground state is being measured using bremsstrahlung photons. These data are currently being analyzed. The positron converter on the LLL Linac is being upgraded to provide a more intense beam. When this upgrade is complete, annihilation photons will also be used in photoneutron studies. The combination of monoenergetic annihilation photons and time-of-flight spectrometry will make it possible to identify and to study all neutron decay modes of a nucleus excited by photons.

A. NEUTRON CROSS SECTIONS (DIRECT AND INDIRECT)

1. Charged Particle Reactions Related to Li(n,t)^{4}He

a. $^3H(\alpha,^6Li)n$ Reaction at Zero Degrees (Brown, Haglund, Jarmie, Ohlsen)

We are studying the $^3H(\alpha,^6Li)n$ reaction by measuring the ^6Li yield at 0° (lab) produced by α bombardment of a Ti-tritide target. The ^6Li ions are detected by a 17 μm solid-state detector after being spatially separated from the α beam in a magnetic field. The ^6Li yield is normalized to the α+t elastic yield as measured by four ΔE-E systems at ±15° and ±30° (lab).

Zero degree cross sections for ^6Li production have been obtained at 15 energies from 11.3 to 12.0 MeV (lab) which cover the resonance region corresponding to lab neutron energies from 0.08 to 3.9 MeV for the inverse reaction. Depending on difficulties encountered in the final analysis, we hope for 2 to 5% accuracy. The data should have an impact on both the energy scale and the absolute cross section, and should be an important contribution to the R-Matrix analysis of the mass-7 system.[1]

b. $^4He(t,t)^4He$ Elastic Scattering (Jarmie, Ohlsen, Hardekopf, Poore, Stupin, Anderson)

Accurate cross sections and analyzing powers have been measured from 7 to 14 MeV. Both angular distributions and excitation functions were taken. The accuracy of the analyzing powers is ±0.005 and of the differential cross sections is from 0.5 to 1.0%. Certain corrections for multiple scattering have to be made before final values are presented. Graphs of the cross section data are shown in Figs. A-1 and A-2. The resonance behavior near 8.7 MeV corresponds to the 240 keV resonance in the $^6Li(n,\alpha)T$ reaction.

2. Total Cross Section of Tritium (Seagrave, with B. L. Berman, T. W. Phillips, W. A. Barletta, LLL)

Using the LLL 100-MeV Linac, we have acquired neutron-transmission data for tritium and hydrogen samples in the neutron energy

[1]G. M. Hale in Nuclear Cross Sections and Technology, NBS425 (1975), Vol. I, p. 302; Also see Section D-1 of this report.

range from 50 keV to 50 MeV. The 200,000-Ci high-pressure tritium sample, the equivalent hydrogen sample, and an evacuated sample container were cycled alternately into the neutron beam along a 250-m flight path. These data have been analyzed to obtain the neutron total cross section for ^{3}H. That part of the present results which lies within the appropriate energy range is in reasonable agreement with the results of the only previous measurement of this cross section.[2]

G. Hale has provided results from the LASL Energy Dependent Four-Body Interaction Code for comparison. Predictions from the p-He^3 code resemble, but lie well below the n-^{3}H data. Inclusion of the LASL n-T elastic differential cross sections is in progress.

3. Double Differential Neutron Cross Sections for Beryllium at Incident Neutron Energies of 5.9, 10.1, and 14.2 MeV (Drake, Auchampaugh, Arthur, Ragan, and Young)

Neutron-production cross sections for beryllium have been measured over the energy range from 0.4 to 14.0 MeV by the time-of-flight technique with incident neutron energies of 5.9, 10.1, and 14.2 MeV, and at labatoratory angles of 25°, 27.5°, 30°, 35°, 45°, 60°, 80°, 100°, 110°, 125°, and 145°. The differential elastic and inelastic cross sections at the three energies are given in Table A-1. Comparison of our emission energy spectra with calculations using the ENDF/B-IV beryllium cross sections show that the ENDF/B cross sections strongly overemphasize the low-lying states in ^{9}Be.

4. Spectra of Equilibrium Delayed Neutrons from Fast Fission of ^{235}U, ^{238}U, and ^{239}Pu (Evans and Krick)

A ^{3}He neutron spectrometer of the Shalev type[3] has been used to measure the energy spectrum of delayed neutrons in equilibrium with fission induced by sub-MeV neutrons incident upon ^{235}U, ^{238}U, and ^{239}Pu. Delayed-neutron spectra of groups 1 through 4 have previously been measured for thermal fission[4,7] and for 14-MeV fission.[7]

---

[2] Los Alamos Physics and Cryogenics Groups, Nucl. Phys. 12, 291 (1959).

[3] J. Cuttler, S. Shalev, and Y. Dagan, Trans. Am. Nucl. Soc. 12, 63 (1969).

[4] R. Batchelor and H. R. Mck Hyder, J. Nucl. Energy 3, 7 (1956).

[5] S. Shalev and J. M. Cuttler, Nucl. Sci. Eng. 51, 52 (1972).

[6] W. R. Sloan and G. L. Woodruff, Trans. Am. Nucl. Soc. 15, 942 (1972).

[7] G. Fieg, J. Nucl. Energy 26, 585 (1972).

Table A-1

Beryllium Differential Neutron Cross Sections

E_n	5.9 MeV		10.1 MeV		14.2 MeV	
θ_L	Elastic (mb/sr)	Inelastic (2.43 MeV state[a]) (mb/sr)	Elastic (mb/sr)	Inelastic (2.43 MeV state[a]) (mb/sr)	Elastic (mb/sr)	Inelastic (2.43 MeV state[a]) (mb/sr)
25°	443 ± 57	80 ± 13	480 ± 62	68 ± 14		
27.5°					338 ± 43	
30°					335 ± 37	
35°	320 ± 42	65 ± 11	285 ± 37	49 ± 10	234 ± 26	
45°	180 ± 23	57 ± 10	151 ± 20	43 ± 9	119 ± 13	21 ± 8
60°	75 ± 10	42 ± 7	40 ± 5	35 ± 7	31.1 ± 3.4	18.4 ± 5.5
80°	23 ± 3.1	32 ± 5	15 ± 2.0	26 ± 5.2	11.5 ± 1.3	14.2 ± 4.6
100°	26 ± 3.4	28 ± 4.8	24 ± 3.1	22 ± 4.4	23.0 ± 2.5	13.8 ± 4.1
110°	32 ± 4.0	30 ± 5.2				
125°	31 ± 4.0	28 ± 4.7	15 ± 2.0	26 ± 5.2	9.5 ± 1.1	9.9 ± 3.0
145°					5.7 ± 0.7	7.9 ± 2.4

[a]Defined as those inelastic reactions which proceed through the states at 1.69-, 2.43-, 2.8-, and 3.06-MeV excitation energy in ^{9}Be.

The method has been described previously.[8] Protons from the LASL R-1 Van de Graaff were used to produce a spectrum of 80 to 420 keV ^{7}Li(p,n) neutrons. The beam was pulsed on for 35 ms out of each 100 ms. The delayed neutron spectrum was measured by gating the spectrometer on for 40 ms during the beam-off period. Samples 75 mm square were placed adjacent to and in front of the target. Sample weights and isotopic purities were: 111 g, 97% for ^{235}U; 229 g, 99.7% for ^{238}U and 136 g, 98% for ^{239}Pu. The spectrometer was located with its axis 16 cm in front of target, perpendicular to the beam line. The spectrometer was surrounded by 19 mm of lead around which was placed a ^{10}B-Al pressed cylinder containing 163 mg/cm^2 of ^{10}B. An additional 38-mm thick lead block was placed between the sample and the detector. Each pulse-height distribution required about 50 hours to accumulate.

The energy response of the spectrometer, with the above described shielding in place, was measured with monoenergetic neutrons between 0.125 and 2.0 MeV produced by protons on a thin Li target. The calibration runs were normalized to the 0° cross section of the ^{7}Li(p,n)^{7}Be reaction and target current-integrator data. Pulse-shape discrimination was used to suppress the spectrometer pulses from gamma radiation and ^{3}He recoils. The data were analyzed with a simple subtractive unfolding technique.

The data are shown in Fig. A-3. The complex structure observed for Group I-IV spectra[4,7] is evident. Major peaks at 70, 130, 185, 256, 375, 475, 500, and 562 keV correspond to prior results. The average energies are approximately 600 keV, somewhat in disagreement with prior results. This may be due in part to the inclusion of the shorter-lived delayed neutron groups, which have not been previously measured, and which may have higher average energies. Also, no correction has been made for sample multiplication, which is estimated to contribute as much as 4% to the observed spectra; correction for the presence of the prompt fission neutrons can reduce the average energy by as much as 50 keV. Finally, the spectrum intensity below about 300 keV is very sensitive to the wall-effect subtraction, and hence part of the average-energy difference could be experimental error.

See Bull. Am. Phys. Soc. 21 655 (1976).

---

[8]A. E. Evans and L. V. East, Trans. Am. Nucl. Soc. 19, 396 (1974).

5. Photon Production From Thermal Neutron Capture in Thorium (Jurney)

The gamma-ray spectrum from $^{232}Th(n_{th},\gamma)$ has been measured at the LASL Omega West reactor capture gamma facility using a 6.3 cm diam by 15-cm long NaI scintillator surrounded by a 20-cm diam by 25-cm long NaI annulus. Effective rejection of unwanted (non-photopeak) pulses was realized by operating the annulus in anticoincidence with the central analyzing detector. The unfolded pulse-height spectrum is shown in Figure A-4; Figure A-5 shows the first 1 MeV of the spectrum displayed in narrow energy bins to preserve detail.

Gamma-ray intensities in the Th spectrum were computed in units of partial capture cross section by comparing them with the intensity of the 2223-keV deuterium ground-state transition resulting from capture by ^{1}H in a 100-mg target of polyethylene. The thermal neutron capture cross section of ^{232}Th, determined from summing the spectrum of Fig. A-4, is 7.1 ± 0.6 barns. For reference, the value given in BNL-325 is 7.4 ± 0.1 barns.

6. Neutrons From Spontaneous Fission (Veeser, Hoffman, Ford)

We are measuring $\bar{\nu}$, the number of neutrons per fission, as a function of the fragment mass for several spontaneous-fissioning nuclei, using a 75-cm-diam liquid scintillator tank. The measurements are made by recording the fragment energies and the number of neutrons from one of the fragments for each of about 5×10^4 fission events. We have completed measurements for ^{250}Cf, ^{252}Cf, and ^{256}Fm, and we are presently measuring ^{257}Fm. Following data reduction we hope to be able to determine improved mass distributions for the fermium isotopes. Since ^{257}Fm sometimes fissions symmetrically, $\bar{\nu}(M)$ is of special interest because this is the first known measurement of the neutrons from symmetric fragments.

7. Neutron-Induced Fission of ^{230}Th (Veeser, Muir)

We measured the cross section for $^{230}Th(n,f)$ near 720 keV using neutrons from an underground nuclear explosion. It has been postulated that the large resonance near 720 keV results from a vibrational band of levels in the second well of a double-humped potential barrier in ^{231}Th, but previous measurements have not shown any fine structure in the resonance cross section. Our measurements were made with 2.7 keV resolution, which is about two times better than the best previous resolution, and show some structure, although the levels are not yet very well resolved. We are now analyzing the data to determine the parity of the resonance and possibly the energies and spins of the fine-structure states. We hope to derive values for the moment of inertia and the decoupling parameter which would permit a better calculation of the depth of the potential well.

8. A Compilation of Yields from Neutron-Induced Fission of ^{232}Th ^{235}U, ^{236}U, ^{237}Np, ^{238}U, and ^{239}Pu Measured Radiochemically at Los Alamos (Ford, Norris)

Los Alamos report LA-6129 (February, 1976) is a compilation of radiochemically measured relative fission yields from targets of ^{232}Th, ^{235}U, ^{236}U, ^{237}Np, ^{238}U, and ^{239}Pu that were irradiated with neutrons, the average energies of which were in the 0.0253-eV to 14-MeV range. The relative fission yields were converted to absolute values through use of the two-mode-of-fission hypothesis.

Most targets were irradiated in the following Los Alamos reactors: BIG-TEN, Clementine, Flattop (oralloy core), Flattop (Pu core), Godiva-I, Godiva-IV, Jezebel (Pu core), Jezebel (^{233}U core), Topsy, Tungsten-Carbide Critical Assembly, and Water Boiler. Other targets were irradiated at the Los Alamos Cockcroft-Walton and Van de Graaff accelerators. Still others were irradiated in the Coupled Fast Reactivity Measurements Facility at INEL.

For each irradiation, the yields of some nuclides in the following list were measured: ^{82}Br, ^{83}Br, ^{89}Sr, ^{90}Sr, ^{91}Sr, ^{91}Y, ^{95}Zr, ^{96}Nb, ^{97}Zr, ^{103}Ru, ^{105}Rh, ^{106}Ru, $^{109}Pd^{g}$, ^{111}Ag, $^{115}Cd^{m}$, $^{115}Cd^{g}$, ^{127}Sb, ^{129}Sb, ^{131}I, ^{132}Te, ^{136}Cs, ^{137}Cs, ^{139}Ba, ^{140}Ba, ^{141}Ce, ^{143}Ce, ^{144}Ce, ^{147}Nd, ^{153}Sm, ^{156}Eu, and ^{161}Tb.

These fission yield measurements are useful for nuclear diagnostic work. The measurements of fission yields at selected neutron energies to 14-MeV are expected to be useful in calculations of fission product build-up in nuclear power reactors in general and breeder reactors in particular.

9. Neutron-Induced Fission Cross Section of ^{243}Cm (Silbert)

From data obtained by LASL experimenters from the underground nuclear explosion Physics-8, we have generated the cross section for $^{243}Cm(n,f)$ over the neutron energy range from 15 eV to 3 MeV. This intense, single-pulse neutron source was employed in a time-of-flight measurement over an evacuated 240-m flight path. A thin 210-μg sample of 89% ^{243}Cm and 11% ^{244}Cm (prepared by R. W. Hoff and coworkers at LLL) was exposed to a well-collimated neutron beam, together with samples of ^{6}LiF and $^{235}UO_2$ that served as flux monitors.

This fission cross section was heretofore known only sketchily. We find, as expected for an even-odd target actinide, and consistent with the known 600 b thermal cross section, abundant fission over the region observed. The cross section in the few-MeV plateau region is 2.3 ± 0.3 b, in agreement with systematics. A study of the resonance region from 15 to 80 eV yields the following preliminary parameters (assuming Γ_γ = 40 meV):

(1) mean level spacing <D> (corrected for missed levels, both spin states included) = 0.85 ± 0.09 eV;

(2) neutron strength function $10^4\ S_o$ = 1.04 ± 0.30;

(3) mean fission width $<\Gamma_f>$ = 225 meV.

A tabular presentation of the cross section is given in report LA-6239-MS.

10. Direct Reaction Fission Studies (Britt, Gavron, Goldstone, Schoenmackers, Weber, and Wilhelmy)

During the past year this program has concentrated a multi-facited effort to (1) measure fission probability distributions in energy regions from below the barrier up to about the threshold for second chance fission; (2) try to further develop realistic microscopic models for fitting these data and; (3) use these models and the experimental data to extract systematic information on fission barrier parameters. Highlights of this program are as follows.

a. Γ_n/Γ_f for Actinide Nuclei Using (^{3}He,df) and (^{3}He,tf) Reactions

The fission probability was measured for a series of actinide nuclei as a function of the excitation energy using (^{3}He,df) and (^{3}He,tf) reactions. From these data Γ_n/Γ_f was determined from threshold up to ~12 MeV of excitation energy and fitted by evaporation calculations which do not contain any arbitrary normalization factors. Generally, these fits are possible only if one assumes the fission process to proceed through a first saddle point which is not axially symmetric. These results and calculations also reproduce previously known empirical trends of average values of Γ_n/Γ_f, as a function of A and Z. The data and theoretical fits are shown in Fig. A-6. These results are scheduled for publication in Physical Review C in May, 1976; also see Phys. Rev. Lett. 34 827 (1975).

b. Fission of Heavy Actinides

Using targets of ^{241,243}Am, ^{245,246,248}Cm, ^{250}Cf and ^{254}Es the fission of the compound nuclei $^{241-250}$Cm, $^{245-249}$Bk, $^{250-252}$Cf and ^{250,251,255}Es have been studied via (d,pf), (t,pf), (^{3}He,df), (^{3}He,tf) and (p,p'f) reactions. Near the N = 152 shell the results for even-even nuclei tend to show broad structures that are not reproduced in our microscopic statistical model fits. Further analysis of these results and experiments on targets of ^{249}Bk and ^{249}Cf are in progress.

c. Fission of ^{228}Ra

Fission probabilities and mass distributions have been measured as a function of excitation energy for ^{228}Ra excited in the ^{226}Ra(t,pf) reaction. Triple peaked mass distributions are observed for which the symmetric component has an apparent higher threshold by over 1 MeV. Results are analyzed in a statistical model which suggests the presence of a resonance in the fission probability for the asymmetric mass component and the need for level density enhancements (possibly due to axial asymmetry at the barrier) in the analysis of the fission probability for the symmetric component. These results are scheduled for publication in Physical Review C in June, 1976.

d. Li-Induced Fission Reactions

Exploratory experiments with a 39 MeV ^{6}Li beam were begun. Initial investigations were performed on ^{236}U and ^{237}Np targets with (^{6}Li,αf), (^{6}Li,df) and (^{6}Li,tf) reactions. Preliminary results indicate that the reactions (^{6}Li,αf) and (^{6}Li,tf) may be useful for studying fission probabilities in the excitation energy regions 15-25 MeV and 12-18 MeV, respectively, but in both cases there are experimental problems that must be studied further before a realistic evaluation of the technique can be obtained. In the (^{6}Li,αf) studies the singles spectra contain α particles from the breakup reaction (^{6}Li,αd) and this must be understood in more detail before absolute fission probabilities can be obtained. In the (^{6}Li,tf) studies the cross sections are small and further studies are necessary to see if the tritons can be clearly separated from other events in the charged particle telescope. In the (^{6}Li,df) measurements we found that the deuteron singles spectrum was dominated by deuterons from reactions in carbon and oxygen in the targets and, therefore, this reaction will probably not be useful for obtaining fission probability measurements.

e. Analysis of Barrier Heights and Transition States in ^{238}U

For the compound nucleus ^{238}U we have a unique case where information on fission probabilities exist from three complementary sources. These sources are (1) (t,pf) results in the subbarrier resonance region,[9] (2) (γ,f) results in the subbarrier resonance region[10] and (3) (γ,f) results in the 6-20 MeV excitation energy region.[11] The requirement to simultaneously fit all three sets of data with our statistical model provides a much more stringent test of the model and should allow us to eliminate some of the ambiguities in parameters.

In the analysis of the resonance data we assume that (1) resonant photofission proceeds through the $J^\pi = 1^-$ level of the $K^\pi = 0^-$ band, (2) the (t,pf) resonance is predominantly $J^\pi = 0^+$, and (3) $K = 0^+$ and $K = 0^-$ bands are degenerate at the second saddle point because of the mass asymmetric shape. Then simultaneous fits to the (t,pf) and (γ,f) results require $E_A \cong$ 5.9 and 6.4 MeV for $K = 0^+$ and $K = 0^-$, respectively with $E_B \cong 6.1$ MeV for both bands. Analysis of the angular distributions from the ^{236}U(t,pf) reaction indicate the existence of additional transition states $K = 0^-$, 2^+, 2^- at average excitation energies above the barrier of ~200 keV (0^-, 2^+) and ~400 keV (2^-).

With the barrier parameters fixed by fits to the resonance data we then tried to fit the higher excitation energy photofission data. These results indicate that we can reproduce the absolute value of the measured fission probability at $E_{ex} \sim 10$ MeV only if it is assumed that there exists a large collective enhancement in the level density at the second barrier. The magnitude of the enhancement needed corresponds to a stable γ deformation or several low energy vibrations. This represents the first case where we have been able to establish a definite need for collective enhancements at the second barrier.

f. Simulated Neutron Cross Sections For Lighter Nuclei From Charged Reactions

We have performed initial experiments to determine the feasibility of using direct charged particle reactions to simulate neutron induced cross sections. The first reactions studied have been $^{90}Zr(^3He,d)\ ^{91}Nb^* \rightarrow {}^{90}Zr + p$ and $^{91}Zr(^3He,t)\ ^{91}Nb^* \rightarrow {}^{90}Zr + p$ which simulates the $^{90}Nb + n \rightarrow {}^{90}Zr + p$ reaction. In these experiments we were

---

[9] J. D. Cramer and H. C. Britt, Phys. Rev. C2 2350 (1970); B. B. Back et al., Phys. Rev. C9, 1924 (1974).

[10] P. Dickey and P. Axel, Phys. Rev. Lett. 35, 501 (1975).

[11] J. T. Caldwell, E. J. Dowdy, R. A. Alvarez, B. L. Berman, P. Meyer and T. F. Godlove, private communication.

attempting to determine the probability of proton emission (P_p) as a function of excitation energy in ^{91}Nb. The experimental arrangement consisted of two counter telescopes which were used to particle identify and energy measure: (1) the outgoing direct reaction particle (d or t) and, (2) the evaporated proton. From the kinematics and Q value for the reaction it was possible to determine the excitation energy of the ^{91}Nb. The P_p was obtained from a ratio of the number of times the ^{91}Nb was produced in a particular excitation energy interval to the number of observed coincidences with emitted protons (corrected for the counter telescope geometry) from the same excitation energy interval. The isotope ^{91}Nb was chosen for this initial study because it is a very favorable case for proton emission since it has a high neutron binding energy (B_n = 12.052 MeV) and a low proton binding energy (B_p = 5.158 MeV).

Initial analyses of the experimental data have shown some of the anticipated effects. The P_p is quite large and increases monotonically from our detectable threshold (at about 6 MeV excitation energy in ^{91}Nb) to the neutron binding energy threshold at 12 MeV where it reaches a value of P_p of ~0.3-0.4. Above the neutron binding energy the competition with the now open neutron decay channels causes the P_p value to decrease, but still remain quite detectable, up to the ~16 MeV maximum excitation energy obtained in these experiments. There are, however, difficulties with the interpretation of these results. Angular distribution studies of the ^{90}Zr(^{3}He,d)^{91}Nb* $\rightarrow$ ^{90}Zr + p reaction imply that there are serious "break-up" effects of the ^{3}He dissociating into a deuteron and proton in the presence of the target Coulomb field. Further experiments are planned to study these effects in more detail. We shall also investigate other direct reaction mechanisms such as (t,α), (^{6}Li,d), (^{6}Li,t), (^{6}Li,α) and (^{7}Li,t) for producing the desired excited nuclei.

11. Measurements of (n,2n) and (n,3n) Cross Sections (Veeser, Arthur)

We are measuring (n,2n) and (n,3n) cross sections using a 75-cm-diam liquid scintillator tank to detect the neutrons. Compared with the more common procedure for measuring such cross sections, activation of a sample and radiochemical analysis of the decay products, this method has the advantage that it is insensitive to the decay of the residual nucleus and therefore can be used for cases where the final nucleus has a lifetime or a decay scheme which is unsuitable for radiochemical analysis. Figure A-7 shows the results for targets of ^{9}Be, ^{45}Sc, ^{89}Y, ^{169}Tm, ^{175}Lu, and ^{197}Au. The solid symbols show the results of radiochemical measurements[12] from the thresholds to 28 MeV, and the open symbols are our results from 14.7 to 24.0 MeV. The curves are from a statistical model calculation reported in Ref. 12. We plan to make a similar comparison using the code GNASH calculations as described in Sec. D-3 of this report. All of our (n,2n) results are in agreement with Ref. 12 except those for lutetium, where ours are higher. Because of problems arising from decay scheme uncertainties and a large background from the naturally occurring radioisotope ^{176}Lu, the lutetium radiochemical measurements are difficult to make and have a large uncertainty. Our (n,3n) results are slightly lower than those of Ref. 12. For thulium and gold there are differences of about 10% and 15% respectively, and for lutetium the difference is about 20%. We do not know of any reason why our (n,3n) measurements should be discrepant, particularly when the (n,2n) results are not. Instead, it seems likely that the radiochemical (n,3n) results are too high by a factor of 1.1 to 1.2 because of the difficulties pointed out above.

We have completed measurements for ^{59}Co, ^{93}Nb, ^{103}Rh, ^{181}Ta, and ^{209}Bi and are now analyzing the data. In addition we are continuing the measurements for several other targets, and we intend to try to measure the ^{238}U (n,xn) cross sections above 14 MeV.

12. Spin Assignments for Resonances in (^{235}U + n) (Keyworth, Moore, Moses; J. W. T. Dabbs, N. W. Hill, ORNL)

A second series of runs was made in 1974 on the ORELA to obtain spin information on resonances in (^{235}U + n) using the polarized-neutron and polarized-target technique. These data contained high enough statistical accuracy to permit a clear separation of the observed count rates into effective rates for each spin. A typical presentation of the data in this way is shown in Fig. A-8; it is evident that the contributions from each spin, and the resulting spin assignments of the resonances, can generally be made without any ambiguity. All spin assignments previously reported by Keyworth, et al. (Phys. Rev. Lett. 31, 1077 [1963]) have been verified in the present work, and a large number of new assignments has been made, as shown in Table A-2. We expect to be able to assign spins to most of the observed structure in ^{235}U below 200 eV.

[12] B. P. Bayhurst, J. S. Gilmore, R. J. Prestwood, J. B. Wilhelmy, Nelson Jarmie, B. H. Erkkila, and R. A. Hardekopf, Phys. Rev. C 12, 451 (1975).

Table A-2

Spin Assignments for Resonances Observed Below 90 eV

Resonance Energies (Except for Those Not Previously Observed)

Are Taken From Mughabghab (BNL-325)

E_o	J	E_o	J	E_o	J	E_o	J
1.14	4[a]	21.07	4[a]	42.23	4	63.63	3
2.03	3[a]	22.14	(3)	42.50	3	64.28	4
2.84	4	22.94	4[a]	42.70	4	65.80	3
3.15	3[a]	23.42	4[a]	43.40	3	66.38	4
3.62	4[a]	23.63	3[a]	43.94	4[a]	67.28	(4)
4.85	4[a]	24.25	3[a]	44.60	4[a]	68.50	3
5.45	4	25.59	3[a]	44.80	3	69.30	4
6.21	3[a]	26.49	4[a]	45.79	4[a]	70.5	b
6.39	4[a]	26.60	3	46.79	4	71.55	4
7.08	4[a]	27.16	3	47.98	4[a]	72.40	4
8.78	4[a]	27.82	4[a]	48.30	3[a]	72.91	3
9.28	4[a]	28.36	3[a]	48.80	3[a]	74.5	b
9.74	3	28.72	4	49.43	4[a]	75.54	3
10.18	4[a]	29.65	4[a]	50.49	3	77.50	4
10.80	3	30.59	3[a]	51.02	3	78.11	3
11.66	4[a]	30.86	4[a]	51.27	4[a]	79.70	4
12.39	3[a]	32.02	4[a]	52.23	3	80.36	3
12.85	4[a]	32.10	3	53.46	3	81.45	3
13.28	4	33.53	4[a]	54.10	4	82.67	4
13.69	(3)	34.39	4[a]	55.08	4[a]	83.59	3
14.02	3[a]	34.85	3[a]	55.85	4	84.04	4
14.51	3[a]	35.10	4[a]	56.02	3	84.35	3
15.40	4[a]	35.20	3[a]	56.50	4[a]	85.31	3
16.08	4[a]	38.36	4[a]	58.08	3	86.65	4
16.68	4[a]	39.41	4[a]	58.69	4	86.85	3
18.05	3[a]	39.90	3	59.75	4	87.54	3
18.96	4[a]	40.52	4	60.20	3	88.60	3
19.30	4[a]	41.30	4	60.85	4	90.30	4
20.13	3	41.55	3	61.17	3	90.60	3
20.62	4[a]	41.88	3[a]	62.40	4	91.28	3

[a]Present measurement verifies results reported previously by Keyworth, et al.

[b]Structure at both 70.5 and 74.5 eV consists of a mixture of levels; ratio of 3^- to 4^- strengths is ~2:1 in both cases.

13. 180° n-p Cross Sections Near 25 MeV (Drosg)

In addition to its interest for understanding the n-p interaction, for fast neutron work above ~20 MeV the uncertainty in the $^{1}H(n,n)^{1}H$ cross section is the limiting factor in the accuracy of proton-recoil telescopes. The results of two measurements show that the 180° cross section as calculated by the YALE and LRL-CONSTRAINED phase shifts are too high by ~5% for laboratory neutron energies near 25 MeV.

The first measurement consisted of a comparison of a proton-recoil telescope with a TOF system calibrated to ±1% against precision charged particle cross sections. At five neutron energies between 23 and 29 MeV, the experimental 180° $^{1}H(n,n)^{1}H$ cross sections were (5.7 ± 3.3)% lower than the predictions of the YALE phase shifts, but only (0.6 ± 3.3)% lower than the predictions of the LRL-UNCONSTRAINED phase shifts (and also within 1% of the Gammel estimate).

The second measurement compared the energy dependence of the 180° $^{1}H(n,n)^{1}H$ cross section by measurements at 11.2 and 25.3 MeV. Here, only the relative (rather than absolute) efficiency of the TOF comparison detector at the two energies was pertinent. The measured ratio (180°, 11.2 MeV):(180°, 25.3 MeV) was 2.22 ± 0.06. This can be compared with a value of 2.08 from the YALE prediction and a value of 2.15 from the LRL-UNCONSTRAINED prediction, favoring the latter.

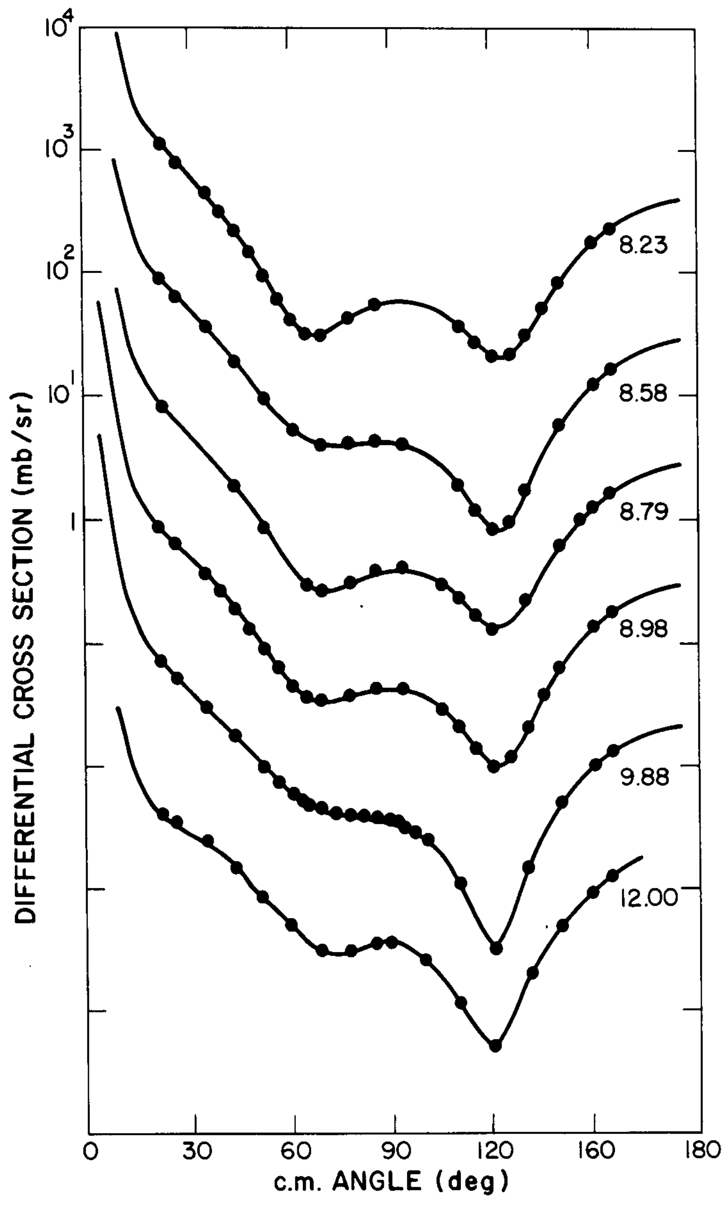

Fig. A-1. Differential cross section as a function of c.m. angle for $^4He(t,t)^4He$ elastic scattering at the idicated triton incident energies (MeV). The ordinate scale applies to the top curve only; the lower curves have been displaced downward in successive one decade steps.

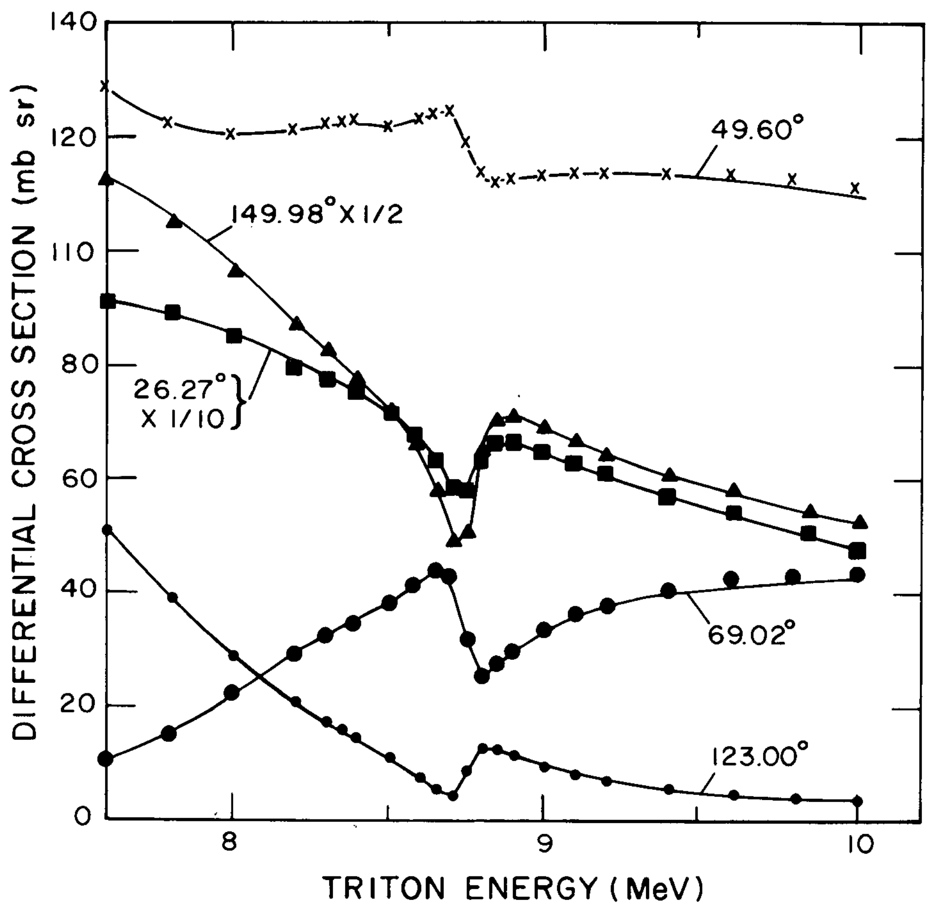

Fig. A-2. Differential cross section as a function of incident triton energy for $^4He(t,t)^4He$ at the indicated c.m. angles.

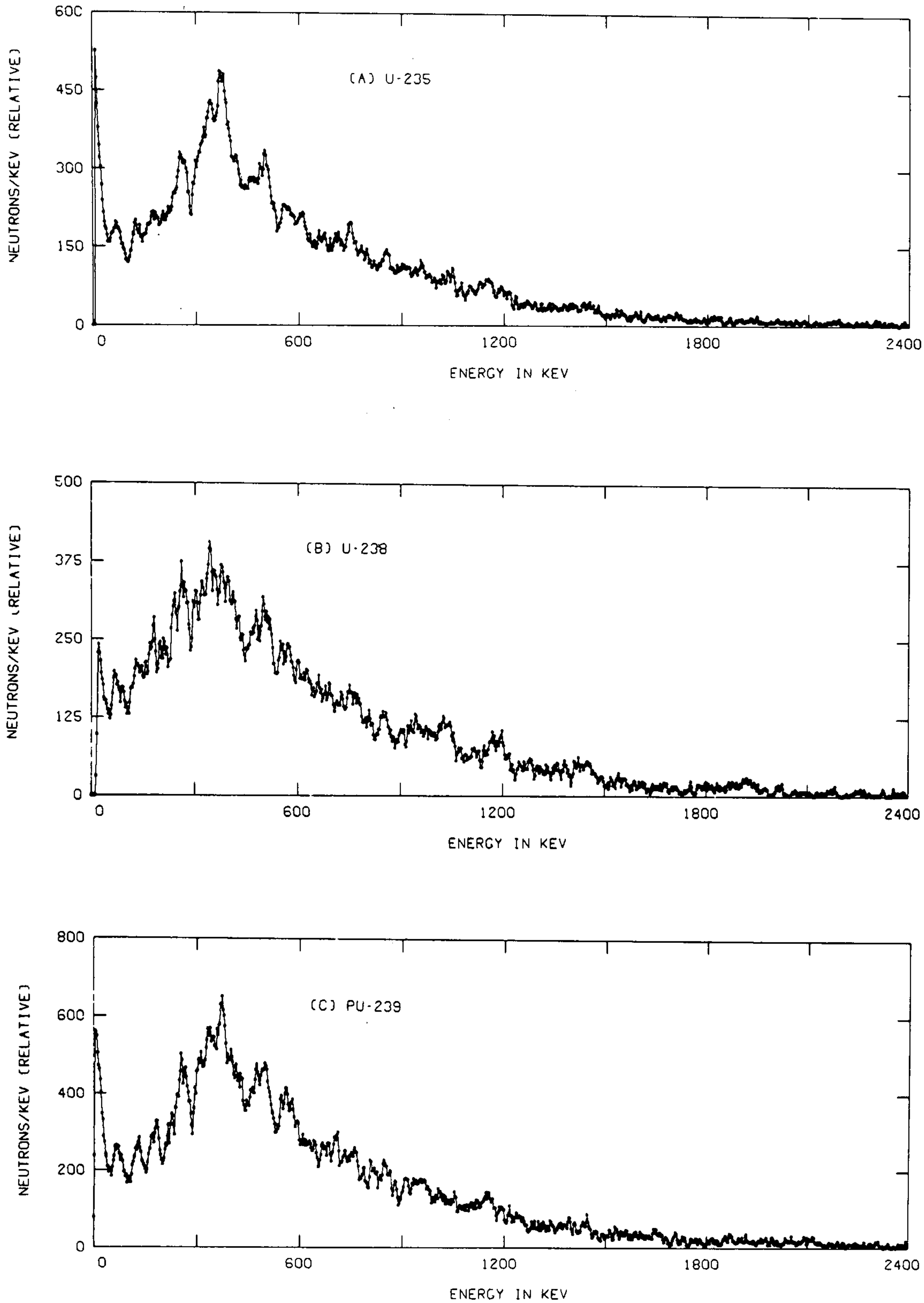

Fig. A-3. Equilibrium spectra of delayed neutrons from fast fission of (a) ^{235}U; (b) ^{238}U; and (c) ^{239}Pu. Energy resolution of the spectra varied from 16 keV for thermal neutrons to 54.3 keV for 1.5-MeV neutrons.

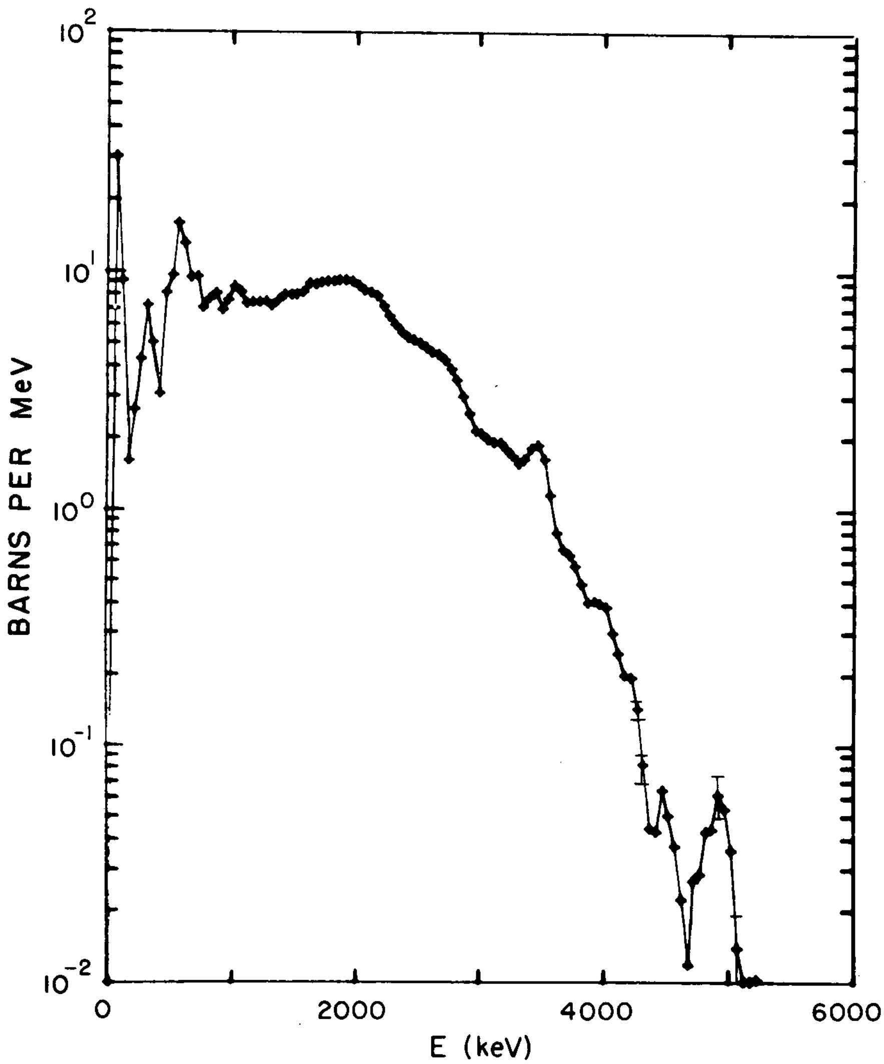

Fig. A-4. Cross section for producing gamma rays of energy E in the $^{232}Th(n_{th},\gamma)$ reaction.

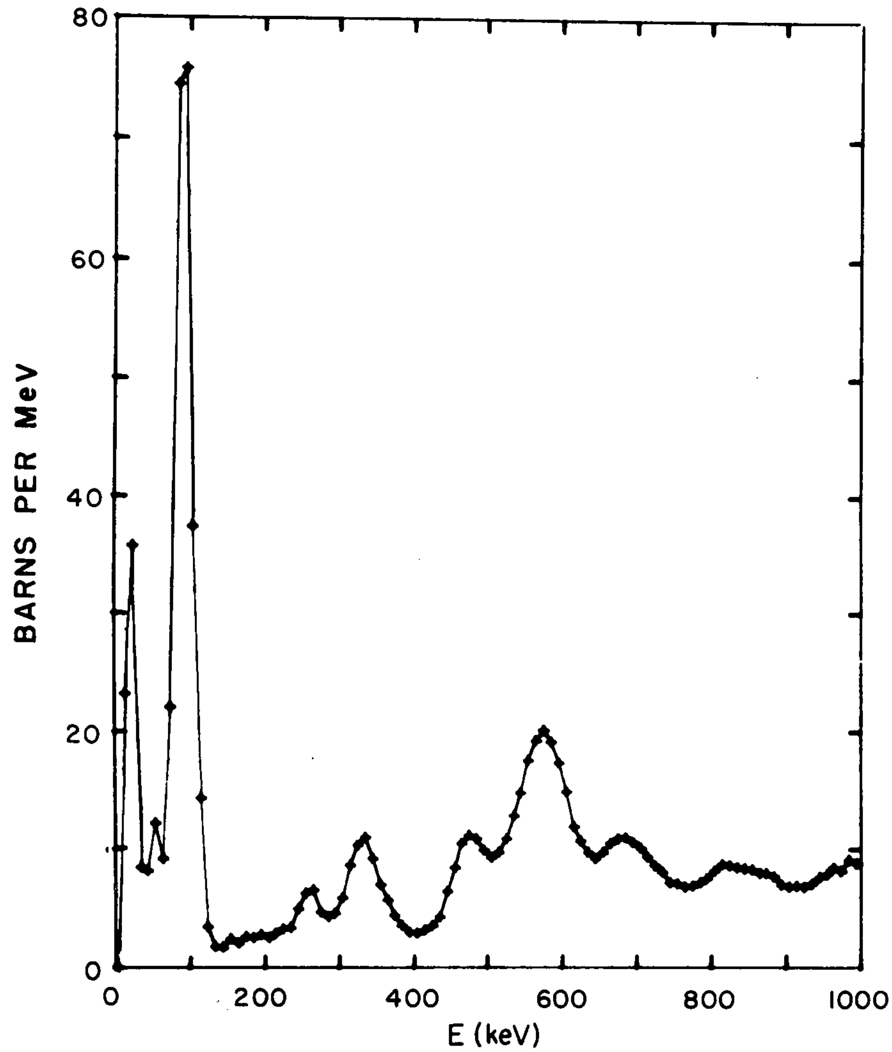

Fig. A-5. Details of the first 1 MeV of the $^{232}Th(n_{th},\gamma)$ spectrum.

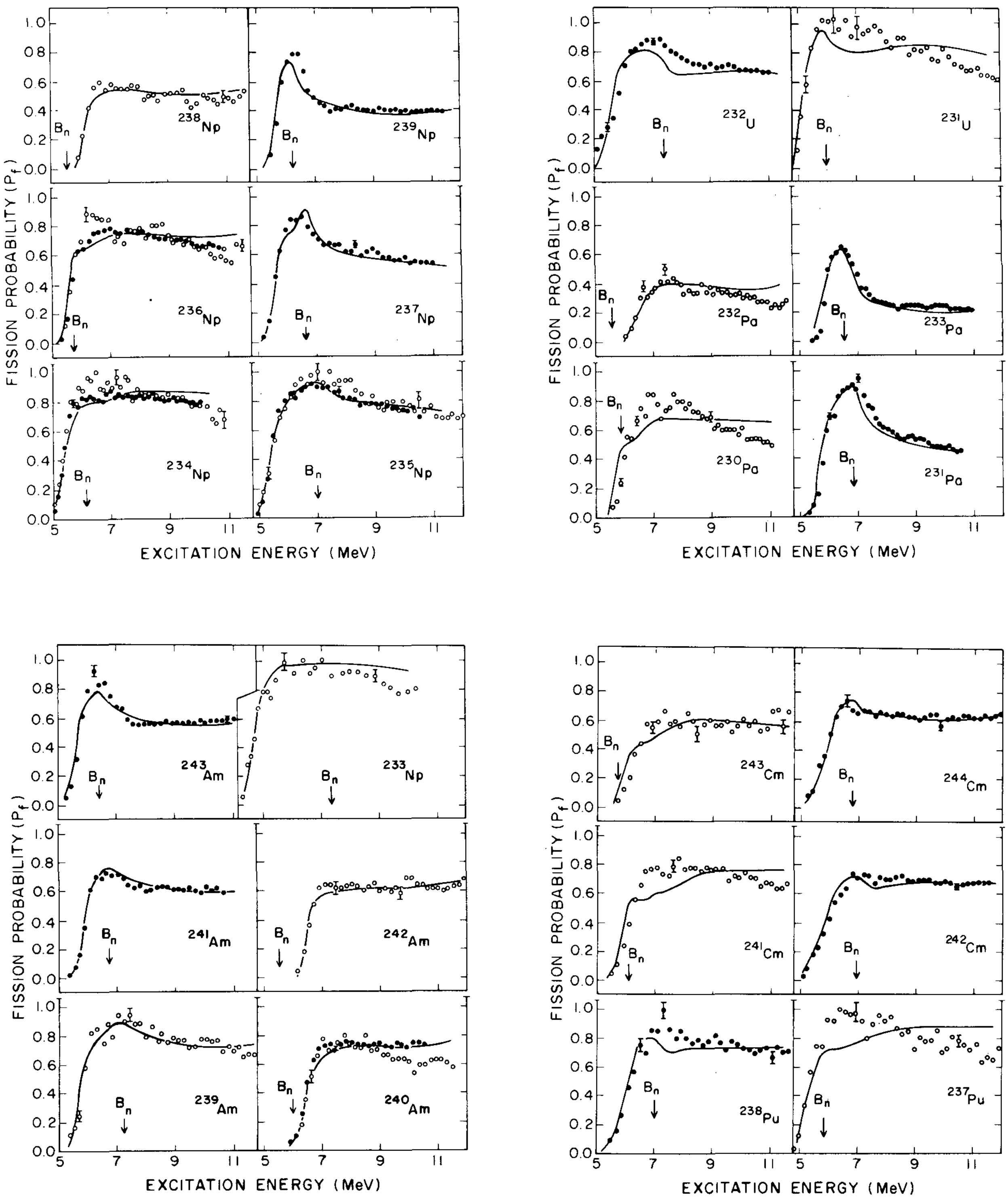

Fig. A-6. Measured fission probabilities: open circles, from (^{3}He,tf) reactions; closed circles, from (^{3}He,df) reactions; full lines, model fits as discussed in the text.

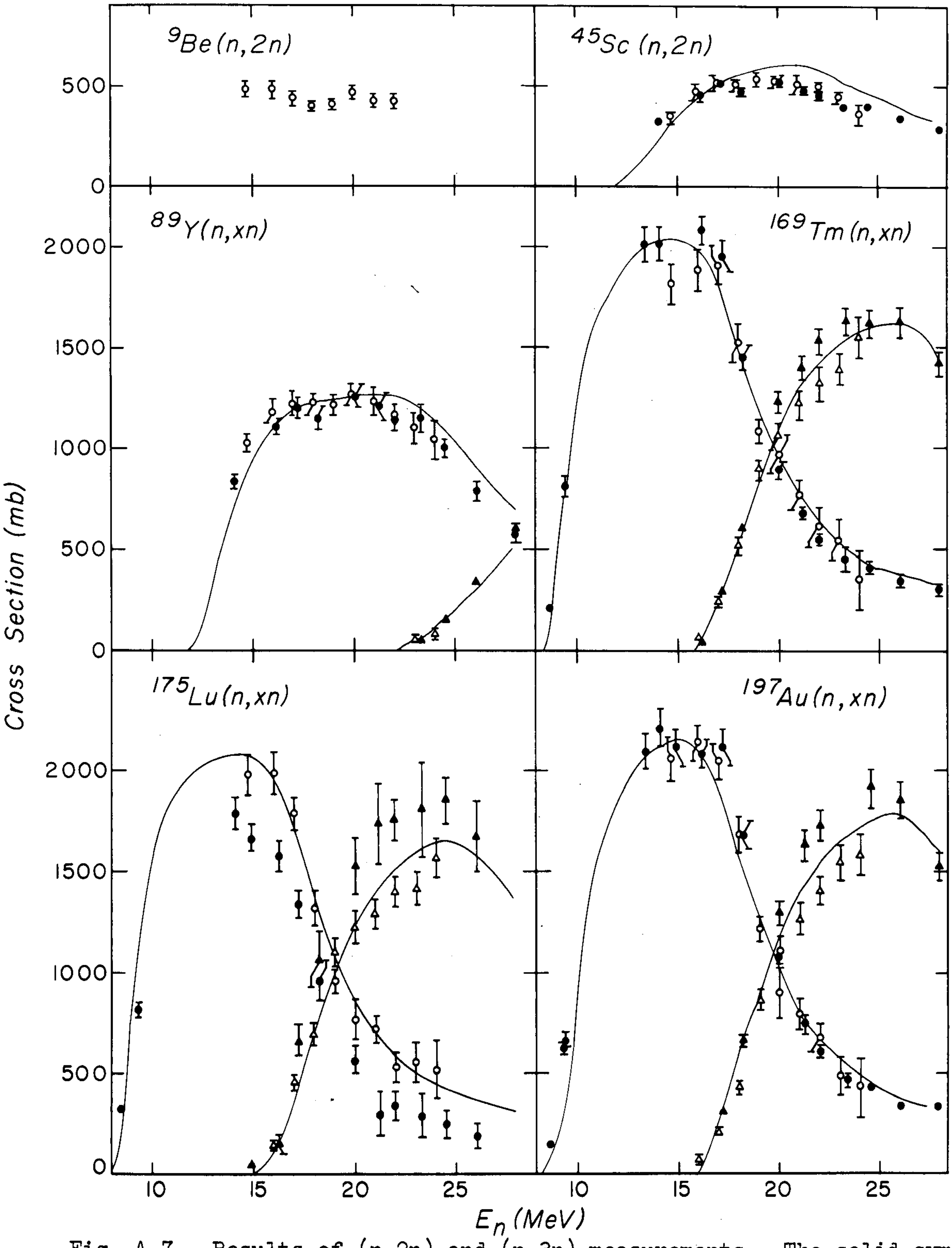

Fig. A-7. Results of (n,2n) and (n,3n) measurements. The solid symbols show radiochemical measurements given in Ref. 1, and the open symbols are our results. Circles are the (n,2n) measurements and triangles are the (n,3n) results. The curves are calculations from Ref. 12.

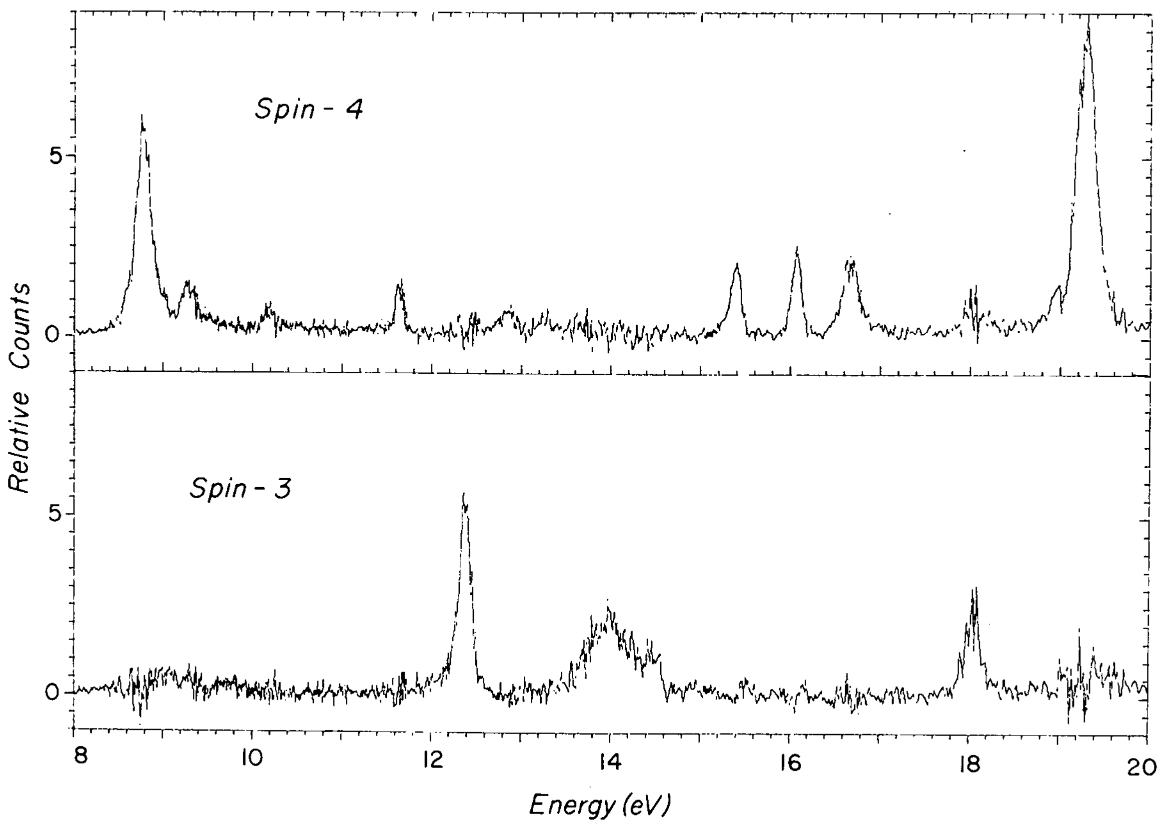

Fig. A-8. Plot of the net relative observed counts separated into the two spin components from 8 to 20 eV.

B. OTHER NUCLEAR DATA

1. Proton-Proton Analyzing Power Measurements at 16 MeV (Lovoi, Ohlsen, Jarmie, Moss, and Stupin)

Proton-proton elastic scattering analyzing powers are very small at low energies because of the nature of the P-wave forces. Only recently has this observable been measured with significant precision: by Hutton, Haeberli and Knutson at Wisconsin[1] at 10 MeV; and by our group at 16 MeV.[2,3] Both groups attained accuracies of ±0.0002.

Our results are given in Table B-1. The errors given are dominated by the statistical error. The beam energy was 16 MeV ±15 keV. The Livermore phase shift prediction[4] is in relatively good agreement. The Wisconsin results at 10 MeV were somewhat smaller than the LRL prediction.[4] The significance of the analyzing power measurements, in particular their effect on the tensor and spin-orbit terms of the nuclear force, await detailed analysis.

Table B-1

Proton-Proton Analyzing Power at 16 MeV

θ(lab) deg.	θ(cm) deg.	Analyzing Power	
10.00	20.08	-0.0043	±0.0004
11.50	23.09	-0.0041	±0.0002
13.00	26.10	-0.0035	0.0003
15.00	30.11	-0.0027	0.0002
16.00	32.12	-0.0018	0.0007
18.00	36.14	-0.0007	0.0008
20.00	40.15	-0.0010	0.0003
25.00	50.18	-0.0000	0.0012
35.00	70.22	+0.0001	0.0007

[1] J. D. Hutton, W. Haeberli, and L. D. Knutson, Bull. Am. Phys. Soc. 20, 576, (1975).

[2] P. A. Lovoi, N. Jarmie, G. G. Ohlsen, C. E. Moss, Bull. Am. Phys. Soc. 20, 85 (1975).

[3] P. A. Lovoi, "Proton-proton analyzing power measurements at 16 MeV," (unpublished) Ph.D. dissertation, U. of New Mexico (1975).

[4] M. H. MacGregor, R. A. Arndt, and R. M. Wright, Phys. Rev. 182, 1714 (1969).

2. $^4He(p,p)^4He$ Elastic Scattering (Jarmie, Hale, Dodder, and Hardekopf)

An extensive R-matrix analysis of the p-alpha system from 0 to 18 MeV is underway. The inclusion of new A_y data at 12 and 17 MeV has improved the fit. We are now able to predict any cross section or other observable in this system in statistical agreement with the known experimental data. The results are important in two ways. First this reaction is frequently used as a polarization analyzer, and second this will be the first complete and statistically reliable phenomenological fit of few nuclear reaction data outside of nucleon-nucleon scattering.

3. Few Nucleon Experiments with Polarized Triton Beams (Ohlsen, Haglund, Jarmie, Brown, Poore, Hardekopf, Walter, Lisowski)

Extensive studies of the polarization analyzing powers of several triton-induced reactions have been made. These include $^4He(\vec{t},t)^4He$ elastic scattering (7-14.2 MeV); $^3He(\vec{t},t)^3He$ elastic scattering (9-17 MeV); the reaction $^3He(\vec{t},d)^4He$ (9-17 MeV); $D(\vec{t},t)D$ elastic scattering (10.5 MeV), and the reaction $D(\vec{t},{}^4He)n$ (10.5 MeV). Most of the data are currently being analyzed via the LASL R-matrix code EDA and should contribute to the understanding of their particular mass system. In particular the reaction $^3He(\vec{t},d)^4He$ is of interest because the isospin symmetry of the initial reactants leads to an expected symmetry of the outgoing particles. The $D(\vec{t},{}^4He)n$ reaction should prove useful in the analysis of the $T(d,n)^4He$ neutron source reaction.

4. Optical Model Studies with Polarized Tritons (Hardekopf, Veeser, Keaton, Haglund, Ohlsen)

We have begun to study the elastic scattering of polarized tritons from intermediate and heavy nuclei to investigate the optical model potential, particularly its spin-orbit component. Optical model studies for deuterons have not been successful in reproducing polarization measurements, probably because of the complexity of the second-rank tensor potentials needed to describe scattering of spin-one particles. We hope that by starting with the simpler case of spin-1/2 particles, tritons, we might have more success in determining an optical model potential for composite particles. Until now it has usually been assumed that the triton spin-orbit potential is negligible. Our early results for 15-MeV tritons (Hardekopf, Veeser and Keaton, Phys. Rev. Letters **35**, 1623, 1975) indicate that this assumption is not correct.

We have recently measured the triton analyzing power at 17 MeV from 20 - 160° (5° steps) for the following nuclei:

^{40}Ca	^{54}Fe	^{60}Ni	^{94}Zr	^{208}Pb
^{46}Ti	^{56}Fe	^{68}Zn	^{116}Sn	
^{48}Ti	^{58}Ni	^{90}Zr	^{140}Ce	

We expect to measure a few more targets at this energy and perhaps at lower energies for the lighter elements. We also need to obtain cross sections in closer angular steps. Following data reduction we will undertake an optical-model analysis of the data to obtain a fairly complete, mass-dependent parameterization of the triton optical model.

5. Lifetime and Character of the Lowest Two-Quasiparticle State in ^{240}Pu (Bunker, Nielsen, Starner, Orth and Naumann)

The lifetime of the 1030.6-keV level of ^{240}Pu has been measured, using a delayed-coincidence technique. The level was populated via the electron-capture decay of ^{240}Am (51 h), produced in an underground nuclear explosion. The main purpose of the experiment was to obtain further information on the character of the 1030.6-keV state. Various arguments[5] had suggested that it was the band head of a $K^{\pi} = 3^{+}$ two-quasiparticle band.

The half-life was measured to be $T_{1/2}$(1030.6 keV) = 1.32 ± 0.15 ns, which is consistent with a K, $I^{\pi} = 3,3^{+}$ two-quasiparticle assignment and excludes a $2,3^{+}$ rotational assignment. This result, coupled with other data on the 1030.6-keV state, suggests a two-neutron Nilsson configuration of $[n622\uparrow + n631\downarrow]_{+}3^{+}$. In agreement with a prediction by Voros *et al.*,[6] this particular 3^{+} state appears to lie lowest of all two-quasiparticle states in ^{240}Pu. The energy and quantum character of such states provide important information about the nuclear pairing interaction.

---

[5] I. Ahmad, R. F. Barnes, R. S. Sjoblom, and P. R. Fields, J. Inorg. Nucl. Chem. 34, 3335 (1972).

[6] T. Voros, V. G. Soloviev, and T. Siklos, Izv. AN (ser. fiz.) 26, 1045 (1962).

C. INTEGRAL EXPERIMENTS

1. Tritium Production from the $^6Li(n,\alpha)t$ and $^7Li(n,n'\alpha)t$ Reactions (Ragan, Hemmendinger, Shunk, and Ellis)

We have made integral measurements to study the production of tritium from the $^6Li(n,\alpha)t$ and the $^7Li(n,n'\alpha)t$ reactions. A 30-cm radius sphere of LiD was placed around an isotropic source of 14-MeV neutrons produced by bombarding a tritium-titanium target with 300-keV deuterons from a Cockcroft-Walton accelerator. Quartz ampules of two sizes containing about 0.15 or 1.0 g of LiH were distributed at 5 radii in the sphere. Ampules containing ^{7}LiH(99.9% ^{7}Li) were placed in one plane at 115° to the beam and ampules of ^{6}LiH(95% ^{6}Li) were placed in a plane at 70° to the beam. These ampules will be analyzed for their tritium content after irradiation by $\sim10^{16}$ source neutrons.

In order to check the tritium assay procedure, ampules containing ^{6}LiH(0.1% ^{6}Li) and .0508-mm diameter gold wire were irradiated in the thermal column of the Omega West Reactor. At thermal energies the $Au(n,\gamma)$ and $^6Li(n,\alpha)t$ cross sections are well known, and by counting the 412-keV γ-rays from the activated gold with a Ge(Li) detector whose efficiency was measured, the neutron flux and thus the amount of tritium was determined. The analysis of these thermal irradiated samples is proceeding.

2. Neutron Spectrum From a ^{235}U Sphere Bombarded by 14-MeV Neutrons (Ragan, Auchampaugh, Hemmendinger, Silbert)

A benchmark measurement of the neutron leakage spectrum from a pulsed 38-kg oralloy (93.5% ^{235}U) sphere has been made using time-of-flight (TOF) techniques. The sphere had a multiplication of approximately 11 for 14-MeV neutrons, and a neutron hold up time of ~40 ns. The centrally located source of 14.1 ± 0.8 MeV neutrons, produced by bombarding a tritium gas target with pulses of low-energy deuterons, was isotropic to ± 7.7%. Neutrons in the 0.18 - 16.0-MeV energy range were detected at the end of a 39-m flight path by an Ne-213 liquid scintillator employing pulse shape discrimination. The uncertainty in the detector efficiency dominates the overall error in the measured spectra at low energies. In Figure C-1, the measured neutron flux as a function of energy is compared with the results of Monte Carlo calculations performed with the code MCN. Uranium cross sections from ENDF/B-IV and an older set from the Lawrence Livermore Laboratory were used in these calculations. The results calculated using the ENDF/B-IV cross sections are in good agreement with the measurements, especially in the 1- to 6-MeV energy region where the uncertainties in both the calculated and experimental results are the smallest.

This work is to be published in Nuclear Science and Engineering; also see Trans. Am. Nucl. Soc. 22 716 (1975).

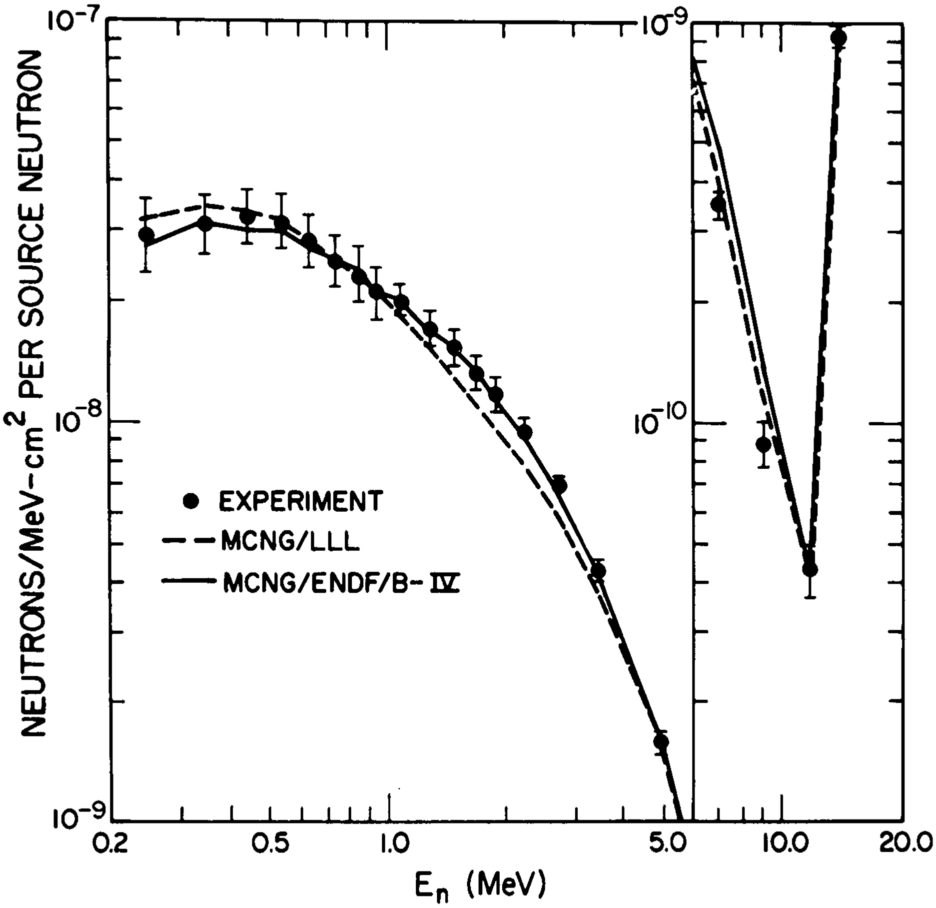

Fig. C-1. Measured and calculated neutron leakage spectrum from a 38-kg sphere of 93.5% ^{235}U with a central 14 MeV neutron source.

D. EVALUATIONS

1. $^{6}Li(n,\alpha)$ (Hale and Dodder)

A new evaluation of the neutron cross sections for ^{6}Li at low energies has just been completed, based on an extension of the comprehensive R-matrix analysis of the ^{7}Li system described at the Conference on Nuclear Cross Sections and Technology.[1] The n + $^{6}Li^{*}(2.185)$ channel has been added in the present analysis, since the data now extend to energies above its threshold. These data include final values of the precise $^{4}He(t,t)$ differential cross sections[2] and new measurements of the $^{4}He(\vec{t},t)^{4}He$ analyzing power[3] done at LASL. Recent measurements of the neutron total cross section[4] and of the $^{6}Li(n,\alpha)$ integrated cross section[5] were also included in the analysis. Figure D-1a shows that the calculated $^{6}Li(n,\alpha)$ cross section is quite consistent with the preliminary new measurements below 600 keV. These calculated values have been proposed for use as an ENDF/B-V standard at energies below 150 keV; they are estimated to be determined to within ±3% even at energies over the resonance.

2. $^{10}B(n,\alpha)$ (Hale and Arthur)

A new evaluation of the neutron cross sections for ^{10}B at low energies has also been completed recently. The evaluation is based on a multichannel, multilevel R-matrix analysis of reactions in the ^{11}B system similar to that which was used to provide the boron cross sections for ENDF/B-IV. New data that were considered in the present analysis include relative measurements of the $^{10}B(n,\alpha\gamma)$ integrated cross

---

[1] G. M. Hale, Proceedings, Conference on Nuclear Cross Sections and Technology, NBS Special Publication 425, p 302 (1975).

[2] N. Jarmie et al., Bull. Am. Phys. Soc. 20, 596 (1975).

[3] R. A. Hardekopf, N. Jarmie, G. G. Ohlsen, and R. V. Poore, Proceedings of the Fourth International Symposium on Polarization Phenomena in Nuclear Reactions, Zurich, 1975 (to be published).

[4] J. A. Harvey and N. W. Hill, Proceedings, Conference on Nuclear Cross Sections and Technology, NBS Special Publication 425, p 244 (1975), and private communication (1976).

[5] G. Lamaze, National Bureau of Standards, private communication (1976).

section[6] and absolute measurements of the $^{10}B(n,\alpha\gamma)$ angular distribution.[7]

The resulting fit to the $^{10}B(n,\alpha)$ integrated cross section is seen in Fig. D-1b to be almost identical to the Version IV calculations at energies below 200 keV, while it decreases more rapidly than before at energies up to 1 MeV. The calculated values of the $^{10}B(n,\alpha)$ cross section have been proposed for use as an ENDF/B-V standard at energies below 150 keV.

3. Statistical-Preequilibrium Model Code Development (Arthur and Young)

The development of the new preequilibrium-statistical nuclear model code GNASH has continued with the addition of an improved preequilibrium form[8] to account for semidirect processes in excitation cross sections and spectral yields. The capability to calculate individual component spectra from complex reactions such as (n,2n) and (n,3n) has been added. As described previously,[9] the code offers considerable flexibility in the calculation of reaction and level excitation cross section isomer ratios, and neutron, gamma-ray, and charged-particle spectra from particle-induced reactions.

Recent calculations using this code have centered around two main areas of interest. The first is concerned with calculation of charged-particle spectra and production cross sections from 15-MeV neutron bombardment of various materials of CTR interest. The calculated proton spectrum for the Al(n,xp) reaction obtained using global input parameters compares favorably with the preliminary measurements

---

[6] R. Schrack, National Bureau of Standards, private communication (1976).

[7] R. M. Sealock and J. C. Overley, "$^{10}B(n,\alpha)^7Li$, $^7Li^*$ Differential Cross Section Measurements between .2 and 1.25 MeV," submitted to Phys. Rev. C (1976); R. M. Sealock, "A Measurement of Differential Cross Sections for the $^{10}B(n,\alpha)$ ^7Li, $^7Li^*$ Reactions," Dissertation, University of Oregon, unpublished (1975).

[8] L. Milazzo-Colli and G. M. Braga-Marcazzan, Nucl. Phys. A210, 297 (1973).

[9] E. D. Arthur and P. G. Young, "A New Statistical Preequilibrium Nuclear Model Code," to be presented at the ANS Annual Meeting, Toronto (1976).

of Haight et al.[10] Similar calculations have been performed for ^{46}Ti, ^{48}Ti, ^{51}V, ^{58}Ni, ^{59}Co, and ^{93}Nb.

The second class of problems has been concerned with the calculation of the spectra of first and second neutrons from (n,2n) reactions, and the first, second and third neutron spectra from (n,3n) reactions. The calculated spectra have been used by Veeser et al.[11] to make efficiency corrections for (n,xn) reactions measured with a large liquid scintillator tank. Figure D-2 shows an example of the calculated first neutron spectra for Au(n,xn) reactions induced by 24 MeV neutrons. Figure D-3 shows the overall agreement of the calculated Au(n,xn) cross section with recent experimental measurements.[11,12] This spectrum capability is also important for meeting requirements of the ENDF/B evaluated data file. Other nuclei for which similar calculations have been made are ^{89}Y, ^{175}Lu, ^{181}Ta, ^{204}Pb, ^{206}Pb, ^{207}Pb and ^{208}Pb.

4. New Evaluation of n + ^6Li Cross Sections Above 1 MeV (Stewart and Young)

Because much of the ^6Li evaluated data in the ENDF/B-IV general purpose file is based on a rather old United Kingdom data set,[13] we have re-evaluated the ^6Li data incorporating more recent experimental results. Modifications were made to the total, elastic, (n,n'd), (n,p), and (n,α) cross sections, to the elastic angular distributions, and to the energy and angular distributions of secondary neutrons from (n,n'd) and (n,2n) reactions.

The most significant revision was in the representation of secondary neutrons from the $^6Li(n,n'd)^4He$ reaction. In order to include energy-angle correlations in the data without introducing new requirements on ENDF/B processing codes, we used "pseudo levels" and phase-space arguments to represent the neutron continuum from the (n,n'd)

---

[10] R. C. Haight et al., Lawrence Livermore Laboratory UCRL-77151 (preprint) (1975).

[11] L. R. Veeser and E. D. Arthur, Bull. Am. Phys. Soc. 20, 1196 (1975).

[12] B. P. Bayhurst et al., Phys. Rev. C12, 451 (1975).

[13] E. D. Pendlebury, Atomic Weapons Research Establishment report AWRE 0-60/64 (July 1974) and AWRE 0-61/64 (July 1974).

reaction. In Fig. D-4, experimentally measured[14] neutron spectra at 30 and 134° for 5.74-MeV incident neutrons are compared to nonelastic neutron spectra from the pseudo-level representation and from the older ENDF/B-IV temperature representation. The ENDF/B-IV data do not describe the inelastic group to the 2.2-MeV state of ^{6}Li very well and predict too hard a spectrum at back angles. Indeed, nonelastic neutrons in the 134° spectrum have energies higher than the elastic peak. Similar effects appear in comparisons at other energies and angles.

5. Beta and Gamma Spectra and Total Decay Energies from Fission Products (England and Stamatelatos)

The ENDF/B-IV fission product files[15] contain data for some 711 radioactive nuclides of which 180 also have spectral data (end-point beta energies, gamma energies, and intensities). In order to test this data base, we have performed various calculations of gamma and beta spectra and total decay energies for comparison with new benchmark experiments at LASL, ORNL, and IRT. Summation calculations of total energies and spectra are made with an extended version of the CINDER-7 code,[16] and comparisons are given in Table D-1, with new measurements of total gamma energies by Dickens et al.[17]

6. Energy Release from Gaseous and Solid Fission Products Following ^{235}U and ^{239}Pu Fission (England)

We have calculated for a variety of irradiation conditions the energy release as a function of cooling time after thermal and fast fission of ^{235}U and ^{239}Pu for both gaseous fission products and for the total conglomerate of products.[18] The CINDER[16] code was used with the

[14] John C. Hopkins, D. M. Drake, and H Condé, Nucl. Phys. A107, 139 (1968) and Los Alamos Scientific Laboratory report LA-3765 (Nov. 1967).

[15] T. R. England and R. E. Schenter, Los Alamos Scientific Laboratory report LA-6116-MS (ENDF-223) (Sept. 1975).

[16] T. R. England, R. Wilczynski, and N. L. Whittemore, Los Alamos Scientific Laboratory report LA-5885-MS (April 1975).

[17] J. K. Dickens et al., Oak Ridge National Laboratory report ORNL-TM-5156 (Nov. 1975).

[18] T. R. England, R. E. Schenter, and N. L. Whittemore, Los Alamos Scientific Laboratory report LA-6021-MS (July 1975).

Table D-1

Comparison of Calculated Total Gamma Heating With Recent Measurements

2.4s ^{235}U Irradiation

Cooling Interval (sec)	Integrated MeV/Fission		% Difference (Calc-Exp)/Exp
5-7	0.164	7.9%	-13
7-9	0.133	8.3	-11
9-14	0.242	9.5	-5
14-19	0.178	6.2	-2
19-29	0.260	5.8	-1
29-39	0.190	5.8	0
39-59	0.278	5.8	-2
59-79	0.195	5.7	-0.5
79-99	0.149	5.4	-0.7
99-149	0.254	5.5	+0.8
149-199	0.163	5.5	+3
199-299	0.206	5.8	+5
299-600	0.307	6.5	+8

100.4s ^{235}U Irradiation

10-30	0.227	10 %	+4
30-50	0.161	8.1	+3
50-100	0.266	6.8	+2
100-150	0.169	5.9	+3
150-250	0.212	5.7	+4
250-350	0.138	5.8	+3
350-550	0.186	5.4	+2
550-750	0.129	5.4	+2
750-950	0.101	5.9	+3
950-1450	0.185	5.4	+5
1450-1950	0.132	5.3	+9
1950-2450	0.100	6.0	+13
2450-14400	0.636	6.5	+9

latest ENDF/B-IV fission product data for the calculations, which cover the time period 0.1 s to >30 yr. Gases are assumed to be the unstable isotopes of Br, Kr, I, and Xe, whether formed directly in fission reactions or as radioactive daughter nuclei. The total decay power calculation involves some 711 nuclides; 150 of these are precursors to ~80 gaseous nuclides which were coupled in 61 linear chains for the gas calculation.

The fractional content and gamma-ray energy release from gaseous fission products are plotted in Fig. D-5 as functions of time following an instantaneous fission burst of ^{239}Pu. While the relative number of gaseous nuclides formed is not large (<25% of all times), their energy release rate becomes important at times greater than 1 h and approaches 50% of the total gamma-ray energy at times near 1 day. An integral of the energy release for the important time period 0.1 to 50 h shows that ~30% of the gamma-ray energy released in that time region is from gaseous products. While other factors such as gas entrapment and decay of solid daughters from gaseous precursors need to be considered, the present results show that substantial amounts of energy are produced by decay of volatile fission products.

7. Time-Dependent Spectra of Photons for Applied Problems (Foster and England)

Because of its possible importance in electromagnetic pulse calculations, we have evaluated the absolute photon spectrum emitted by ^{235}U and ^{239}Pu from the instant of a very short (<1 ns) fission burst to 10^8 seconds. The prompt spectrum has an average energy of about 0.9 MeV. The energy drops to 0.4 MeV by 1 ns, then rises monotonically to 1 MeV at about 60 s after fission. The data out to 15 s are from fairly recent direct measurements.[19-23] The data for later times were

[19] R. E. Sund and R. B. Walton, Phys. Rev. 146, 824 (1966).

[20] R. B. Walton and R. E. Sund, Phys. Rev. 178, 1894 (1969).

[21] V. V. Verbinski and R. E. Sund, General Atomic report GA-9148 (1969).

[22] R. E. Sund, H. Weber, and V. V. Verbinski, Phys. Rev. C10, 853 (1974).

[23] P. C. Fisher and L. B. Engle, Phys. Rev. 134, B796 (1964).

originally taken from rather old work,[24] but we are now replacing them with a detailed calculation using ENDF/B-IV fission-product data in the CINDER code.[15,16]

[24] F. C. Maienschein, R. W. Peelle, W. Zobel, and T. A. Love, Proc. 2nd Internl. Conf. Peaceful Uses of Atomic Energy (United Nations, Geneva, 1958) V. 15, p 366.

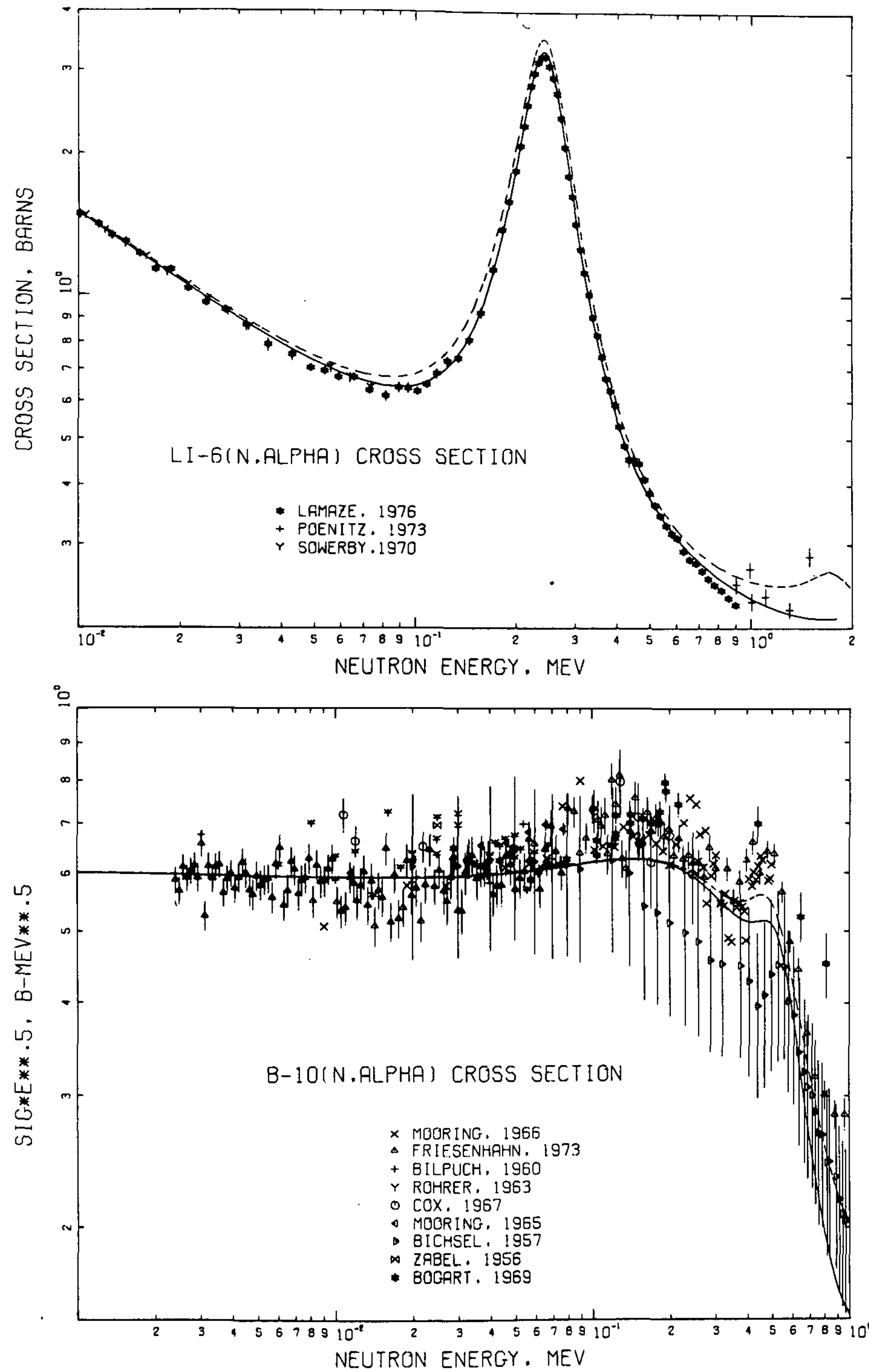

Fig. D-1. Comparison of calculated and measured values of (a) the ^{6}Li(n,α) cross section between 0.01 and 1 MeV, and (b) the ^{10}B(n,α) cross section between 1 keV and 1 MeV. The solid curves are the present analyses; the dashed curves are ENDF/B-IV.

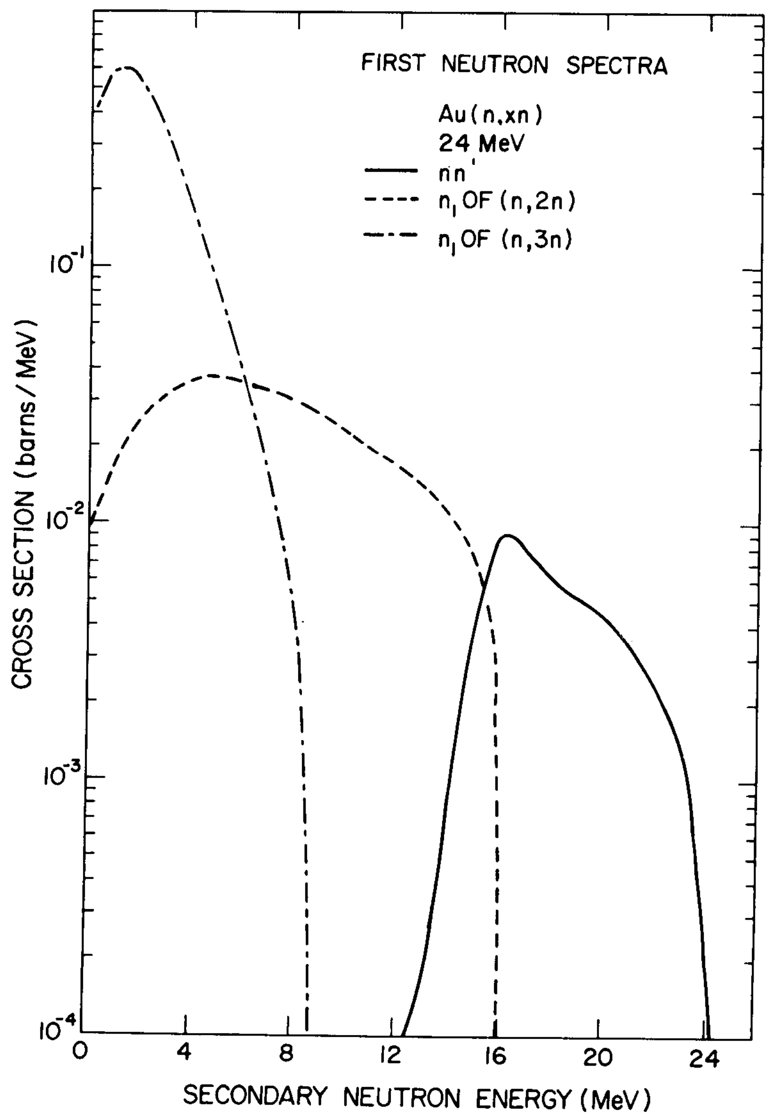

Fig. D-2. Calculated first neutron spectra for Au(n,xn) reactions induced by 24 MeV neutrons.

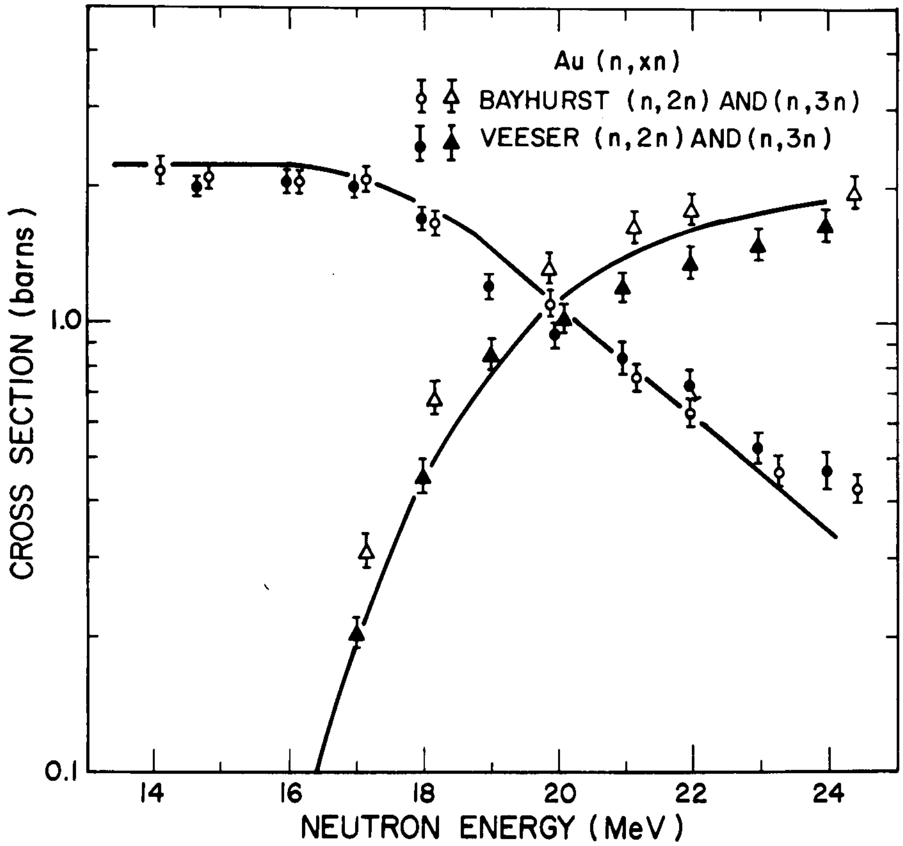

Fig. D-3. A comparison of GNASH calculated results with recent Au(n,xn) measurements of Bayhurst et al. and Veeser et al.

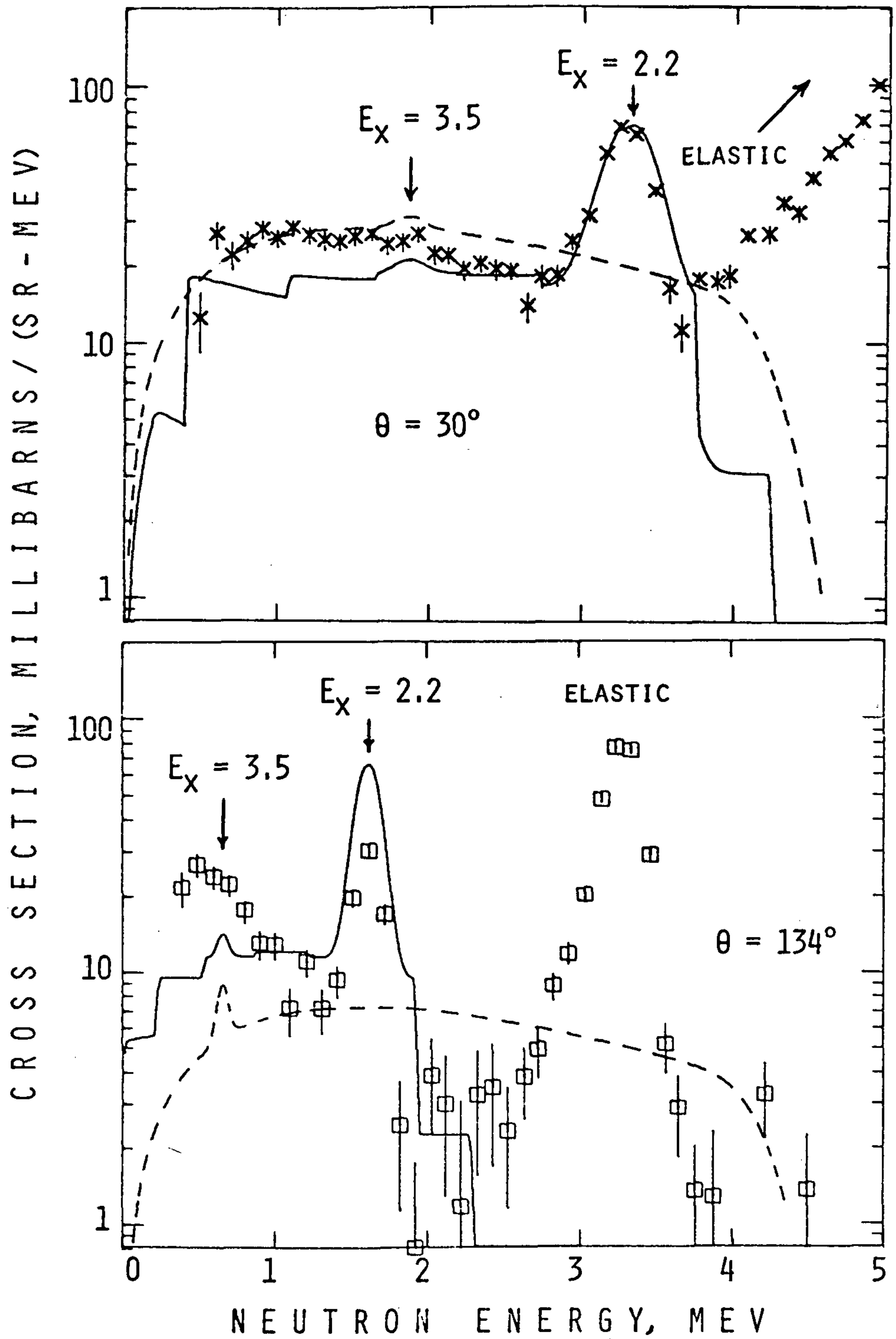

Fig. D-4. Laboratory energy spectra of the neutrons scattered by 5.74-MeV neutrons from ^6Li. The curves represent the nonelastic neutrons; the dashed curve is from ENDF/B-IV whereas the smooth curve includes a "pseudo-level" representation of the (n,n'd) neutrons. The points are the experimental data from Ref. 4.

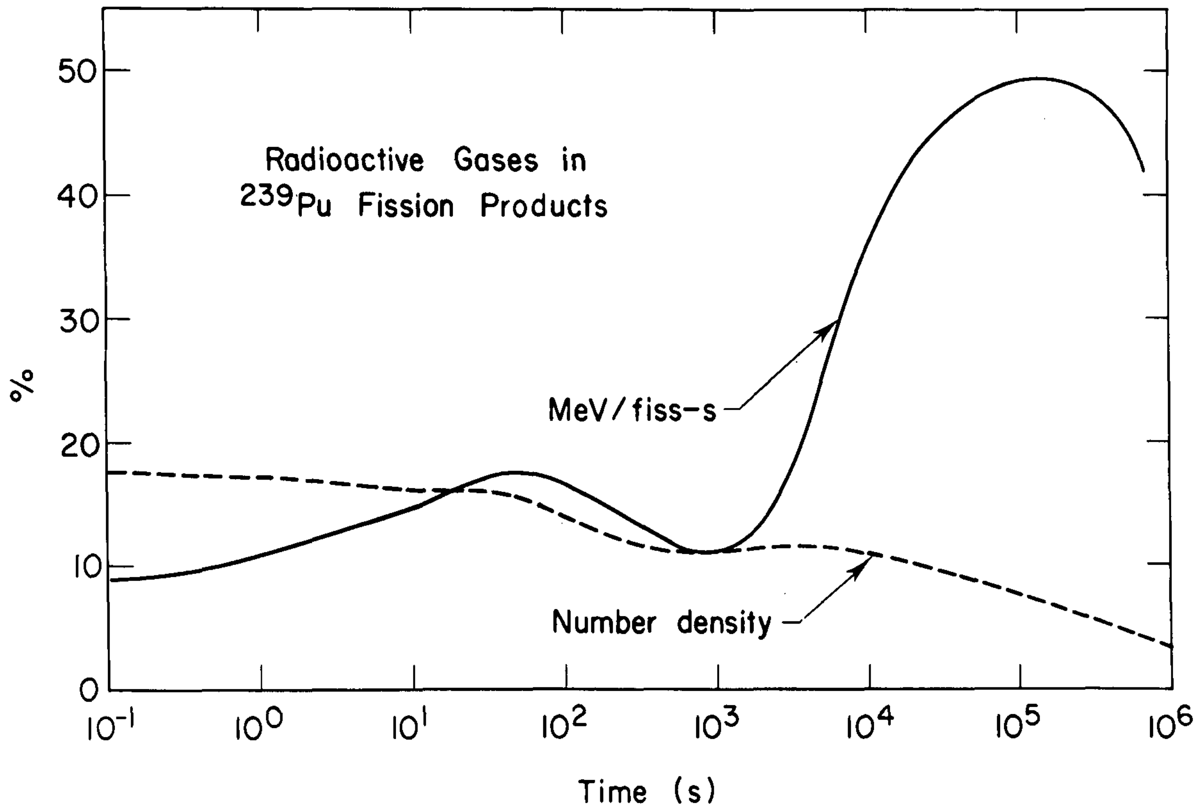

Fig. D-5 Percentage of the total number of nuclei produced and gamma-ray energy released that are attributed to gaseous products.

E. APPLICATIONS, SOURCES, FACILITIES

1. Signal-to-Background Ratio for Neutron Production Between 6 and 14 MeV by the Reactions $^3H(p,n)^3He$, $^1H(t,n)^3He$, and $^2H(d,n)^3He$ (Drosg, Auchampaugh, Gurule)

In employing "monoenergetic" neutron sources in the energy range from 6 to 14 MeV, it is of importance for many measurements that the primary reaction dominate and that extraneous neutrons from target gas breakup, beam window and beam stop reactions, and upstream slit and aperture reactions be minimized. We have investigated combinations of source reactions, target windows, and beam stops to determine the best signal-to-background ratio. A 3.7-m TOF system was used with the LASL tandem Van de Graaff accelerator. The reactions $^3H(p,n)$, $^1H(t,n)$ and $^2H(d,n)$ were compared and the effects due to target gas were separated from those due to the window and beam stop.

The $^3H(p,n)$ source gave signal to background ratios better by factors of ~15 at 14 MeV neutron energy than the $^2H(d,n)$ source yielding the same energy neutrons. The comparison is shown in Fig. E-1.

With respect to window and beam stop materials, consideration was given to molybdenum and ^{58}Ni windows and gold, tantalum, ^{12}C, ^{28}Si, and ^{58}Ni beam stops. If signal to background ratio is the primary factor, the $^3H(p,n)$ reaction with ^{58}Ni window and ^{28}Si beam stop is the optimum practical source. It must be noted, however, that for the same beam current and gas pressure, a $^1H(t,n)$ source yields nearly 20 times more primary neutrons. In gamma-ray sensitive experiments the (p,γ) reaction on ^{58}Ni may rule this material out. In this case the $^1H(t,n)$ source at high pressure may be preferable. Clearly, the best source for a specific purpose will depend on the experimental parameters.

2. Low-Level Uranium Assay by Delayed Neutron Counting (Minor, Bunker, Balestrini)

Facilities for the rapid assay of water and solids for trace concentrations of uranium, using a delayed-neutron counting method, have been built at the Omega West Reactor. The apparatus was designed specifically for use in the National Uranium Resources Evaluation (NURE) program, administered by the Grand Junction Office of ERDA. During the next four years, over 200,000 stream and stream sediment samples from New Mexico, Colorado, Wyoming, Montana, and Alaska will be assayed.

The neutrons are detected with an array of ^3He counters embedded in a cylinder of polyethylene. In the case of water, 40-ml samples are typically bombarded 60 sec in a thermal flux of 1.2×10^{13} n/cm^2 sec, then counted for 60 sec following a 30-sec delay (which eliminates interference from ^{17}N). The resulting sensitivity for uranium is about 0.5 parts per billion, with the dynamic range spanning many orders of magnitude. At present, only those samples having >10 ppb are being analyzed by this method; those with <10 ppb are being assayed by a fluorimetric technique in LASL's CMB Division. All sediments are being assayed by the delayed-neutron method. A 3-gm sample of screened material is bombarded for 20 sec and then counted for 20 sec following a 10-sec delay, yielding a cycle time of 1 assay/min and a U sensitivity of less than 0.1 parts per million. By fall of 1976, the assay system will be fully automated, with all timing of counting and sample movement controlled by a small computer.

3. Intense Neutron Source Facility - Status (Emigh)

In the document, USNDC-7, prepared for the U. S. Nuclear Data Committee meeting at Oak Ridge National Laboratory, 18-20 June 1973, a description of possible uses of the INS facility for obtaining nuclear data using 14-MeV neutrons was presented. These objectives remain part of the experimental program associated with the operation of the facility. At the present time, the INS facility has been authorized by Congress and an appropriation for construction is in the President's Budget for FY-77. Should this schedule be maintained, the facility will become operational and available for experimental operation early in 1981. The facility will contain two 14-MeV neutron sources, each capable of producing 10^{15} neutrons/sec with a maximum flux of $\sim 10^{14}$ neutrons/cm^2 sec on a continuous basis.

4. Determination of Boron Content of Materials Through the $^{10}B(n,\alpha)^7Li$ Reaction (Gladney, Jurney, Curtis)

We have investigated the analytical capabilities of a procedure based on the $^{10}B(n,\alpha)^7$ Li reaction for the precise determination of boron content in bulk samples of complex matrices. The doppler-broadened 478-keV gamma transition from $^7Li^*$ is compared in intensity with a dominant gamma (either prompt or delayed) from neutron capture in a standard having a well-known (n,γ) cross section, e.g. ^1H or ^{197}Au. The high reaction cross section of ^{10}B for thermal neutrons results in a correspondingly high sensitivity for the procedure; we have been able to make useful determinations of less than 0.1 μg of boron in gram quantities of material. The precision of the method has been demonstrated through analysis of various industrial and environmental NBS Standard Reference Materials.

Although boron is known to be an important element in plant metabolism, with a relatively narrow range between deficiency and toxicity in many agriculturally important plants, the geochemistry of B and the impact of its dissemination into the environment by industrial processes have not been widely studied because of the relative difficulty and other shortcomings of available procedures. We believe the analytical method described here can make an important contribution to these studies.

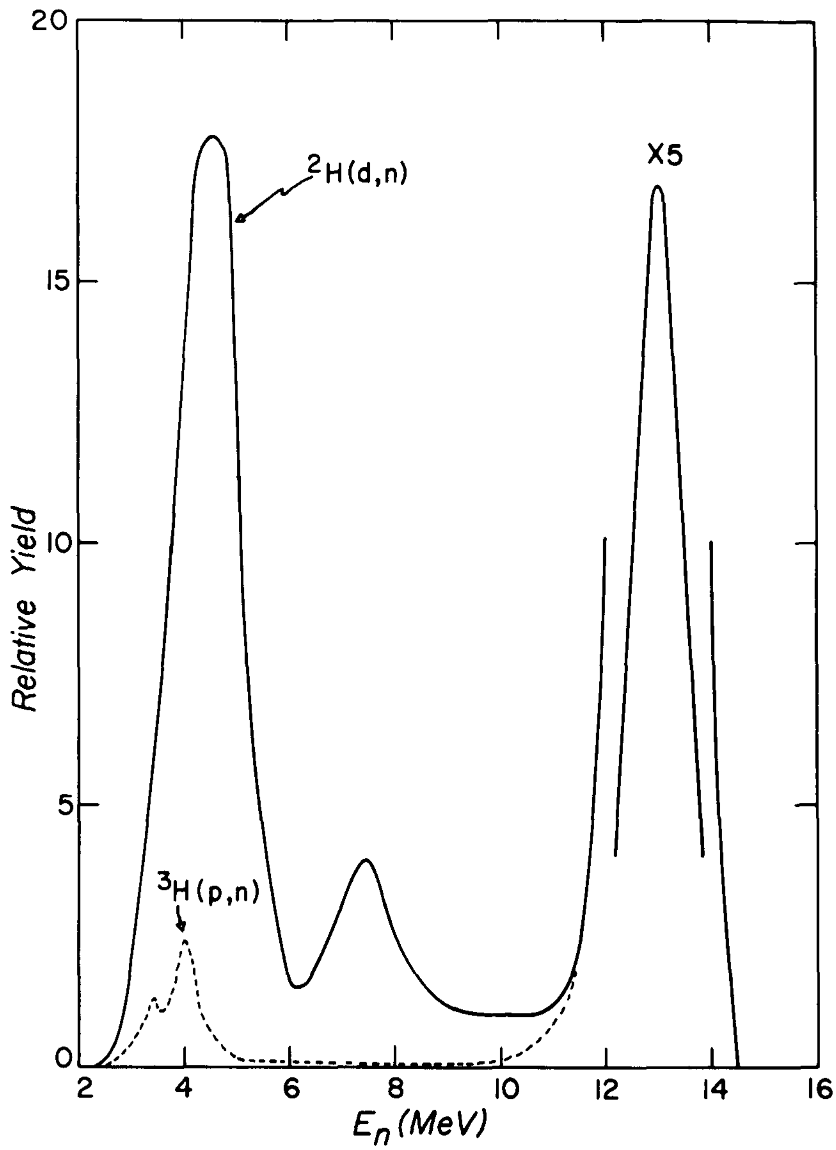

Fig. E-1. Comparison between the two source reactions $^2H(d,n)^3He$ and $^3H(p,n)^3He$ at $E_n = 13$ MeV. The spectra were taken with identical resolution and have been normalized at the primary neutron peak in order to permit direct signal-to-background comparison. The $^3H(p,n)^3He$ spectrum was measured using a ^{58}Ni beam stop to minimize background resulting from (p,n) reactions. Clearly, the low-energy background in the $^2H(d,n)^3He$ spectrum would make this reaction a poor source of primary neutrons for measuring the emission of low-energy neutrons such as the majority of inelastic neutrons and those produced in the (n,2n) reaction.

F. PARTIAL BIBLIOGRAPHY OF RECENT PUBLICATIONS

G. F. Auchampaugh and L. W. Weston	Parameters of the Subthreshold Fission Structure in ^{240}Pu	Phys. Rev. C12 1850 (1975)
D. M. Barton, B. C. Diven, G. E. Hansen, G. A. Jarvis, P. G. Koontz, and R. K. Smith	Measurement of the ^{235}U Fission Cross Section Over the Neutron Energy Range 1 to 6 MeV	To be publ. in Nuc. Sci. and Eng.
R. E. MacFarlane, M. Becker	Self Shielded Cross Sections for Neutron Transport in Iron	Trans. ANS 22 668 (1975)
J. Weber, A. Gavron, J. Wilhelmy, and B. R. Erdal	Mass and Kinetic Energy Measurements of Fragments from the Isomeric and Excited State Fission of ^{242}Am	Phys. Rev. C13 189 (1976)
A. I. Gavron, H. C. Britt, and J. B. Wilhelmy	Evidence for a Triple Hump Shaped Fission Barrier in Light Actinides	To be publ. in Phys. Rev. C
S. J. Balestrini and L. Forman	Independent Fission Yields of Rubidium and Cesium from Thermal Neutron Induced Fission of ^{239}Pu	Phys. Rev. C12 413 (1975)
J. Weber, H. C. Britt, A. I. Gavron, and E. Konecny	Fission of ^{228}Ra	To be publ. in Phys. Rev. C
A. I. Gavron	Angular Distribution of Neutrons from Fission Fragments	To be publ. in Phys. Rev. C
D. C. Hoffman, et al.	Discovery of ^{259}Fm	Third Intl. Conf. on Nuclei Far from Stability, Corsica, 1976

D. C. Hoffman	Low Energy Fission Systematics of the Fermium Isotopes: The Transition from Mass Asymmetry at ^{254}Fm to Symmetry at ^{259}Fm	Third Intl. Conf. on Nuclei Far from Stability, Corsica, 1976
G. M. Hale and D. C. Dodder	Polarization for Reactions in the ^{7}Li System	Proc. Fourth Intl. Symposium on Polarization Phenomena in Nuclear Reactions, Zurich, 1975. To be published.
R. A. Hardekopf, et al.	Neutron Polarization and Analyzing Power in the H(t,n)^{3}He Reaction Using a Polarized Triton Beam	1975 Pol. Sym., Zurich
R. L. Walter, P. W. Lisowski, G. G. Ohlsen, R. A. Hardekopf	^{4}He(n,n)^{4}He Analyzing Power in the 20 to 30 MeV Energy Range	1975 Pol. Sym., Zurich
P. W. Liskowski, R. L. Walter, R. A. Hardekopf, and G. G. Ohlsen	Absolute Neutron Polarization from Measurements of A(ZZ) (0 deg) in the T(D,n)^{4}He Reaction	1975 Pol. Sym., Zurich
G. G. Ohlsen, R. A. Hardekopf, R. L. Walter, P. W. Lisowski	Polarization Transfer in the D(t,n)^{4}He Reaction	1975 Pol. Sym., Zurich
J. P. Coffin, E. R. Flynn, R. A. Hardekopf, J. Sherman, J. W. Sunier	Analyzing Power for the ^{90}Zr(t,α)^{89}Y and ^{206,208}Pb(t,α ^{205,207}Tl Reactions	1975 Pol. Sym., Zurich

P. W. Keaton, Jr.	Optical Model Potentials for Deuterons, Tritons and Helions	1975 Pol. Sym., Zurich
J. M. Potter	Tests of Parity Conservation in Proton - Proton and Proton - Nucleus Scattering	1975 Pol. Sym., Zurich
R. A. Hardekopf, L. R. Veeser, P. W. Keaton, Jr.	Polarization Measurements and Optical Model Potential for Tritons	Phys. Rev. Lett. 35, 1623 (1975)
J. C. Allred, L. Rosen	First Observations of Fusion Neutrons from a Thermonuclear Weapon Device	Adventures in Experimental Physics 5 33 (1976)
R. A. Hardekopf, G. G. Ohlsen, R. V. Poore, N. Jarmie	Location of a Polarization Extremum in Triton - Alpha Scattering and Its Application to a New Polarized Triton Source	To be publ. in Phys. Rev. Ltrs.
M. J. Throop, et al.	Inelastic Proton Scattering as a Test of Surface Delta Wave Functions	Phys. Rev. Lett. 35, 16 (1975)
N. Jarmie, J. H. Jett, P. W. Keaton, Jr., R. A. Nisley, K. H. Witte	Tabulated P-^{4}He Phase Shifts	LA-6186-MS
W. Von Oertzen, E. R. Flynn	Test of the Generalized Pauli Principle and of Supermultiplet Symmetry in the Reactions t + $^{9}Be \rightarrow$ ^{6}Li + ^{6}He, $^{6}Li^{*}(0^{+})$ + ^{6}He	To be publ. in Annals of Physics
E. R. Flynn, O. Hansen, J. Sherman, N. Stein, J. W. Sunier, R. K. Sheline	Study of the $^{210}Bi(t,\alpha)^{209}Pb$ Reaction	To be publ. in Nucl. Phys.
J. Sherman, O. Hansen, J. R. Powers, H. T. Fortune	$^{24}Mg(t,\alpha)$ and $^{28}Si(t,\alpha)$ Reactions	To be publ. in Nucl. Phys.

E. R. Flynn, R. A. Hardekopf, J. Sherman, J. W. Sunier, J. P. Coffin	Total Spin Measurement of Proton Hole States by the (t,α) Reaction	To be publ. in Phys. Rev. Ltrs.
D. Burke, E. R. Flynn, J. Sherman, J. W. Sunier	Studies of States in ^{153}Eu and ^{155}Eu with the (t,p) Reaction	To be publ. in Nucl. Phys.
E. R. Flynn, J. Sherman, N. Stein, D. K. Olsen, P. J. Riley	Study of the ^{84}Kr(t,p)^{86}Kr and ^{86}Kr(t,p)^{88}Kr Reactions	To be publ. in Phys. Rev. C
E. R. Flynn, O. Hansen, J. Sherman, N. Stein, J. W. Sunier	^{88}Sr(t,p)^{90}Sr Reaction at 20 MeV and the Systematics of Pairing Excitations Near N = 50	To be publ. in Nucl. Phys.
E. R. Flynn, D. Burke, J. Sherman, J. W. Sunier	Study of Particle Pairing Vibration Multiplets in ^{211}Bi	To be publ. in Nucl. Phys.
C. E. Moss, J. Sherman	Excitation Energies of Levels in ^{27}Al and ^{28}Si	To be publ. in Nucl. Phys.
M. J. Bennett, R. K. Sheline	Study of the Nuclear Levels in ^{161}Dy by the (d,p), (d,t), and (n,γ) Reactions	To be publ. in Phys. Rev. C
A. I. Gavron	(^{3}He,2p) Reaction on ^{208}Pb	Phys. Rev. C13, 98 (1976)
J. A. Barclay, S. S. Rosenblum, W. A. Steyert, Jr., K. S. Krane	Nuclear Orientation of ^{76}As	To be publ. in Phys. Rev. C
K. S. Krane, C. E. Olsen, S. S. Rosenblum, W. A. Steyert, Jr.	Gamma Ray Angular Distributions in the Decays of Polarized ^{171,172}Lu	To be publ. in Phys. Rev. C

K. S. Krane, S. S. Rosenblum, W. A. Steyert, Jr.	Nuclear Magnetic Moment of ^{65}Ni	To be publ. in Phys. Rev. C
K. S. Krane, S. S. Rosenblum W. A. Steyert, Jr.	Determination of the Nuclear Magnetic Moment of ^{175}Hf by Nuclear Orientation	To be publ. in Phys. Rev. C
B. T. Murcoch, C. E. Olsen, W. A. Steyert, Jr.	Tests for Violation of Time Reversal Invariance in the 922 keV Gamma Ray of ^{184}W	To be publ. in Phys. Rev. C
K. S. Krane, C. E. Olsen, S. S. Rosenblum, W. A. Steyert, Jr.	Gamma Ray Angular Distributions and Parity Tests in the Decays of Polarized ^{173}Lu and $^{174m,g}Lu$	Phys. Rev. C12, 1999 (1975)
K. S. Krane, C. E. Olsen, S. S. Rosenblum, W. A. Steyert, Jr.	Nuclear Orientation of $^{95,97}Nb$ and ^{95}Zr in Zirconium Ferride	To be publ. in Phys. Rev. C
G. P. Ford	Calculation of Nuclear Level Densities for ^{56}Fe, ^{59}Co, ^{60}Ni, ^{61}Cu, ^{62}Ni, ^{63}Cu, and ^{65}Cu	To be publ. in Phys. Rev. C
D. C. Hoffman, J. W. Barnes, B. J. Dropseky, F. O. Lawrence, G. M. Kelley, M. A. Ott	Half Lives of ^{129m}Xe, ^{131m}Xe, ^{133m}Xe, ^{133g}Xe, and ^{135g}Xe	J. Inorg. Nucl. Chem. 37 2336 (1975)
D. C. Hoffman, W. R. Daniels, J. B. Wilhelmy, M. E. Bunker, J. W. Starner, E. K. Hulet, J. H. Landrum, R. W. Lougheed, J. F. Wild	Discovery of a 7.6 Hour High Spin Isomer of ^{256}Es	Third Intl. Conf. on Nuclei Far From Stability, Corsica, 1976

E. B. Shera	Measurement of the Energy of the 6129 keV Gamma Ray of ^{16}O	Phys. Rev. C12 1003 (1975)
H. A. Smith, M. E. Bunker, J. W. Starner, Jr., C. J. Orth, K. E. Lobner	States in ^{126}Sb Populated in the Beta Decay of 10,000 Year ^{126}Sn	Phys. Rev. C13 387 (1976)
H. C. Britt, B. H. Erkkila, R. H. Stokes, H. H. Gutbrod, F. Plasil, R. L. Ferguson, M. Blann	Argon and Krypton Induced Reactions at Energies of 4-7 MeV/AMU	To be publ. in Phys. Rev. C
D. W. Muir, M. E. Wyman	Neutronic Analysis of a Tritium Production Integral Experiment	Publ. in Proc. Technology of Controlled Thermonuclear Fusion Experiments and the Engineering Aspects of Fusion Reactors, p. 910 (Austin, 1972)
H. C. Paxton	Los Alamos Critical Mass Data	LA-3067-MS, Rev.
C. E. Ragan, G. F. Auchampaugh, A. Hemmindinger, M. G. Silbert	Neutron Spectrum from a ^{235}U Sphere Bombarded by 14 MeV Neutrons	To be publ. in Nucl. Sci. and Eng.
D. W. Muir, P. G. Young, Jr.	Applied Nuclear Data Research and Development, April 1 - June 30, 1975	LA-6123-PR
C. I. Baxman, P. G. Young, Jr.	Applied Nuclear Data Research and Development, July 1 - September 30, 1975	LA-6164-PR
D. R. Harris, W. A. Reupke, W. B. Wilson	Consistency Among Differential Nuclear Data and Integral Observations: The ALVIN Code for Data Adjustment, for Sensitivity Calculations, and for Identification of Inconsistent Data	LA-5987

R. B. Kidman, R. E. MacFarlane	LIB-IV, A Multigroup Library From MINX	1976 Toronto Mtg. ANS
R. E. MacFarlane, R. M. Boicourt	NJOY: A Neutron and Photon Cross Section Processing System	Trans. Am. Nucl. Soc. 22 720 (1975)
D. W. Muir, et al.	Cross Section Uncertainty Analysis	Trans. Am. Nucl. Soc. 22 794 (1975)
S. A. W. Gerstl	Summary of Common Interests Identified by Sensitivity Analysis	Proc. OECD-NEA Mtg. on Sens. Studies Paris, 1975
T. R. England, R. E. Schenter	ENDF/B-IV Fission Product Files: Summary of Major Nuclide Data	LA-6116-MS
D. J. Dudziak, R. G. Palmer	Neutron Spectrum Calculations Applied to Reactor Materials Dosimetry: A Review	ASTM-EURATOM, Petten, 1975
M. S. Moore	Status of Neutron Cross Sections of Transactinium Isotopes in the Resonance and Fast Energy Regions - Underground Nuclear Explosion Measurements	IAEA, Karlsruhe, 1975
S. A. W. Gerstl	Sensitivity Analysis in Shielding: An Overview	Trans. Am. Nucl. Soc. 22 791 (1975)
G. M. Hale	Use of Multichannel R-Matrix Theory in Evaluating Data for Light Elements	IAEA, Trieste, 1975
D. C. Dodder	R-Matrix Analysis	1975 Pol. Sym., Zurich
L. Stewart, G. M. Hale	$T(d,n)^4He$ and $T(t,2n)$ Cross Sections at Low Energies	LA-5828-MS

D. C. Dodder, J. K. Fink	Energy Dependent Phase Shift Analyses and Renormalization of Low Energy Proton - Proton Differential Cross Sections	To be publ. in Phys. Rev. Lett.
K. T. R. Davies, A. J. Sierk, J. R. Nix	Effect of Viscosity on the Dynamics of Fission	To be publ. in Phys. Rev. C
P. Möller and J. R. Nix	Macroscopic Potential Energy Surfaces for Symmetric Fission and Heavy Ion Reactions	To be pul. in Nucl. Phys.
L. Forman, M. G. Silbert A. D. Schelberg	Time of Flight Neutron Spectroscopy Using Approximately 20 Meter Flight Paths to a Nuclear Device	Nucl. Instrum. Methods 128 607 (1975)
G. G. Ohlsen, P. A. Lovoi	Supercube Scattering Chamber for Spin 1/2 and Spin/Analyzing Power Measurements	1975 Pol. Sym., Zurich
R. A. Hardekopf	Operation of the LASL Polarized Triton Source	1975 Pol. Sym., Zurich
R. A. Hardekopf, G. G. R. V. Poore, N. Jarmie	Calibration of a Polarized Triton Beam	1975 Pol. Sym., Zurich
E. R. Flynn, S. D. Orbesen, J. Sherman, J. W. Sunier	Q3D Spectrometer With a Helix Detector System	Nucl. Instrum. Methods 128 35 (1975)
E. A. Plassmann	Central Neutron Spectrum of the Fast Critical Assembly Big-Ten	Nucl. Technol. 25 381 (1975)
T. F. Wimett	Fast Burst Reactors	Book to be publ. by ANS

G. A. Cowan	Oklo Phenomenon: A Natural Nuclear Reactor	IAEA, Franceville, 1975
R. D. Walton, Jr., G. A. Cowan	Relevance of Nuclide Migration at Oklo to the Problem of Geologic Storage of Radioactive Waste	IAEA, Franceville, 1975
G. A. Cowan	Oklo: A Prehistoric Natural Fission	LA-UR-75-2040
G. A. Cowan, E. A. Bryant, W. R. Daniels, W. J. Maeck	Some U.S. Studies of the Oklo Phenomenon	LA-UR-75-1127
H. O. Menlove	Applications of Californium -252 in the Nuclear Industry	Int. Sym. on ^{252}Cf Util., Paris, 1976
E. Storm	Bremsstrahlung Induced K Fluorescent Radiation	To be publ. in J. Appl. Phys.
A. E. Evans, H. C. Menlove, R. B. Walton, D. B. Smith	Radiation Damage to Helium -3 Proportional Counter Tubes	To be publ. in Nuc. Inst. Meth.
A. N. Goland, D. M. Parkin	Dependence of Radiation Damage Analysis on Neutron Dosimetry	ASTM-Euratom, Petten, 1975

A. INTRODUCTION

Since its inception, the Cross Section Project at The University of Michigan has stressed the absolute measurement of neutron-induced cross sections in the 100-1000 keV energy range. Our particular emphasis is to provide absolute data which do not rely to any significant extent on any other cross section data. These independent measurements are intended to provide absolute normalization points for the extensive collection of cross section shape data produced at linacs and other TOF facilities. Our techniques are based on the use of small short-lived photoneutron sources which are calibrated relative to the secondary national neutron standard NBS-II using The University of Michigan manganese bath.

Facilities have been developed for the uniform activation, rapid transfer, and experimental utilization of these sources. The cross section measurements are carried out in a low-albedo laboratory with all walls, floors, and ceilings lined with anhydrous boric acid. The small component of room-return flux which remains is determined by carrying out multiple measurements using variable source-target spacing.

The absolute neutron flux is calculated from the geometry of the experiment and the measured total emission rate of the source. Nearly all our measurements are carried out with the source centered between two symmetric targets to minimize the variation in total reaction rate with small geometric uncertainties.

The two photoneutron sources previously described (Na-Be and Na-D) have been supplemented over the past year with two additional sources (Ga-D and La-Be). The set now provides us with the capability of carrying out measurements at four energies ranging from 140 to 960 keV. We are also undertaking some similar measurements using a Cf-252 spontaneous fission neutron source.

B. PHOTONEUTRON SOURCE CHARACTERISTICS

Together with the original Na-Be source, we now have a set of three photoneutron cores along with two target shells of differing material. The cores and target shells are interchangeable. The cores are of similar construction: aluminum spheres filled with NaF, Ga_2O_3, or La_2O_3 powder. The target shells are deuteriated polyethylene and beryllium. The combinations of Ga-D, Na-D, and La-Be were checked for neutron source activity, gamma impurities, self-absorption, decay characteristics, and photoactivation of the Mn bath. Approximate neutron emission rates at the time of removal from the reactor core are as follows:

Source	Median Energy	Yield	Half-Life
Na-Be	964 keV	6×10^7 neutrons/sec.	15 hours
Na-D	265 keV	2×10^7 neutrons/sec.	15 hours
Ga-D	140 keV	6.7×10^6 neutrons/sec.	14 hours
La-Be	770 keV	1.5×10^6 neutrons/sec.	40 hours

The half-lives of the photoneutron cores have been measured using the manganese bath. Photoactivation of the Mn bath was easily determined due to the removability of outer target shells from the core.

Self-absorption measurements of the photoneutron sources were also carried out. Absorbing materials were placed in the dry well of the Mn bath together with the source, and the resulting bath activation was compared to bath runs with the source alone.

C. ABSOLUTE CROSS SECTION MEASUREMENTS

1. ^{235}U Fission Cross Section (M. C. Davis, G. F. Knoll)

Two additional measurements of the ^{235}U fission cross section have been carried out in the past year to supplement the measurements at 960 and 265 keV reported earlier. These two new points at 140 and 770 keV correspond to measurements completed using a Ga-D source and a La-Be source, respectively. All these absolute cross sections will carry a standard deviation in the neighborhood of 2 - 3%. Analysis of the data is nearing completion and results will be given in a comprehensive journal article.

The four data points will contribute information about cross section shape as well as its absolute value. Since a number of factors are common to all four uranium measurements (foil mass, NBS-II normalization, etc.) we are able to eliminate some significant uncertainties when considering the relative ratio of these data points.

2. ^{239}Pu Fission Cross Sections (M. C. Davis, J. C. Robertson, G. F. Knoll)

Completed work reported at the November, 1975 ANS Annual Meeting in San Francisco includes the absolute fission cross section measurements for ^{239}Pu at 964, 265, and 140 keV. These measurements used Na-Be, Na-D, and Ga-D photoneutron sources, respectively. Runs were made at two different source-to-foil spacings using the dual limited solid-angle detector method as in earlier experiments with ^{235}U. One important difference in experimental technique was that the experiment was done in an evacuated brass cylinder rather than in a helium environment. Results for these measurements are 1.68 ± .04, 1.44 ± .04, and 1.46 ± .04 barns at 964, 265, and 140 keV, respectively. These values differ somewhat from those given in the *Transactions* due largely to a re-evaluation of published angular distribution data needed for anisotropy corrections.

Experimental runs have recently been completed on a ^{239}Pu fission cross section measurement at 770 keV using a La-Be photoneutron source. Data evaluation is still underway. This measurement is the last in our set of absolute differential fission cross section measurements for ^{239}Pu and the set will be described in a forthcoming journal article.

Since the original mass assay of the ^{239}Pu foil deposits was carried out, the ^{239}Pu deposits were gold overlayed at ORNL. This necessitated a second assay which was conducted this past June at the National Bureau of Standards. One of our group (M. C. Davis), in collaboration with D. M. Gilliam of NBS, carried out this determination by comparison of alpha activities with standard foils. As a check on the procedure used, the ^{235}U foil deposits were also assayed. The method was alpha counting using a large solid-state silicon detector in a carefully measured limited solid angle geometry. The ^{235}U foils were absolutely counted in a precise geometry with the results in excellent agreement with the original mass assay done at the Isotope Target Laboratory at ORNL.

3. Fission Cross Section Measurements Using ^{252}Cf Fission Neutrons (M. C. Davis, J. C. Engdahl)

Integral measurements of ^{235}U and ^{239}Pu over the ^{252}Cf spontaneous neutron spectrum have been completed. Important corrections determined include manganese bath leakage and fast capture losses. Leakage was measured using a long counter to be 0.24% for a ^{252}Cf neutron spectrum, with a bath radius of 50 cm and bath density of 1.31 gm/cc. Transport calculations using the ANISN code produced excellent agreement. Measurement of the change in bath efficiency due to oxygen and sulphur fast neutron capture using a 4" O.D spherical graphite moderator gave inconclusive results. Because of the excellent agreement in case of leakage between measurement and calculation, our ANISN results along with other references will be used in this correction.

The fission rate determinations were carried out in a vacuum with the remaining experimental technique the same as that used in the differential fission cross section measurements.

4. The ^{6}Li(n,α) Cross Section (J. C. Engdahl, G. F. Knoll)

The previously-reported value for this cross section at 964 keV[1] after further analysis has been found to be 12 to 15% too high due to the underestimation of the yield of protons from the (n,p) reaction in the atmosphere surrounding the experiment. Due to the extreme difficulties encountered in operating a Si surface barrier detector in the high gamma-ray flux from our photoneutron sources, we have abandoned further attempts to improve the accuracy of this measurement using similar methods. Instead, we have begun an evaluation of a different experimental scheme which will substitute track-etch techniques to determine reaction rates.

A supply of LR-115 film has been received and initial tests have been performed. So far, it has been determined that the alpha counting efficiency in the energy range 1 - 2 MeV is approximately 100% with a very low background, $\sim$1 - 2 counts/mm^2.

A method to be investigated will be to sandwich two layers of cellulose nitrate such that the first layer records the α tracks and degrades the triton energies, so the second layer can record the tritons. The degradation is necessary due to the minimum -dE/dx requirement for track registration. This method will be tested in a thermal beam. This could prove useful in the determination of the angular dependence of alphas and tritons.

If results of this preliminary evaluation are sufficiently encouraging, we plan to repeat the ^{6}Li(n,α) measurement at 964 keV as well as our other available energies.

5. Capture Cross Section of In-115 (J. C. Robertson, M. C. Davis)

Motivation for our interest in this cross section is contained in our report of a year ago. The 4π continuous flow proportional counter has been put into operation and calibration measurements undertaken. We expect first cross section data to be taken within several months and plan the initial effort with the Na-Be source at 964 keV. The feasibility of extending the measurement to our other available energies will be evaluated.

---

[1] W. P. Stephany and G. F. Knoll, Proc. of Conference on Nuclear Cross Sections and Technology, NBS-425, p. 236 (1975).

D. FISSION FRAGMENT ANGULAR DISTRIBUTION MEASUREMENTS (S. Hsue)

It is becoming increasingly apparent that anisotropy in the angular distribution of fission fragments is emerging as the largest unresolved uncertainty in our fission cross section measurements. We have deliberately chosen to collect fragments in a restricted solid angle near normal to the foil in order to avoid the large corrections and uncertainties which result from 2π fission fragment counting arising from fragments emitted near the plane of the foil. The price we pay for this approach is a dependence on a prior knowledge of the anisotropy of fission fragment emission at the appropriate neutron energy. Unfortunately the previous measurements[2,3] on ^{235}U(n,f) angular distribution have substantial deviations at various energies. For example, the reported fragment anisotropy (W(0)/W(90°) - 1) of ^{235}U at a neutron energy of 1 MeV ranges from 11.4 ± 1.2%[2] to 17 ± 2%[3]. In our measurements, we will attempt to resolve some of the discrepancies in the fragment anisotropy. In addition, we can measure the fragment angular distribution at the same neutron energy as in the cross section measurements, thereby reducing the possible error due to extrapolation.

We have undertaken a series of experimental measurements using the Tandem Dynamitron at Argonne (courtesy Dr. A. B. Smith). This work has been made possible through the collaboration of Dr. J. M. Meadows of the Applied Physics Division at Argonne. A set up consisting of a track foil holder and vacuum chamber has been built for the fragment angular distribution experiment.

We have obtained a total of 72 hours of beam time and have made fission fragment anisotropy measurements with ^{235}U at neutron energies of 265 keV, and 965 keV. Track counting and data analysis is now in progress and we expect results to be complete in several months. These data will then replace our dependence on anisotropy values based on previously published data. Further measurements on Pu-239 are in the planning stage.

E. CALIFORNIUM-252 NU-BAR (H. Bozorgmanesh, G. F. Knoll)

An accurate absolute value of nu-bar (the average number of prompt neutrons per spontaneous fission) of Cf-252 is a desirable and important

---

[2] V. G. Nesterov, G. N. Smirenkin, and D. L. Shpak, Sov. J. Nucl. Phys. **4**, 713 (1967).

[3] J. Caruana, J. N. Mathur, J. W. Boldeman, and R. L. Walsh, meeting report at Indian Nuclear Physics and Solid State Physics Symposium, Bombay, December, 1974.

standard in reactor design and related areas. This source is widely used in experiments as a reference and frequently the ratio of $\overline{\nu}$ for a given relevant fissile isotope to that of Cf-252 is measured.

In the present direct measurement experiment the absolute fission rate and the absolute neutron emission rate are measured separately.

The neutron source emission rate is obtained in The University of Michigan manganese bath. The nature of the background associated with the bath and the desired accuracy of the measurement (0.5%) require a source with neutron emission rate of $\sim 10^6$/sec. The associated fission rate (2.5×10^5/sec) and decay rate (7.5×10^6/sec) is clearly too high for accurate 2π geometry counting of the fission fragments. We have, therefore, elected to count using a restricted solid angle near the normal to the plane of deposit, using a heavy-ion silicon surface barrier detector behind variable defining apertures. Any accurate determination of the fission rate requires the discrimination of the fission fragments from competing events superimposed in the lower tail of the pulse height spectrum.

Potential competing processes which can lead to pulses in the low amplitude tail of the fission fragment distribution are:

1) Multiple pile-up of decay alpha particles,

2) Low-angle scattering of fission fragments,

3) Energy loss of fission fragments within the source,

4) Long-range alpha particles from tertiary fission (3.27×10^{-3} per binary fission).

Alpha pile-up was eliminated by restricting the solid angle, such that the corresponding alpha rates were less than a few hundred per second. Fragment scattering was minimized by tailoring the shape of the aperture edge and by avoiding observation angles near the plane of the foil. The thin deposit (1.5 μgm/cm^2) and evaporated gold cover (40 μgm/cm^2) led to minimal fragment energy loss in the direction of the aperture. The long-range alpha particles were separately recorded by stopping the fission fragments and decay alphas in an aluminum foil of 8 mg/cm^2 thickness. Pulse height analysis of the transmitted long-range alphas produced a broad peak (Fig. E-1) centering around 15 MeV (corrected for energy loss in the aluminum absorber). This contribution amounted to 0.2% of all fission events.

The spectrum plotted in Fig. E-1 shows the excellent separation of the fission fragments obtainable under these conditions. A series of these rate determinations using solid angles ranging from 2 x 10^{-5} to 60 x 10^{-5} steradian shows a self-consistency of approximately 0.15%.

The correction factors for neutron rate determination in The University of Michigan manganese bath were thoroughly examined. A long counter was employed to directly determine the neutron leakage rate of the NBS-II photoneutron source as well as a 5 μgm Cf-252 source. The efficiency of the long counter was experimentally determined by source comparison technique. ANISN modeling of the bath and the Cf-252 source resulted in a leakage correction factor in good agreement with the experimental value. A portion of the californium neutron spectrum consists of fast neutrons with energies above the thresholds for charged particle reactions, $O(n,\alpha)^{13}C$, $^{32}S(n,p)^{32}P$ and $^{32}S(n,\alpha)^{29}Si$. Since neutrons captured in these charged particle reactions do not contribute to the measured activity of $^{56}M_n$, corrections must be made to "oxygen loss" and "sulphur loss".

These parasitic absorptions in the bath as well as source and support self-absorption corrections were calculated with the transport code. Comparative studies of these values with published values under similar conditions were carried out. Several absolute neutron emission rate determinations were conducted in The University of Michigan manganese bath. A consistent (within statistical uncertainty) value of absolute neutron emission rate was obtained.

All data are now complete for this experiment and analysis is underway. A nu-bar value will be reported in several months.

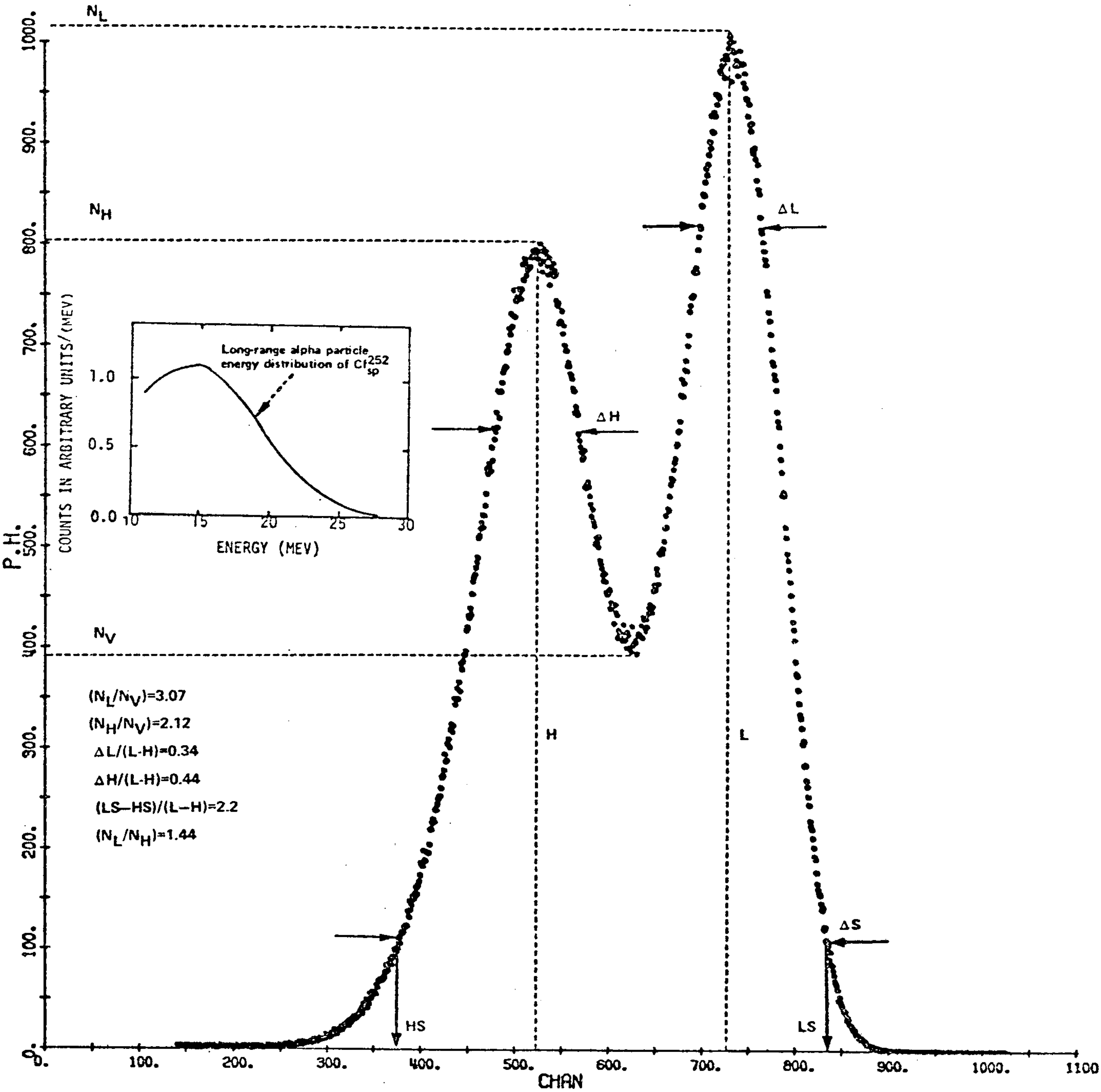

N_L
N_H
N_V
1000.
900.
800.
700.
600.
500.
400.
300.
200.
100.
0.
P.H.
0.
100.
200.
300.
400.
500.
600.
700.
800.
900.
1000.
1100
CHAN
ΔL
ΔH
ΔS
H
L
HS
LS
Long-range alpha particle energy distribution of Cf^{252}_{sp}
COUNTS IN ARBITRARY UNITS/(MEV)
ENERGY (MEV)
(N_L/N_V)=3.07
(N_H/N_V)=2.12
$\Delta L/(L\text{-}H)$=0.34
$\Delta H/(L\text{-}H)$=0.44
(LS—HS)/(L—H)=2.2
(N_L/N_H)=1.44

Fig. E-1

NATIONAL BUREAU OF STANDARDS

A. NEUTRON PHYSICS

1. A New Measurement of the $^6Li(n,\alpha)T$ Cross Section from 10 - 500 keV (G. P. Lamaze, O. A. Wasson, and R. A. Schrack)

The $^6Li(n,\alpha)T$ cross section has been measured from 10 to 500 keV neutron energy at the NBS Linac above ground neutron time-of-flight facility. The experiment was conducted along the 200 meter drift tube. The $^6Li(n,\alpha)T$ events were detected at 69.25 m in a 0.5 mm thick ^6Li loaded glass scintillator (NE912) coupled to an RCA 8850 photomultiplier tube. The phototube was pulsed off during the gamma flash to suppress afterpulsing. The neutron flux was monitored at 200 m with a 5.08 cm x 60.96 cm hydrogen filled proportional counter. Both pulse height and flight time were recorded for each event in each detector. Events were sorted on line and dumped onto a 5.4 million byte moving head disc. The results have been included in ENDF-B/V and are in excellent agreement with an R-matrix analysis of the ^7Li system performed by G. Hale of LASL.

2. A Measurement of the $^{10}B(n,\alpha_1\gamma)^7Li$ Cross Section in the keV Energy Region (R. A. Schrack, O. A. Wasson, and G. P. Lamaze)

The $^{10}B(n,\alpha_1\gamma)$ relative cross section has been measured from ~5 to ~700 keV at the NBS Linac Neutron Time-of-Flight Facility. Two techniques have been utilized to detect the 478 keV gamma rays resulting from neutron absorption in ^{10}B. The ^{10}B sample is a disk of sintered boron enriched to 95% ^{10}B. The first technique of gamma ray detection employed a 3" x 3" encapsulated NaI detection system which was pulsed off during the gamma flash. The second system utilized an 18% efficiency coaxial Ge(Li) detector. These experiments were located at the 69 m station of the 200 m flight path. The neutron flux was monitored at the 200 m end station using a 61 cm long hydrogen gas proportional counter operated with one atmosphere of gas. The pulse height information for 1024 time channels was recorded for each of the experiments using our magnetic disk based data acquisition system.

The results of the two experiments agree to within $\pm$ 4% between 5 and 300 keV. Inelastic neutron scattering in the NaI detector causes a large background that makes the NaI results less reliable above 300 keV. The results obtained with the Ge(Li) detector are in agreement with ENDF IV data up to 300 keV except for a dip of about 3% centered around 40 keV. The data of this experiment fall below the ENDF IV values above 300 keV by 8% at 500 keV and 16% at 700 keV. The data have been fit by an R-matrix analysis code by G. Hale of LASL.

3. Measurement of the $^{235}U(n,f)$ Reaction Cross Section from 5 - 800 keV Neutron Energy (O. A. Wasson)

The shape of the $^{235}U(n,f)$ cross section from 5 - 800 keV neutron energy was measured relative to the neutron-proton scattering cross section using the 200 m flight path at the NBS linac. The uncertainty in the relative cross section is $\pm$ 3%, which includes counting statistics, background determination, detector efficiencies, multiple scattering, and beam line transmissions. In a separate experiment on the 20 m flight path, the $^{235}U(n,f)$ cross section was measured in the neutron energy region from 6 eV to 30 keV using the 0.5 mm thick ^{6}Li glass scintillator as a flux monitor. This experiment, which yielded an average $^{235}U(n,f)$ cross section for the 10-20 keV neutron energy interval which agreed within 2% with the value of Gwin, Silver, Ingle, and Weaver (Nucl. Sci. and Eng. 59, 79 (1976)), was used to normalize the $^{235}U(n,f)$ cross section shape measurement from the hydrogen counter. Although the ^{235}U cross section shape follows that of Gayther, Boyce, and Brisland (Proc. 2nd IAEA Panel on Neutron Standard Reference Data, p201, Vienna (1974)) the absolute value from 500-800 keV is $\sim$ 6% less than that obtained from non-thermally normalized data.

4. Neutron Capture Cross Sections for ^{186}Os and ^{187}Os and the Age of the Universe (J. C. Browne,* G. P. Lamaze, and I. G. Schröder)

The relative neutron capture cross sections for ^{186}Os and ^{187}Os have been measured using the NBS 25-keV filtered beam facility. The knowledge of these cross sections calibrates the $^{187}Re \rightarrow {}^{187}Os$ nuclear β-decay clock and thus makes possible a new determination of the age of the universe. A value for the ratio $(\bar{\sigma}_{186}/\bar{\sigma}_{187}) = 0.41 \pm .04$ was obtained. This leads to an age of the universe of $\sim 2 \times 10^{10}$ years. A paper has been submitted to Physical Review C.

* Lawrence Livermore Laboratory

5. Black Detector Calibration (M. M. Meier and A. D. Carlson)

The first application of the associated particle technique at NBS has been the calibration of a "Black Detector,"[1] a large scintillator with a response that can be calculated by Monte Carlo techniques.[2]

Despite considerable experimental effort, a discrepancy of about seven percent has persisted between calculation and experimental calibration at 300 keV neutron energy. The 25^{o} chamber has been installed recently and a calibration performed at 850 keV. Here agreement between the two techniques is satisfactory. The low energy problem may be associated with the program which does not explicitly take into account the Poisson statistics of photoelectron production which becomes important at low light output from the scintillator. Along with investigation and modification of the Monte Carlo program, we plan to further study the experimental problem, and particularly, to compare the 10^{o} and 25^{o} chambers at an overlapping energy. At energies where agreement is better than three percent, we will begin using the detector for flux monitoring in cross section and dosimetry experiments.

6. ^{235}U(n,f) Cross Section in the MeV Energy Region (A. Carlson)

With the completion of diagnostic investigations, high accuracy shape measurements of the ^{235}U fission cross section will begin soon at the 60 m end station of the linac neutron time-of-flight facility. The neutron flux will be measured with a proton counter telescope used in ring geometry with a tapered lead rod shielding the Si(Li) proton detector from the direct beam. The ^{235}U fission reaction events are detected with a parallel plate ionization chamber. Both of these detectors are located at the 60 m station. It is anticipated that these measurements will extend down to $\approx$ 0.5 MeV. These data will provide a tie in with the recently completed NBS ^{235}U(n,f) measurements from 5 to 800 keV neutron energy.

---

1 Lamaze, Meier, and Wasson, Nuclear Cross Sections and Technology, 1 (1975) 73.

2 W. P. Poenitz, ANL-7915, Argonne National Laboratory (1972).

7. Doppler-Free Neutron Spectroscopy (C. D. Bowman and G. P. Lamaze)

For many years the obtainable experimental resolution in neutron spectroscopy has been much finer than the broadening introduced by thermal motion of target nuclei. The purpose of this work is to demonstrate that the Doppler effect can be avoided entirely by three different techniques--none of which have been theoretically or experimentally explored. All three methods involve the measurement of elastic scattering. The first is simply small angle forward scattering at angles of about 15^{o} or less. At these angles, the nuclear recoil energy is small enough that Mössbauer-like binding of the nucleus in the lattice can take place. The second is by coherent scattering at neutron resonances. Near the resonances the coherent scattering can become very large. The atoms acting coherently and therefore without recoil scatter neutrons strongly at the Bragg angle. The third is by resonance "total" reflection which takes place at the interface of two media when the index of refraction (which depends on the scattering length at resonance) of the two media differs. These three effects exist also in the nuclear scattering of γ-rays. Modest experimental efforts are now underway at NBS and perhaps elsewhere to investigate these techniques both for neutrons and for γ-rays.

8. A Gamma Ray Laser Using Existing Technology (C. D. Bowman)

In exploring the influence of solid state on neutron physics several unexplored phenomena were recognized which have an analog with the influence of solid state on the physics of γ-ray interactions and transport. From these studies has emerged a concept for a γ-ray laser based on nuclear transitions and using the above phenomena for control (focusing, dispersion, reflection, background reduction) of the laser beam. The laser is based on the 9.3 keV transition in ^{83}Kr which apparently can be pumped either by (γ,n) or (n,γ) reactions with our most intense presently available laboratory sources of neutrons and bremsstrahlung. Support is being sought for a series of nuclear data measurements to confirm the theoretical estimates of the important parameters underlying the concept.

9. Total Cross Section of ^4He (H. T. Heaton II and A. D. Carlson)

The total cross section of ^4He is being measured as a method of studying the d,T cross section by its inverse reaction. Investigations of this cross section using the NBS electron linac as a pulsed neutron source for time-of-flight measurements have been made to see if resolution of better than 0.1% at 22.15 MeV (the level in ^5He system) can be obtained with reasonable counting statistics. To achieve this resolution with the linac it is necessary to: (1) use the longest flight path--200 m, (2) use the shortest possible beam width--the rf microstructure, (3) use thin plastic scintillators on fast photomultipliers to minimize flight path uncertainty--hence multiple detector assemblies which must be optically decoupled, (4) use a physically small neutron source yet one which produces sufficient high energy neutrons to do the experiment in a finite time. Studies on suitable neutron sources have been made. Investigations on the use of the rf microstructure are currently under way, as is the measurement of the best way to achieve the subnanosecond "electronic" resolution necessary for this experiment.

10. Absolute ^{235}U Fission Cross Section for ^{252}Cf Spontaneous Fission Neutrons (H. T. Heaton II, J. A. Grundl, V. Spiegel, D. M. Gilliam, and C. Eisenhauer)

A measurement of the absolute ^{235}U fission cross section for ^{252}Cf spontaneous fission neutrons has been performed with two double fission chambers in compensated beam geometry. The fission chambers are mounted 10 cm apart on opposite sides of a small volume single encapsulated ^{252}Cf source (4×10^9 n/sec, 0.34 cm^3 capsule vol; $\sim$2 g steel and aluminum). In this geometry the effect of source position errors is small. The ^{252}Cf neutron source strength was determined with a Manganous Sulfate Bath relative to the internationally compared Ra-Be photoneutron standard neutron source, NBS-I, presently known to $\pm$ 1.1%. Uncertainty in the Manganous Bath comparison of NBS-I and the Cf source was $\pm$ 0.4%; the ^{235}U fissionable deposit masses have been ascertained to $\pm$ 1.3%. Five scattering corrections were applied to the data: source capsule (0.8 $\pm$ 0.3)%, fission chamber (1.1 $\pm$ 0.4)%, support structure (0.6 $\mp$ 0.5)%, platinum deposit backing (1.3 $\pm$ 0.8)%, and total room return (0.5 $\pm$ 0.2)%. The observed ^{235}U fission cross section is 1205 $\pm$ 27 mb. A computed value of 1245 mb is obtained using an evaluated ^{252}Cf fission neutron spectrum and ENDF/B-IV for the ^{235}U (n,f) cross section.

11. Spectral Indices For the BIG-10 Critical Facility: Spectrum-Averaged Fission Cross Section Ratios for ^{235}U, ^{238}U, ^{239}Pu, ^{237}Np (D. M. Gilliam and J. A. Grundl, NBS; G. E. Hansen and H. H. Helmik, LASL)

Absolute fission rate ratio measurements were performed in the Big Ten Critical Assembly at the Los Alamos Scientific Laboratory. Preliminary results given in this report last year are now superseded by the final results given below.

The NBS double fission chamber was placed in a close-fitting cavity (Test Region I) at the center of the BIG-10 facility, and fission ratios were observed for back-to-back deposits of the isotopes of interest (^{235}U, ^{238}U, ^{239}Pu, and ^{237}Np). The fission counts were recorded by means of a dual triple-scaler counting system as described in Ref. 1. The triple-scaler counting system was compared with a PDP-8 computer-based analyzer system using LASL-built live-timing circuitry. In nine comparisons, an rms discrepancy of 0.2% was obtained between the two independent systems. In addition, a check of the NBS dead-time corrections was made by the variance-to-mean method using LASL multiscaling hardware. The NBS dead-time corrections were found to agree with the variance-to-mean results within $\pm$0.2% over the count rate range used in the present measurements. Fourteen deposits from the NBS set of reference and working fissionable deposits were employed in the measurements. NBS personnel spent two and one-half man-weeks at the LASL Pajarito site, making sixteen spectral index runs and some subsidiary deposit mass assay comparisons in the Big-10 system. The results are summarized in the table below.

BIG-10 SPECTRAL INDICES

Nuclides Compared	Fission Cross Section Ratio--*in situ*	Fission Cross Section Ratio--in Unperturbed BIG-10	Observed/ENDF/B-IV for Unperturbed BIG-10
^{238}U/^{235}U	0.0366 $\pm$ 1.8%	0.0372 $\pm$ 1.9%	1.106
^{239}Pu/^{235}U	1.198 $\pm$ 1.5%	1.198 $\pm$ 1.5%	1.021
^{237}Np/^{235}U	0.314 $\pm$ 2.1%	0.317 $\pm$ 2.2%	0.985
^{239}Pu/^{237}Np	3.79 $\pm$ 2.1%	3.76 $\pm$ 2.2%	1.031

In subsequent high-fluence irradiations of dosimetry activation foils, a run-to-run fluence normalization accuracy of ±0.3% was achieved, based on corroboration by a multiplicity of redundant monitors.

J. A. Grundl, D. M. Gilliam, N. D. Dudey, and R. V. Popek, "Measurement of Absolute Fission Rates," Nuclear Technology, 25 (1975), 237.

12. Fission Cross Section Ratios in the ^{252}Cf Neutron Spectrum (D. M. Gilliam, C. Eisenhauer, H. T. Heaton II, and J. A. Grundl)

A paper of this title was presented at the Nuclear Cross Sections and Technology Conference, Washington, D.C., March 3-7, 1975. The abstract is given below. The paper is available in the proceedings of the conference, NBS Special Publication 425, Vol. I, p.270.

Abstract:
"In a ^{252}Cf neutron field, ratios of spectrum-averaged fission cross sections have been measured by back-to-back counting in a double fission ionization chamber with interchangeable deposits of ^{235}U, ^{238}U, ^{239}Pu, and ^{237}Np. These ratio measurements provide integral tests for evaluated cross section data. The dominant error in the ratio measurements was the $\pm$1.4% to $\pm$2.1% uncertainty in the fissionable deposit masses. Redundant mass assay methods were employed for all deposit nuclides. Corrections of up to (1.4 $\pm$ .7)% were necessary for inelastic scattering effects on the neutron energy distribution in the cases of ^{238}U and ^{237}Np. For ^{235}U and ^{239}Pu fission rates, a correction of (0.45 $\pm$ .20)% was made for the contribution of neutrons moderated and back-scattered by laboratory structures. The cross section ratios observed in the present measurements were as follows: 1.000: 0.266 $\pm$ 1.7%: 1.500 $\pm$ 1.6%: 1.105 $\pm$ 2.2% for ^{235}U: ^{238}U: ^{239}Pu: ^{237}Np, respectively. In comparison to the observed integral cross section ratios, the corresponding values derived from ENDF/B-IV data were 2.3% to 6.0% lower."

The results are given more fully in the tables below:

FISSION CROSS SECTION RATIOS FOR ^{252}CF FISSION-SPECTRUM NEUTRONS

NUCLIDES	σ_f RATIO	TOTAL UNCERTAINTY	MASS ASSAY UNCERTAINTY	σ_f RATIO, ENDF/B-IV	DISCREPANCY PRESENT WORK/ENDF
	PRESENT WORK				
$^{238}U/^{235}U$	0.266	± 1.7%	± 1.5%	0.251	6.0%
$^{239}Pu/^{235}U$	1.500	± 1.6%	± 1.4%	1.440	4.2%
$^{237}Np/^{235}U$	1.105	± 2.2%	± 2.1%	1.080	2.3%

ABSOLUTE CROSS SECTION VALUES
(10^{-24} cm^2)

NUCLIDE	$\sigma_f(\chi_{Cf})$ PRESENT WORK	$\sigma_f(\chi_{Cf})$ ENDF/B-IV	DISCREPANCY PRESENT WORK/ENDF
^{238}U	0.320 ± 2.8%	0.312_5	2.4%
^{239}Pu	1.80_4 ± 2.5%	1.79_0	0.8%
^{237}Np	1.33_2 ± 2.8%	1.34_3	-0.8%

13. Measurement of ^{235}U Thermal Neutron Fission Yields (D. Gilliam, J. A. Grundl, and V. Spiegel, Jr.; with staff members of ANC, ANL, ARHCO, and HEDL)

A first measurement of the yields of five long-lived fission products was undertaken at the NBS reactor thermal column in cooperation with four nuclear energy development laboratories. A summary of the experimental procedure and results obtained follow.

Three ^{235}U fission activation foils were irradiated separately in the thermal column of the NBS Reactor. During each irradiation, the integrated fission density (fissions/mg ^{235}U) was determined by observing ^{235} fissions from a calibrated depleted uranium deposit by means of the NBS Double Fission Chamber. The activation foil was positioned inside of the chamber adjacent to the calibrated deposit. Corrections relating the specific fission count from the deposit to the fission density sustained in the activation foil were computed and tested experimentally. These included self-absorption in the activation foils ($\pm$ 0.5% maximum) and fission fragment and dead time losses in the fission chamber ($\sim$3% and 1.4% respectively). Fission densities of around 1×10^{13} fissions/mg ^{235}U were obtained with an accuracy of $\pm$ 1.7% to $\pm$ 2.0%. The dominating errors in the fission density measurement were the uncertainty in the mass of the reference ^{235}U deposit ($\pm$ 1.2%), the uncertainty in the correction for ^{238}U fission in the depleted uranium working deposit ($\pm$ 0.63 to 1.25%), and the uncertainty in the calibration of the working deposit mass relative to the reference deposit ($\pm$ 0.72%).

The total number of fissions in the activation foils was inferred from the observed fission density and the activation foil masses as reported by the supplier, the Isotope Target Laboratory at ORBL. These masses remain to be confirmed by an independent mass analysis. Four participating laboratories-ANC, ANL, ARHCO, and HEDL-received irradiated activation foils and determined absolute fission product activities using Ge(Li) spectrometers. The gamma counting results have been combined with the fission counting data and foil mass data to obtain absolute fission yeilds. The foil to foil precision from separate irradiations and gamma counting groups for ^{95}Zr, ^{103}Ru, ^{132}Te, ^{137}Cs, and ^{140}Ba fission products agree well with the estimated (1σ) uncertainties, typically 3 to 4%.

Thermal-fission yeilds, laboratory-averaged values relative to the ^{140}Ba fission yield, are shown in Table II; They are not to be taken as final values for this effort.

TABLE II

YIELDS RELATIVE TO ^{140}Ba

(FOR THERMAL NEUTRON FISSION OF ^{235}U)

Fission Product Nuclide	Yield[a] Relative to ^{140}Ba (Average of Tests 74-1,2,3)
^{95}Zr	1.03 ± 3.3%
^{97}Zr	1.11 ± 2.9%[b,c]
^{99}Mo	1.00 ± 3.3%[b,c]
^{103}Ru	0.491 ± 4.2%
^{131}I	0.478 ± 2.8%[b,c]
^{132}Te	0.690 ± 7.4%
^{133}I	1.06 ± 2.8%[b,c]
^{137}Cs	1.00 ± 3.6%
^{141}Ce	1.12 ± 3.1%[b,c]
^{143}Cc	0.95 ± 2.8%[b,c]
^{144}Ce	0.96 ± 7.6%

[a] The error in the relative yields is taken as the root-sum-square combination of the gamma counting errors in the ^{140}Ba yield and the gamma counting errors in the yield of the nuclide of interest. (These relative yields are independent of errors in the fission counting or foil mass analysis.)

[b] No error was assigned to the branching ratio.

[c] Only one laboratory reported a result for this nuclide.

15. Evaluation of Fission Neutron Spectra (J. Grundl and C. Eisenhauer)

In our paper at the Nuclear Cross Sections and Technology Conference in March we presented our evaluation in terms of a reference Maxwellian of the form $M(E) = c\sqrt{E}\exp(-1.5\,E/\bar{E})$, where $\bar{E}$ is the average energy of the Maxwellian. Departures of the data from the reference Maxwellian were expressed by a constant adjustment in each of seven energy groups. The segment adjusted fission spectrum is suitable for estimating detector responses but it has the disadvantage of being discontinuous. Since then we have updated the evaluation by specifying the adjustment in terms of a piecewise continuous function $\mu(E)$ over five energy intervals between zero and 20 MeV.

The final evaluation is given as the product $X(E)$ of the reference Maxwellian and the adjustment:

$$X(E) = M(E)\,\mu(E)$$

The reference Maxwellians are

$$M(E) = 0.7501\sqrt{E}\exp(-1.5E/1.97),$$ thermal-neutron-induced fission of ^{235}U

and

$$M(E) = 0.6672\sqrt{E}\exp(-1.5E/2.13),$$ spontaneous fission in ^{252}Cf

The adjustment functions are as follows:

Table I. Adjustment Functions

Energy Interval (MeV)	$\mu(E)$, ^{235}U	$\mu(E)$, ^{252}Cf
0.0 - 0.25	$1 + 0.8E - 0.153$	$1 + 1.20E - 0.237$
0.25 - 0.8	$1 - 0.14E + 0.082$	$1 - 0.14E + 0.098$
0.8 - 1.5	$1 + 0.040E - 0.062$	$1 + 0.024E - 0.0332$
1.5 - 6.0	$1 + 0.01E - 0.017$	$1 - 0.0006E + 0.0037$
6.0 - 20.0	$1.043\exp[-0.06(E-6.0)/1.043]$	$1.0\exp[-0.03(E-6.0)/1.0]$

14. Calculations for Intermediate-Energy Standard Neutron Field (ISNF) (C. Eisenhauer, J. Grundl)

The Intermediate-Energy Standard Neutron Field (ISNF) is a one-dimensional spherically symmetric neutron field operated in the graphite thermal column of the NBS reactor. This facility makes available a primary standard neutron field with a smoothly varying energy spectrum that may be accurately calculated. The system consists of a 30 cm dia. spherical cavity in thick graphite, a thin 13 cm dia. ^{10}B shell mounted at the center of the cavity, and a set of ^{235}U fission disks placed near the cavity wall. The fission disks convert the incident thermal flux to fission neutrons which diffuse into the graphite. The neutrons which return from the graphite along with the direct fission source neutrons are transmitted by the ^{10}B shell and give rise to the ISNF field at the center of the cavity. Field characteristics are as follows:

Total flux intensity	1×10^9 n/cm^2 sec
Median spectrum energy	0.56 MeV
90% spectrum interval	8 keV to 3.5 MeV
Uniformity of total flux	< 3% variation over 5 cm

Computations of the scalar flux in this system have been performed using the ANISN discrete ordinates code primarily but complemented with Monte-Carlo calculations. Sensitivity of central flux to changes in system parameters such as graphite density, cross section variations, and cavity radius have also been investigated. Calculated detector responses for the ISNF spectrum using ENDF/B-IV tabulations have been obtained for over 30 reactions important for nuclear energy developments.

Average values of the reference Maxwellian spectra and the evaluated spectra over seven energy groups are shown in Table II. From both tables I and II it can be seen that the departures of the evaluated spectra from the reference Maxwellians are only a few percent for energies between 0.25 MeV and 8 MeV. The spectra were evaluated on the basis of sixteen published fission spectrum measurements covering the period from 1952 through 1974. The 1σ and 2σ uncertainties judged from variations of the experimental data from the evaluated spectra are also given in Table II. This evaluation allows us to ascribe maximum uncertainties to the flux $\phi(E)$ when comparing the results of integral experiments $\int\phi(E)\sigma(E)dE$ to calculations with differential cross sections $\sigma(E)$.

TABLE II. Group-Averaged Values of Reference Maxwellians and Evaluated Spectra for ^{252}Cf and ^{235}U

Energy Boundaries (MeV)	Californium-252 (Spontaneous Fission) Reference Maxwellian (E_{av} = 2.13 MeV)	[a]Evaluated Spectrum		Uranium-235 (Thermal-neutron-induced) [a]Reference Maxwellian (E_{av} = 1.97 MeV)	[b]Adjusted Maxwellian Segments	
		1σ	2σ		1σ	2σ
0.0						
	(0.050)	0.047 ±13%	± 26%	(0.056)	0.054 ± 16%	±32%
0.25						
	0.179	0.184 ± 1.1%	± 3.3%	0.195	0.197 ± 4.1%	± 6.2%
0.8						
	0.222	0.220 ± 1.8%	± 3.6%	0.233	0.229 ± 3.0%	± 4.8%
1.5						
	0.193	0.194 ± 1.0%	± 3.1%	0.195	0.195 ± 3.1%	± 5.2%
2.3						
	0.199	0.200 ± 2.0%	± 3.0%	0.190	0.192 ± 2.0%	± 3.0%
3.7						
	0.147	0.146 ± 2.1%	± 4.8%	0.124	0.127 ± 4.8%	± 8.0%
8						
	(0.0104)	0.0087 ± 8.5%	± 17%	(0.0068)	0.0054 ± 5.3%	± 11%
12						

[a]Listed uncertainties, 1σ and 2σ, are judged from departures of data subsets after adjustment.

16. Filtered Beams at the NBS Reactor (R. B. Schwartz, I. G. Schroder, and E. D. McGarry*)

We have installed the third, and last, of our filtered beams in a through tube at the NBS Reactor. An 81 cm silicon filter, viewing a graphite scatterer, produces a 144 keV neutron beam. A contaminant peak at 55 keV is easily removed by the addition of ∿2cm of titanium. The gamma ray background with this filter is approximately 350 mr/hr. This will soon be reduced to approximately 12 mR/hr by an additional 55 cm of silicon. The neutron flux is approximately 10^6 neutrons/cm^2-sec. A series of measurements to accurately determine the characteristics of the three beams (2 keV, 25 keV, and 144 keV) is well under way.

*Harry Diamond Laboratory

B. ELECTRONUCLEAR PHYSICS

1. Measurement of Nuclear Structure (S. Penner, J.W. Lightbody, Jr., X.K. Maruyama, and F.J. Kline)

The following paper was submitted for presentation at the Washington Meeting of the American Physical Society. The abstract follows:

Measurement of the rms Nuclear Charge Radius of ^{3}He by Elastic Electron Scattering. (Z.M. Szalata,[1] J.M. Finn,[1] J.B. Flanz,[1] G.A. Peterson,[1] F.J. Kline, J.W. Lightbody, Jr., X.K. Maruyama, and S. Penner)--Electrons have been scattered from ^{3}He at the 140 MeV Linear Electron Accelerator Facility at the National Bureau of Standards. Two identical 350 cm^3 sealed gas target cells were used. One contained CH_4 for normalization purposes, and the other an accurately known mixture of ^{3}He and CH_4. Cross sections were measured in the range of momentum transfer squared between 0.035 and 0.31 fm^{-2} with scattered electron energy resolution of about 0.2%. A value of the rms nuclear charge radius accurate to about 1% was obtained in a nearly model independent analysis.

Several papers were submitted to the Physical Review C. The abstracts follow:

Shapes of deformed nuclei as determined by electron scattering: ^{152}Sm, ^{154}Sm, ^{166}Er, ^{176}Yb, ^{232}Th, and ^{238}U. (T. Cooper,[2] W. Bertozzi,[2] J. Heisenberg,[2] S. Kowalski,[2] W. Turchinetz,[2] C. Williamson,[2] L. Cardman,[3] S. Fivozinsky, J. Lightbody, Jr., and S. Penner)--Electron scattering experiments have been performed on the deformed nuclei ^{152}Sm, ^{154}Sm, ^{166}Er, ^{176}Yb, ^{232}Th, and ^{238}U at momentum transfers between 0.5 fm^{-1} and 1.3 fm^{-1}. The cross sections for the 0^+, 2^+, and 4^+ rotational states of these nuclei have been obtained and together with other information on the electromagnetic properties of these nuclei, these data lead to information about the deformed shapes. The shapes of ^{166}Er and ^{176}Yb are quite different from the shapes of ^{152}Sm and ^{154}Sm and require a varying skin thickness. The Sm isotopes require a constant skin thickness. Results are presented for $\rho_0(\gamma)$, $\rho_2(\gamma)$ and $\rho_4(\gamma)$.

Electroexcitation of the T_0+1 Giant M1 Resonance in ^{58,60}Ni. (R.A. Lindgren,[4] W.L. Bendel,[4] E.C. Jones, Jr.,[4] L.W. Fagg,[4] X.K. Maruyama J.W. Lightbody, Jr., and S.P. Fivozinsky)--Using inelastic electron scattering, several isobaric analog 1^+ states between 9 and 12 MeV excitation in ^{58}Ni and ^{60}Ni have been found. They are identified as components of the T_0+1 giant M1 state in ^{58,60}Ni.

---

[1]University of Massachusetts, Amherst, Mass.
[2]Massachusetts Institute of Technology, Boston, Mass.
[3]University of Illinois, Champaign, Ill.
[4]Naval Research Laboratory, Washington, D.C.

Electron Scattering From Vibrational Nuclei. (J.W. Lightbody, Jr., S. Penner, S.P. Fivozinsky, P.L. Hallowell,[5] and Hall Crannell[6])-- We present electron scattering form factors for the ground states and several low energy quadrupole excitations of the nuclei ^{52}Cr, ^{110}Pd, ^{114}Cd and ^{116}Sn. For ^{116}Sn we also present the form factor for the lowest octupole excitation. From these data we derive ground state charge distribution parameters as well as B(EL) values. We attempt to interpret the observed 2^+ states as the one- and two-phonon states of an anharmonic vibrational model. Predictions are made for the electromagnetic decay branching ratios and excited state electric quadrupole moments.

---

[5]Operations Research, Inc., Silver Spring, Md.

[6]The Catholic University of America, Washington, D.C.

C. DATA COMPILATION

1. X-Ray and Ionizing Radiation Data Center (J. H. Hubbell)

The compilation "Atomic Form Factors, Incoherent Scattering Functions, and Photon Scattering Cross Sections," developed in collaboration with Wm. J. Veigele and E. A. Briggs (now at SAI), R. T. Brown and D. T. Cromer (LASL) and R. J. Howerton (LLL) described in previous ERDA-NDC reports is now published in J. Phys. Chem. Ref. Data 4, 471 (1975). This data set has been incorporated by R. Roussin et al (RSIC, ORNL) into the latest ENDF/B photon interaction data library tape.

As a further evaluation phase for the new general-purpose photon cross section and x-ray attenuation coefficient compilation now in progress, a report "Comparison of Theoretical and Experimental Photoeffect Data 0.1 keV to 1.5 MeV," co-authored with Wm. J. Veigele (SAI), was published as NBS Tech. Note 901 (1976), with particular emphasis on the extensive photoeffect calculations by Veigele and by J. Scofield (LLL).

Based on a new pair production evaluation as well as the above new scattering and photoeffect data, a report "Photon Mass Energy-Absorption Coefficient Air/Medium Ratios for Ionometric Dosimetry 0.1 keV to 20 MeV" was presented at the "Measurements for the Safe Use of Radiation" Symposium at NBS March 1-4, 1976. A more detailed account of this material, including explicit cross sections and energy-absorption coefficients for five low-Z elements and seven composites of dosimetric interest, is being prepared for publication in Radiation Research.

D. FACILITIES

1. 3 MV Positive Ion Van de Graaff and Associated Particle Facility (M. M. Meier)

Machine operation has been satisfactory. Changes in the beam transport system, including installation of an electrostatic quadrupole after the tube extension, have effected a threefold increase in analyzed, pulsed beams.

The data analysis system continues to be upgraded. Software for use with the CAMAC system and program selector board[1] are essentially complete. On order or under construction are 2.7 Mbyte disc, additional 8k of core (new total - 24k), high speed teletype and multiplexer for two-parameter acquisition.

Collimators and beam line hardware are being designed for cross section measurement and dosimetry experiments. This facility will employ the "Black Detector"[2] as a flux monitor and is expected to be operational in the coming summer.

The associated particle chambers have been in routine operation as a calibrated neutron source for the energy range 100 keV to 1 MeV. It was found that the $\theta(^3He) = 25^o$ chamber which produces neutrons in the range 500 to 1000 keV can be operated with acceptable backgrounds without electrostatic deflection.

---

[1] Schrack, Heaton, and Green, Nuclear Cross Sections and Technology, 1 (1975) 97.

[2] Lamaze, Meier, and Wasson, Nuclear Cross Sections and Technology, 1 (1975) 73.

OAK RIDGE NATIONAL LABORATORY

A. CROSS SECTION MEASUREMENTS

1. Gamma-Ray Production Data

During the reporting period the following gamma-ray production data obtained at ORELA were released:

a. Production of Low Energy Gamma Rays by Neutron Interactions with Fluorine for Incident Neutron Energies Between 0.1 and 20 MeV*,** (G. L. Morgan and J. K. Dickens)

Differential cross sections for the production of low-energy gamma rays (< 240 keV) by neutron interactions in fluorine have been measured for neutron energies between 0.1 and 20 MeV. The Oak Ridge Electron Linear Accelerator was used as the neutron source. Gamma rays were detected at 92° using an intrinsic germanium detector. Incident neutron energies were determined by time-of-flight techniques. Tables are presented for the production cross sections of three gamma rays having energies of 96, 110, and 197 keV.

b. The V(n,xγ) Reaction Cross Section for Incident Neutron Energies Between 0.2 and 20.0 MeV†,‡ (E. Newman and G. L. Morgan)

Differential cross sections for the neutron-induced gamma-ray production from natural vanadium have been measured for incident neutron energies between 0.2 and 20.0 MeV. The Oak Ridge Electron Linear Accelerator (ORELA) was used to provide the neutrons and a NaI spectrometer to detect the gamma rays at 125°. The data presented are the double differential cross section, $d^2\sigma/d\Omega dE$, for gamma-ray energies between 0.3 and 10.6 MeV for coarse intervals in incident neutron energy. The integrated yield of gamma rays of energies greater than 300 keV and higher resolution in the neutron energy is also presented. The experimental results are compared with the Evaluated Neutron Data Files (ENDF).

---

* Abstract of ORNL-TM-4823.
** Relevant to request No. 74180.
† Abstract of ORNL-TM-5299, ENDF-221.
‡ Relevant to request No. 74224.

c. The Cr(n,xγ) Reaction Cross Section for Incident Neutron Energies Between 0.2 and 20.0 MeV*,** (G. L. Morgan and E. Newman)

Differential cross sections for the neutron-induced gamma-ray production from natural chromium have been measured for incident neutron energies between 0.2 and 20.0 MeV. The Oak Ridge Electron Linear Accelerator (ORELA) was used to provide the neutrons and a NaI spectrometer to detect the gamma rays at the laboratory angle of 125°. The data presented are the double differential cross section, $d^2\sigma/d\Omega dE$, for gamma-ray energies between 0.3 and 10.6 MeV for coarse intervals in incident neutron energy. The integrated yield of gamma rays of energies greater than 300 keV and higher resolution in the neutron energy is also presented. The experimental results are compared with the Evaluated Neutron Data Files (ENDF).

d. The Cu(n,xγ) Reaction Cross Section for Incident Neutron Energies Between 0.2 and 20.0 MeV†,‡ (G. T. Chapman)

Differential cross sections for the neutron-induced gamma-ray production from copper have been measured for incident neutron energies between 0.2 and 20.0 MeV. The Oak Ridge Electron Linear Accelerator (ORELA) was used to provide the neutrons and a NaI spectrometer to detect the gamma rays at 125°. The data presented are the doubly differential cross section, $d^2\sigma/d\Omega dE$, for gamma-ray energies between 0.3 and 10.6 MeV for coarse intervals in incident neutron energy. The integrated yield of gamma rays of energies greater than 300 keV with higher resolution in the neutron energy is also presented. The experimental results are compared with previous measurements made at ORELA and with the Evaluated Neutron Data File (ENDF/B-IV, MAT 1295).

e. The Nb(n,xγ) Reaction Cross Section for Incident Neutron Energies Between 0.65 and 20.0 MeV¶ (Dickens, Morgan and Newman)

Differential cross sections for the neutron-induced gamma-ray production from niobium have been measured for neutron energies between 0.65 and 20 MeV. The Oak Ridge Electron Linear Accelerator (ORELA) was used to provide the neutrons and a NaI spectrometer to detect the gamma rays at 90°. The data presented are the double differential cross section, $d^2\sigma/d\Omega dE$, for gamma-ray energies between 0.75 and 10.5 MeV and coarse intervals in the incident neutron energy. The integrated yield of gamma rays of energies greater than 0.75 MeV and higher resolution

---

* Abstract of ORNL-TM-5098, ENDF-222.
** Relevant to request Nos. 74230 and 72037.
† Abstract of ORNL-TM-5215.
‡ Relevant to request No. 74304.
¶ Abstract of ORNL-TM-4972, ENDF-219.

in the incident neutron energy is also presented. The experimentally determined results are compared with the Evaluated Neutron Data Library.

f. <u>The Mo(n,xγ) Reaction Cross Section for Incident Neutron Energies Between 0.2 and 20.0 MeV</u>*,** (G. L. Morgan and E. Newman)

Differential cross sections for the neutron-induced gamma-ray production from natural molybdenum have been measured for incident neutron energies between 0.2 and 20.0 MeV. The Oak Ridge Electron Linear Accelerator (ORELA) was used to provide the neutrons and a NaI spectrometer to detect the gamma rays at 125°. The data presented are the double differential cross section, $d^2\sigma/d\Omega dE$, for gamma-ray energies between 0.3 and 10.6 MeV for coarse intervals in incident neutron energy. The integrated yield of gamma rays of energies greater than 300 keV and higher resolution in the neutron energy is also presented. The experimental results are compared with the Evaluated Neutron Data Files (ENDF).

g. <u>Gamma-Ray Production due to Neutron Interactions with Silver for Incident Neutron Energies Between 0.3 and 20 MeV: Tabulated Differential Cross Sections</u>† (Dickens, Love and Morgan)

Numerical values of differential cross sections for gamma rays produced by neutron reactions with silver have been obtained for neutron energies between 0.3 and 20 MeV for $\theta_\gamma = 125°$. The $d^2\sigma/d\omega dE$ values were obtained using a NaI spectrometer. These data are presented as gamma-ray production group cross-section values of $d^2\sigma/d\omega dE$ for $0.3 \leq E_\gamma \leq 10.5$ MeV, with gamma-ray intervals ranging from 15 keV for $E_\gamma \leq 0.4$ MeV to 160 keV for $E_\gamma \sim 9$ MeV. Neutron energy intervals varied from 0.10 MeV for E_n between 0.3 and 0.4 MeV to 3 MeV for E_n between 14 and 20 MeV.

h. <u>The Au(n,xγ) Reaction Cross Section for Incident Neutron Energies Between 0.2 and 20.0 MeV</u>‡ (G. L. Morgan and E. Newman)

Differential cross sections for the neutron-induced gamma-ray production from natural gold have been measured for incident neutron energies between 0.2 and 20.0 MeV. The Oak Ridge Electron Linear Accelerator (ORELA) was used to provide the neutrons and a NaI spectrometer to detect the gamma rays at 125°. The data presented are the double differential cross sections, $d^2\sigma/d\Omega dE$, for gamma-ray energies between 0.3 and 10.6 MeV for coarse intervals in incident neutron energy. The integrated yield of gamma rays of energies greater than 300 keV and higher resolution in the neutron energy is also presented. The experimental results are compared with the Evaluated Neutron Data Library (ENDL).

---

* Abstract of ORNL-TM-5097, ENDF-220.
** Relevant to request No. 74313.
† Abstract of ORNL-TM-5081.
‡ Abstract of ORNL-TM-4973.

2. Capture Cross Sections

The following are abstracts of papers written or published during the reporting period:

a. Neutron Capture and Transmission by ^{24,25,26}Mg *,** (H. Weigmann,† R. L. Macklin and J. A. Harvey)

Resonance neutron capture and transmission by the stable isotopes of magnesium were measured at the Oak Ridge Electron Linear Accelerator time-of-flight facility; capture by separated isotope and natural metal samples at 40 meters and transmission by a natural metal sample (78.7% ^{24}Mg) at 200 meters. Twenty-six resonances in ^{24}Mg + n up to 1.8 MeV were fitted with R-matrix parameters. The data were sufficient to assign spin and parity to 19 of these. The capture data were analyzed up to 850 keV for ^{24}MeV + n, 265 keV for ^{25}Mg + n (17^{+} resonances), and 440 keV for ^{26}Mg + n (4 resonances). Average capture at stellar interior temperatures was calculated. The ^{24}Mg + n data serve to assess the isospin impurities in three isobaric analogue states. Three other states exhibit reduced neutron widths each several percent of the Wigner limit which may be understood in terms of simple shell model configurations.

b. The Neutron Capture Cross Section of Natural Silicon‡,¶ (Boldeman,§ Allen,§ Musgrove§ and Macklin)

The neutron capture cross section of natural silicon has been measured to 1500 keV using the capture cross section facility at the 40 m station of the Oak Ridge Electron Linear Accelerator. Analysis of the present data, in combination with existing total cross section information, has provided almost complete resonance data for ^{28}Si. On the other hand, the capture kernel only ($g\Gamma_n\Gamma_\gamma/\Gamma$) has been obtained for neutron capture resonances in ^{29}Si and ^{30}Si. A strong positive correlation has been observed between the radiative width and the corresponding reduced neutron width for p-wave resonances in ^{28}Si, confirming significant valence effects. It is noted that a quantitative valence calculation provides only an approximate estimate of the valence strength for this nucleus. It was not possible to confirm from the present measurements, reported asymmetry observed in two resonances in the ^{29}Si(γ,n) reaction.

---

* To be published in Phys. Rev. C.
** Relevant to request No. 74181.
† Visiting Scientist from CBNM, Geel, Belgium.
‡ Nuclear Physics A252, 62 (1975).
¶ Relevant to request No. 74182.
§ Australian Atomic Energy Commission, Lucas Heights, NSW, Australia.

c. Kilovolt $^{33}S(n,\alpha_0)$ and $^{33}S(n,\gamma)$ Cross Sections: Importance in the Nucleosynthesis of the Rare Nucleus ^{36}S*,** (Auchampaugh,† Halperin, Macklin and Howard‡)

The $^{33}S(n,\alpha_0)$ and $^{33}S(n,\gamma)$ cross sections have been measured from $\sim$ 10 to $\sim$ 700 keV. Resonance parameters are given for 39 resonances. The level spacing is determined to be 9.1 ± 0.9 keV. The $\sigma(n,\alpha_0)$ and $\sigma(n,\gamma)$ cross sections are averaged over a Maxwellian distribution for values of kT from 25 to 275 keV. When these cross sections are used in a nucleosynthesis calculation of the rare isotope ^{36}S, the overproduction of this isotope, relative to the other nuclei formed in the universe, is reduced from a factor of 10 to 2.5.

d. Resonant Neutron Capture in ^{40}Ca ¶,§ (Musgrove, Allen, Boldeman, Chan,+ and Macklin)

The neutron capture cross section of ^{40}Ca has been measured with $\sim$ 0.2 percent energy resolution below E_n = 300 keV. Resonance parameters have been extracted for many new p- and d-wave resonances.

Gamma-ray spectra were also measured following capture in one doublet and two resolved resonances below 50 keV. Strong feeding of low lying p-wave levels was observed in all cases. Calculations showed that valence transitions were inadequate to account for the observed dominance of these transitions and a further mechanism is required.

The average resonance parameters obtained from the data are as follows: $\langle D \rangle = 37 \pm 4$ keV, $10^4 S_1 = 0.16 \pm 0.05$, $10^4 S_1 = 2.0 \pm 0.7$. The average radiative widths and standard deviations of their distributions were found to be strongly ℓ-dependent as follows: $\langle\Gamma_\gamma\rangle_s = 1.5 \pm 0.9$ eV, $\langle\Gamma_\gamma\rangle_p = 0.36 \pm 0.09$ eV and $\langle\Gamma_\gamma\rangle_d = 0.75 \pm 0.36$ eV.

---

* Phys. Rev. C 12, 1126 (1975).
** Relevant to request Nos. 74023 and 74024.
† Los Alamos Scientific Laboratory, Los Alamos, New Mexico 87544.
‡ Astronomy Department, University of Illinois, Urbana, Illinois 61801.
¶ Submitted for publication in Nuclear Physics.
§ Relevant to request Nos. 74029 and 74030.
\+ University of Melbourne, Victoria, Australia.

e. Neutron Capture Cross Section of ^{59}Co in the Energy Range 2.5 - 1000 keV*,** (R. R. Spencer and R. L. Macklin)

Time-of-flight measurements of the capture cross section of ^{59}Co were carried out in the neutron energy region 2.5 - 1000 keV using the Oak Ridge Electron Linear Accelerator and a pair of nonhydrogenous liquid-scintillator gamma-ray detectors. Resonance energies and capture areas were determined for a large number of resolved resonances up to 85 keV neutron energy, and radiation widths for 35 known s-wave resonances were derived. Significant positive correlations ($\rho \simeq 0.3$) were found between the radiative widths and neutron reduced widths of these s-wave resonances for both possible spin states.

f. High Resolution Neutron Capture Cross Sections in ^{63}Cu and ^{65}Cu.†,‡ (M. S. Pandey,¶ J. B. Garg,¶ R. Macklin and J. Halperin)

Neutron capture cross sections in separated isotopes of copper (^{63}Cu and ^{65}Cu) from a few keV to a few hundreds of keV were measured using the ORELA time-of-flight facility. From these measurements the capture yields of resonances were accurately determined giving precise values of $g\Gamma_n$ and Γ_γ up to a maximum neutron energy of 50 keV. For ^{63}Cu one obtains a value of $\langle\Gamma_\gamma\rangle$ = (507 ± 30) meV, p-wave average level spacing $\langle D\rangle_{\ell=1}$=(.495 ± .026) keV and strength function $S_1 = (0.44 \pm 0.07)10^{-4}\text{eV}^{-1/2}$. The corresponding s-wave mean level spacings for ^{63}Cu and ^{65}Cu are (1.04 ± 0.11) keV and (1.47 ± 0.19) keV respectively. Some few of the narrowest levels have been assumed formed by d-waves.

g. Valence Neutron Capture in ^{88}Sr § (Boldeman, Allen, Musgrove and Macklin)

The neutron capture cross section of ^{88}Sr has been measured with high energy resolution between 2.5 and 400 keV using the capture cross section facility at the 40 m station on the Oak Ridge Electron Linear Accelerator. Strong positive correlations have been observed between the reduced neutron and radiative widths for both $p_{3/2}$ and $p_{1/2}$ resonances. The data provide an unambiguous quantitative verification of the valence model.

---

* Submitted for publication in Nucl. Sci. Eng.
** Relevant to request No. 69106.
† Submitted for publication in Phys. Rev.
‡ Relevant to request Nos. 69132 and 74307.
¶ State University of New York at Albany.
§ Submitted for publication in Nuclear Physics.

h. Valence Component in the Neutron Capture Cross Section of ^{90}Zr*,** (Boldeman, Allen, Musgrove and Macklin)

The neutron capture cross section of ^{90}Zr has been measured with high energy resolution between 3 and 200 keV using the capture cross section facility at the 40 m station on the Oak Ridge Electron Linear Accelerator. Through the comparison of the present data with the total cross-section and inverse $^{91}Zr(\gamma,n)$ data from Toohey and Jackson, complete resonance parameters have been extracted for 37 $p_{3/2}$ and $p_{1/2}$ and 11 s-wave resonances out of a total of 101 observed resonances. The neutron strength functions extracted from the resonance parameters are $S_0 = 0.56 \times 10^{-4}$, $S_1 = 3.8 \times 10^{-4}$, $S_1(p_{3/2}) = 4.7 \times 10^{-4}$ and $S_1(p_{1/2}) = 1.9 \times 10^{-4}$. It is noteworthy that the $S_1(p_{3/2})$ strength function is significantly larger than the $S_1(p_{1/2})$ strength function in agreement with theoretical expectation.

A significant correlation ($\rho = 0.58$) exists between the reduced neutron widths and the radiative widths for the 37 $p_{3/2}$ resonances. The data give strong confirmation of the valence neutron model. With standard valence calculations all radiative widths can be calculated reasonably from the associated reduced neutron width. However, to explain the measured correlation coefficient, it has been necessary to include with the valence component, single-particle transitions to the ground and low excited states of ^{91}Zr, which are uncorrelated with the resonance reduced neutron width.

The average capture γ-spectrum for neutron capture in ^{90}Zr between 2 and 80 keV has been calculated from the valence model and the present data and is found to be in very close agreement with published experimental data.

i. Neutron Capture Cross Section of Niobium-93 from 2.6 to 700 keV†,‡ (R. L. Macklin)

The neutron capture cross section of stable ^{93}Nb was measured by time-of-flight methodology at the Oak Ridge Electron Linear Accelerator. Individual resonances were parameterized to 7.4 keV with energy resolution $\leq$ 0.14% full-width-at-half-maximum. The average cross section was deduced from 3 to 700 keV with an accuracy estimated at 3 to 5% SD. The average data to 100 keV are well fitted by strength functions, but the fluctuations about the fit are not consistent with an energy-independent level density proportional to 2.1 + 1 beyond 20 keV.

---

* Nuclear Physics A246, 1 (1975).
** Relevant to request Nos. 69142, 69151 and 72062.
† Nucl. Sci. Eng. 59, 12 (1976).
‡ Relevant to request Nos. 62049 and 62050.

j. Average Neutron Resonance Parameters and Radiative Capture Mechanisms for the Isotopes of Molybdenum*,**
(Musgrove, Allen, Boldeman and Macklin)

The neutron capture cross sections of the stable molybdenum isotopes have been measured with high energy resolution between 3 and 90 keV at the 40 m station of ORELA. Average resonance parameters are extracted for s- and p-wave resonances. The s-wave neutron strength function is close to 0.5×10^{-4} for all isotopes, but the p-wave strength function exhibits a well defined peak near $A \sim 95$.

Both s- and p-wave radiative widths decrease markedly as further neutrons are added to the closed shell. The p-wave radiative widths are generally greater than the s-wave widths showing the presence of non-statistical γ-decay mechanisms.

Valence neutron theory fails to explain the magnitude of the p- to s-wave radiative width discrepancy and doorway state processes are invoked. The existing data for ^{92}Mo and ^{98}Mo are reviewed and the possible radiative mechanisms are outlined.

In particular, the data for ^{98}Mo provide a clear violation of the usual valence theory, since no correlations between radiative and neutron strengths are found. Further, the radiative widths are far smaller than can be explained on the valence model. An explanation for this loss of valence strength is advanced.

Interpolated resonance parameters allow an estimate for the unknown cross section for ^{99}Mo(n,γ).

k. keV Neutron Capture Cross Sections of ^{134}Ba and ^{136}Ba †
(Musgrove, Allen, Boldeman, and Macklin)

The neutron capture cross sections of ^{134}Ba and ^{136}Ba have been measured in the energy region 3 to 100 keV. The following average quantities were deduced from the extracted resonance parameters: $\langle D \rangle$ = 127 ± 10 eV, $10^4 S_0 = 0.85 \pm 0.3$, $10^4 S_1 = 0.8$, $\langle \Gamma_\gamma \rangle = 120 \pm 20$ MeV for ^{134}Ba. Analysis of the ^{136}Ba data gave $\langle \Gamma_\gamma \rangle = 125 \pm 30$ meV for s-wave neutrons. The average 30 keV capture cross sections for these two s-process nuclei were found to be 225 ± 35 mb for ^{134}Ba and 61 ± 10 mb for ^{136}Ba.

---

* To be submitted for publication in Nuclear Physics.
** Relevant to request No. 72072.
† Nuclear Physics A256, 173 (1976).

ℓ. keV Neutron Resonance Capture in Barium-135 * (Musgrove, Allen and Macklin)

The neutron capture cross section of ^{135}Ba has been measured with high resolution at the Oak Ridge Electron Linear Accelerator in the energy range 3 to 100 keV. From over ninety observed resonances in the 3 to 6 keV energy range, the average resonance parameters obtained were: $<\Gamma_\gamma> =$ 150 ± 20 meV; $<\Gamma_\gamma> = 39.3 \pm 4$ eV and $10^4 S_1 = 0.8 \pm 0.2$. The quoted radiation width and p-wave strength function also have a normalization error of ± 20 percent. The method of separation of s- and p-wave populations by statistical methods is described.

m. keV Neutron Resonance Capture in ^{138}Ba ** (Musgrove, Allen, Boldeman and Macklin)

The neutron capture cross section of ^{138}Ba has been measured with high resolution to 100 keV and resonance parameters have been extracted. A number of new levels are observed. The s-wave radiative width is found to be six times the p-wave radiative width and is also considerably larger than for other nuclei in this mass region. Valence capture and enhanced decay to single-particle final states could account for the large s-wave radiative strength. A large positive correlation between Γ_n^0 and Γ_γ for ten s-wave levels was found ($\rho = 0.67$). The following average resonance parameters were deduced: $<D> = 7.5 \pm 1.5$ keV, $S_0 = (0.9 \pm 0.4) \times 10^4$, $S_1 \approx 0.5 \times 10^{-4}$; $<\Gamma_\gamma>_s = 310 \pm 25$ meV and $<\Gamma_\gamma>_p = 47 \pm 5$ meV. Evidence for a predominant direct capture mechanism for thermal capture is presented.

n. The ^{165}Ho(n,γ) Standard Cross Section from 3 to 450 keV † (R. L. Macklin)

The ^{165}Ho(n,γ) cross section was measured at the Oak Ridge Electron Linear Accelerator neutron time-of-flight facility. Nonhydrogenous scintillation detectors were used with pulse-height weighting to measure the prompt photon yield, normalized to the saturated 3.92-eV resonance in (^{165}Ho + n) and the shape of the ^{6}Li(n,α) cross section. Resonance parameters for many of the observed peaks below 3 keV were determined by a nonlinear least-squares fit. The data to 100 keV were well fitted with energy-independent strength functions $10^4 S^0 = 1.33 \pm 0.14$, $10^4 S^1 = 1.36 \pm 0.24$, $10^4 S_2 = 1.19 \pm 0.76$ and $\overline{\Gamma}_\gamma / D_0 = 0.076/(3.23 \pm 0.55$ eV). The fluctuations of the cross section about the strength function fit are analyzed for 250-eV averages. The Wald-Wolfowitz "Runs" test is consistent with no additional nonrandom structure in the cross section.

* INDC(AUL)-23/L.

** Nuclear Physics, to be published.

† Nucl. Sci. Eng. 59, 231 (1976).

o. Gold Neutron-Capture Cross Section from 3 to 550 keV *,**
(R. L. Macklin, J. Halperin and R. R. Winters†)

A careful remeasurement of the $^{197}Au(n,\gamma)$ cross section using the pulse height weighting technique in small scintillators has been completed. The 4.9 eV resonance was used for calibration and the $^{6}Li(n,\alpha)$ cross section for flux shape. Estimated errors range from 1.4% near 30 keV to 3.3% at 550 keV. Individual resonance parameters were deduced in the 2.6-4.9 keV range and the fluctuations over 10's of resonances were analyzed below 90 keV. The fluctuations are larger than expected, limiting the precision attainable with monoenergetic sources using this standard. The fluctuation intensity appears to indicate intermediate resonance structure in the compound nucleus with ∿ 10 keV width and ∿ 40 keV spacing.

p. Stellar Neutron Capture in the Thallium Isotopes‡ (R. L. Macklin and R. R. Winters)

High resolution neutron capture cross section data for isotopically enriched samples of ^{203}Tl and ^{205}Tl were taken at the Oak Ridge Electron Linear Accelerator time-of-flight facility. The resonance parameter data were used to calculate neutron capture probabilities over a range of stellar interior temperatures. A semi-empirical estimate is also interpolated for the radioactive ^{204}Tl and ^{205}Pb and the results used to recalculate the time scale of s-process nucleosynthesis.

q. The Neutron Strength Functions and Radiation Widths of ^{206}Tl Resonances¶ (Winters, Earle,§ Harvey and Macklin)

The parameters of ^{206}Tl resonances have been determined from neutron total cross section measurements and neutron capture measurements on the Oak Ridge Electron Linear Accelerator.

The neutron strength function $\Sigma g\Gamma_n^0/\Delta E$ for known s-wave resonances is 0.2×10^{-4} below 50 keV and 1.1×10^{-4} above 50 keV. The strength function $\Sigma g\Gamma_n^1/\Delta E$ for known p-wave resonances is 0.5×10^{-4} below 65 keV and 1.5×10^{-4} above. The contribution to these strength functions of unidentified resonances is too small to modify the conclusion that both exhibit a change of slope at around 60 keV. This effect could be interpreted as evidence for intermediate structure (as has previously been seen[1]) for s-wave resonances in the Pb isotopes; however, it is seen for both s- and p-wave resonances at about the same energy.

---

* Phys. Rev. C 11, 1270 (1975).
** Relevant to request Nos. 67082 and 72073.
† Denison University.
‡ To be published in Journal of Astrophysics.
¶ Abstract of paper to be presented at 1976 Int. Conf. Interactions of Neutrons with Nuclei, Lowell, Massachusetts, 6-9 July 1976.
§ Chalk River Nuclear Laboratory, AECL, Chalk River, Ontario.
[1] H. W. Newson, Statistical Properties of Nuclei, Ed. J.B. Garg, Plenum Press (1972) p. 309 and references cited therein.

The radiative widths fall into two groups depending on the parity of the resonances. The s-wave resonances have Γ_γ in the range 0.8 to 6 eV while the p-wave resonances have Γ_γ in the range 0.04 to 0.2 eV. It is suggested that this unusual separation of radiative widths into two families is due to the nature of the low lying states. Since all known states below 2 MeV have high spin or negative parity there can be no high energy E1 primaries from p-wave resonances whereas many E1 transitions from each s-wave resonance are possible.

r. Resonance Neutron Capture by ^{209}Bi * (R. Macklin and J. Halperin)

Neutron capture measurements were made for bismuth samples up to the inelastic scattering threshold at 901 keV (lab). All resonance peaks (ℓ = 0.1) between 2.6 keV and 30 keV were fitted to single level parameters by least squares adjustment. From 30 to 70 keV the resonances reported from recent neutron transmission studies were fitted. Average radiative widths found were (164 ± 45) meV for ℓ = 0 and (33.7 ± 3) meV for ℓ = 1. The average spacing of p-wave levels was 1.14 ± .25 keV for the energy interval 2.6-30 keV. The astrophysical average capture (10.7 mb at kT = 30 keV) is little different from earlier estimates but the rate of change with stellar temperature is slower.

3. Total Cross Sections

a. Measurement of the Neutron Total Cross Section of Sodium**,† (D. C. Larson, J. A. Harvey and N. W. Hill)

Recent sensitivity analyses[1] for the CRBR upper axial shield indicate that 40% of the integrated tissue dose sensitivity to the sodium total neutron cross section comes from the interference minimum of the 300-keV resonance. With the large quantities of liquid sodium coolant present in the CRBR, the cross section minimum for this resonance takes on new significance. Recent thick sample measurements on sodium minima by Brown et al.[2] show a significant discrepancy with the present ENDF/B-IV evaluation[3] for the 300-keV resonance. The evaluation in this region is

* To be submitted for publication in Phys. Rev. C.

** Abstract of paper to be presented at 1976 Int. Conf. Interactions of Neutrons with Nuclei, Lowell, Massachusetts, 6-9 July 1976.

† Relevant to request Nos. 74010 and 74011.

[1] E. M. Oblow, "Survey of Shielding Sensitivity Analysis Development and Applications Program at ORNL," ORNL-TM-5176 (January 1976).

[2] P. H. Brown, B. L. Quan, J. J. Weiss and R. C. Block, Trans. Am Nucl. Soc. 21, 505 (1975).

[3] N. C. Paik and T. A. Pitterle, "Evaluation of Sodium-23 Neutron Data for the ENDF/B Version III File," Appendix A, WARD-3045T4B-2, Westinghouse Advanced Reactors Division (April 1972), and ENDF/B-IV, MAT 1156, NNCSC, Brookhaven National Laboratory (1974).

based on the data of Cierjacks et al.,[1] which show a much sharper minimum than revealed by the measurement of Brown. In addition to the 300-keV resonance problem, no high resolution total cross section data were available from ∿ 40 keV to 300 keV, leading to large uncertainty estimates for this energy region in the evaluation.

In order to provide consistent high resolution data for the ENDF/B-V evaluation, as well as to verify the high resolution data of Cierjacks, we have measured the transmission of neutrons through a 8.1-cm (1/n = 4.90 b/atom) sample of pure sodium from 40 keV to 20 MeV. The transmitted beam was detected by a NE-110 proton recoil detector located at the 200-m flight path of the Oak Ridge Electron Linear Accelerator (ORELA). A 5-ns electron beam burst width was used, with a repetition rate of 800 sec^{-1}. The data were corrected for dead-time effects (maximum of 9% in the cross section at 1.1 MeV), and background (varying from 0.1-0.2% between 100 keV and 2 MeV, rising to 1% at 8 MeV). The 50,000 channels of transmission data were suitably averaged to improve counting statistics while preserving the resonance structure and were then converted to cross section versus energy.

We observe eight resonances in the region of 190 to 310 keV, four of which have not been seen in previous transmission measurements. Resonance energies are 201.2, 214, 236.8,* 239.5, 243.1,* 298.1, 299.4* and 305.2* keV, where the asterisk labels the new resonances. The present data near the 300-keV minimum agree well with data of Brown et al. The largest deviation of the present data from the evaluation in the vicinity of the minimum is -12%.

In summary, the present measurement points out several areas for improvement in the sodium evaluation for ENDF/B-V, the most important being the broadening of the minimum at 300 keV.

b. Measurements on Total Neutron Cross Sections of ^{32}S **
(Johnson, Halperin, Winters and Macklin)

In the valency model for neutron capture enhanced dipole transitions occur from states with relatively large neutron widths to final states with large neutron spectroscopic factors. In order to study this phenomenon we need to know not only Γ_γ for each resonance but also the neutron widths and J^π-values. The observed total cross sections give the neutron width and J-values for well-resolved resonances. The parity can also be deduced if the non-resonant phase shift is large enough to give an interference pattern.

---

[1] C. Cierjacks, P. Forti, D. Kopsch, L. Kropp, J. Neve and H. Unseld, "High Resolution Total Neutron Cross Sections Between 0.5 to 30 MeV," Karlsruhe report KFK-1000 (June 1968).

** Relevant to request Nos. 74021 and 74022.

We have measured the neutron total cross section of ^{32}S using the 200 m flight path with 5 nsec pulses at ORELA to supplement our earlier neutron capture data obtained at the 40 meter station. From these data we have determined Γ_n and J^π for 15 of the $\sim$ 60 resonances observed in capture. There is no obvious correlation of Γ_n and Γ_γ. But the radiative widths predicted from the valency model from the observed Γ_n and J^π are large fractions of the observed Γ_γ. Furthermore, resonances predicted to have relatively large valency capture are observed to have relatively intense high energy gamma rays in the emitted spectra.

c. Neutron Total Cross Sections and Resonance Parameters of ^{63}Cu and ^{65}Cu * (Pandey, Garg and Harvey)

The neutron total cross sections of the isotopes of copper have been measured with high resolution using the ORELA neutron facility. From the area and shape analysis of the transmission and total cross section data, precise values of the resonance parameters, such as E_0, Γ_n^0, Γ_n^1, J^π, etc., have been determined. For example, for ^{63}Cu many s-wave resonances have been observed from 10 to 150 keV giving values of $\langle D\rangle_{J=1}=(2.7\pm0.3)$ keV, $\langle D\rangle_{J=2}=(4.0\pm0.5)$ keV, $\langle D\rangle_{J=1+2}=(1.63\pm0.13)$ keV, $S_{o_{J=1}}=(2.8\pm0.6)\times10^{-4}$ $eV^{-1/2}$, $S_{o_{J=2}}=(1.9\pm0.5)\times10^{-4}$ $eV^{-1/2}$, $S_{o_{J=1,2}}$ = $(2.4\pm0.4)\times10^{-4}$ $eV^{-1/2}$. For ^{65}Cu s-wave resonances were observed giving values of $\langle D\rangle_{J=1}=(3.6\pm0.4)$ keV, $\langle D\rangle_{J=2}=(5.2\pm0.7)$ keV, $\langle D\rangle_{J=1+2}=(2.12\pm0.19)$ keV, $S_{o_{J=1}}=(2.8\pm0.6)\times10^{-4}eV^{-1/2}$, $S_{o_{J=2}}=(1.8\pm0.5)\times10^{-4}$ $eV^{-1/2}$, $S_{o_{J=1,2}}$ = $(2.3\pm0.4)\times10^{-4}$ $eV^{-1/2}$.

d. Resonances in ^{207}Pb+n Including d+s Wave Admixture** (Horen, Harvey and Hill)

High resolution ($\sim$ 0.07%) neutron transmission data of ^{207}Pb (enriched to 92.4%) taken at the 200-meter flight path at ORELA are being analyzed to determine resonance parameters. Of particular interest is the observation of a large d- and s-wave admixture in the 256.25-keV resonance ($J^\pi = 1^-$, Γ = 3.2 keV). Analysis of this resonance assuming only s-wave contribution leads to an abnormally large radiation width, $\Gamma_\gamma \approx 1$ keV. The resonance was therefore analyzed using a 2-channel, single-level, R-matrix formalism which gave $\Gamma_n^d = 0.71\ \Gamma_n^s$. This result is consistent with photonuclear polarization and angular distribution studies.[1] Similar analyses indicate that the 101.78-keV ($J^\pi = 1^-$, Γ = 75 eV) resonance also contains a d-wave component. These d-wave components correspond to a few percent of the Wigner limit. A neutron scattering experiment at the

---

* Submitted for publication in Phys. Rev.

** Relevant to request No. 74315.

[1] R. Holt, private communication, January 1976.

200-meter flight path is in progress. Preliminary data show that the shapes of a number of resonances are strongly angular dependent, and indicate such measurements will be valuable in assigning unambiguous ℓ-values. Our results indicate numerous discrepancies with previously reported values.

e. Resonant States of ^{209}Pb from Neutron Total Cross Section Measurements* (Fowler, Johnson and Hill)

By the use of a suitable combination of three natural samples of lead in a transmission experiment we have measured the total neutron cross section of effectively 99.6% ^{208}Pb. The Oak Ridge Electron Linear Accelerator, ORELA, time-of-flight facility provided 4-5 ns pulses of neutrons for the 200 meter flight path. We observed $\sim$100 resonances between .7 MeV and 1.5 MeV, about twice as many as were seen in a previous experiment[1] carried out with ^{7}Li(p,n) neutrons. In this energy interval our resolution varied from $\sim$.6 keV at 0.7 MeV to $\sim$1.4 keV at 1.5 MeV. The improved energy resolution and statistics from this experiment together with differential cross sections from the previous experiment[1] will enable us to identify the J values, parities and reduced widths of the resonant states of ^{209}Pb more definitely than was possible earlier. In the case of the other doubly closed shell nuclei such data give information of the fragmentation of shell model states.[2]

4. Scattering and Reactions

a. Angular Anisotropy in the ^{6}Li(n,α) T Reaction** (Harvey, Halperin, Hill and Raman)

The yield of tritons and alphas in forward and backward directions ($\Omega \gtrsim \pi$) from the interaction of neutrons with ^{6}Li has been measured from a thin sample of ^{6}LiF (101 μgm/cm^2) from 0.5 to 25000 eV. The measurements were made with a diffused junction Si detector located 9.03 meters from the water-moderated Ta-target at ORELA. The alpha and triton groups at 2.06 and 2.73 MeV are well resolved enabling one to obtain an accurate ratio of their intensity as a function of neutron energy. The intensity of the alpha peak was greater than the intensity of the triton peak in the forward direction but less in the backward direction. This difference is measureable down to 10 eV. An anisotropy has already been reported for

---

* Relevant to request No. 74315.

[1] J. L. Fowler, Phys. Rev. 147, 870 (1966).

[2] J. L. Fowler, C. H. Johnson and R. M. Feezel, Phys. Rev. C 8, 545 (1973) and C. H. Johnson, Phys. Rev. C 7, 561 (1973).

** Relevant to request Nos. 69009-11.

25 keV neutrons by Schroder et al.[1] who made measurements using an iron-filtered neutron beam. In the 10 eV to 10 keV energy region, our results give an energy dependence for the alpha to triton ratio at 180° (or triton to alpha ratio at 0°) of the form $1 + cE^{0.54}$ where c is $\sim$0.005 and E is the neutron energy in eV. At 100 eV this ratio equals 1.06. It is necessary to consider this angular anisotropy when the $^{6}Li(n,\alpha)$ cross section is used as a standard. This angular anisotropy probably arises from the interference between the large p-wave resonance at 245 keV and many s-wave resonances which account for the large 1/v (n,α) thermal cross section.

b. High Resolution Neutron Scattering Experiments at ORELA* (W. E. Kinney, J. W. McConnell and T. A. Love)

Neutron elastic and inelastic scattering data taken with 0.2-0.3 nsec/m resolutions have been reduced to cross sections from 500 to 3000 keV in 1-keV intervals. The results include: 1) Na, Si, and Fe differential (n,n) cross sections at 8 angles from 24° to 155° relative to C; 2) Na and Fe differential $(n,n'\gamma)$ cross sections at 30°, 90°, and 125° relative to the ^{7}Li 478-keV γ-production cross section; 3) Na, Al, Si, V, and Fe $(n,n'\gamma)$ measured with $\sim$30% 4π geometry relative to the ^{7}Li 478-keV γ-production cross section.

c. Cross Sections for the Al(n,xn) and Al$(n,x\gamma)$ Reaction between 1 and 20 MeV**,† (G. L. Morgan and F. G. Perey)

Differential cross sections for the production of secondary neutrons and photons from aluminum have been measured at 127° (lab) for incident neturon energies in the range 1 to 20 MeV. An electron linac was used as a neutron source with a white spectrum. Incident neutron energies were determined using time-of-flight techniques for a source-to-sample distance of 48 m. Secondary spectra were determined by unfolding the pulse-height distributions observed in a NE-213 scintillation counter. The results are compared to the current evaluated data file (ENDF/B-IV, MAT 1193).

---

[1] I. G. Schroder, E. D. McGarry, G. deLeeuw-Gierts and S. deLeeuw, Conference on Neutron Cross Sections and Technology, NBS Special Publication 425 (1975) p. 240.

* Relevant to request Nos. 74012-13, 62007, 69045, 69084-87, 66016-17.

** Abstract of ORNL-TM-5241; paper submitted for publication in Nucl. Sci. Eng.

† Relevant to request Nos. 74162-63, 74215, 17268-69.

d. (n,α), (n,p), (n,γ) and Total Neutron Cross Section Measurements upon ^{59}Ni (Harvey, Halperin, Hill, Raman and Macklin)

In addition to (n,γ) and total neutron cross section measurements upon ^{59}Ni we have made (n,α) and (n,p) measurements at ORELA from $\sim$0.01 eV to $\sim$20 keV. The thermal and resonance (n,α) cross sections of this isotope which are produced from $^{58}Ni(n,\gamma)$ are important due to helium embrittlement and swelling of the structural material of power reactors.

The (n,α) and (n,p) measurements were made simultaneously with a diffused junction Si detector located 9.03-meter from the water-moderated neutron target at ORELA resulting in a neutron energy resolution of 0.5% (FWHM). A sample of ^{59}Ni (95%, 91 μgms/cm^2) was electroplated upon a 1-mil Pt foil and a deposit of ^6Li (95%, 104 μgm/cm^2) was evaporated on top of this ^{59}Ni deposit. The triton and alpha groups (2728 and 2056 keV for thermal neutrons) from the ^6Li (n,α) reaction were easily resolved from the 4759-keV alpha group from the ^{59}Ni (n,α) reaction. The ^{59}Ni (n,p) measurements were made with a deposit of only ^{59}Ni since the 1827-keV protons were difficult to separate from the alphas from ^6Li.

The (n,γ) cross section measurement was made with a 3.136-gram Ni sample 2.54-cm dia. enriched to 2.96% in ^{59}Ni. The measurements were made from 100 to 12000 eV with an energy resolution of 0.15% using the total energy detector located at a 40-meter flight path. Since the sample contained a small amount of ^{60}Co, the bias level on this gamma ray detector was set $\sim$2 MeV involving an uncertainty of 10 $\pm$ 5%. Another measurement is planned with a "clean" sample to reduce the uncertainty due to this extrapolation.

Neutron total cross section measurements were also made with this 3.136-gm sample with an inverse thickness of 5295 barns/atom of ^{59}Ni using an 80-meter flight path. The total cross section of the 203.4-eV resonance obtained with this sample was 1.32 times that obtained from earlier measurements using the $\sim$9-mg, 95%-enriched sample reported in last year's report.[1] This $\sim$9-mg sample has been emptied, reweighed on a microbalance and examined for oxygen by measuring the ^{16}N activity produced by the $^{16}O(n,p)$ reaction with 14-MeV neutrons. These measurements confirmed the neutron analysis that the original sample contained only 7.0 mg of Ni rather than 9.2 mg. This increases the thermal capture and absorption cross sections reported last year to 70 $\pm$ 5 and 87 $\pm$ 6 barns respectively.

The measurements on ^{59}Ni in the thermal energy range yield a value of 12 $\pm$ 1 barns for the (n,α) cross section and 2.0 $\pm$ 0.5 for the (n,p) cross section. This (n,α) result is to be compared with earlier

---

[1] S. Raman, E. T. Jurney, J. A. Harvey and N. W. Hill, NCSAC Report (1975).

values of 13.7 ± 1.2, 18.0 ± 1.6, and 22.3 ± 1.6 barns reported by Eiland and Kirouac,[1] by Werner and Santry,[2] and by McDonald and Sjöstrand[3] respectively. The (n,p) result is lower than the value of 4 ± 1 barns reported by McDonald and Sjöstrand. The results of our four experiments have been combined to produce the following parameters for the 203.4-eV resonance E_0 = 203.4 ± 0.2 eV, Γ = 13.3 ± 0.2 eV, g = 3/8, J = 1, Γ_n = 8.50 ± 0.15 eV, Γ_γ = 4.0 ± 0.6 eV, Γ_α = 0.50 ± 0.03 eV and Γ_p = 0.063 ± 0.006 eV. Assuming that the thermal cross sections arise mainly from the large 203.4-eV resonance, the (n,p) thermal cross section would be expected to be 1/8 the (n,α) cross section or 1.5 barns.

Fifteen higher energy resonances have been observed in the four types of experiments. The alpha and proton widths of the resonances vary widely due to selection rules and because they are essentially single channel processes to the ground state. For example, for the 2^- resonance at 3203 eV, Γ_α is $\lesssim 0.01\ \Gamma_p$ but for the 1^- resonance at 203.4 eV and the 9103-eV resonance, Γ_α is $\gtrsim 7\ \Gamma_p$.

5. Capture γ-Rays

a. Determination of Parity of ^{98}Mo Resonances With Low Energy γ Rays (S. F. Mughabghab,* O. A. Wasson,** G. G. Slaughter and S. Raman)

Low energy γ rays were utilized to determine the spin and parity of neutron resonances. The spins of resonances at 429, 467, 613, 1525, 2178, 2462, 2947, 3293, 5432, 5617 eV were found to be 1/2 while those at 12, 402, 818, 1123, 1922, 2565, 2615, 3264, 3797, 4013, 4574, 4861, 5288 eV are J=3/2, and as a result are formed by p-wave neutrons.

b. Neutron Interactions with ^{100}Mo (Weigmann, Raman, Slaughter, Harvey, Macklin and Halperin)

Neutron capture in the isotopes ^{92}Mo and ^{98}Mo is known to be dominated by the "valence capture" mechanism. Among these observations related to valence capture are strong correlations between reduced neutron widths of p-wave resonances and partial radiation widths to final states with large (d,p) spectroscopic factors such as the ground state. ^{100}Mo was considered another candidate for valence capture, particularly because a strong concentration of p-wave strength occurs between 1 and 2.5 keV neutron energy. Therefore, neutron capture γ-ray spectra were measured in separated resonances of ^{100}Mo. As neutron widths given in

---

[1] H. M. Eiland and G. J. Kirouac, Nucl. Sci. Eng. 53, 1 (1974).
[2] R. D. Werner and D. C. Santry, Nucl. Sci. Eng. 56, 98 (1975).
[3] J. McDonald and N. G. Sjöstrand, submitted to Atomkernenergie.
* Brookhaven National Laboratory, Upton, New York.
** National Bureau of Standards, Washington, D. C.

the literature for the resonances in question are strongly discrepant, a transmission measurement was also performed to redetermine neutron widths. Simultaneously, total capture data, measured earlier with the ORELA neutron capture cross section measurement facility, have been analyzed.

The capture γ-ray spectra were measured with a 40 cm^3 Ge(Li) detector, using a 10.2 m flight path for neutron time-of-flight spectroscopy. Capture γ-ray spectra have been obtained for individual resonances up to about 5 keV neutron energy. The transmission measurement has been performed at an 80 m flight path and resonance analysis is being done up to about 25 keV.

Although analysis of the data is still in progress, two main results may already be given: (1) The neutron widths of the strong p-wave resonances between 1 and 2.5 keV neutron energy are considerably (up to a factor of three) smaller than those given in BNL-325. This reduces the probability that valence capture dominates and may in part explain the second observation; (2) Valence capture does not play a dominant role in these resonances: For instance, a transition to the ground state of ^{101}Mo (spectroscopic factor 0.42) is not observed in 3 of the 4 strongest p-wave resonances.

c. Neutron Capture Gamma-Ray Studies (S. Raman, G. G. Slaughter, R. F. Carlton,* J. C. Wells, Jr.** and D. A. McClure†)

The tin isotopes are well suited to a study of nuclear structure within the framework of the nuclear shell model because the magic number of protons (Z = 50) minimizes the need for considering n-p pairing interactions in theoretical calculations and because the large number of stable isotopes makes it possible to study systematic trends in both experimental and shell model features. The existing experimental data on the odd-A tin isotopes are not as extensive as one might expect on the basis of their theoretical importance. Thermal neutron capture studies have not been widely used due to the extremely small capture cross sections for the heavier even-A tin isotopes. Most experimental studies (especially nucleon transfer studies) are beset with the problem of interference from isotopic impurities. This usually necessitates an extensive study of all tin isotopes before conclusive results may be obtained. Resonance neutron capture offers a powerful technique for studying tin isotopes because interference from unwanted isotopes can be greatly suppressed through the combination of enriched targets and selection of resonances known to be in the nucleus under study. We have, therefore, undertaken a systematic investigation of the level structure of six odd tin isotopes between A = 115 and A = 125.

---

* Middle Tennessee State University, Murfreesboro.
** Tennessee Technological University, Cookeville.
† Georgia Institute of Technology, Atlanta.

Measurements have been completed on all except ^{115}Sn and ^{117}Sn which will be carried out in the near future. In the case of ^{121}Sn, treated here as a typical case, capture γ-rays (18 primary and 32 secondary) from 16 neutron resonances up to 7 keV, obtained with a Ge(Li) detector, have been utilized to determine 20 excited levels in ^{121}Sn. Several new levels have been found. Spin and parity assignments have been made to many of the levels. When the present series of studies has been completed, the resulting level schemes for the tin isotopes are expected to significantly increase our understanding of their energy systematics.

We have also begun (n,γ) measurements in the lead region aimed at obtaining information on absolute γ-ray transition widths and on reaction mechanisms. Measurements have been completed on enriched ^{206}Pb and ^{207}Pb targets. Unlike the case of the tin isotopes, the γ-ray spectra in lead isotopes are strikingly simple composed of less than 5 primary γ-ray transitions. The idea then would be to combine the relative γ-ray intensities obtained with a Ge(Li) detector (or even a NaI detector) with the total γ-ray widths obtained with a total energy detector in order to deduce the partial widths. In this manner, we have been able to determine the E2 radiation widths for the ground state transitions in ^{208}Pb from 2^+ neutron resonances at 3.1, 10.2 and 16.2 keV. The observed strengths represent only $\approx$ 0.3% of the energy-weighted sum-rule strength. By extending the (n,γ) measurements to higher neutron energies, we hope to locate other pieces of the E2 strength as well as the E1 and M1 strengths. Initial results obtained with a large NaI detector up to a neutron energy of 200 keV are very encouraging.

d. Neutron Transmission and Capture Gamma-Ray Measurements of ^{120}Sn + n * (R. F. Carlton,** S. Raman, J. A. Harvey and G. G. Slaughter)

Neutron transmission and neutron capture γ-ray measurements have been performed upon 98.45% enriched samples of ^{120}Sn. The transmission measurements were made at 18-m and 80-m neutron flight paths. Neutrons were detected by a ^{6}Li glass scintillator. Parameters have been obtained for 251 resonances up to 98 keV. From the shapes of the resonances, ℓ-value assignments have been made for 70% of the resonances. Level spacings and strength functions for s- and p-wave neutrons have been obtained. Neutron capture γ rays from 16 resonances, obtained with a Ge(Li) detector, have been utilized to determine the levels in ^{121}Sn. New spin and parity assignments have been made for many of the levels. Four new levels have been found. The neutron separation energy was determined to be 6170.3±2.0 keV. The ^{121}Sn level scheme has been compared with those for ^{117}Sn and ^{119}Sn to investigate systematic behavior.

---

* Submitted for publication in Phys. Rev.

** Middle Tennessee State University, Murfreesboro.

e. Search for Non-Statistical Effects in $^{173}Yb(n,\gamma)\ ^{174}Yb$
(S. F. Mughabghab, A. I. Namenson,* G. G. Slaughter and S. Raman)

Capture γ-ray spectra due to neutron capture in an enriched ^{173}Yb sample were measured with a Ge(Li) detector at ORELA for the purpose of determining the correlation coefficient between partial radiative widths and neutron reduced widths. Spins of resonances were also determined.

6. Actinides

a. $\bar{\nu}_p$ of ^{252}Cf ** (R. R. Spencer)

The most important parameter required in the design of nuclear power systems is $\bar{\nu}$ (the average number of neutrons emitted in fission) for the fissile isotopes and its dependence on the energy of the neutrons inducing fission. Measurements of $\bar{\nu}_p(E)$ are most conveniently carried out as a ratio to $\bar{\nu}_p$ for spontaneous fission of ^{252}Cf. Therefore it is necessary to know the value of this standard to a high accuracy (of the order of 1/4%). At ORNL measurements of $\bar{\nu}_p$ for ^{252}Cf are being pursued using a Gd-poisoned, liquid scintillator tank to detect the neutrons. Preliminary experiments have been carried out using the ORELA neutron source and an NE-213 proton recoil detector to "tag" neutrons scattered into the tank over a range of angles and neutron energies while simultaneously detecting the neutrons from a presently available (undocumented) ^{252}Cf source in a fission chamber. A three-dimensional data acquisition program, necessary for the proton recoil data, was developed by the computer section and successfully used in these experiments. The proton recoil data are being compared to Monte Carlo and Discrete Ordinate Transport (DOT) calculations of the tank absorption efficiency carried out by the neutron transport group at ORNL and to Monte Carlo calculations provided by a similar group at BAPL (Westinghouse). The calculations will be used to extend the measured detection efficiency over the full angular range of the tank and over the energy range necessary to describe the ^{252}Cf neutron spectrum. Support measurements of the tank time-of-absorption of neutrons have been performed in addition to a number of tests of the statistical consistency of the fast counting system. A new, low mass, fission chamber containing documented ^{252}Cf is under construction. A solid state proton recoil detector is being designed for use in the tank efficiency calibration at low neutron energies.

---

* U.S. Naval Research Laboratory, Washington, D. C.
** Relevant to request Nos. 69359, 72103 and 74130.

b. Neutron Energy Dependence of the Number of Prompt Neutrons Emitted in Fission of ^{235}U and ^{239}Pu * (Gwin, Ingle, Spencer, Todd and Weston)

Measurements of the neutron energy dependence of $\bar{\nu}$ the average number of prompt neutrons emitted per fission have been made on ^{235}U and ^{239}Pu over the neutron energy range from about 0.005 eV to a few tenths of an eV. In addition, a set of measurements was made for ^{239}Pu which extended to about 6 MeV. All of these measurements utilize ^{252}Cf as a standard.

Figure 1 shows the measured ratio of $\bar{\nu}$ for ^{239}Pu to that for ^{252}Cf over the neutron energy region from 0.003 to 0.3 eV. The increase in $\bar{\nu}$ for ^{239}Pu, shown in Fig. 1, as the energy decreases has been observed by Weinstein et al.[1] Also shown in Fig. 1 is the measured ratio of $\bar{\nu}$ for ^{235}U to that for ^{252}Cf. At the present level of the analysis, there is no demonstrated neutron energy dependence of $\bar{\nu}$ for ^{235}U over the energy region shown on Fig. 1. The background on the measurements shown in Fig. 1 was less than .05 cts compared to 3.14 cts for ^{252}Cf.

The absolute value of the $\bar{\nu}$ ratios is of importance and the data shown in Fig. 1 for the ratio of $\bar{\nu}$ for ^{239}Pu to that for ^{252}Cf near 0.0253 eV is about 0.6% higher than the value given by Lemmel.[2] The present experimental data have been corrected for the electronic dead time and preliminary calculations show that the correction for differences in the neutron fission spectrum is less than 0.1%. The measured ratio of $\bar{\nu}$ for ^{235}U to that for ^{239}Pu for the neutron energy region about 0.02 eV is within 0.1% of the value of 0.840 given by Lemmel.[2]

Two ^{252}Cf fission sources were used in the course of the present experiments and the effective $\bar{\nu}$ for these two sources differ by 0.25%. It is not knownat this time whether the disagreement results from contamination of either or both samples or whether the discrepancy results from fragment detection differences for the two chambers. The data reported here utilized the ^{252}Cf source which had the same physical g metry and electronics as the ^{235}U and ^{239}Pu samples, and the composition of this ^{252}Cf source is known. Use of the other ^{252}source, in a separately contained chamber, results in a lower value by 0.25% for the present measurements relative to ^{252}Cf.

---

* Relevant to request Nos. 69250, 69253-55, 66050, 66066, 66069 and 66072.

[1] S. Weinstein, R. Reed and R. C. Block, "Neutron Multiplicity Measurements for ^{233}U, ^{235}U and ^{239}Pu Resonance Fission," IAEA-SM-122/113.

[2] H. D. Lemmel, "The Third IAEA Evaluation of the 2200 m/sec and 20°C Maxwellian Neutron Data for ^{233}U, ^{235}U, ^{239}Pu and ^{241}Pu," Proc. Conf. Neutron Cross Sections and Technology, March 3-7, 1975, Washington, D.C.

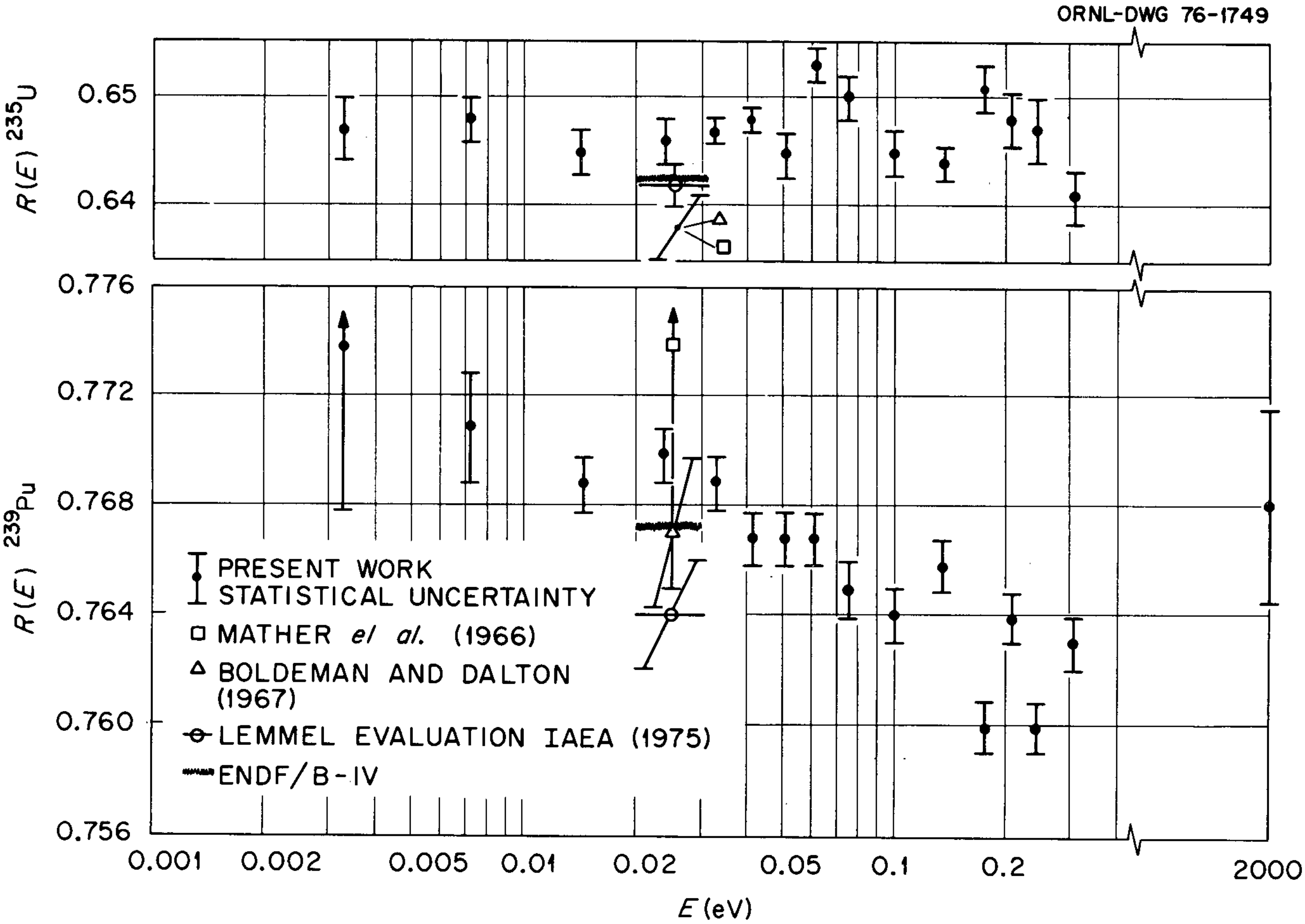

Figure A-1. Energy dependence R(E) the ratio of $\bar{\nu}_p$ for ^{239}Pu and ^{235}U to $\bar{\nu}_p$ for ^{252}Cf below 0.5 eV.

Figure A-2 shows a plot of $\bar{\nu}$ for ^{239}Pu over the neutron energy range from 0 to 8 MeV. Also shown are the results obtained simultaneously for the ^{252}Cf Monitor. These experiments were performed at a 20 m flight path to aid in establishing operating conditions for the main experiments which are scheduled to be performed at an 85 m flight path. It is emphasized that the present results are preliminary.

c. Preliminary Fission Product Energy Release Measurements for Thermal Neutron Fission of ^{235}U * (Dickens, Love, McConnell, Emery and Peelle)

An experimental system to measure time-dependent spectra of beta and gamma rays from fission-product production by thermal neutron fission of ^{235}U is described, and for each component (beta and gamma) the system has been tested with a pilot data-accumulation run. Data reduction techniques are described and test results given. Gamma-ray spectra are compared with calculations using ENDF/B-IV data files. Both beta- and gamma-ray spectra were integrated to give total yields and total energy-release results for times after fission between 3 and 14400 sec. These preliminary integral data are compared with previous measurements and with integral calculations using ENDF/B-IV data files.

Figure A-3 shows $tf_\gamma(t)$ vs time after a fission, where $f_\gamma(t)$ is the gamma-ray energy emission rate (MeV/sec) following fission. Figure A-4 shows a sample photon spectrum compared to calculations based on known fission product yields and decay spectra.

d. Measurement of the Neutron Capture and Fission Cross Sections of ^{239}Pu and ^{235}U, 0.02 eV to 200 keV, the Neutron Capture Cross Sections of ^{197}Au, 10 to 50 keV, and Neutron Fission Cross Sections of ^{233}U, 5 to 200 keV **,† (Gwin, Silver, Ingle and Weaver)

The neutron absorption and fission cross sections for ^{239}Pu and ^{235}U have been measured over the neutron energy range from 0.02 eV to 200 keV. In addition, the neutron capture cross section for ^{197}Au was measured from 10 to 50 keV and the fission cross section of ^{233}U was measured from 0.1 to 100 keV. Normalization of the ^{239}Pu and ^{235}U data was made over the energy region from 0.02 to 0.4 eV to the ENDF/B-III neutron cross sections for these isotopes, Mat 1159 and 1157, respectively. The capture cross section for ^{197}Au was normalized using the saturated resonance method for the 4.9-eV resonance. For ^{233}U fission,

---

* Abstract of ORNL/TM-5273.

** Nucl. Sci. Eng. 59, 79 (1976).

† Relevant to request Nos. 62037, 62039-40, 66043, 67089, 69226, 69241, 69245, 69307, 69439, 69449, 69452, 69467, 72085 and 74207.

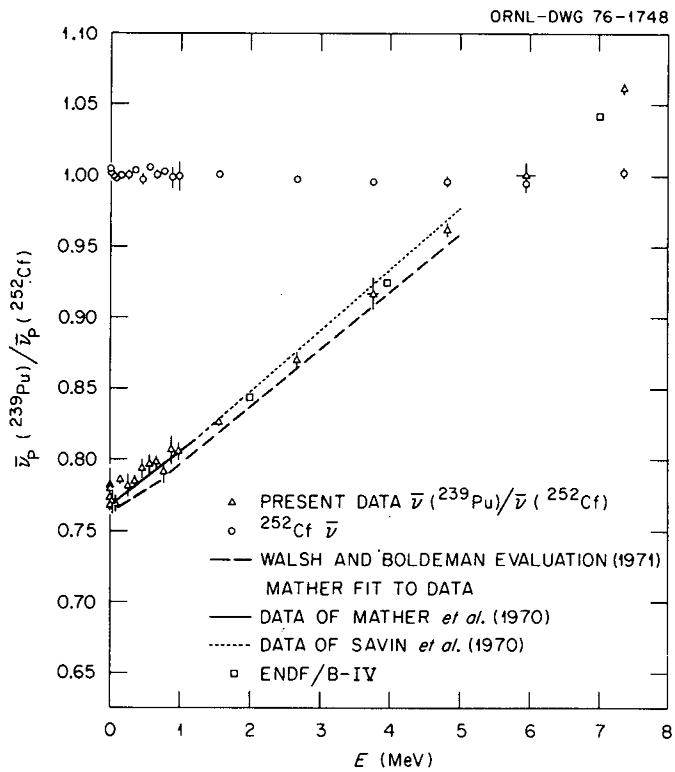

Figure A-2. $\bar{\nu}_p$ ^{239}Pu relative to $\bar{\nu}_p$ for ^{252}Cf vs energy, 0 to 8 MeV.

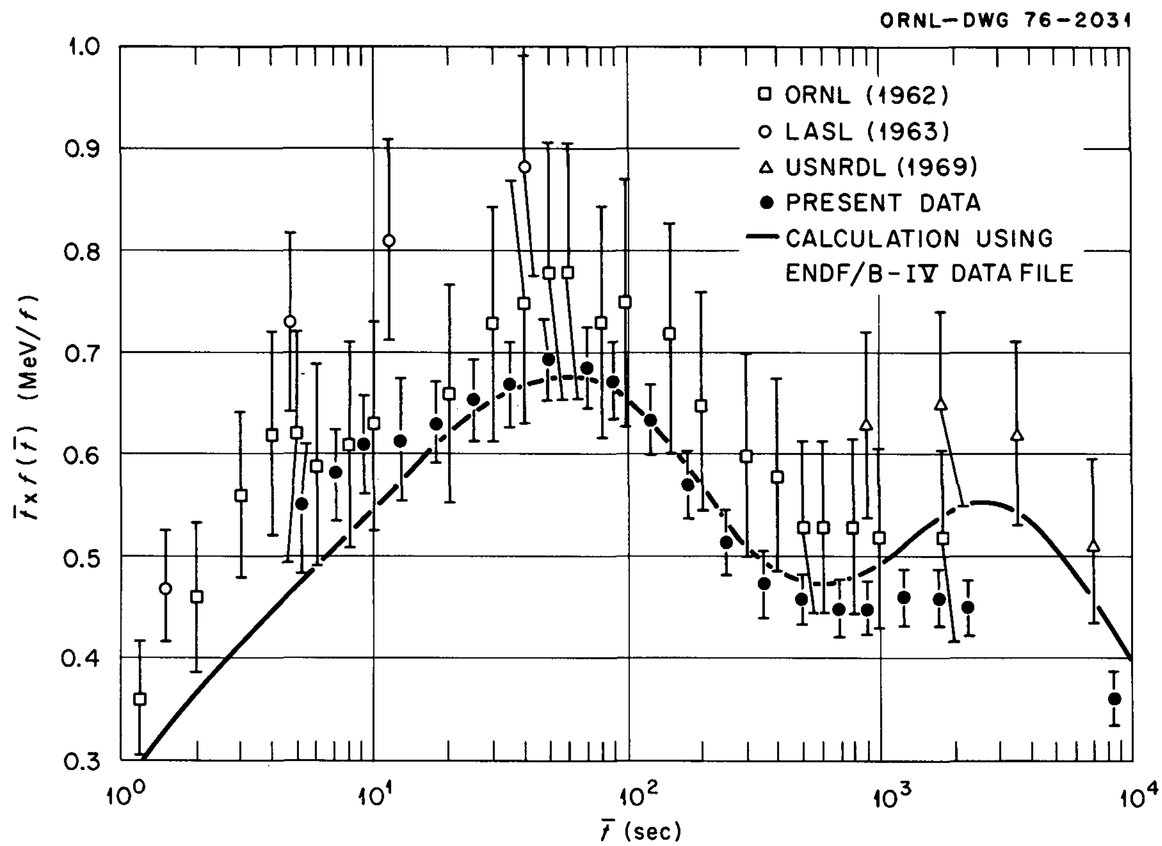

Figure A-3. Photon energy emission rate for thermal-neutron fission of ^{235}U. The open squares are the data of Peelle, et al., open circles represent data of Fisher and Engle, and the open triangles are data of Bunney and Sam. The calculation was carried out by R. Schenter (Hanford) using the RIBD code and the ENDF/B-IV data file.

ORNL-DWG 76-1618

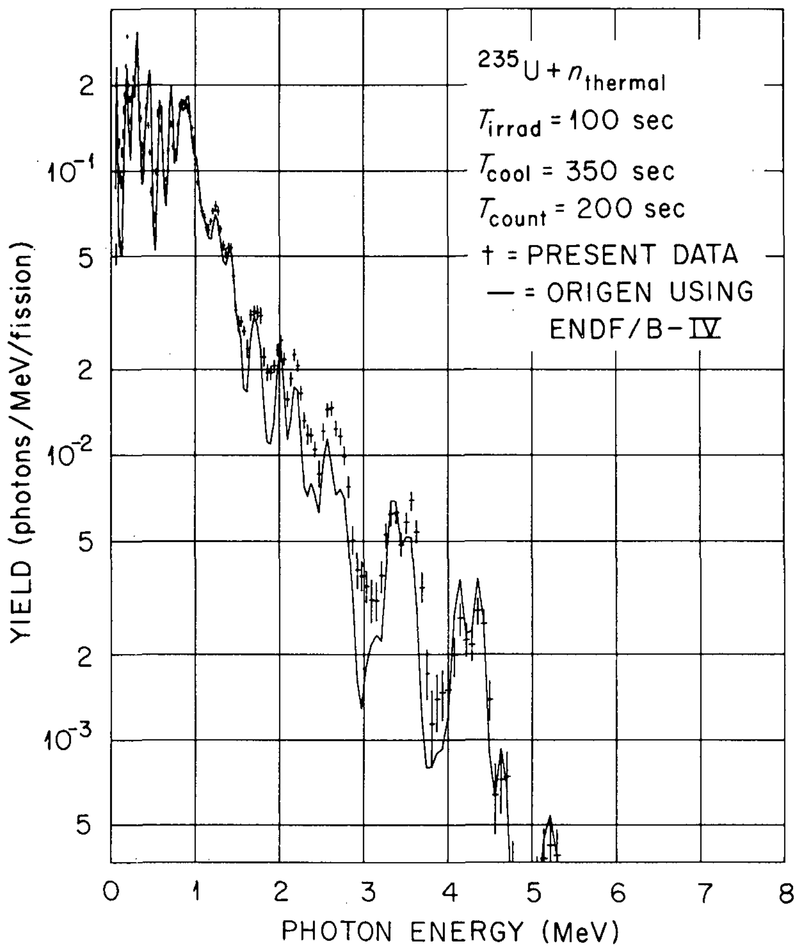

Figure A-4. Comparison of present gamma-ray spectra (crosses) from thermal-neutron fission of ^{235}U with calculated spectra (solid line) using ORIGEN. The irradiation time was 100 sec. The cooling time and counting interval is given in the legend.

the normalization was made using the results of Weston et al. The neutron flux was measured using the $^{10}B(n,\alpha)$ reaction; the energy variation used for this reaction was that given in ENDF/B-III.

The pulsed-neutron beam for these measurements was generated using the Oak Ridge Electron Linear Accelerator. A large liquid scintillator about 40 m from the neutron source was used to detect the prompt gamma-ray cascades resulting from neutron absorption in the sample. The time interval between the burst of neutrons and the detection of the absorption event was used to establish the neutron energy scale. The sample of the fissile isotopes was contained in multiplate (pulse) ionization chambers and those neutron absorption events detected in coincidence with a pulse from the ionization chamber were defined as fission events.

In general for ^{239}Pu and ^{235}U, these experiments indicated lower neutron fission cross sections than contained in ENDF/B-III for energies above 10 keV. The measured values of the ratio α, neutron capture-to-neutron fission, for ^{239}Pu agree within errors with those derived from ENDF/B-III, Mat 1159. For the present measurements, the uncertainty on α for ^{239}Pu is $\sim$11% at 10 keV and increases to $\sim$30% at 100 keV.

The experimental results for the neutron capture cross section for ^{197}Au are $\sim$15% lower than the ENDF/B-III values. The measurements of the ratio of the neutron fission cross section for ^{233}U to that for ^{235}U are generally higher than the ENDF/B-III values by $\sim$5%.

e. Parameters of the Subthreshold Fission Structure in ^{240}Pu *,**
(George F. Auchampaugh† and Lawrence W. Weston)

The neutron subthreshold fission cross section of ^{240}Pu has been measured from 500 eV to 10,000 eV using the Oak Ridge Electron Linear Accelerator neutron facility. A total of 82 fission widths were obtained from area and shape analysis of those resonances which define the class II states at $\cong$ 782 eV, $\cong$ 1405 eV, $\cong$ 1935 eV, and $\cong$ 2700 eV. The average square of the coupling matrix element for the first three class II states is 1.85 ± 1.43 eV^2 (S.D.). The average class II fission width is 2.5 ± 1.0 eV (S.D.). Approximately 22 clusters of class I resonances were observed below 10 keV, which results in a value of 450 ± 50 eV for the average class I level spacing. Assuming parabolic inner and outer barriers, the following barrier parameters were obtained:

$$V_A - B_n / h\omega_A = 0.71 \begin{smallmatrix} +0.21 \\ -0.09 \end{smallmatrix} \quad \text{and} \quad V_B - B_n / h\omega_B = 0.53 \begin{smallmatrix} +0.09 \\ -0.06 \end{smallmatrix}$$

* Abstract of LA-UR 75-1318, LASL; also submitted for publication in Phys. Rev.
** Relevant to request Nos. 67130, 72089-90.
† Los Alamos Scientific Laboratory, Los Alamos, New Mexico 87545.

f. The ^{238}U Subthreshold Neutron Induced Fission Cross Section*,**
(F. C. Difilippo,† Perez, de Saussure, Olsen and Ingle)

Subthreshold fission in the ^{238}U nucleus has been measured by Silbert and Bergen,[1] Block et al.,[2] and Blons.[3] We report here recent high resolution measurements performed at the ORELA facility for neutron energies between 600 eV and 2 MeV. The ORELA was operated at 800 pps with neutron bursts 30 nsec wide and a power of 40 kW on target. The resolution was 2 eV at 600 eV and 500 eV at 100 keV. The detector was a fission chamber divided in two sections. The first section contained 4.5 g of ^{238}U (2 ppm of ^{235}U) and the second section had .65 g of highly enriched ^{235}U.

The time-of-flight spectrum between 600 eV and 100 keV is shown in Fig. A-5. The data were reduced to fission cross sections by a ratio measurement to the ^{235}U count rate and the ENDF/B-IV evaluation of the ^{235}U fission cross section.

The average subthreshold fission cross section between 10 and 100 keV was found to be 44 ± 6 μb, which compares well with the values of 50 ± 15 μb and 41 ± 16 μb obtained by Silbert and Bergen[1] and Block et al.,[2] respectively.

Between 600 eV and 57 keV, 28 subthreshold fission clusters were clearly identified. The fission clusters at 721 eV and 1.2 keV were resolved into five and four resonances, respectively.

The present results have been interpreted on the basis of Strutinsky's[4] double-humped fission barrier and the formalism of Weigmann[5] and Lynn.[6] The average level spacing for the Class II levels was D_{II} = 1.8 keV. This yields E_{II} = 1.8 MeV for the height of the second minimum of the fission barrier above the ground state.

The fission areas for the two resolved clusters are in good agreement with the data of Block et al.[2] A value of 1.4 ± .3 meV was found for the fission width of the 721-eV resonance. For the unresolved fission clusters, the average fission width of the Class II levels was found to be $\langle\Gamma_f^{II}\rangle$ = .8 ± .2 meV. The distribution of the Class II fission widths was a χ^2-distribution consistent with the presence of two open fission channels. From the present value of $\langle\Gamma_f^{II}\rangle$, the Hill-Wheeler formula and

* Abstract of paper to be presented at ANS Meeting, Toronto, June 1976.
** Relevant to request Nos. 67203 and 69416.
† An IAEA fellow from Comission Nacional Energia Atomica, Argentina.
[1] M. B. Silbert and D. W. Bergen, Phys. Rev. C 4, 220 (1971).
[2] R. C. Block, et al., Phys. Rev. Letters, 31 247 (1973).
[3] J. Blons, C. Mazur and D. Paya, Conference on Neutron Cross Sections and Technology, NBS Special Publication 425 (1975) p. 642.
[4] V. M. Strutinsky, Nucl. Phys. A95, 420 (1967).
[5] H. Weigmann, Z. Phys. 214, 7 (1968).
[6] J. E. Lynn, AERE-R5891 (1968).

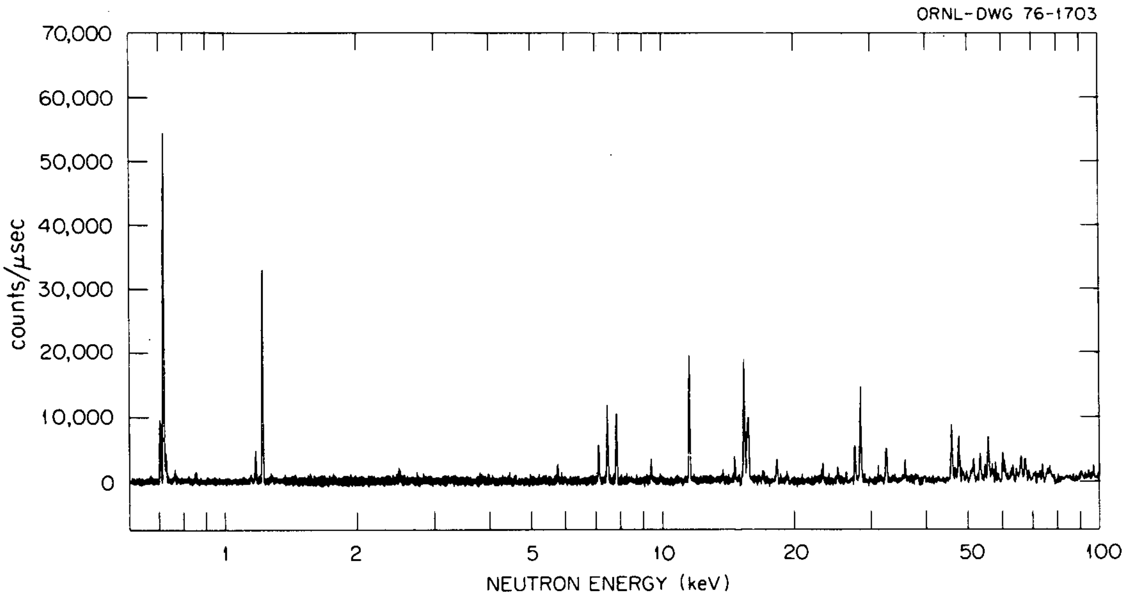
ORNL-DWG 76-1703
70,000
60,000
50,000
40,000
30,000
20,000
10,000
0
counts/μsec
1
2
5
10
20
50
100
NEUTRON ENERGY (keV)

Figure A-5

Specht's[1] systematics for the lifetime of the shape fission isomers, one obtains a value of 6.3 MeV for the height of the second barrier and a value of .7 MeV for the inverse curvature of the second barrier. Both values are in good agreement with the evaluation of Back et al.[2]

From the high energy data and the neutron binding energy in the ^{238}U nucleus, an upper bound of the height of the fission barrier was estimated at 6.3 MeV. This indicates that the height of the first barrier is either equal to or smaller than 6.3 MeV.

h. High Resolution Measurement of the Neutron Induced ^{238}U Subthreshold Fission Cross Section*,** (Difilippo, Perez, de Saussure, Olsen and Ingle)

Subthreshold fission in the ^{238}U nucleus has been measured by Silbert and Bergin,[3] Block et al.,[4] and Blons.[5] We report here recent high resolution measurements performed at the ORELA facility for neutron energies between 600 eV and 1 MeV. The ORELA was operated at 800 pps with neutron bursts 5 nsec wide and a flight path of about 40 m. The detector was a fission chamber divided in ten sections. The first eight sections contained a total of 4.5 g of ^{238}U (2 ppm of ^{235}U) and the last two sections had a total of .65 g of highly enriched ^{235}U.

The experimental resolution varied between 6 to 10 eV in the region between 600 eV and 10 keV, and was 100 eV at 100 keV. The good resolution achieved in this experiment allows, in principle, resolving of the fission clusters below 20 keV, in terms of Class I levels. The analysis of the data up to 100 keV indicates an average level spacing for the Class II levels of about 2 keV.

In a previous measurement,[6] performed on a 20 m flight path at ORELA, a large fission cluster was observed around 150 keV, which was tentatively identified with a vibrational cluster. With the present resolution this cluster split into individual clusters with an average spacing of 4 keV, which is consistent with the expected spacing for a Class II, J = 3/2, family of levels.

---

* Abstract of paper to be presented at 1976 Int. Conf. Interactions of Neutrons with Nuclei, Lowell, Massachusetts, July 6-9, 1976.

** Relevant to request Nos. 67203 and 69416.

[1] H. J. Specht, Physica Scripta 10A (1974).

[2] B. B. Back et al., Third Conf. Physics and Chemistry of Fission, Rochester (1973), p. 8, IAEA-SM-174/201.

[3] M. G. Silvert and D. W. Bergin, Phys. Rev. C 4, 220 (1971).

[4] R. C. Block et al., Phys. Rev. Letters 31, 247 (1973).

[5] J. Blons et al., Proc. Conf. Nuclear Cross Sections and Technology, NBS Special Publication 425 (1975) p. 642.

[6] F. C. Difilippo et al., Trans. Am. Nucl. Soc., Toronto, June 1976, to be published.

In the energy range between 200 keV up to the first fission cross section plateau at 900 keV, several fission clusters have been observed. Their average spacing of around 50 keV is too small for vibrational clusters. One tentatively concludes that we are observing clusters arising from the coupling of rotational bands and particle levels in the second well.

Similar structures were observed in the measurement of the subthreshold fission cross section of ^{232}Th, by Blons,[1] and have been discussed by Michaudon.[2]

h. Neutron Absorption Cross Section of ^{241}Am *,** (L. W. Weston and J. H. Todd)

The ^{241}Am neutron absorption cross section, which is predominantly capture, has been measured from 0.01 eV to 370 keV neutron energy. The Oak Ridge Electron Linear Accelerator (ORELA) was used as the source of pulsed neutrons. Resonance parameters (SLBW) have been derived for the data up to 50 eV. The capture gamma-ray detector used was the "total energy detector," which is a modification of the Moxon-Rae detector. This detector required that the events be weighted by their pulse height in the detector and that the net efficiency of the detector be low. The cross section was normalized at thermal neutron energies (0.02 to 0.03 eV) and the shape of the neutron flux was measured relative to the $^{10}B(n,\alpha)$ cross section up to 2 keV and relative to the $^{6}Li(n,\alpha)$ cross section at higher neutron energies. The results of the measurement indicate a lower cross section ($\sim$ 25%) between 0.3 and 100 eV than has been previously indicated and an appreciably higher cross section (by 100% at 100 keV) from 20 to 370 keV.

Figures A-6 and A-7 give the results compared to ENDF/B-IV.

i. The Neutron Total Cross Section and Resonance Parameters of ^{249}Bk † (J. A. Harvey, R. W. Benjamin,‡ N. W. Hill and S. Raman)

Several years ago a cooperative program was initiated between ORNL and the Savannah River Laboratory to measure the neutron total cross section of the heavy actinides as samples became available. Initially the interest in the cross sections of the transplutonium isotopes was to enable more accurate calculations of ^{252}Cf production. Recently, however,

* Submitted for publication in Nucl. Sci. Eng.
** Relevant to request Nos. 67135-36, 70048, 72099 and 74127.
† Relevant to request No. 67151.
‡ Savannah River Laboratory, Aiken, S.C.
[1] J. Blons et al., Proc. Conf. Nuclear Cross Sections and Technology, NBS Special Publication 425 (1975) p. 642.
[2] A. Michaudon, ibid., p. 202.

ORNL-DWG 72-6741R4

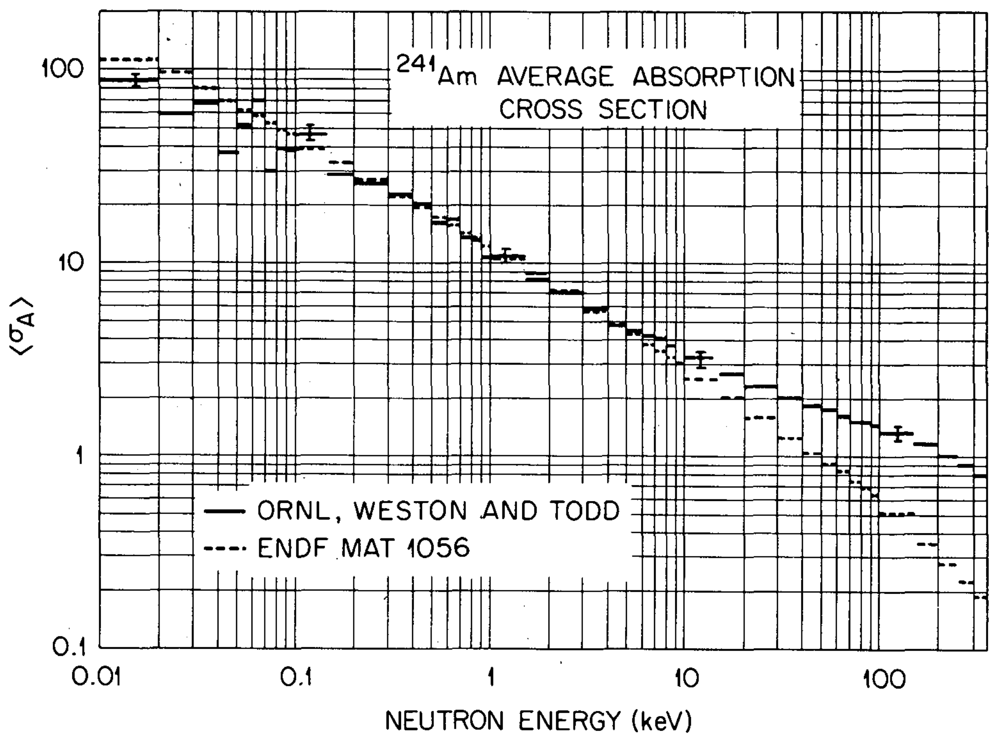

Figure A-6

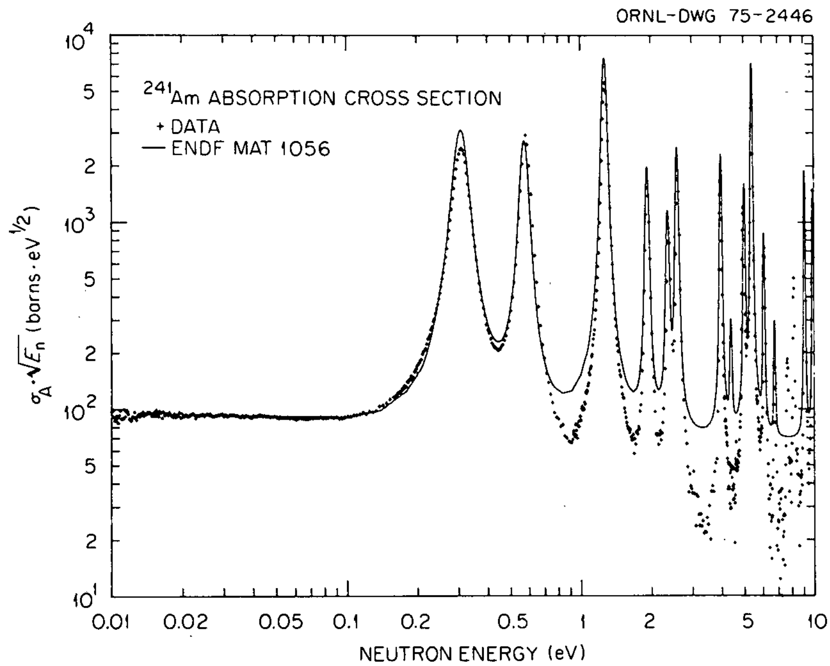

ORNL-DWG 75-2446
^{241}Am ABSORPTION CROSS SECTION
+ DATA
— ENDF MAT 1056
$\sigma_A \cdot \sqrt{E_n}$ (barns · eV$^{1/2}$)
NEUTRON ENERGY (eV)

Figure A-7

the study of the problem of managing radioactive wastes, particularly the long-lived actinides, and the possibility of recycling these long-lived actinides has emphasized the need for additional and better data on many heavy isotopes. Neutron total cross section measurements upon small samples (too small and/or radioactive to permit a direct capture cross section measurement) can readily be interpreted to yield the absorption cross section in the thermal energy range and often up to ∿100 eV.

This year a 6-mg sample of ^{249}Bk became available through the cooperation of John Bigelow of the TRU facility. Two samples were prepared from this material, a "thick" sample containing 5.3 mg (N = 0.00061 atoms/barn) and a "thin" one containing ∿0.8 mg. The sample holders had inside diameters of only 1.6 mm and the neutron beam was collimated to a diameter of 1.3 mm. The samples were cooled with liquid nitrogen to reduce the Doppler broadening which is greater than the neutron energy resolution up to ∿100 eV. Measurements were made upon the samples using a 11.0-cm diameter, 1.3-cm thick ^{6}Li-glass scintillator located at a 17.87 meter flight path. The measurements covered the energy range from 0.005 to ∿10000 eV with an energy resolution of 0.3%.

A total of 47 resonances below ∿130 eV were observed. A large resonance was observed at 0.197 eV which is responsible for most of the thermal absorption cross section, which departs markedly from a 1/v energy dependence. The average level spacing based on the resonances up to 20 eV is 1.1 eV. The large resonance in ^{249}Cf at 0.70 eV was also observed even though there was only ∿2% ^{249}Cf in the sample (i.e., ∿10 μgm) at the time of measurement. Additional measurements will be made after about half of the 330-day ^{249}Bk has decayed into ^{249}Cf in order to obtain parameters for the resonances in ^{249}Cf as well as its thermal absorption cross section. These measurements will be combined with the fission cross section measurements of Dabbs et al.[1] to obtain a complete set of parameters of the low energy resonances of ^{249}Cf.

j. Fission Cross Section Measurements on ^{245}Cm and ^{243}Cm *,**
(Dabbs, Hill, Bemis and Raman)

Fission cross-section determinations are in progress with small ultra-pure and highly alpha active actinide samples using a new type of hemispherical plate ionization chamber and fast current sensitive amplifiers.[2] 10 μg samples are adequate for such measurement at a 10 m flight path at ORELA, using irradiations of several hundred hours and power levels above 40 kW. The basic resolution is about 4 ns/m. In the case

* Abstract of paper to be presented at 1976 Int. Conf. Interactions of Neutrons with Nuclei, Lowell, Massachusetts, July 6-9, 1976.

** Relevant to request No. 67145.

1 "Neutron-Induced Fission of ^{249}Cf," J. W. Dabbs et al., Physics Division Annual Report, ORNL-4937, May 1974, p. 181.

2 J. W. T. Dabbs et al., Proc. Conf. Nuclear Cross Sections and Technology, NBS Special Publication 425 (1975) p. 81.

of ^{243}Cm a clear determination of a spontaneous fission rate of 0.01 counts/sec in the presence of an alpha particle emission rate of 10^7/sec has been demonstrated, with >95% efficiency for the fission counts. Preliminary results showing a number of new resonances at low energies will be presented. The importance of such measurements to the nuclear waste question will be discussed briefly.

k. Measurement of Neutron Transmissions from 0.52 eV to 4.0 keV Through Seven Samples of ^{238}U at 40 m *,** (Olsen, de Saussure, Perez, Silver, Ingle and Weaver)

Neutron transmission through 1.5-, 5-, 10-, 30-, 100-, 425-, and 1425-mil samples of depleted ^{238}U were measured from 0.52 eV to 4.0 keV using the ORELA pulsed electron linac neutron source and time-of-flight technique with a 1-mm ^6Li-glass detector with a flight path of 40 m. The measurements are tabulated and compared with transmission calculated from the ENDF/B-IV total cross section. In addition, the 1425-mil transmission from 50 to 300 eV is compared with transmissions calculated by using multilevel formalisms, and some neutron widths are extracted with area analysis and compared with those from previous measurements.

ℓ. Resonance Parameters of the 6.67-, 20.9-, and 36.8-eV Levels in ^{238}U †,** (Olsen, de Saussure, Perez and Difilippo)

The ENDF/B-IV ^{238}U cross sections (NAT-1262) yield an effective capture resonance integral in strongly self-shielded situations which is too high.[1] This situation suggests that the ENDF/B capture widths for the first few s-wave levels may be too large. Recent ORELA measurements[2] of transmission through ^{238}U have been analyzed with a multilevel formula to determine the parameters of the 6.67-, 20.9-, and 36.8-eV levels. These three levels provide 86% of the infinitely dilute capture resonance integral.

---

* Abstract of ORNL/TM-5256 (March 1976).

** Relevant to request Nos. 69286-89.

† Abstract of paper to be presented at ANS Meeting, Toronto, June 1976.

[1] An extended discussion on this problem is contained in the various papers of Seminar on ^{238}U Resonance Capture, Brookhaven National Laboratory, BNL-NCS-50451, ed., S. Pearlstein, 1975.

[2] D. K. Olsen, G. de Saussure, E. G. Silver, and R. B. Perez, Seminar on ^{238}U Resonance Capture, Brookhaven National Laboratory, BNL-NCS-50451, p. 95, ed., S. Pearlstein, 1975; D. K. Olsen, G. de Saussure, E. G. Silver, and R. B. Perez, Trans. Am. Nucl. Soc. 21, 505 (1975); and D. K. Olsen, G. de Saussure, R. B. Perez, E. G. Silver, R. W. Ingle, and H. Weaver, "Measurement of Neutron Transmission from 0.52 eV to 4.0 keV Through Seven Samples of ^{238}U at 40 m," ORNL/TM-5256, January 1976.

The data consist of transmissions through 3.62-, 1.08-, 0.254-, 0.0762-, 0.0254-, 0.0127-, and 0.0036-cm metal samples. These seven transmissions were simultaneously analyzed over many resonances with the least-squares computer code SIOB[1] which contains Gaussian resolution and Doppler broadening and employs a multilevel Breit-Wigner cross section formalism[2] with "picket fences" terms to account for distant levels, both bound and unbound. In addition to the resonance parameters, the code allows the effective radius, normalizations, backgrounds, and picket fence terms to be fitted parameters.

An effective radius of .949 x 10^{-12} cm was obtained, independent of the details of the bound levels, by fitting the transmission data from 55 to 500 eV. The cross section of the energy region of interest from 0.52 to 55.0 eV is sensitive to the bound levels. Both the same effective radius of .948 x 10^{-12} cm and a minimum in $\chi^2$was obtained for this lowest energy region with a picket fence of bound levels extending from -80 eV to - ∞. Fig. A-8 shows this fit.

Table A-1 compares the neutron and radiation widths from this fit with those contained in ENDF/B-IV. The errors immediately following these widths are the statistical standard deviations from the fit. The numbers in parentheses are deviations corresponding to the uncertainty in the effective Doppler temperature, i.e. 300° ± 5°K. The statistical standard deviations for the widths are small. However, the widths depend strongly on the cross-section model and parameters, and the statistical errors contain no estimate of the systematic errors in the data. The uncertainties associated with systematic errors in the data are estimated to be an order of magnitude larger than the statistical errors quoted in Table A-1. It is concluded that radiation widths smaller than those contained in ENDF/B-IV are required to reproduce these transmission data. These smaller capture widths would significantly reduce the discrepancies between calculated and measured capture resonance integrals.[3]

TABLE A-1. Neutron and Radiation Widths

	LEAST-SQUARES FIT		ENDF/B-IV	
E (eV)	Γ_n(meV)	Γ_γ(meV)	Γ_n(meV)	Γ_γ(meV)
6.67	1.482 ± .002 (± .006)	22.96 ± .04 (± .02)	1.50	25.6
20.9	10.19 ± .01 (± .03)	22.46 ± .04 (± .02)	8.80	26.8
36.8	33.85 ± .03 (± .05)	22.29 ± .03 (± .02)	31.1	26.0

[1] G. de Saussure, D. K. Olsen, and R. B. Perez, to be published.
[2] H. A. Bethe, Rev. Mod. Phys. 9, 69 (1937); also H. A. Bethe and G. Placzek, Phys. Rev. 51, 450 (1939).
[3] M. R. Bhat, Seminar on ^{238}U capture, Brookhaven National Laboratory, BNL-NCS-50451, p. 244, ed., S. Pearlstein, 1975.

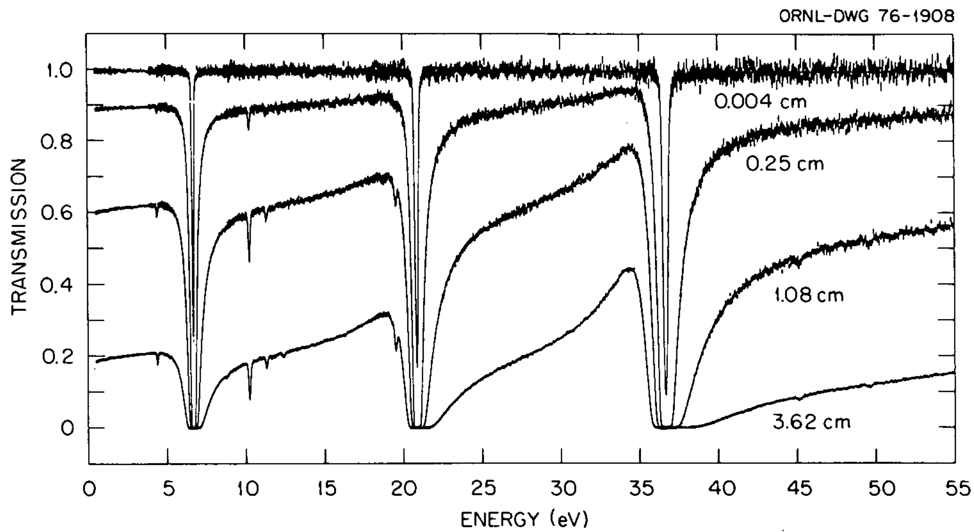

Figure A-8. Simultaneous least-squares fit with the multilevel computer code, SIOB, to neutron transmission from 0.52 to 55.0 eV through 3.62-, 1.08-, 0.254-, 0.0762-, 0.0254-, 0.0127-, and 0.0035-cm samples of ^{238}U. For clarity the fit to the data from the 0.0762-, 0.0254-, and 0.0127-cm samples is not shown.

m. Three papers were presented at the IAEA Advisory Group Meeting on Transactinium Isotope Nuclear Data at Karlsruhe, 1975, and will be published in the proceedings:

General Survey of Applications Which Require Actinide Nuclear Data (S. Raman)

This review paper discussed the actinide waste problem, the buildup of toxic isotopes in the fuel, the neutron activity associated with irradiated fuel, the ^{252}Cf buildup problem, and the production of radioisotope power sources as broad areas that require actinide cross-section data. Decay data enter into the area of radiological safety and health physics. This paper also discussed a few cross-section measurements in progress at the Oak Ridge Electron Linear Accelerator. The availability of actinide samples through the Transuranium Program at Oak Ridge is discussed in considerable detail. The present data status with respect to the various applications is reviewed along with recommendations for improving the data base.

Some Activities in the United States Concerning the Physics Aspects of Actinide Waste Recycling (S. Raman)

This review paper briefly discussed the reactor types being considered in the United States for the purpose of actinide waste recycling. The reactor types include thermal reactors operating on the 3.3% ^{235}U-^{232}U and the ^{233}U-^{232}Th fuel cycles, liquid metal fast breeder reactors, reactors fueled entirely by actinide wastes, gaseous fuel reactors and fusion reactors. This paper also discusses cross section measurements in progress or planned toward providing basic data for testing the recycle concept.

Neutron Capture Cross Sections of the Actinides (L. W. Weston)

7. Integral Measurements

Measurement of Secondary Neutrons and Gamma Rays Produced by Neutron Interactions with Nitrogen and Oxygen over the Incident Energy Range 1 to 20 MeV* (G. L. Morgan)

The spectra of secondary neutrons and gamma rays produced by neutron interaction in thick samples ($\approx$ 1 mean free path) of liquid nitrogen and liquid oxygen have been measured as a function of the incident neutron energy over the range 1 to 20 MeV. Data were taken for angles of 30°, 55°, 90°, and 125°. A linac (ORELA) was used as a neutron source with a 47-m flight path. Incident energy was determined by time-of-flight,

* Abstract of ORNL-TM-5023 (October 1975).

while secondary spectra were determined by pulse-height unfolding techniques. The results of the measurements are presented in forms suitable for comparison to calculations based on the evaluated data files.

b. Measurement of Secondary Neutrons and Gamma Rays Produced by Neutron Interactions in Aluminum over the Incident Energy Range 1 to 20 MeV * (G. L. Morgan)

The spectra of secondary neutrons and gamma rays produced by neutron interaction in a thin sample ($\approx$ 1/6 mean free path) of aluminum have been measured as a function of the incident neutron energy over the range 1 to 20 MeV. Data were taken at an angle of 125°. A linac (ORELA) was used as a neutron source with a 47-m flight path. Incident energy was determined by time-of-flight, while secondary spectra were determined by pulse-height unfolding techniques. The results of the measurements are presented in forms suitable for comparison to calculations based on the evaluated data files.

c. Measurement of Secondary Neutrons and Gamma Rays Produced by Neutron Interactions in Silicon Dioxide over the Incident Energy Range 1 to 20 MeV ** (G. L. Morgan)

The spectra of secondary neutrons and gamma rays produced by neutron interactions in a thick ($\approx$ 1 mean free path) sample of silicon dioxide have been measured as a function of the incident neutron energy over the range 1 to 20 MeV. Data were taken at an angle of 90°. A linac (ORELA) was used as a neutron source with a 47-m flight path. Incident energy was determined by time-of-flight, while secondary spectra were determined by pulse-height unfolding techniques. The results of the measurement are presented in forms suitable for comparison to calculations based on the evaluated neutron data files.

d. Measurement of Secondary Neutrons and Gamma Rays Produced by Neutron Bombardment of Water over the Incident Energy Range 1 to 20 MeV † (G. L. Morgan)

The spectra of secondary neutrons and gamma rays produced by neutron bombardment of a thick ($\approx$ 1 mean free path) sample of water have been measured as a function of the incident neutron energy over the range 1 to 20 MeV. Data were taken for angles of 90° and 140°. A linac (ORELA) was used as a neutron source with a 47-m flight path. Incident energy was determined by time-of-flight, while secondary spectra were determined by pulse-height unfolding techniques. The results of the measurements are presented in forms suitable for comparison to calculations based on the evaluated data files.

* Abstract of ORNL-TM-5072 (November 1975).
** Abstract of ORNL-TM-5024 (September 1975).
† Abstract of ORNL-TM-5018 (August 1975).

8. Experimental Techniques

a. Monte Carlo Calculations of Multiple-Pulse Pileup (J.W.T. Dabbs)

In fission cross-section measurements, it is often desired to make measurements in the presence of an intense alpha particle background. It is obvious that with sufficiently fast electronic equipment the alpha pulse pileup can be reduced to unimportance but quantitative knowledge of the problem is needed to choose the allowable amounts of material with particular ionization chambers, gas scintillator systems, or segmented ionization chambers.

A new method for Monte Carlo calculations, which is applicable to pulse pileup to any desired multiplicity of pileup, has been developed and used with a minicomputer for pileups with as many as 20 pulses. Previously, closed-form calculations have been presented only for four pulses, except in the trivial case of square pulses. The present calculations are easily adaptable to unusual geometries such as in the hemispherical-plate fission chamber work describer elsewhere in this report.

The method consists of setting up a table of 32 values (nominally one value per nanosecond) for the pulse shape in question. A double interval in time, 64 units long, is established. Then, for each multiplicity k (from 1 to some upper limit, say, 20) of pulses in the interval, 2k such pulses are distributed, to begin randomly in time over the double interval, and their amplitudes are added in each unit of the second half of the double interval, thus generating 32 values of pulse height for that k. After 250 repetitions of this process for each k value, one has an 8000-member height distribution for that k. The pulse-height distributions are then weighted by the Poisson distribution factor, p_k, for the particular counting rate involved and are summed to give the final pulse-height distribution. Comparison with observed values in a practical case has established the validity of the calculation. Such calculations have been used in designing three experiments so far.

b. An Experimental System for Providing Data to Test Evaluated Secondary Neutron and Gamma-Ray-Production Cross Sections over the Incident Neutron Energy Range from 1 to 20 MeV * (G. L. Morgan, T. A. Love and F. G. Perey)

A system is described which allows simultaneous measurement of secondary neutron and gamma-ray-production cross sections. Measurements can be made rapidly over wide energy ranges. An electron linac is used as a neutron source. Annular scattering samples located 47 m from the neutron source are viewed by a NE-213 scintillation counter. Multiparameter data acquisition is done by on-line computer for incident neutron energies from 1 to 20 MeV.

* Nucl. Intrum. Methods 128, 125 (1975).

B. DATA ANALYSES

Most of the data procurement activities reported in the previous section were mainly motivated by a need in some application. Much work remains to be done after some data have been obtained before they become useful to applied users. In this section we report on some of these activities bearing directly upon this work: theoretical calculations, compilations, evaluations, validation of evaluated data, and sensitivity studies aimed at establishing adequacy of the data.

1. Theoretical Calculations

a. Calculated Nucleon Spectra at Several Angles from 192-, 500-, 700-, and 900-MeV Carbon-12 on Iron-56 * (H. W. Bertini, R. T. Santoro and O. W. Hermann)

Neutron spectra were calculated as a function of angle between 0 and 110° for ^{12}C on ^{56}Fe at 192, 500, 700, and 900 MeV. Proton spectra were calculated for the same angular range but for only 192-MeV ^{12}C on ^{56}Fe. The most significant property of these spectra is that there is an appreciable number of neutrons emitted with energies greater than the incident energy per nucleon at all angles investiaged.

b. Calculated Neutron Cross Sections for Cu and Nb up to 32 MeV for Neutron Damage Analysis** (C. Y. Fu and F. G. Perey)

Cross sections for neutron interaction with Cu and Nb, with emphasis on spectra of light particles from binary reactions, are calculated for neutron energies from 4 to 32 MeV for estimating recoil probability densities for the analysis of damage experiments with a Be(d,n) neutron source. Nuclear model parameters were adjusted to reproduce the available cross-section data around 14 MeV. Helium production cross sections were also calculated for ^{63}Cu for neutrons below 20 MeV, as an illustration of the Hauser-Feshbach method for calculating tertiary reaction cross sections.

---

* Abstract of ORNL/TM-5161 (February 1976); also submitted for publication in Phys. Rev. C.

** Submitted for publication in Journal of Nuclear Materials.

2. ENDF/B Related Evaluations

a. An Evaluation of Neutron and Gamma-Ray-Production Cross-Section Data for Lead* (C. Y. Fu and F. G. Perey)

A survey was made of the available information on neutron and gamma-ray-production cross-section measurements of lead. From these and from relevant nuclear-structure information on the Pb isotopes, we prepared recommended neutron cross-section data sets for lead covering the neutron energy range from 0.00001 eV to 20.0 MeV. The cross sections are derived from experimental results available to February 1972 and from calculations based on optical-model, DWBA, and Hauser-Feshbach theories. Comparisons which show good agreement between theoretical and experimental values are displayed in a number of graphs. Also presented graphically are smoothed total cross sections, Legendre coefficients for angular distributions, and a representative energy distribution of gamma rays from resonance capture.

b. Consistent Calculations of Neutron and Gamma-Ray-Production Cross Sections for Ca-40 from 1 to 20 MeV (C. Y. Fu)

Cross sections of neutron interaction with ^{40}Ca and the subsequent production of gamma rays are calculated and compared with experiments. Various nuclear models are judiciously applied for the calculation. The Hauser-Feshbach theory for binary reactions is extended to include tertiary reactions, which are important for ^{40}Ca from 10 to 20 MeV. Continuum-level spins and parities are included in the gamma-ray production calculation to conserve angular momentum. An extensive measurement of gamma-ray production cross sections, available after all model parameters were fixed, is used to test the predictability of the models, particularly in the high energy range, where tertiary reactions contribute significantly.

c. Note on the ENDF/B-IV Representation of the ^{238}U Total Cross Section in the Resolved Resonance Energy Region** (de Saussure Olsen and Perez)

The ENDF/B-IV prescription fails to represent correctly the ^{238}U total (and scattering) cross section between the levels of the resolved range. We show how this representation can be improved by properly accounting for the contribution of levels outside the resolved region to the cross section at energies inside the resolved region, and by substituting the more precise multilevel Breit-Wigner formula for the presently used single level formula. We illustrate the importance of computing accurately the minima in the total cross section by comparing values of the self-shielded capture resonance integral computed with ENDF/B-IV and with a more accurate cross-section model.

---

* Atomic Data and Nuclear Data Tables 16, 409 (1975).
** Submitted for publication in Nuclear Science and Engineering.

d. SUR, A Program to Generate Error Covariance Files* (F. C. Difilippo)

Covariance matrices were calculated for the ^{238}U, ^{241}Pu, and ^{239}Pu fission cross sections and for the ^{238}U, ^{240}Pu, ^{241}Pu, and ^{239}Pu capture cross sections. A computer program was written which uses the evaluated ENDF/B data files and the measured or evaluated (from other evaluations) cross sections for the calculation of the uncertainty files. An effort has been made to make the output of the program consistent with the ENDF/B error files format. A user's manual for the present code and references utilized in the covariance matrix calculations are given.

e. The Energy Dependence of the Neutron Absorption and Fission Cross Sections of ^{235}U and ^{239}Pu Below 1 eV and the Wescott g Factors** (R. Gwin)

The energy dependence of recently published[1] neutron absorption and fission cross sections [$\sigma_a(E)$ and $\sigma_f(E)$] of ^{235}U and ^{239}Pu has been reexamined. The published data[1] are normalized to ENDF/B-III values of σ_f and σ_a. This paper compares the data of Ref. 1 to the recently released ENDF/B-IV values σ_f and σ_a for ^{235}U and ^{239}Pu. Wescott g factors are calculated for fission (g_f) and for absorption (g_a).

f. A New Perturbation Formalism for the Complex Widths and Poles of the Transition T-Matrix† (Perez, de Saussure and Olsen)

The T-matrix of nuclear reaction theory can be written in the form

$$T_{cc'} = i \sum_{v} \frac{g_{vc} g_{vc'}}{\varepsilon_v - E} \quad ,$$

where g_{vc} is the complex width for channel c and ε_v the complex poles of the transition T-matrix. We have shown that, in terms of a parameter τ ($0 < \tau \leq 1$), the complex widths and poles of the T-matrix are obtained via the solution of two coupled Volterra equations.

In the present formalism the interaction contains both changes in the hamiltonian operator and the boundary conditions. The convergence of the method depends on the ratio of the elements of the interaction matrix

* Abstract of ORNL/TM-5223 (March 1976).

** Submitted for publication in Nuclear Science and Engineering.

† Abstract of paper to be presented at 1976 Int. Conf. Interactions of Neutrons with Nuclei, Lowell, Massachusetts, July 6-9, 1976.

[1] R. Gwin, et al., "Measurement of the Neutron Capture and Fission Cross Sections of ^{239}Pu and ^{235}U, 0.02 eV to 200 keV, the Neutron Capture Cross Sections of ^{197}Au, 10 to 50 keV, and Neutron Fission Cross Sections of ^{235}U, 5 to 200 keV," Nucl. Sci. Eng. 59, 79 (1976).

to the spacing of the complex poles rather than on the same ratio expressed in terms of the spacing of the R-matrix poles on the real axis, as it is the case in the usual perturbation approach.

The present method has been applied to neutron cross section calculations in cases of large level interference and to the study of intermediate structure phenomena.

3. Validation of ENDF/B Evaluations Through Integral Measurements

a. Critical Experiments and the 2200 m/sec Neutron Parameters*
(R. Gwin)

The use of critical volumes of aqueous homogeneous solutions of uranium in defining the 2200-m/sec neutron parameters for ENDF/B has been examined. The parameters for ^{233}U and ^{235}U are constrained by relating $(\overline{\eta} - 1)\overline{\sigma}_{ax}$ to the constant K obtained from the analysis of the critical systems. K is directly proportional to the hydrogen capture cross section at 2200 m/sec. This paper suggests that the capture cross section of hydrogen be removed from K and that a new constant K/σ_{aH} be defined by the critical systems. This new constant is the hydrogen to uranium ratio for an infinite critical system populated with neutrons having a Maxwellian energy distribution.

b. Analysis of Neutron Scattering and Gamma-Ray Production Integral Experiments on Nitrogen for Neutron Energies from 1 to 15 MeV **
(S. N. Cramer and E. M. Oblow)

Two integral experiments of neutron scattering and gamma-ray production from nitrogen samples performed at Intelcom Radiation Technology and Oak Ridge National Laboratory were analyzed with Monte Carlo calculations. The experimental results include angular-dependent NE-213 detector count rates for both scattered neutrons and gamma-ray production from a spherical dewar of liquid nitrogen pulsed with a neutron beam with energies from 1 to 20 MeV. Additional results were reported in the ORNL experiments for unfolded scattered neutron and gamma-ray production spectra as a function of detector angle in broad incident neutron energy bins. Multigroup Monte Carlo calculations were made to analyze all the reported results. Conclusions were drawn about the status of the ENDF/B-IV nitrogen cross-section data file from the comparison of calculated and experimental results.

---

* Abstract of ORNL-TM-4550 (January 1975); paper submitted for publication in Nuclear Science and Engineering.
** Abstract of ORNL/TM-5220.

c. Analysis of Neutron Scattering and Gamma-Ray Production Integral Experiments on Carbon for Neutron Energies from 1 to 14 MeV *

The results of two integral experimenta on carbon, performed at ORNL and IRT, were compared with Monte Carlo calculations to test evaluated carbon neutron and gamma-ray production data sets. In both experiments NE-213 detectors were used to measure the angular dependence of neutron scattering and gamma-ray production from thick (1 mfp) carbon sample in the energy range from 0.5 to 20 MeV. Additional measurements from the ORNL experiment also provided angular-dependent, energy distributions of the scattered neutrons. Multigroup Monte Carlo calculations modeling the two experimental arrangements were made to compare with the measured data. Both ENDF/B-III and ENDF/B-IV carbon data were used in the computations. The results indicate that such experiments are adequate for testing processed neutron scattering and gamma-ray production data (both integral and double differential) to within 10-20% over a wide range of incident neutron energies (1 to 15 MeV). Also, on the whole, calculations with the carbon ENDF/B-IV data compared favorably with the measured results over the energy range tested. The only notable exceptions were the disagreements in the neutron result comparisons above 9 MeV which were attributed for the most part to errors in the evaluated $C(n,n')3\alpha$ and elastic angular distribution cross sections in this range.

d. Comparison of Measurements and Calculations for ORNL Integral Neutron Scattering Experiment for Iron** (S. N. Cramer and E. M. Oblow)

Calculations of an integral neutron scattering experiment on an iron sample have been performed using the ENDF/B-IV data set MAT 1192 (DNA MAT 4192). The neutron source incident on the sample ranged from 20 MeV to 1 MeV. Comparisons between experimental and calculated results are given as neutron count rates and neutron secondary energy spectra.

e. Experiment on Secondary Gamma-Ray Production Cross Sections Averaged Over a Fast-Neutron Spectrum for Each of 13 Different Elements Plus a Stainless Steel† (R. E. Maerker)

The experimental and calculational details for a CSEWG integral data testing shielding experiment are presented. This particular experiment measured the secondary gamma-ray production cross sections averaged over a fast-neutron spectrum for iron, oxygen, sodium, aluminum, copper, titanium, calcium, potassium, silicon, nickel, zinc, barium, sulfur, and a type 321 stainless steel. The gamma-ray production cross sections were binned into $\sim$ 0.5-MeV wide gamma-ray energy intervals.

---

* Abstract of paper submitted for publication in Nucl. Sci. Eng.

** Abstract of paper to be presented at ANS Meeting, June 1976, Toronto, Canada.

† Abstract of ORNL-TM-5204, ENDF-228 (January 1976).

f. Neutron Total Cross Section Checks for Iron, Chromium, Nickel, Stainless Steel, Sodium and Carbon* (R. E. Maerker and F. J. Muckenthaler)

Utilizing detectors in good geometry at the Tower Shielding Facility behind various thicknesses of iron, chromium, and nickel provided experimental data for checking neutron total cross sections of these elements. In addition, data behind a type 304L stainless steel and carbon were also obtained, as were some data behind sodium. These data were then compared with data from the total cross section files of both versions III and IV of ENDF/B. Results of these comparisons indicate version IV to be generally superior to version III, but further improvement in version IV is possible for all elements tested. In particular, minima in the total cross sections for both chromium and nickel are apparently still poorly represented in version IV for all energies above 10 keV.

4. Sensitivity Studies

a. The Frequency of Occurrence of Various Nuclear Reactions When Fast Neutrons ($\lesssim$ 50 MeV) Pass Through Tissue-Equivalent Material** (R. G. Alsmiller, Jr. and J. Barish)

Calculated results are presented for the frequency with which various partial nuclear-reaction cross sections are utilized when fast neutrons ($\lesssim$ 50 MeV) are transported through a tissue-equivalent phantom to obtain an indication of which cross sections are of most importance for radiotherapy applications and are therefore in need of experimental verification.

b. Survey of Shielding Sensitivity Analysis Development and Applications Program at ORNL† (E. M. Oblow)

The cross-section sensitivity analysis program at ORNL is reviewed with emphasis on present computer code capabilities and past successful applications in the radiation shielding area. The FORSS sensitivity code system is discussed in regard to objectives, methodology, and code specifications. Examples of past shielding applications of FORSS emphasize the success of fine energy grid sensitivity studies and group structure selection, the use of evaluated error files in problem uncertainty estimation, two-dimensional shield sensitivity analysis and integral experiment design for fast reactors, data studies for the LMFBR program

---

* Abstract of ORNL-5013 (January 1976).

** Abstract of ORNL-TM-4970.

† Abstract of ORNL-TM-5176; paper presented at the Specialists' Meeting on Sensitivity Studies and Shielding Benchmarks, IECD - Paris, France, October 7-10, 1975.

related to sodium and iron evaluations, and iron data problems in CTR shield design. Conclusions are drawn about the adquacy of present ENDF/B data files for sodium and iron and the general applicability of sensitivity studies in future shield design and analysis.

c. Preliminary Cross-Section Sensitivity Analysis for an Air-Over-Ground Environment* (J. V. Pace, III and D. E. Bartine)

Two-dimensional sensitivity calculations have been made for an air-over-ground geometry to determine the effect of air and ground cross-section perturbations on the total neutron and gamma-ray dose near the air/ground interface and 415 meters above the ground. ENDF/B 22 neutron and 18 gamma group Version IV cross sections were used in all computations.

d. Cross-Section Sensitivity of the D-T Fusion Probability and the D-T and T-T Reaction Rates** (R. T. Santoro and J. Barish)

The cross-section sensitivity of the fusion probability has been calculated for various conditions of incident deuteron energy and plasma electron temperature. The fusion probability is most sensitive to the D-T cross section at the higher energies ($\gtrsim$ 50 keV), and, based on the reported errors in the cross section, the errors in the calculated fusion probabilities should be $\lesssim$ 10%.

The cross-section sensitivities of the D-T reaction rate in a D-T plasma and the T-T reaction rate in a tritium plasma have also been calculated for various assumed values of the plasma ion temperature.

e. Uncertainties in Calculated Heating and Radiation Damage in the Toroidal Field Coil of a Tokamak Experimental Power Reactor due to Neutron Cross-Section Errors† (Alsmiller, Barish and Weisbin)

Calculated results are presented of the uncertainties in the neutron scalar flux, the energy deposition per unit volume, and the displacements per atom in the toroidal field coil of a tokamak experimental power reactor due to neutron cross-section errors in iron and carbon which are major constituents of the blanket-shield-coil configuration considered. The calculations were carried out using perturbation theory to obtain sensitivity profiles for the various cross sections of interest, and these profiles were then combined with cross-section error estimates, including correlations, to obtain the uncertainties.

---

* Abstract of paper presented at ANS Meeting, San Francisco, November 16-21, 1975.

** Abstract of ORNL-TM-4933.

† Abstract of ORNL/TM-5198 (March 1976); paper submitted to Nucl. Sci. Eng.

Each of the three responses — the neutron scalar flux, the energy deposition per unit volume, and the displacements per atom — is found to be very sensitive to the cross sections in the energy group which contains the source ($\sim$ 14 MeV since a D-T source is assumed), and each of the responses is found to have a relative standard deviation of approximately 100% due to neutron cross-section errors in iron.

f. Neutronics Calculations for the Tokamak Experimental Power Reactor Reference Design* (R. T. Santoro)

The results of initial one-dimensional calculations evaluating the nuclear performance of the Tokamak Experimental Power Reactor are presented. Estimates of the tritium breeding, nuclear heating, and radiation damage are given for an assumed neutron wall loading of 0.168 MW/m^2 (100 MW).

g. Neutronic Scoping Studies for Tokamak Experimental Power Reactor** (Santoro, E. S. Bettis,† D. G. McAlees,‡ H. L. Watts and M. L. Williams)

One-dimensional neutron and photon radiation transport methods have been used to investigate candidate blanket configurations and compositions for use in the Tokamak Experimental Power Reactor. Seven blanket designs are compared in terms of energy recovery, radiation attenuation, potential radiation damage, and, where applicable, tritium breeding.

h. The Calculated Performance of Various Structural Materials in Fusion-Reactor Blankets¶ (Williams, Santoro and Gabriel)

The calculated nuclear performances of niobium, SS-304, and nimonic-105 as structural materials in a conceptual D-T fusion-reactor blanket model are compared. For each structural material, the tritium breeding ratio, the energy-deposition rate, the operating dose, the time dependence of the neutron-induced activity, the time dependence of the dose from the activation products, the time dependence of the nuclear afterheat, and the atomic displacement rate are calculated. Emphasis is placed on the nuclear response in the first structural wall to the selected structural material for an assumed neutron wall loading of 1 MW/m^2. Taking into account all of the nuclear responses, SS-304 appears to be a reasonable choice as the structural material for fusion-reactor applications.

---

* Abstract of ORNL-TM-5033.

** Abstract of ORNL/TM-5035 (February 1976).

† Consultant to Thermonuclear Division

‡ Exxon Nuclear Company, Inc.

¶ Abstract of ORNL-TM-5036 (December 1975); paper submitted to Nuclear Technology.

5. Multigroup Libraries

After all the nuclear data have been evaluated in the form of microscopic cross sections or data as a function of energy in a library such as ENDF/B, they can then be used directly for applied calculations. However, in most instances, inparticular in applications involving neutron transport, the data must be processed in the form of multigroup cross sections. Until a few years ago most users generated for themselves the multigroup data from the evaluated data files. With the increase in size of the evaluated data files, as they became more detailed and complete, the cost of generating the multigroup data sets and maintaining the processing codes has soared and become prohibitive for many users. As a result, a demand has arisen for processed nuclear data. When processing the evaluations, the group structure must be tailored to the particular application. The Radiation Shielding Information Center has traditionally provided these processed data sets to users and during 1975 several multigroup libraries were generated from ENDF/B-IV for various applications.

We report below on a few of these data sets generated at ORNL and available from RSIC.

a. A 218-Group Master Neutron Cross-Section Library for Criticality Safety Studies* (W. E. Ford, III, C. C. Webster and R. M. Westfall)

A P_3, 218 neutron group master cross-section library has been generated from the latest ENDF/B data for 65 nuclides of primary interest in criticality safety calculations. Procedures used to generate the cross sections and the organization of the master cross-section library are described.

b. Coupled 100-Group Neutron and 21-Group Gamma-Ray Cross Sections for EPR Calculations** (D. M. Plaster, R. T. Santoro and W. E. Ford, III)

Coupled 100-group neutron and 21-group gamma-ray 800°K cross sections have been generated using the latest ENDF/B cross-section data for H, He, ^{6}Li, ^{7}Li, Be, ^{10}B, ^{11}B, C, O, F, Al, Ti, V, Cr, ^{55}Mn, Fe, ^{59}Co, Ni, Cu, Nb, and Pb. The procedures used to generate these cross sections and the organization of the cross-section tape in ANISN format are discussed.

* Abstract of ORNL/CSD/TM report (to be published).
** Abstract of ORNL-TM-4872.

Modification Number One to the Coupled 100n-21γ Cross Section Library for EPR Calculations* (Ford, Santoro, Roussin and Plaster)

The EPR ANISN-formatted 100-group neutron and 21-group gamma-ray cross section library has been modified by the addition of data for 20 materials, by the addition of reaction cross sections for calculating tritium and helium production, and by the addition of kerma factors. The EPR 100-group master cross section library has been modified by the addition of data for 19 materials. Procedures used to generate these cross sections and the organization of the libraries are described.

c. Data Testing of the 126/36 Neutron-Gamma ENDF/B-IV Coupled Library for LMFBR Core and Shield Analysis** (White, Wright, Williams and Weisbin)

The Physics Branch of the ERDA Division of Reactor Development and Demonstration has sponsored the development of a 126/36 neutron/gamma coupled library derived from ENDF/B-IV data. The detailed specifications (e.g., selection of the tailored group structure) and processing methods have already been documented.[1] The purpose of this paper is to describe the testing program and results obtained to date in an effort to gain confidence in the library performance for a variety of important LMFBR core and shield applications.

d. The CTR Processed Multigroup Cross Section Library for Neutronics Studies† (Roussin, Weisbin, White, Greene, R. Q. Wright and J. B. Wright)

The program for the development, generation, validation and distribution of a general purpose, processed multigroup cross section library (PMCSL) for use in CTR neutronics studies is described. The Radiation Shielding Information Center (RSIC) coordinated an effort to establish the CTR-PMCSL based on input requirements specified by ERDA-DCTR contractors. By collaborating with the ORNL Neutron Physics Division Shielding Analysis and Reactor Physics Group (which had a similar mission for the ERDA-DRDD community) it was possible to define a single 171 neutron, 36 gamma-ray group cross-section library useful for both CTR and LMFBR neutronics analysis. The master library was generated using the MINX

---

* Abstract of ORNL/TM-5249.

** Abstract of paper to be presented at ANS Meeting, June 1976, Toronto.

† Abstract of ORNL/RSIC-37; paper to be presented at ANS Meeting, June 1976, Toronto.

[1] C. R. Weisbin, R. W. Roussin, J. E. White and R. Q. Wright, "Specification for Pseudo-Composition-Independent Fine-Group and Composition-Dependent Fine- and Broad-Group LMFBR Neutron-Gamma Libraries at ORNL," ORNL-TM-5142 (ENDF-224) (December 1975).

neutron processor and the gamma-ray processor from the AMPX system. Results of initial testing of the library at ORNL are described. Preliminary release of the library is being made to a group of ERDA contractors in AMPX and CCCC interface forms, along with appropriate retrieval and manipulation programs. Problem-independent and problem-dependent collapsed versions will also be provided. The release is intended to stimulate implementation and testing at several installations for the purpose of improving the quality of the libraries which will ultimately receive general distribution.

e. Radiation-Damage Calculations: Primary Recoil Spectra, Displacement Rates, and Gas-Production Rates* (T. A. Gabriel, J. D. Amburgey and N. M. Greene)

A heavy charged-particle recoil data base [primary knock-on atom (PKA) spectra] and an analysis program have been created to assist experimentalists in studying, evaluating, and correlating radiation-damage effects in different neutron environments. Since experimentally obtained controlled-thermonuclear-reactor-type neutron spectra are not presently available, the data base can be extremely useful in relating currently obtainable radiation damage to that which is anticipated in future fusion devices. However, the usefulness of the data base is not restricted to just CTR needs. Most of the elements of interest to the radiation-damage community and all neutron reactions of any significance for these elements have been processed, using available ENDF/B-IV cross-section data, and are included in the data base. Calculated data such as primary recoil spectra, displacement rates, and gas-production rates, obtained with the data base, for different radiation environments are presented and compared with previous calculations.

---

* Abstract of ORNL/TM-5160 (March 1976).

C. COMPILATION AND NUCLEAR DATA PROJECT

1. Compilation of Phenomenological Optical-Model Parameters 1954-1975* (C. M. Perey and F. G. Perey)

Presented here is a compilation, with bibliography, of optical-model parameters determined by fitting elastic-scattering angular distributions for various incident particles including heavy ions. It includes parameters from previous compilations back to 1954 and from an extensive literature search in the leading journals and publications in nuclear physics up to June 1975 inclusively.

2. Nuclear Data Project Activities – 1975 (R. L. Auble,** F. E. Bertrand,** Y. A. Ellis, W. B. Ewbank, B. Haramatz, D. J. Horen,† H. J. Dim,** D. C. Kocher,** M. J. Martin, F. K. McGowan,** and M. R. Schmorak)

This year has seen the culmination of Nuclear Data Project (NDP) efforts in several areas. The Evaluated Nuclear Structure Data File (ENSDF) has been developed to where it can serve as the focus for NDP evaluation activities. Standard ENSDF data sets are being used routinely to produce computer-printed *Nuclear Data Sheets* as well as drawings. Additional output formats are being developed to meet needs of other users. The Project's file of keyword-indexed references to nuclear structure literature has also been exploited in new ways during the year: a volume of cumulated references to the experimental nuclear structure literature (1969-1974) was issued as a Supplement to Volume 16 of *Nuclear Data Sheets*; the contents of the cumulated volume were also placed on the RECON system for direct interactive search by any qualified user.

The standard formats developed by the Nuclear Data Project for the representation of nuclear structure data are gaining wider understanding and acceptance as the existence of ENSDF becomes known. Tape copies of data sets containing adopted levels and decay schemes have been sent on request to several laboratories in the U.S., Europe, and the Soviet Union. The data center at LINP (Leningrad Institute of Nuclear Physics) has also used the standard formats to describe results of nuclear physics experiments.

a. Evaluated Nuclear Structure Data File (ENSDF)

The data file was designed to organize nuclear structure information in standard format into convenient blocks and to provide tools for storing and retrieving the information as needed. Information in ENSDF is organized into "data sets" of three general types: decay schemes of radioactive nuclei, level structure from nuclear reactions, and adopted level properties. The file is maintained on disk at the ORNL computer center. As of March 1974 the file contained

1230 decay schemes

1800 reaction data sets

1540 adopted levels data sets.

---

* Abstract of paper submitted for publication in Atomic Data and Nuclear Data Tables.

** Part-time assignment to Nuclear Data Project.

† Director, Nuclear Data Project until November 1975.

Selection of particular data from the ENSDF is accomplished by computer scanning of a descriptive keyword string.

b. *Nuclear Data Sheets* from ENSDF

For several years, the drawings in *Nuclear Data Sheets* have been prepared from standard ENSDF data sets. During 1975, the Nuclear Data Project also began preparation of the printed *Data Sheets* from the data file. A standard page layout for presentation of tabular data was first used for A = 75. Addition of a text editor to control the special ORNL 160-character print train now produces acceptable computer-composed pages for photoreproduction.

The NDS listing program has also been used to prepare special responses to requests for nuclear structure information, e.g., a table of all nuclear levels with known lifetimes, an ordered list of γ-rays observed in decay of transactinide nuclei, tabulation of levels and γ-rays observed in (HI,xnγ) reactions.

c. Decay Radiations from ENSDF

One additional output format for information from ENSDF has been tested. The MEDLIST program, which calculates absolute intensities for both atomic and nuclear radiations following radioactive decay, normally prepares a tabular format for photoreproudction (e.g., ORNL-5114). The program was extended in 1975 to also provide a file of these radiations in a card-image format, easily readable by FORTRAN programs. Many conventions of the ENDF/B-IV tapes were adopted to facilitate inclusion of ENSDF data in some future version of ENDF. Radiations from 191 radioactive nuclei were written onto a tape, which has been sent to several users for testing. A copy is also available on data cell for testing by ORNL users of radioactivity data.

Discussions with MIRD representatives and members of the Information Center for Internal Exposure at ORNL have produced tentative agreement to use ENSDF data in future calculations for medical dosimetry and for radiation protection standards.

d. Nuclear Structure References

In support of its data evaluation program, the Nuclear Data Project searches the world's scientific literature for reports of nuclear structure results. Each year approximately 3000 published articles and 2000 preliminary reports are tagged according to data content and added to the indexed nuclear structure reference file. The master file now includes some 55,000 entries on magnetic tape at ORNL.

The cumulated file of Nuclear Structure References, 1969-1974, has been prepared for inclusion among the reference files available from the RECON network. The file can be searched for keyword descriptions and references on nuclear structure topics from any of 27 directly connected RECON sites within the USA. Since the introduction in mid-1975 of a dial-up version of RECON, any ERDA-approved user can search the files from any telephone. The RECON version of the NDP reference files does not take full advantage of the keyword structure, but it does provide an interactive search capability which can include combinations of key terms (isotope, reaction, etc.). The RECON file can also be used to search on author or publication year, and can provide printed references if needed.

OHIO UNIVERSITY ACCELERATOR LABORATORY

A. NEUTRON ELASTIC SCATTERING

1. Neutron Elastic Scattering and the Isospin Dependence of Nucleon-Nucleus Optical Model Potentials* (D. Bainum, T. Cheema, D. Carlson,** J. Ferrer† and J. Rapaport)

a. Experimental Program

Elastic scattering data, has been taken for over 100 cases with monoenergetic neutrons at 7, 9, 11, 20 and 26 MeV. Data has been obtained from $\theta_L = 15°$ to $\theta_L = 155°$ in steps of $\Delta\theta = 5°$ for a total of 29 points, with an average time data taking of about 1.5 hours for each experimental point. This represents well over 4000 hours of data acquisition.

A list of the used scattering samples with their geometrical characteristics is indicated in Table A-1.

A brief description of what has been done according to energy and research interest is discussed below.

a-1. Neutron Scattering at 11 MeV

Elastic scattering of 11 MeV neutrons from Mg, Al, S, Ca, V, Mn, Fe, Co, Ni, Nb, ^{92,96,98,100}Mo, In, ^{120}Sn, Ho, Ta, ^{206}Pb, Pb and Bi have been measured. The required neutrons were produced by the D(d,n)^{3}He reaction. A pulsed beam time-of-flight technique using five large area NE-224 liquid scintillators and a plastic scintillator monitor simultaneously was employed. Zero degree flux measurements were used to normalize the differential cross sections. Energy resolution was approximately 350 keV FWHM. A time-of-flight spectra for a few targets is shown in Fig. A-1, while in Fig. A-2 is shown an example of the peak-fitting procedure used to extract the reaction yield. The measured cross sections were corrected for dead time, detector efficiency, attenuation, multiple scattering, finite geometry, neutron source anisotropy, contaminants and compound elastic contribution. An estimation of

---

* Supported in part by the National Science Foundation, Grant MPS 74-04109 A01.

** Present address: Crocker Nuclear Laboratory, University of California, Davis, California.

† Present address: Fusion Energy Corporation, Princeton, New Jersey.

Table A-1. Scattering Sample Dimensions

Sample	Dimensions height x diam. (cm)	Mass (gm)	Isotopic enrichment (%)
$_{12}Mg$	2.49 x 2.49	23.058	natural
$_{13}Al^{27}$	2.55 x 2.54	34.654	100
$_{14}Si$	1.81 x 2.1	14.836	natural
$_{16}S$	2.13 x 2.08	14.057	natural
$_{20}Ca$	2.28 x 2.16	12.622	natural
$_{23}V^{51}$	2.03 x 2.03	40.156	natural (∿100)*
$_{25}Mn^{55}$	2.51 x 2.51	47.22	100*
$_{26}Fe$	2.10 x 2.05	53.882	natural
$_{27}Co^{59}$	1.78 x 1.78	38.674	100*
$_{28}Ni$	2.50 x 2.49	110.7	natural
$_{40}Zr^{90}$	1.95 x 1.96	36.679	97.72
$_{40}Zr^{92}$	2.00 x 2.00	41.077	95.1
$_{41}Nb^{93}$	2.55 x 2.31	108.7	100
$_{42}Mo^{92}$	2.08 x 1.99	57.866	97.37$^+$
$_{42}Mo^{96}$	2.24 x 1.99	59.678	96.44$^+$
$_{42}Mo^{98}$	2.10 x 2.16	66.463	98.30$^+$
$_{42}Mo^{100}$	2.27 x 2.11	65.705	95.90$^+$
$_{49}In$	2.29 x 2.46	92.01	natural
$_{50}Sn^{120}$	2.814 x 3.00 O.D. x 1.97 I.D.	82.43	98.39$^+$
$_{65}Ho^{165}$	1.78 x 1.78	38.357	100*
$_{73}Ta^{181}$	2.03 x 2.03	109.7	natural (∿100)*
$_{82}Pb^{206}$	2.39 x 1.51	47.08	99.80$^+$
$_{82}Pb^{208}$	1.88 x 2.00	67.08	99.75$^+$
$_{82}Pb$	2.38 x 1.51	46.88	natural
$_{83}Bi^{209}$	2.56 x 2.43	114.7	100

* Borrowed from the Applied Physics Division, Argonne National Laboratory.

$^+$ Loaned by the Isotopes Division, Oak Ridge National Laboratory.

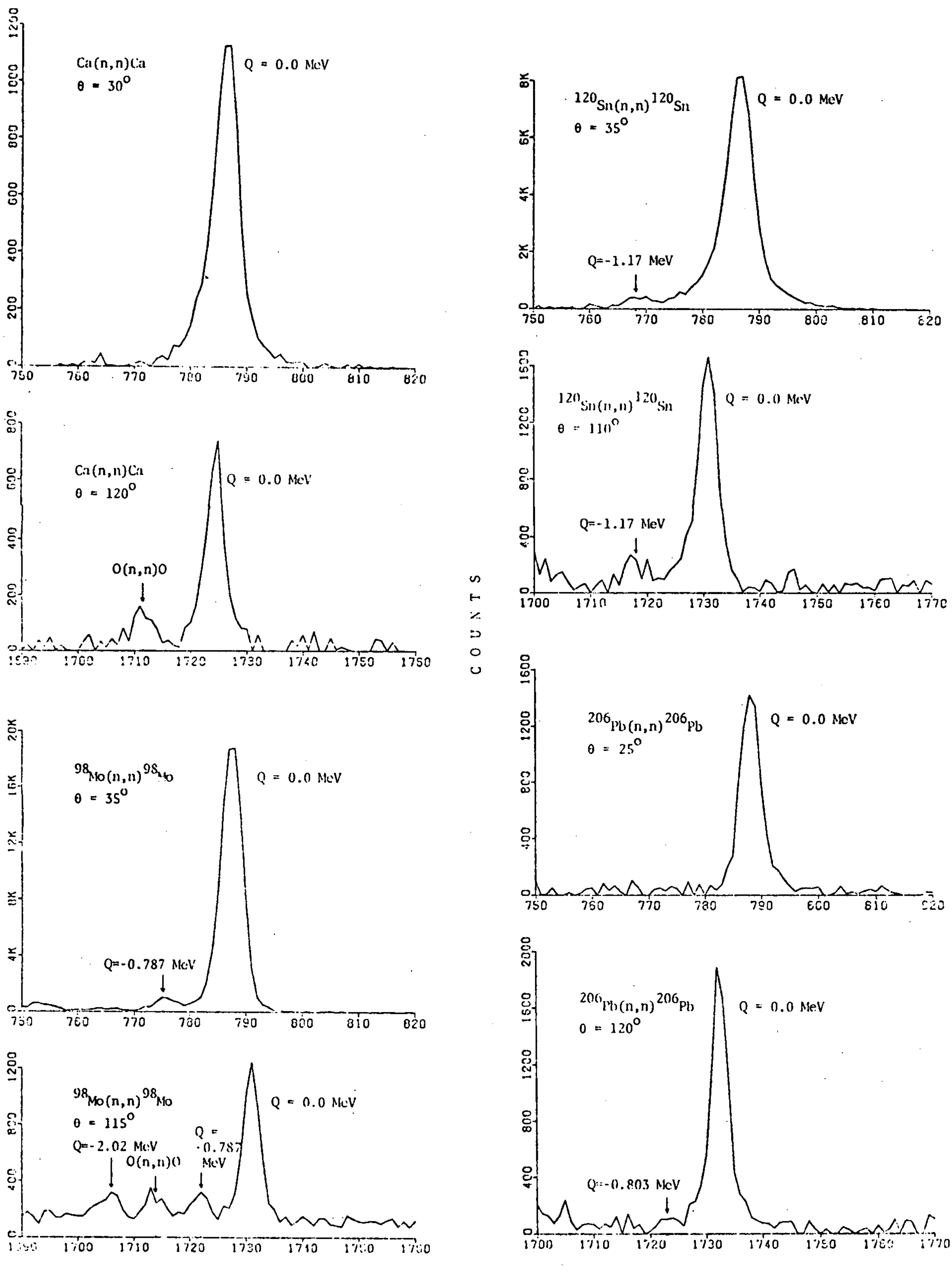

Fig. A-1. Examples of T.O.F. spectra obtained at E_n = 11 MeV.

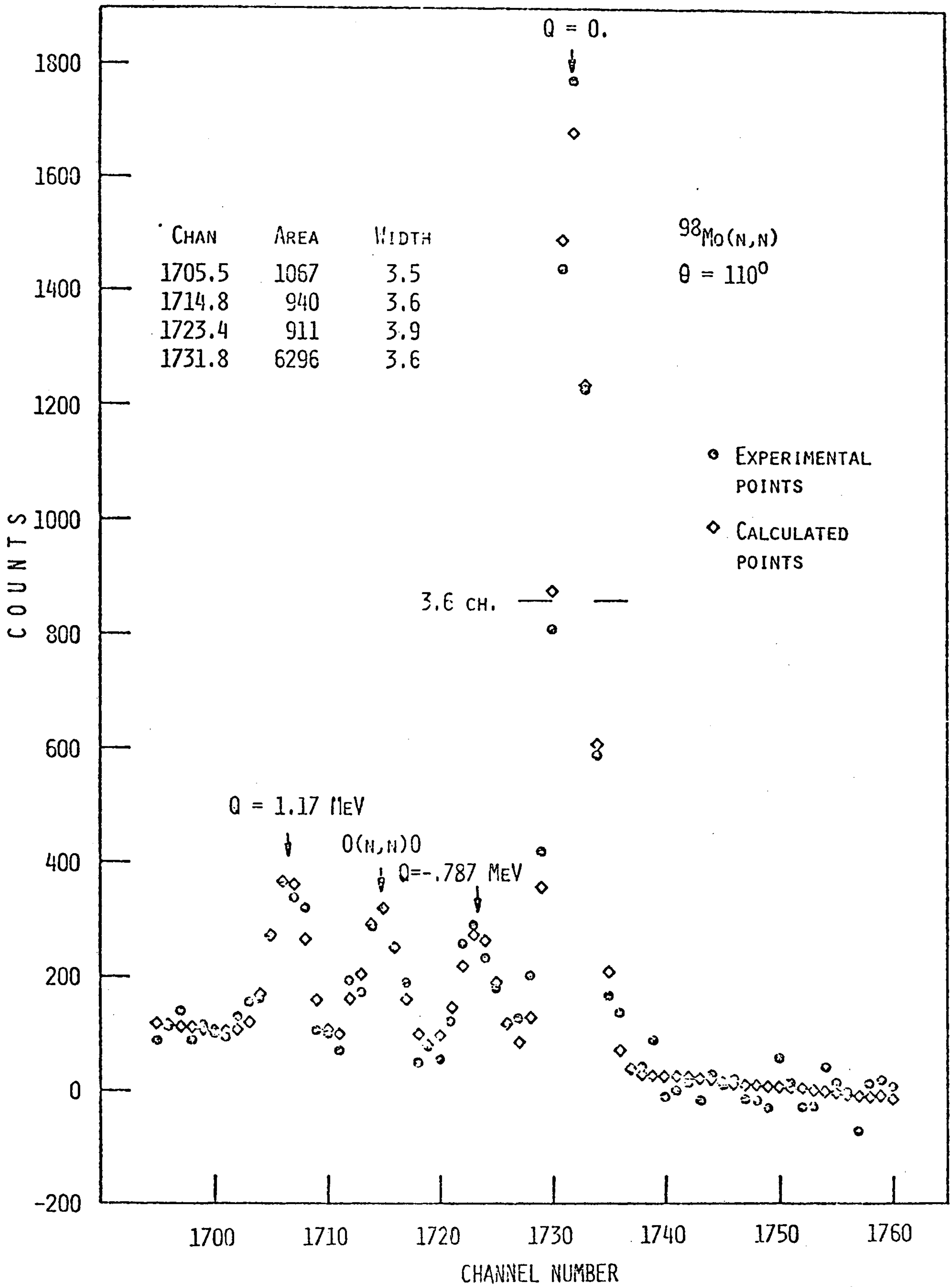

Fig. A-2. Example of the peak fitting procedure. Filled circles are data points while squares are calculated points.

the overall errors involved in the data analysis is presented in Table A-2.

The optical model analysis of this data has been finished.[1] An analysis comparing the (n,n) data with available (p,p) data is shown in Fig. A-3 while the resulting optical model parameters are tabulated in Table A-3. The results of an analysis comparing selected (n,n) cases with (p,p) data such that $E_p = E_n + \Delta E_c$ is presented in Fig. A-4 while the resulting optical model parameters are tabulated in Table A-4. Assuming the same radial dependence of the isospin term and the real term of the optical potential the depth of the isospin term was found to be $V_1 = 21.3 \pm 0.2$ MeV and 22.0 ± 1.2 MeV respectively* while the imaginary part assumed to be surface peaked was estimated to be $W_1 = 12.0 \pm 0.1$ MeV and $W_1 = 1.38 \pm 1.7$ MeV.

a-2. Scattering at 7, 9 and 11 MeV on the Mo Isotopes

(n,n) data at the indicated energies has been taken on separated isotopes of ^{92,96,98,100}Mo targets. Neutrons from the T(p,n) reaction were used at 7 MeV while the D(d,n) reaction was used at 9 and 11 MeV. A single neutron detector plus a monitor was used. In this fashion a substantial background reduction was achieved, especially at the forward angles. Reduction of the data is being performed.

a-3. Scattering at 20 MeV

The T(d,n) reaction has been used to provide 20 MeV monoenergetic neutrons. Data over the complete angular range has been obtained for the following natural samples, Si, S, Ca and Fe as well as the following enriched samples, ^{92,96,98,100}Mo and ^{206,208}Pb. A spectra is shown for S in Fig. A-5. Again as was in a-2 data was taken with only one detector, which helped considerably to achieve a better shielding thus reducing the background. Ideal conditions were achieved when the shadow bar was placed as close to the sample as possible and all the shielding requirements discussed by Hopkins et. al.[2] met.

---

* See Tables A-3 and A-4.

[1] J. C. Ferrer, Ph.D. dissertation, December, 1975, Ohio University, Physics Department; J. C. Ferrer, J. D. Carlson and J. Rapaport, Isospin Dependence of the Nucleon-Nucleus Optical Potential Through Nucleon Elastic Scattering, to be published; J. C. Ferrer, J. D. Carlson and J. Rapaport, Neutron Elastic Scattering at 11 MeV and the Isospin Dependence of the Neutron-Nucleus Optical Potential, to be published.

[2] J. C. Hopkins, J. T. Martin and J. D. Seagrave, Nucl. Inst. and Meth. 56 (1967) 175.

Table A-2

Relative Uncertainties (%)

Statistics in yields:	15° - 125°	< 1 - 5
	130° - 155°	5 - 10
Monitor statistics		< 1
Geometrical factors		< 1
Monte Carlo statistics		1 - 1.4
Compound nuclear contribution		1*
Residual background		< 1
Contaminants		1**
Angular resolution		0.5°†

Normalization Uncertainties (%)

Statistics in yields, 0° flux	< 1
Monitor statistics, 0° flux	1.3
Detector efficiency	1*
Attenuation and multiple scattering correction	3
Dead time correction	< 1
Flux anisotropy correction	1
Total	3.5

* Applicable only to Mg, Al, S and Ca

** Applicable only to Ca, $^{92,96,98,100}Mo$

† Errors in the differential cross section due to this were significant mainly around the first minima where the cross section varies rapidly.

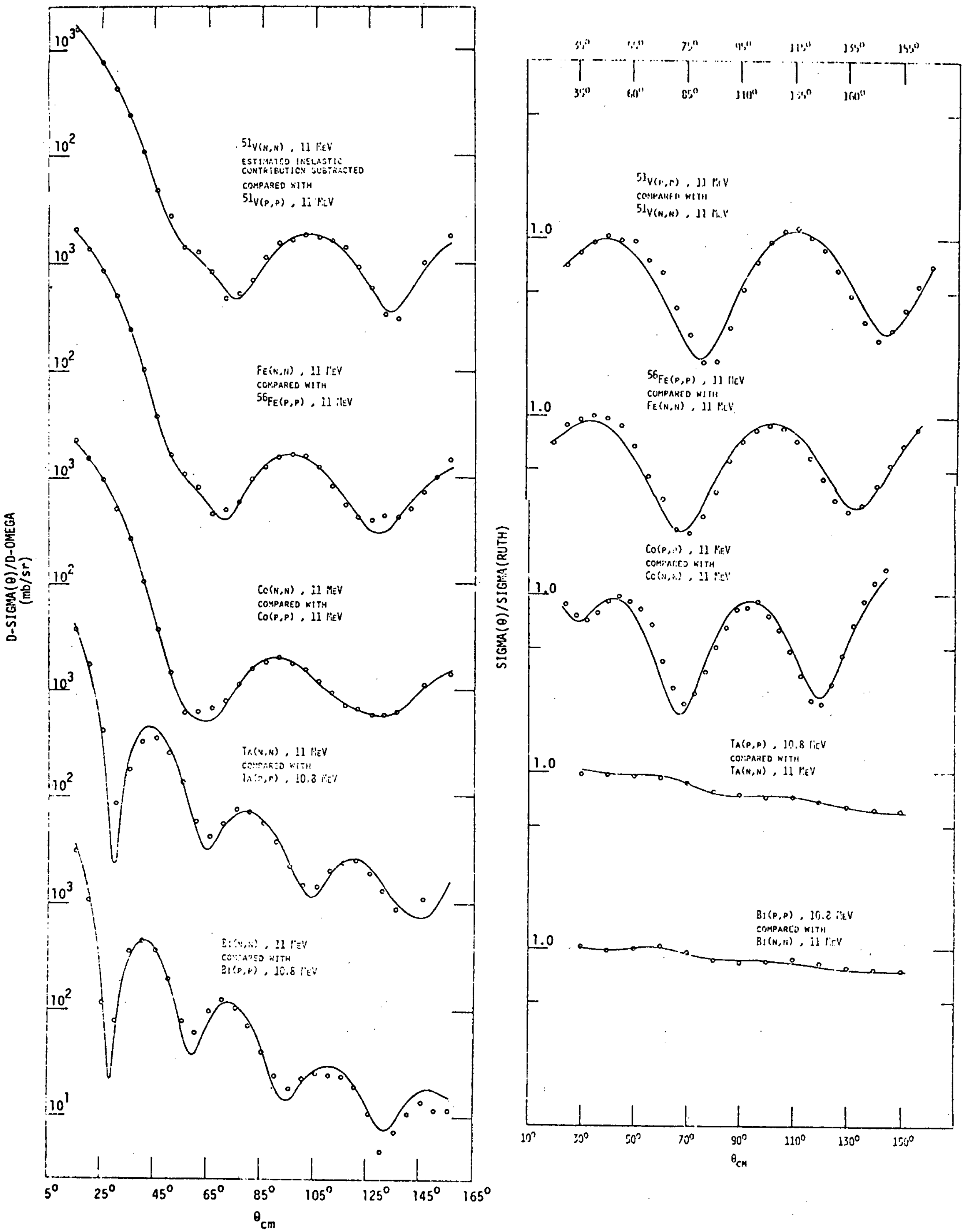

Fig. A-3. Simultaneous fitting of (n,n) and (p,p) data on the same nuclei at E ≃ 11 MeV.

Comparison		Energy (MeV)	V_{0R}	V_{1R}	r_R	a_R	W_{0D}	W_{1D}	a_I	V_{so}	χ^2/N	J/A (MeV fm^3)	$< r^2 >^{1/2}$(fm)
^{51}V	(n,n)	11.0	50.66	20.96	1.200	0.642	9.05	12.04	0.572	6.68	7.53	424.3	4.19
	(p,p)	11.0									7.39	481.8	
^{59}Co	(n,n)	11.0	47.46	20.69	1.246	0.650	9.57	12.16	0.534	7.47	2.10	440.5	4.45
	(p,p)	11.0									5.97	497.1	
^{56}Fe	(n,n)†	11.0	46.19	21.50	1.258	0.656	11.42	11.88	0.496	7.04	7.24	435.4	4.46
	(p,p)	11.0									4.29	495.2	
^{181}Ta	(n,n)	11.0	46.54	21.97	1.260	0.590	6.49	11.95	0.802	7.66	21.82	378.3	5.94
	(p,p)	10.8									16.27	501.1	
^{209}Bi	(n,n)	11.0	47.83	21.65	1.247	0.658	8.59	11.89	0.652	5.95	18.03	380.1	6.23
	(p,p)	10.8									12.61	507.7	
			Ave	21.35				11.98					
				±0.21				±0.05					

† Data is for natural iron.

Table A-3. Results of optical model parameters search for simultaneous fitting to (n,n) and (p,p) data at 11 MeV for the indicated nuclei.

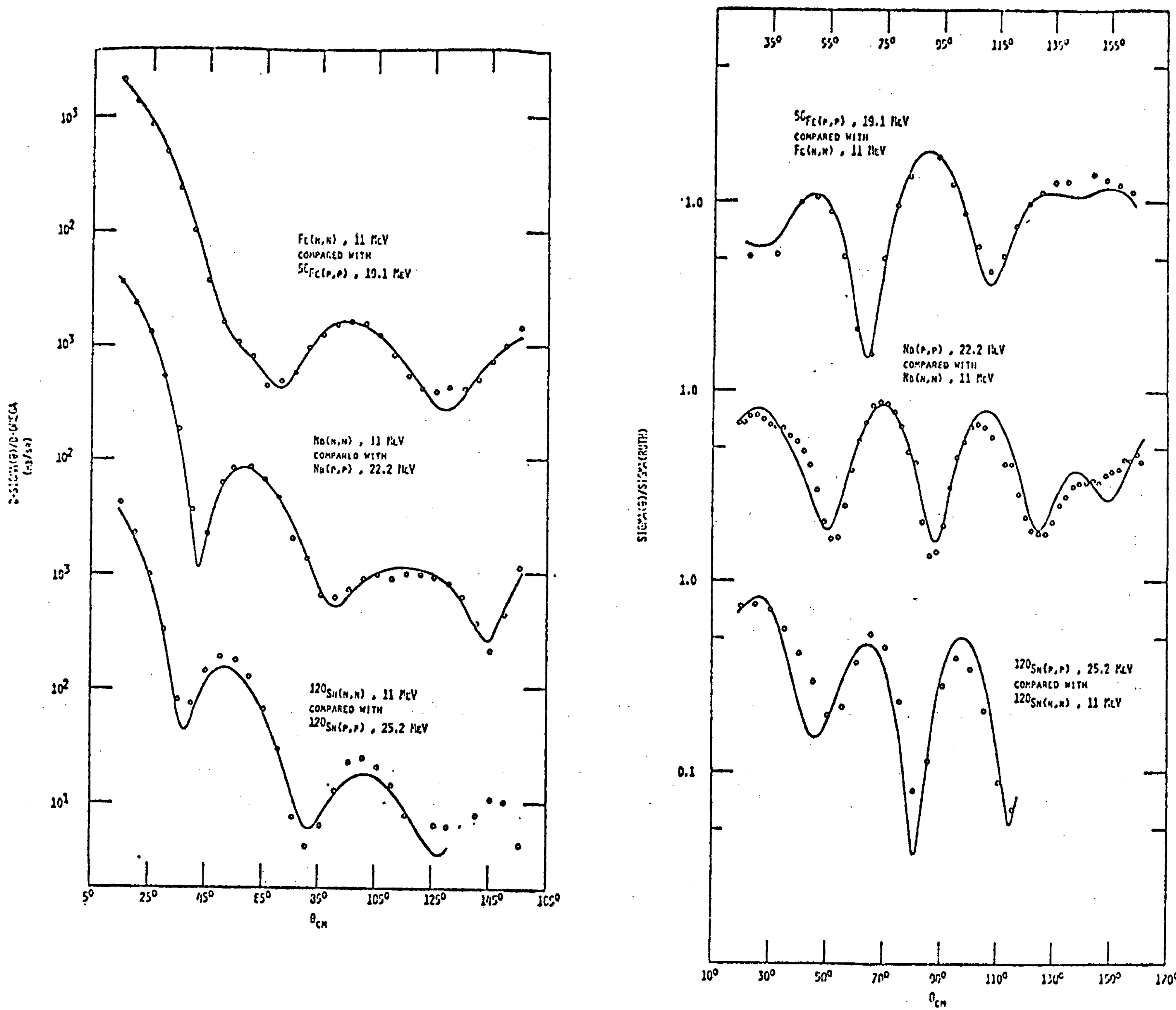

Fig. A-4. Simultaneous fitting of (n,n) and (p,p) data on the same nuclei but with $E_p = E_n + \Delta E_c$.

Comparison		Energy (MeV)	V_{0R}	V_{1R}	r_R	a_R	W_{0D}	W_{1D}	a_I	V_{so}	χ^2/N
^{56}Fe	(n,n)†	11.0	47.19	24.90	1.246	0.636	10.84	10.11	0.520	7.15	6.38
	(p,p)	22.2									1.06
^{93}Nb	(n,n)	11.0	50.88	21.43	1.215	0.596	8.26	14.03	0.728	7.78	9.48
	(p,p)	22.2									3.53
^{120}Sn	(n,n)	11.0	49.91	19.67	1.233	0.740	17.49	17.13	0.408	4.53	41.30
	(p,p)	25.2									25.60
			Ave	22.00				13.76			
				±1.25				±1.66			

† Data is for natural iron.

Table A-4. Results of optical model parameters search for simultaneous fitting to (n,n) and (p,p) data with $E_p = E_n + \Delta E_c$ for the indicated nuclei. (E_n = 11 MeV)

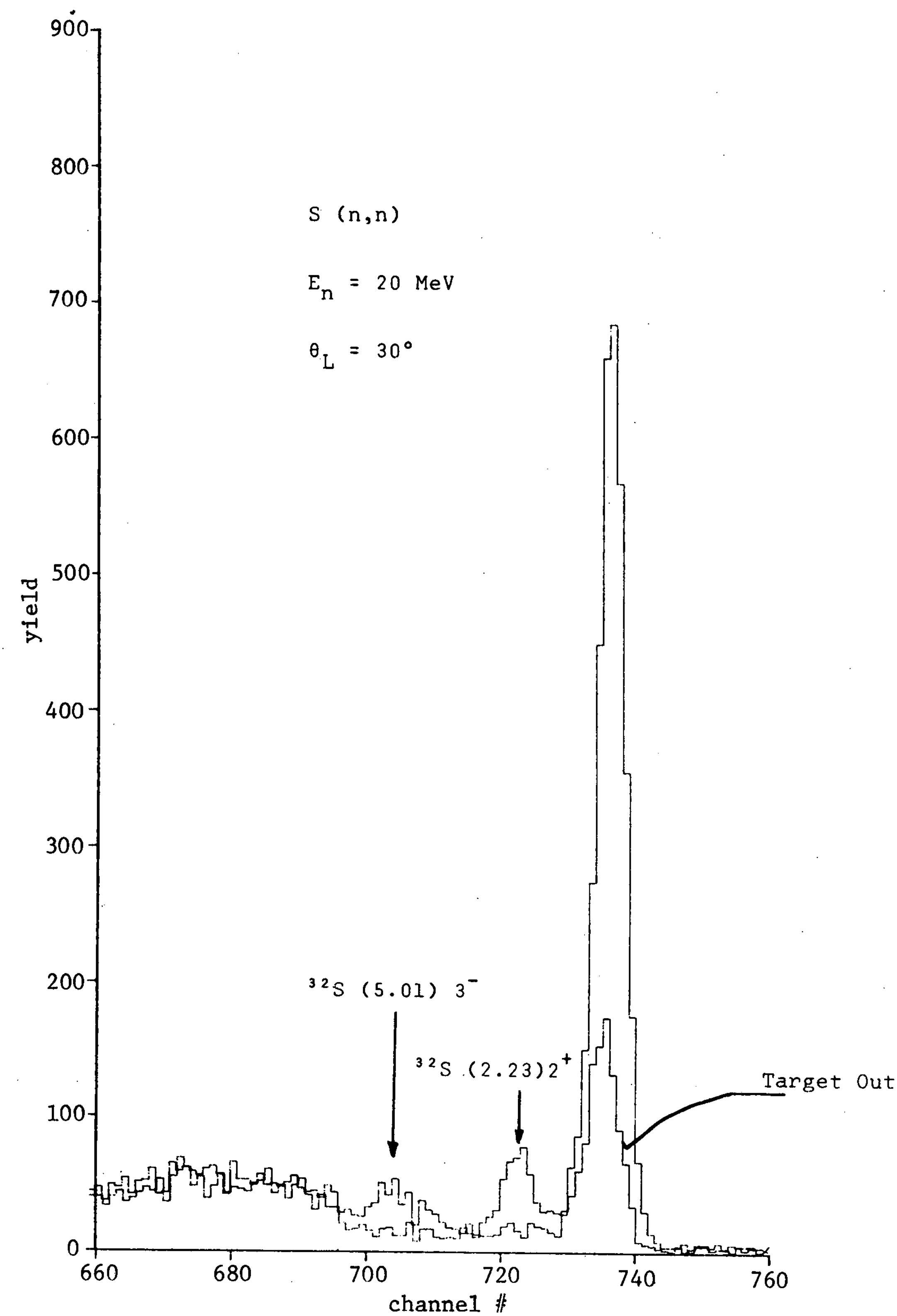
900
800
700
600
500
400
300
200
100
0
yield
S (n,n)
E_n = 20 MeV
θ_L = 30°
^{32}S (5.01) 3^-
^{32}S (2.23)2^+
Target Out
660
680
700
720
740
760
channel #

Figure A-5.

At present the data is being analyzed.

a-4. Scattering at 26 MeV

Neutron elastic angular distributions have been obtained with 26 MeV neutrons using the T(d,n) reaction as a monoenergetic neutron source. Data over the same angular range as in a-1 has been obtained for the following samples: Al, Si, S, Ca, Fe, Nb, and Bi as well as the enriched samples, $^{92,96,98,100}Mo$, ^{120}Sn and $^{206,208}Pb$. A Si(n,n) spectra is shown in Fig. A-6. The uncorrected angular distribution for the Fe(n,n) is shown in Fig. A-7 for E_n = 11, 20 and 26 MeV. At 11 and 20 MeV the $^{56}Fe(n,n')$ to the first excited state ($J^\pi = 2^+$) at 0.85 MeV has been resolved; however, only a shoulder on the low energy side of the elastic is seen at some angles at 26 MeV; the measured β at 20 MeV will be used to subtract the inelastic contribution in the observed elastic yield. Analysis of the data is in progress.

a-5. The $^{120}Sn(n,n)$ reaction at 9.4 and 22.8 MeV

An enriched ^{120}Sn sample (98.39%) was used in this set of elastic scattering measurements in order to complement previously measured proton elastic and (p,n) quasielastic scattering measurements on the same nuclide at 22.8 MeV. Complete neutron, differential elastic scattering cross section have been obtained at 22.8 and 9.4 MeV. The latter energy being chosen since it was equal to the energy of the outgoing neutron in the $^{120}Sn(p,n)$-IAS reaction. The analysis of this data is proceeding in a fashion similar to that explored by Carlson, Zafiratos and Lind.[3]

In this analysis a good proton optical model potential, U_p, is first obtained by fitting the 22.8 MeV $^{120}Sn(p,p)^{120}Sn$ data. Following and in the spirit of the Lane model, a DWBA analysis of the $^{120}Sn(p,n)$-IAS data is used to determine the isospin dependent part, U_1, of the nucleon-nucleus optical potential. Continuing in the spirit of the Lane model, U_p and U_1 are then used to derive a neutron optical model potential, U_n.

Early attempts[3] utilizing the above procedure were encouraging, however, due to the general poor quality of the available neutron scattering data they did not provide a stringent test of the Lane model. In the present work at Ohio University the quality of the neutron elastic scattering data approaches that of the charged particle (p,p) and (p,n) measurements. As seen in Fig. A-8 the predicted neutron elastic scattering cross sections at 9.4 MeV based on the derived U_n are

[3] J. D. Carlson, C. D. Zafiratos and D. A. Lind, Nucl. Phys. A249 (1975) 29; J. D. Carlson, D. A. Lind and C. D. Zafiratos, Phys. Rev. Letters 30 (1973) 99.

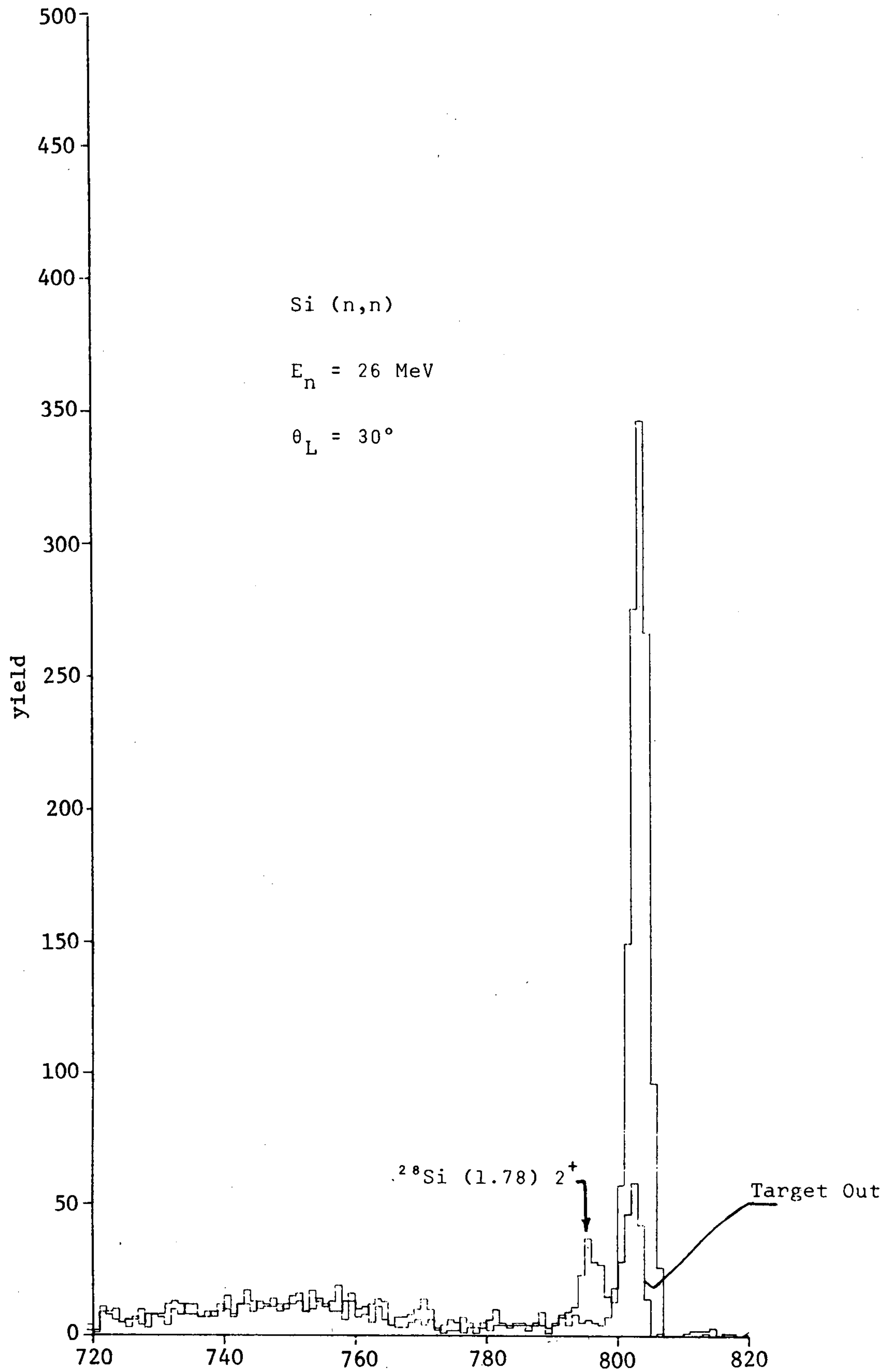

Si (n,n)
E_n = 26 MeV
θ_L = 30°
^{28}Si (1.78) 2^+
Target Out
yield
channel #
500
450
400
350
300
250
200
150
100
50
0
720
740
760
780
800
820

Figure A-6.

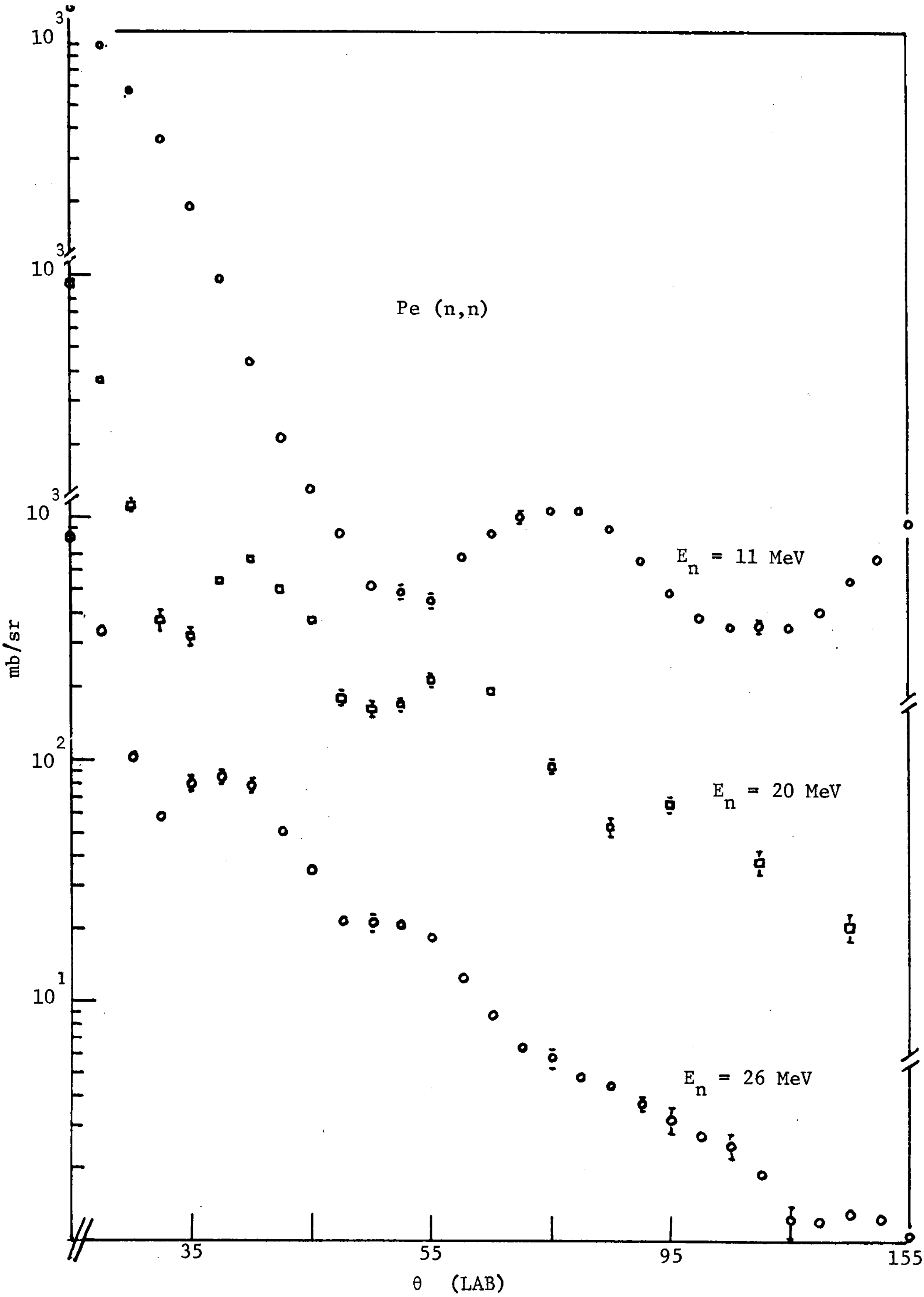

Pe (n,n)
E_n = 11 MeV
E_n = 20 MeV
E_n = 26 MeV
mb/sr
10^3
10^3
10^3
10^2
10^1
35
55
95
155
θ (LAB)

Figure A-7.

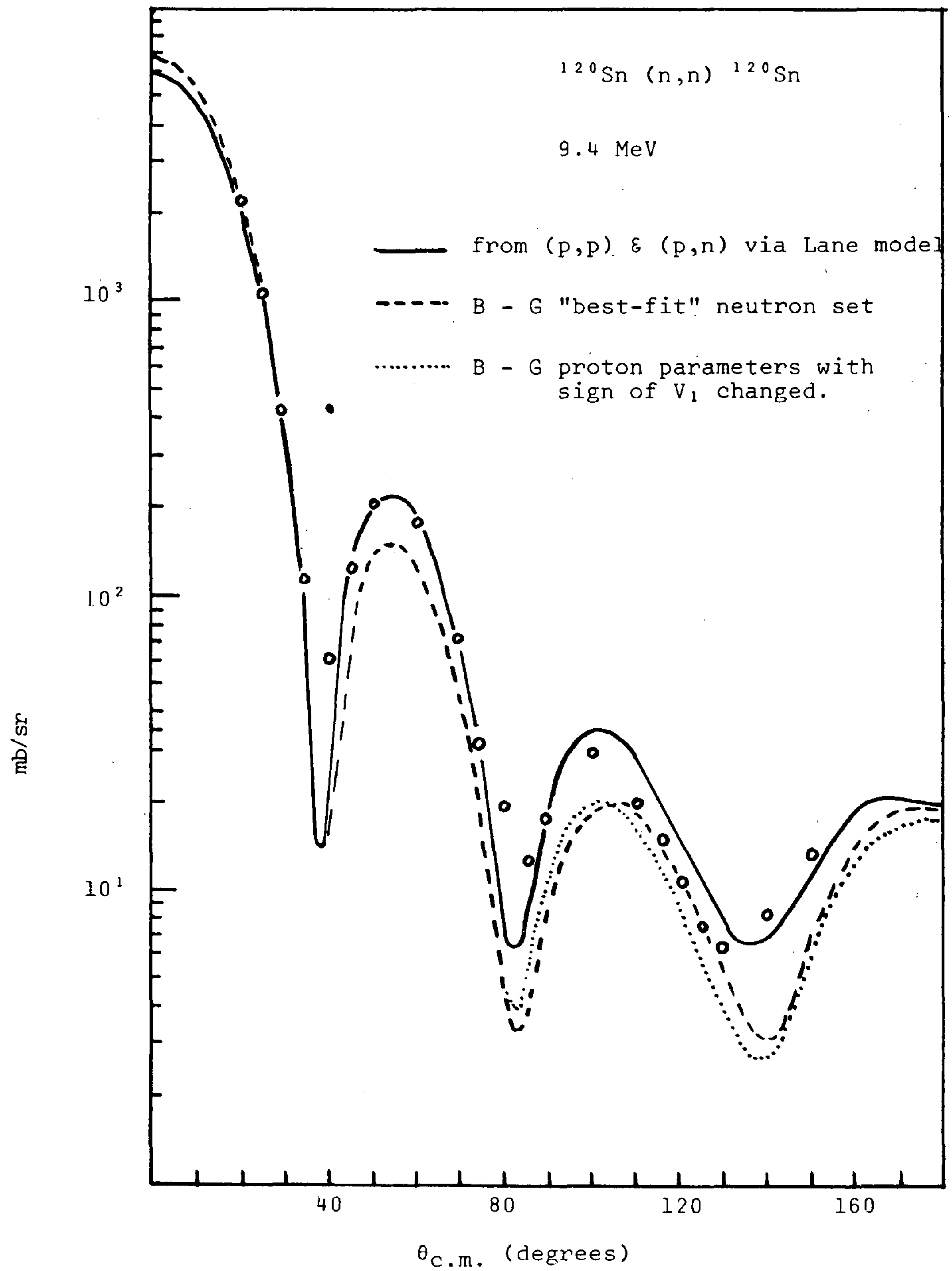

Fig. A-8. Neutron elastic scattering data at 9.4 MeV for ^{120}Sn compared with various O.M. predictions.

in excellent agreement with the measured results. In fact, they are significantly better than predictions based either on a standard set of global, neutron optical model potentials from the Becchetti-Greenlees compilation[4] or a set of neutron optical potentials derived from the Becchetti-Greenlees proton potentials by changing the sign of the appropriate isospin dependent term.

At 22.8 MeV the agreement is not as good, Fig. A-9. The difficulty at this energy ($E_n = E_p$) seems to be in the proper treatment of the Coulomb correction term, V_C. This term needs to be treated explicitly at 22.8 MeV in the generation of U_n from U_p and U_1. However, at 9.4 MeV this does not seem to be as critical. In this instance the difference in proton and neutron energies equals the Coulomb displacement energy, ΔE_C, for ^{120}Sn and the effects due to V_C are cancelled or balanced by the effects due to the energy dependence of the potentials. This is a matter which is currently being explored in detail through the analysis of proton and neutron scattering on T = 0 nuclei at the same energy.

a-6. Consistent Lane Model Analysis of Nuclear Elastic and Quasielastic Scattering on Other Nuclei

Neutron elastic scattering angular distribution have been obtained for several other nuclides at energies which complement ($E_n = E_p$ or $E_n = E_p - \Delta E_C$) existing proton elastic and (p,n) quasi-elastic scattering data. Data have been obtained and the analysis is currently in progress for the following cases: ^{96}Mo(n,n) at 11 MeV to complement (p,p) and (p,n) IAS data at 22.8 MeV, ^{208}Pb(n,n) at 26 MeV to complement (p,p) and (p,n) IAS data at 26 and 45 MeV, ^{56}Fe(n,n) at 11 MeV to complement (p,p) and (p,n) IAS data at 20 MeV and (p,p) data at 11 MeV. The analysis of these data has followed a somewhat different approach than the previous section, although still in the spirit of the Lane model. Rather than using the (p,p) and (p,n) IAS data to generate a neutron optical potential which is then compared with neutron data, the approach here has been to fit the corresponding (p,p) and (n,n) data for a given nuclide separately. The difference of the resulting potentials is then used to determine the isospin dependent portion of the nucleon-nucleus interaction, U_1.

A typical spectrum obtained for ^{96}Mo(n,n) scattering at 11 MeV is shown in Fig. A-10. The complete differential cross section for ^{96}Mo(n,n) is shown in Fig. A-11. These data have been corrected for finite geometry, multiple scattering, attenuation, and source anisotropy effects. Also shown in Fig. A-11 are the corresponding proton elastic and (p,n) quasielastic scattering cross sections for ^{96}Mo at 22.8 MeV. Note that the neutron scattering measurements were made at an energy

[4] F. D. Becchetti, Jr. and G. W. Greenlees, Phys. Rev. 192 (1969) 1190.

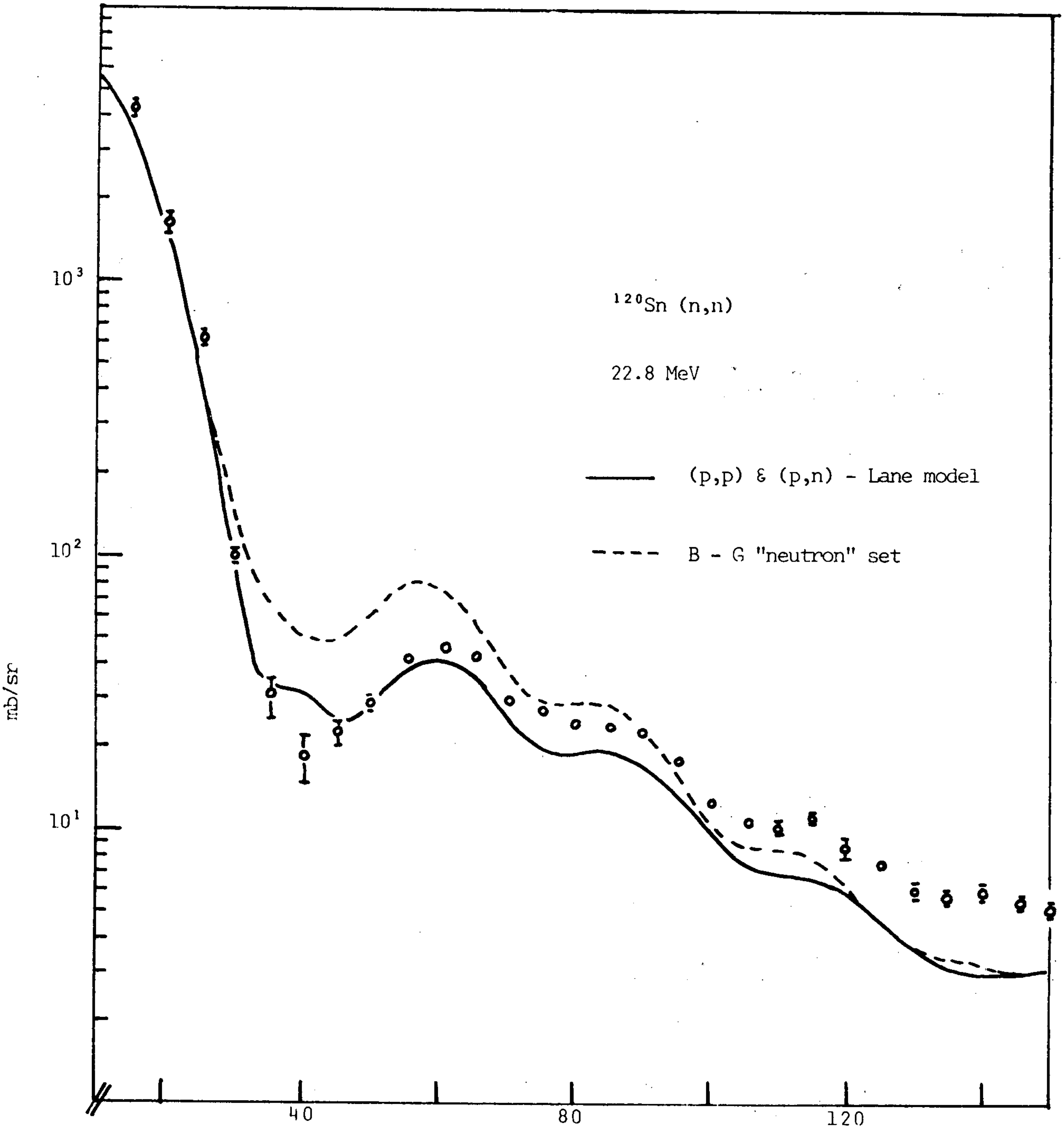

Fig. A-9. Neutron elastic scattering data at 22.8 MeV for ^{120}Sn compared with various O.M. predictions.

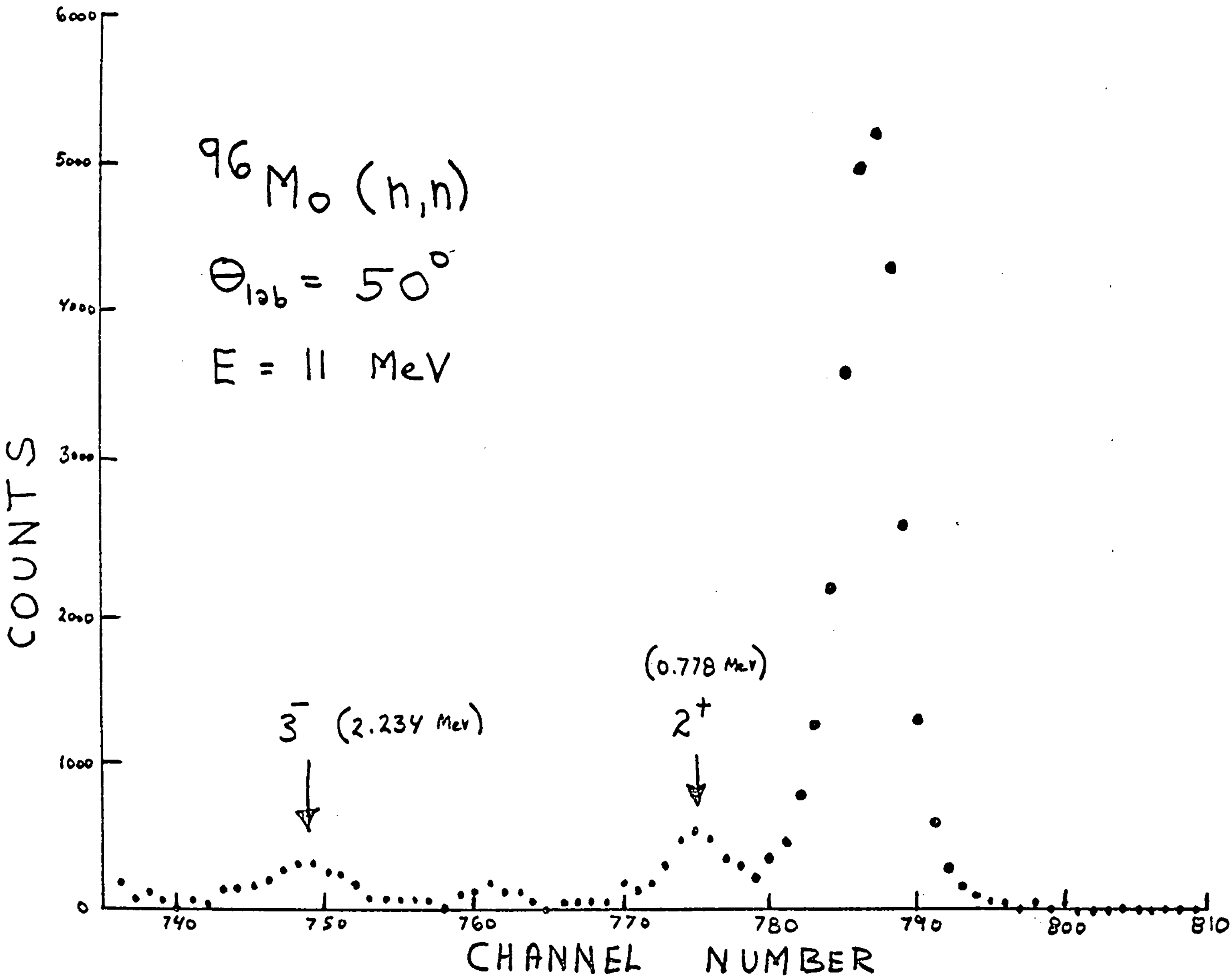

Fig. A-10. Spectrum of 11 MeV neutron scattered from ^{96}Mo at θ_{lab} = 50°.

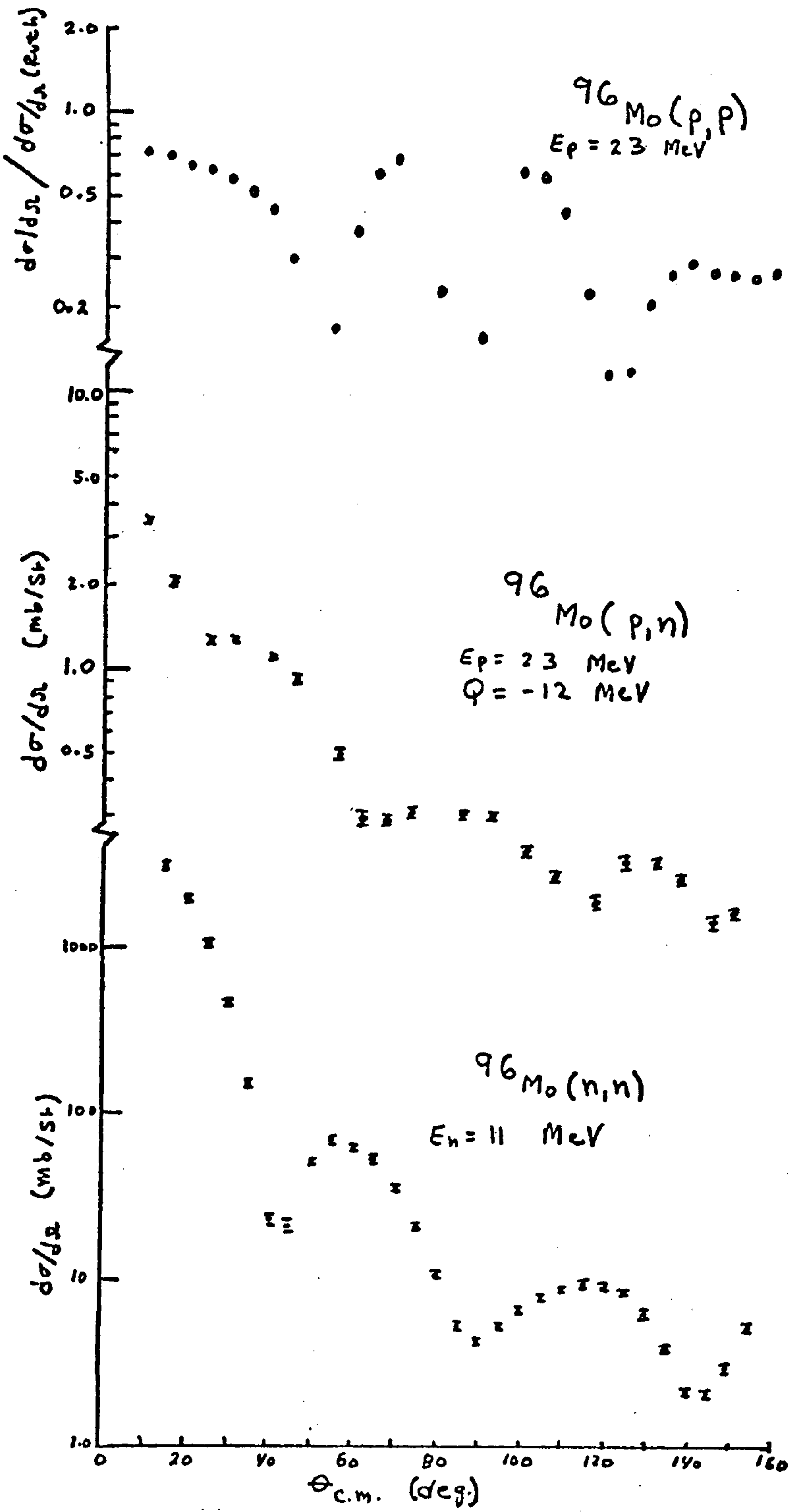

Fig. A-11. Neutron elastic and quasielastic scattering data for ^{96}Mo at equivalent energies.

corresponding to the energy of the outgoing neutron in the $^{96}Mo(p,n)$ IAS reaction.

In Fig. A-12 is shown the fit to the $^{96}Mo(n,n)$ data which results from a six parameter optical model search. The optical model potential consisted of a real volume plus an imaginary surface-peaked term. The six free parameters were the real and imaginary well depths and the corresponding radii and diffuseness. An equally good fit was obtained to the (p,p) data with a similar 6 parameter search.

The difference between these potentials was used to generate a prediction of the (p,n) IAS cross section shown on the bottom line in Fig. A-13. The first attempt was rather disappointing giving a result approximately 50% too low. The difficulty appeared to be in the absolute normalization of the (n,n) data. The absolute normalization for the (p,p) data had been determined by normalizing to the Rutherford scattering at small angles. Although the uncertainty in the relative $^{96}Mo(n,n)$ cross sections was less than ± 5% the uncertainty in the absolute cross sections was ± 10%. In comparing the measured $^{96}Mo(n,n)$ data to various optical model predictions it was found that the forward angles were very insensitive to the specific parameterization. The (n,n) data was therefore renormalized such that the 15°-35° points fit the Becchetti-Greenlees neutron potential[4] results with a minimum χ^2. A 10% shift resulted.

A new (n,n) search was carried out and a new isospin dependent U_1 was determined. The solid line in Fig. A-13 resulted from this second determination of U_1. Also shown is the prediction based on the isospin dependent term found in the Becchetti-Greenlees proton optical potentials.[4]

The real part of U_1 found from this procedure had a strength of approximately 23 MeV. However, the geometric factors of U_p and U_n were quite different, particularly the diffuseness of the real part a_I and the radius of the imaginary part, r_I. The result is that U_1 does not have the same shape as either U_n or U_p. In fact, as shown in Fig. A-14, the real part of U_1 has a peak at the surface and the imaginary part changes sign in the interior of the nucleus.

Questions still persist regarding the proper handling of the Coulomb correction term, V_C, as mentioned in the previous section. It is felt that by combining this analysis with work on T = 0 nuclei that a consistent and straightforward determination of U_1 will result.

b. Analysis of the Data

---

[4] F. D. Becchetti, Jr. and G. W. Greenlees, Phys. Rev. <u>192</u> (1969) 1190.

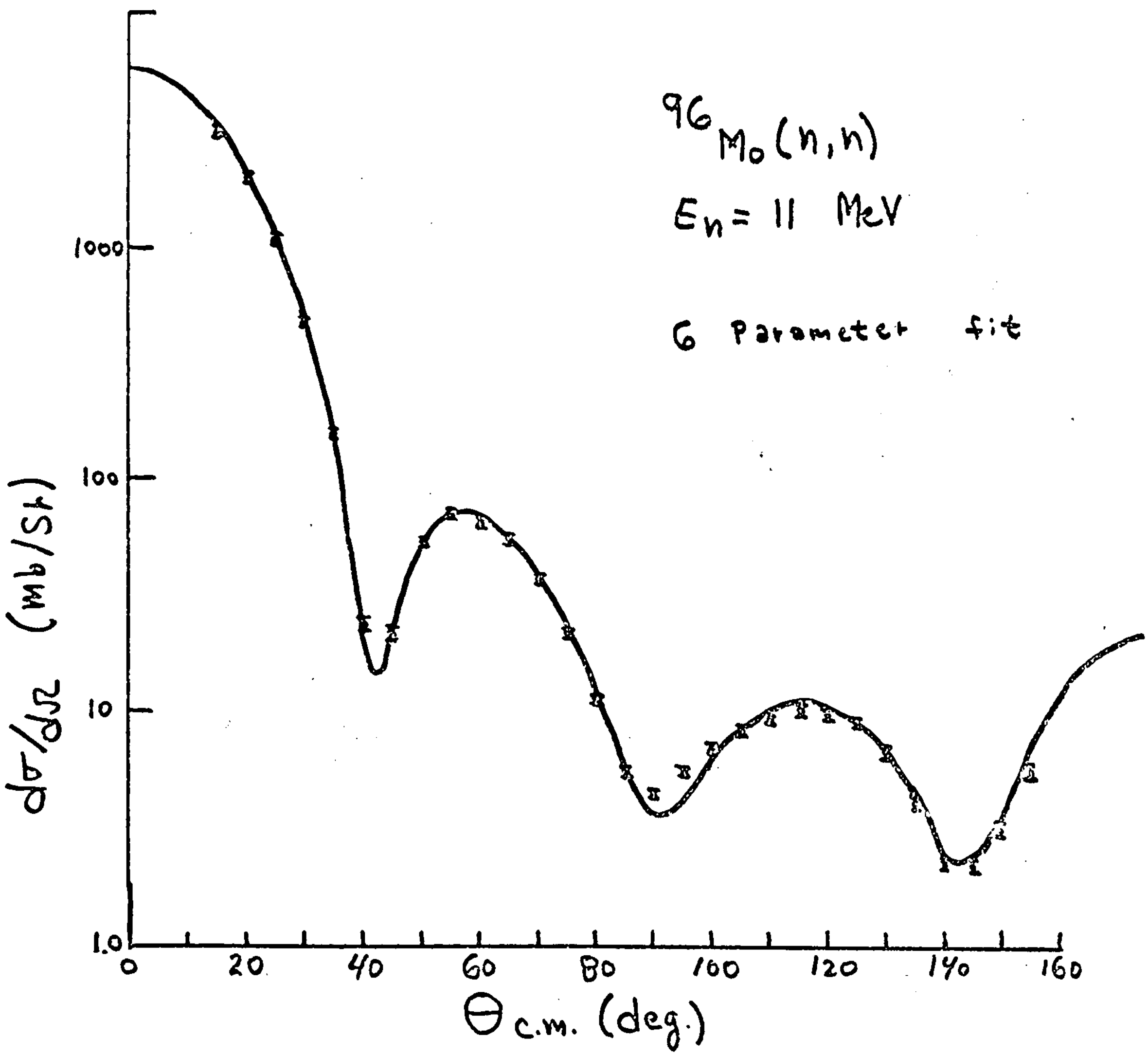

Fig. A-12. O.M. fit to ^{96}Mo(n,n) data.

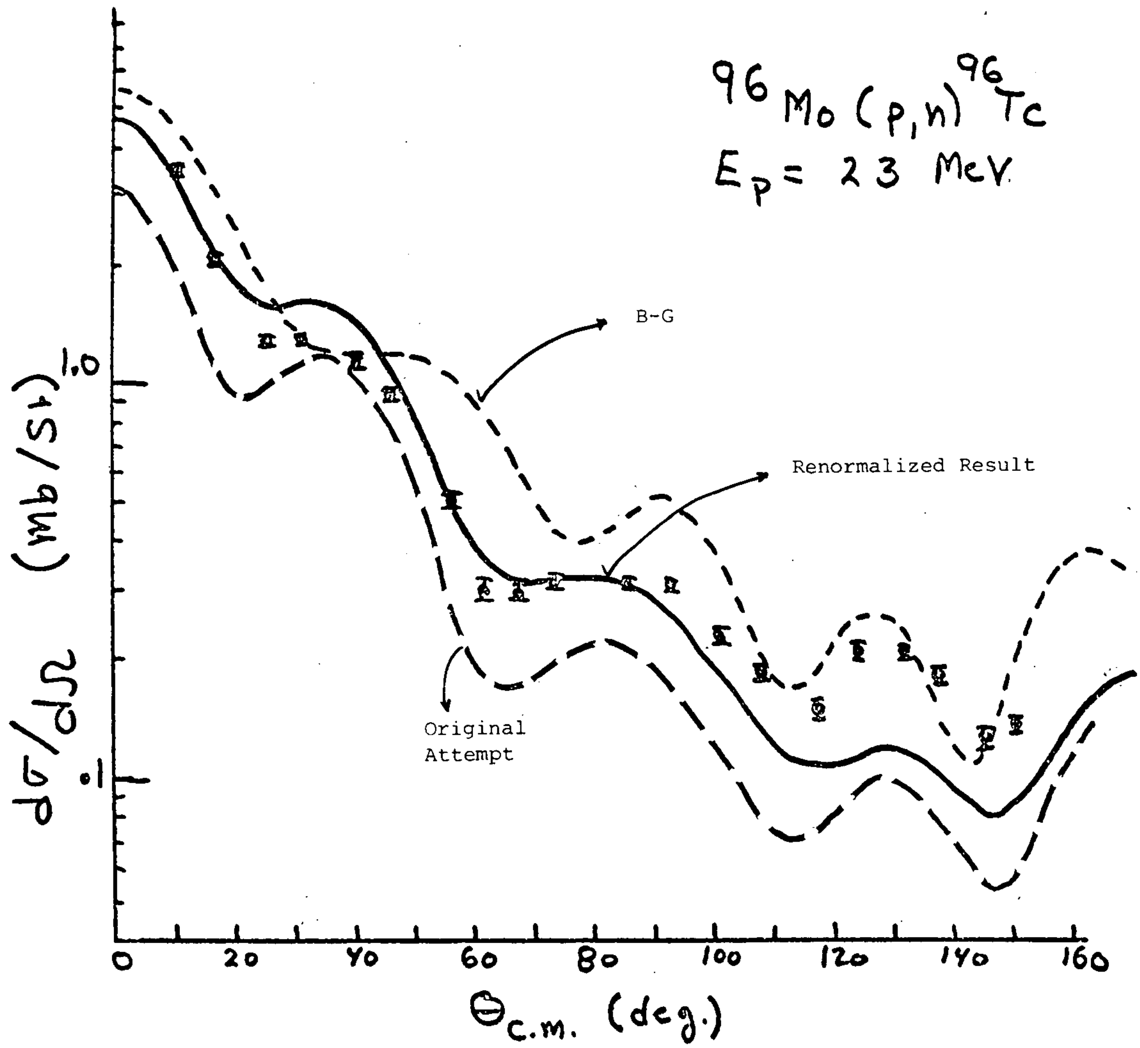

Fig. A-13. ^{96}Mo(p,n) IAS data at 22.8 MeV compared with various predictions based on the difference between proton and neutron optical potentials and the B-G neutron parameters.

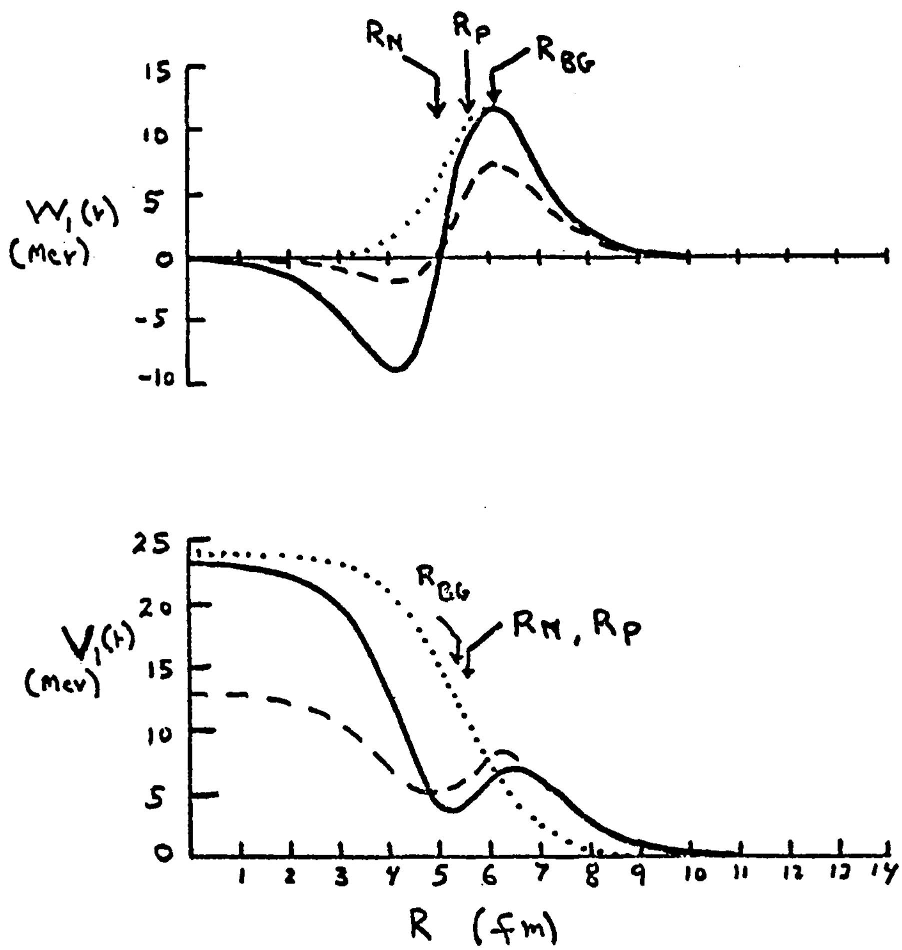

Fig. A-14. Real and imaginary parts of $U_1(r)$ as determined from the difference of proton and neutron optical potentials for ^{96}Mo compared with the Becchetti-Greenlees result. The dashed curve is before renormalization (see text) and the solid curve is after renormalization.

b-1. Corrections

The observed neutron spectrum is corrected by subtracting from it a target-out spectrum properly normalized to the same number of counts in the neutron monitor peak. Dead time and source anisotropy corrections are then included and absolute cross sections are obtained using the 0° flux measurement. We have also measured the 'H(n,n) cross section to obtain absolute values. Correction for contaminants are evaluated which may be quite important. For instance all the enriched Mo samples had oxygen in them[5] which amounted to a few percent (in number of atoms). The Mo(n,n) cross section has at 26 MeV a minimum of about 50 mb/sr at $\theta_L = 40°$; however the O(n,n) has at this angle a cross section value almost two orders of magnitude larger thus making very important its contribution to the observed yield. A separate experiment was done to measure the O(n,n) cross section in the forward angles at all the neutron energies used in the Mo(n,n) studies.

Compound nuclear contributions were evaluated using the code Helene[6] which performs a Hauser-Feshback calculation with a Porter-Thomas width fluctuation correction. This contribution was found to be significant at 11 MeV for the light nuclei reaching in some cases up to 15% in the back angles.

Other corrections which are important are effects due to the finite size of the sample: attenuation of the neutrons as they traverse the sample, multiple scattering within the sample, and single scattering over a range of angles determined by the sample size and source-sample distance, i.e. finite geometry. Treatment of these corrections have been done by using an analytical code[7] and a Monte Carlo code.[8] The second approach, even though much more time consuming is believed to be more accurate and is being used throughout. In general three iterations with 10,000 neutrons per iteration are used.

b-2. Optical Model Parameters

After all the corrections are done, optimum model parameters are obtained by fitting the data with optical model search

---

[5] P. Lambropoulos, P. Guenther, A. Smith and J. Whalen, Nucl. Phys. A201 (1973) 1.

[6] S. K. Penny, ORNL-TM-2590, Oak Ridge National Laboratory, 1969.

[7] W. E. Kinney, Nucl. Inst. and Meth. 83 (1970) 15 and private communication.

[8] W. E. Kinney, private communication (1975).

codes. The code "Genoa"[9] is available at the library of the Ohio University Computer and it allows to search for individual cases as well as for mixed cases.

Some of the obtained parameters for the (n,n) study at 11 MeV have been presented in Tables A-3 and A-4 with the corresponding fits in Fig. A-3 and A-4.

[9] F. G. Perey, private communication (1975).

B. REACTIONS INVOLVING OUTGOING NEUTRONS

1. The Structure of ^{98}Tc* (R. W. Finlay, C. McKenna,** J. R. Comfort† and D. E. Bainum)

Low-lying states in ^{98}Tc have been studied via the ^{98}Mo(p,n)^{98}Tc and ^{98}Mo(p,nγ)^{98}Tc reactions for proton energies between 2.4 and 4.2 MeV. Gamma ray decay schemes have been deduced from measurements of the gamma ray excitation functions, (n,γ) coincidences and (γ,γ) coincidences. Additional information was obtained from the study of the ^{97}Mo(^{3}He,d)^{98}Tc reaction at E_{3He} = 19 and 23 MeV and the ^{97}Mo(d,nγ)^{98}Tc reaction at E_d = 4 MeV. The present study provides evidence for at least 23 states below 700 keV excitation energy. No gamma ray transitions to the (6^+) ground state of ^{98}Tc were observed in the (p,nγ) reaction, but 33 gamma ray transitions were assigned. Structure of the low-lying states is discussed in terms of the anticipated shell model configurations. Candidates are suggested for each member of the $(\pi g_{9/2})(\mu d_{5/2})^{-1}$ and $(\pi p_{1/2})(\mu d_{5/2})^{-1}$ multiplets (Nuclear Physics, in press).

* Supported in part by U. S. ERDA.

** Present address: IBM Laboratories, Fishkill, New York.

† Present address: Indiana University Cyclotron Facility, Bloomington, Indiana.

2. The ^{14}C(p,n)^{14}N Reaction* (R. W. Finlay, H. Weller,** R. Blue** and G. Doukellis)

In order to investigate properties of levels at high excitation energy in ^{15}N, the ^{14}C(p,n)^{14}N reaction was studied for incident proton energies from 3.7 to 7.3 MeV. Preliminary angular distributions for outgoing neutron groups corresponding to the ground state and first excited state (2.313 MeV) in ^{14}N were measured using five simultaneous time-of-flight detectors. The target consisted of an 80 μg/cm^2 deposit of ^{14}C on a thin Ni foil backing. Neutron detector efficiency was determined by measuring the yield from the ^{7}Li(p,n)^{7}Be reaction for the same range of outgoing neutron energies. Preliminary analysis has been confined to the region $5.0 \leq E_p \leq 5.6$ MeV.

---

* Supported in part by the Ohio University Research Committee.

** Physics Department, University of Florida, Gainesville, Florida.

3. Inelastic Scattering of Fast Neutrons* (D. E. Bainum, R. W. Finlay, J. D. Carlson,** J. Rapaport and J. R. Comfort†)

The Ohio University time-of-flight spectrometer has been used to measure inelastic scattering of fast neutrons from nuclei. Approximately 20 angular distributions have been measured at flight paths between 6 and 11 meters. The T(d,n)He and D(d,n)^{3}He reactions were used to produce 26 and 11 MeV neutrons, respectively. Only a few cases have been analyzed to the extent that flux attenuation and multiple scattering corrections have been completed. One case has been reported.

Existing measurements can be classified in four categories:

a. Double-Closed-Shell Nuclei

The ^{208}Pb(n,n')^{208}Pb reaction has been measured at 11 and 26 MeV and ^{40}Ca(n,n')^{40}Ca has been measured at 11 MeV. Scattering samples consisted of natural calcium (97% ^{40}Ca) and isotopically enriched Pb (99.75% ^{208}Pb). Analysis of these measurements in terms of current microscopic theories of inelastic scattering is in progress.

b. Single-Closed-Shell Nuclei

(n,n') measurements have been made on ^{90}Zr and ^{92}Mo at 11 MeV. The remaining N = 50 nuclei (^{88}Sr and ^{89}Y) will be studied in the near future. Measurements are also planned for the Z = 50 region as soon as the separated isotope samples can be obtained.

c. Further Study of the Mass 90-100 Region

The Mo isotopes have been described as a transition region, ^{92}Mo being a single-closed-shell nucleus and ^{100}Mo showing somewhat more collective behavior. Differential cross sections for the lowest 2^+ and 3^- states in ^{92,96,98,100}Mo plus ^{90,92}Zr have been measured and will be analyzed in this spirit.

d. T = 0 Nuclei

Inelastic scattering to the lowest 2^+ states in ^{28}Si and ^{32}S have been measured at several energies. These reactions are technically somewhat easier to study. They provide a useful test of time-of-flight and data reduction methods since, being T = 0 nuclei, they should be free of any isospin-dependent effects. The importance of coupled-reaction-channel effects might also be studied in these cases.

---

* Supported in part by the National Science Foundation.

** Present address: Crocker Nuclear Laboratory, University of California, Davis, California.

† Present address: Indiana University Cyclotron Facility, Bloomington, Indiana.

4. A Thick, Time-Compensated Scintillation Detector for Fast Neutrons* (J. D. Carlson** and R. W. Finlay)

In an effort to improve the detection efficiency for 26 MeV neutrons in elastic and inelastic neutron scattering experiments, a thick, large-area time-compensated, liquid scintillator has been designed, built and tested. An 18 cm diameter x 25 cm thin-walled acrylic tube is joined to tapered acrylic end pieces. The tube is filled with 7.25 liters of NE 224 liquid scintillator. The tapered end sections are machined to fit the convex surface of the photocathode envelopes of RCA 4522 photomultipliers which view the cell from both ends. The detector is intended to detect neutrons traveling parallel to the cell axis since the entire assembly is placed inside an existing neutron shield. Thus it is necessary for the neutron to travel through one photomultiplier and tube base before entering the sensitive volume. Photons generated at the point of interaction inside the scintillator travel to the front and rear faces of the scintillator where they generate pulses in the two photomultipliers. These pulses can be processed in such a manner that an output timing pulse is generated which is compensated for the variations in flight path caused by the 39 cm length of the sensitive volume of the detector. This detector has an efficiency for 26 MeV neutrons approximately 3¼ times greater than that of a standard 5 cm thick Ohio University scintillation detector operated at the same threshold with approximately the same time resolution (to be submitted to Nuclear Instruments and Methods).

---

* Supported in part by the National Science Foundation.

** Present address: Crocker Nuclear Laboratory, University of California, Davis, California.

C. STRUCTURE STUDIES OF LIGHT NUCLEI, $7 \leq A \leq 12$

1. A Neutron T.O.F. System for Measurement of Elastic Differential Cross Sections (R. M. White, H. D. Knox and R. O. Lane)

a. Experimental Design

A neutron T.O.F. spectrometer with associated support system has been developed for rapid measurements and data reduction of neutron elastic differential cross sections with particular emphasis on the light nuclei $7 \leq A \leq 12$. Peculiar to these nuclei is the problem of energy loss of the elastically scattered neutrons due to the kinematics of scattering off very light scatterers. For example, a 4.00 MeV neutron incident on ^6Li will have only 2.07 MeV of energy after elastically scattering 160°. Therefore a larger dynamic range of neutron energies is encountered at various spectrometer angles even for a small range of incident neutron energies. If the neutron detector system is to be biased such that the lowest energy neutrons are detected with good efficiency a well-shielded detector is necessary. Further, if data are to be acquired at a reasonably rapid rate a high current machine coupled to a prolific source of monoenergetic neutrons, a neutron detector of large solid angle, and larger size scattering sample are desirable. However, the larger sample size then requires that accurate codes exist to correct for finite sample size effects. To these ends the Ohio University neutron T.O.F. spectrometer and data reduction system have been developed.

Neutrons are provided by a pulsed proton beam of approximately 4.5 μamps, 0.8 ns width and 5 MHZ repetition rate incident upon a tritium gas cell. The $T(p,n)^3He$ reaction provides a prolific monoenergetic source of neutrons to well beyond 8 MeV with a gas cell pressure of 18 psi. This pressure introduces an energy spready of ± 20 to ± 40 keV in the neutron burst. Scattering samples are cylindrical in shape with sizes approximately 4 cm high by 3.4 cm diameter and are isotopically enriched for ^6Li, ^{10}B and ^{11}B.

The neutron detector is NE 224 liquid scintillator housed in a 5 cm thick x 18 cm diameter lucite container optically coupled to an RCA 4522 PMT. The detector shield consists of 8 inch I.D. 1 inch thick steel pipe around which is a 3 inch thick lead annulus 30 inches long in the region of the scintillator and a 2 inch thick lead annulus 24 inches long extending forward along the pipe. This represents over 1000 pounds of steel and 2000 pounds of lead shielding. Placed around the lead is 1750 pounds of steel shot and outside of that 1000 pounds of paraffin (above 5 MeV the inelastic scattering of neutrons by iron allows it to compare well with hydrogen as neutron shielding material). The total weight of the system neglecting the massive copper shadow bar and support is over 7000 pounds. Use of an air pad system allows movement of the shield by one person. The massive copper shadow bar can be repositioned accurately for different scattering angles and allows wide collimation to the sample. Nine angles are normally measured from 20° to 160° with a neutron flight path of 3.6 meters.

b. Data Reduction Program

One of the most difficult problems in obtaining accurate results from angular distribution measurements is in determining the absolute efficiency of the neutron detector. For the energy range of interest in the present measurements a method has been developed which involves a relative efficiency determination and use of the well-known zero-degree cross sections (absolute yields) for the $T(p,n)^3He$ reaction. These absolute cross sections are known to 2½% and the data reduction program for this experiment utilizes only ratios, i.e., $\sigma(0°,E'_p/\sigma(0°,E_p)$ of these yields which really involves only the relative shape of the curve and that is known to an even better degree. For optimum results in terms of electronic bias settings, voltage ranges of equipment, etc., the measurements are usually carried out in three energy ranges between 4.0 and 8.0 MeV. A relative efficiency run is made for each energy range with the detector at 0° and the monitor at an angle (25°) which remains fixed during both the relative efficiency run and actual data taking. The relative efficiency runs use charge normalization which have been demonstrated to have an accuracy of 1%. The actual data are normalized to monitor counts and the final formula for cross section involves integrated detector and monitor counts, ratios of zero degree cross sections for the $T(p,n)^3He$ reaction, and ratios of relative efficiency measurements for monitor and detector.

The use of a reasonably simple program for reduction of counts to absolute cross section lends itself nicely to a fully automated data reduction system. The neutron T.O.F. spectra for both detector and monitor are accumulated in a MCA and transferred to disk on the laboratory's IBM 1800 computer. A panel of switches allows introduction of various experimental parameters--for example, the accelerator NMR freq., tritium gas cell pressure, run length in accumulated charge, angle of scattering, sample measured, etc. The on-line data reduction program then calculates all kinematics, calls up relevant relative efficiency information, analyzes monitor and detector spectra for dead time corrections, etc., formulates a substracted spectra (sample in-sample out), picks integration channels, makes various corrections for finite geometry, attenuation of incident flux, etc., and presents final cross sections in both lab and cm frames to the control room typewriter in a few seconds. Further, a CRT displays all spectrum analysis that the computer performs on a given energy-angle measurement for visual inspection by the investigator. A full computer log of information is printed on the various experimental parameters and all the above information is transferred to magnetic tape should further off-line data analysis be required. With this system a complete angular distribution can be taken in 4 to 12 hours, depending on the specific nucleus, with final cross sections obtained immediately. While rapid accumulation and reduction of data is desirable for many reasons, the most important benefit comes in allowing an investigator to stay completely on top of his experiment. Accuracy of the system is verified by measurement of certain well-known angular distributions on ^{12}C and from integration of the elastic differential cross section below the inelastic threshold. Further, measurements are taken on polyethylene and compared to the well known H(n,n)H cross sections. The system was designed and maintains accuracy of measurements to within 5 to 6%.

c. Multiple Scattering Corrections

The multitude of problems normally existing with proper and accurate multiple scattering corrections are further complicated on very light nuclei because the energy of scattered neutrons may be considerably less due to kinematic shift and significant resonance structure may exist in the neutron cross section to be corrected. Further, the energy resolution of the T.O.F. system can change from forward to backward angles for a fixed flight path and fixed incident energy and multiple scattering corrections are, of course, sensitive to this energy resolution. In the data reduction program discussed above we have adopted A. B. Smith's Monte-Sample Multiple Scattering Code from ANL. The code has been extensively rewritten to speed up the long Monte-Carlo process and has been checked through more than 45 hours of IBM 360/44 computer time. Plots have been made from 500k to 3M histories vs. correction factors to assure convergence of the corrections per angle and many test cases run on this revised code.

The code will handle elastic and inelastic scattering and reactions, and takes as input information a total cross section library (50) and an angular distribution library (25) and therefore includes energy-dependence of differential cross sections of multiple events necessary for these very light nuclei. The code also employs an energy resolution quantity determined by the T.O.F. system as input information. The code as it has been rewritten at Ohio University runs approximately five times faster than the original Argonne code and while running times vary significantly with sample size, transmission, etc., the code will do on a sample of 80% transmission approximately one million histories in 45 minutes on an IBM 360/44 computer.

The multiple scattering corrections are then applied automatically to the angular distribution by the laboratory's IBM 1800 and finalized data cards are punched out for printing up tables of data for the various nuclei. As the multiple scattering corrections for three distributions can be run overnight, the finalized corrected data on a particular angular distribution can be made available within 24 hours of the measurement of the distribution.

2. <u>Measurements of Differential Elastic Neutron Scattering Cross Sections on ^{10}B, ^{11}B, ^{6}Li and ^{7}Li in the Energy Range 4 MeV $\leq$ $E_n \leq$ 8 MeV</u> (R. O. Lane, R. M. White and H. D. Knox)

Very extensive data have been obtained for differential elastic scattering cross sections for ^{10}B, ^{11}B, ^{6}Li and ^{7}Li from 4 MeV to 8 MeV. The multiple scattering corrections are being completed now and the final data will be presented at the upcoming meetings listed below:

a. Differential Cross Sections for 4.0 to 8.0 MeV Neutrons Scattered from ^{10}B and ^{11}B (R. M. White, H. D. Knox and R. O. Lane)

The ^{10}B and ^{11}B data will be presented at the American Physical Society Meeting in Washington, D.C., April 26-29, 1976, as described by the following abstract:

Differential Cross Sections for 4.0 to 8.0 MeV Neutrons Scattered from ^{10}B and ^{11}B* (R. M. White, J. M. Cox,** H. D. Knox and R. O. Lane)

Neutrons produced by the $T(p,n)^{3}He$ reaction with the Ohio University Tandem Van de Graaff were scattered from enriched samples of ^{10}B (92.3%) and ^{11}B (97.2%). Nine angles were measured from 20° to 160° by time-of-flight methods with a 3.6 meter neutron flight path. Over 50 angular distributions for ^{11}B and 25 for ^{10}B were obtained at energies of 4.0 to 8.0 MeV where data are very scarce because these energies are not practical for neutron work on most accelerators. Results, corrected for attenuation, finite geometry, air scattering, and multiple scattering, show slowly varying cross sections in ^{10}B and little resonance structure. However, ^{11}B shows evidence of considerable interfering resonance structure above 5.0 MeV with large d-wave contributions.

---

* Work supported by U. S. ERDA.

** Present address: Owens-Corning, Granville, Ohio.

b. Elastic Scattering of 4 MeV to 7.5 MeV Neutrons from ^{6}Li and ^{7}Li (H. D. Knox, R. M. White and R. O. Lane)

The ^{6}Li and ^{7}Li data obtained recently up to 5.25 MeV are currently being extended up to 7.5 MeV to form good overlap with other groups, e.g., the Duke results which go up from 7.5 MeV. All the data on ^{6}Li and ^{7}Li will be presented at the 1976 International Conference on the Interactions of Neutrons with Nuclei, July 6-9, 1976, at the University of Lowell, Massachusetts. An abstract on this is given below:

Elastic Scattering of 4 to 5.25 MeV Neutrons from ^{6}Li and ^{7}Li* (H. D. Knox, R. M. White and R. O. Lane)

The differential cross sections of neutrons elastically scattered from ^{6}Li and ^{7}Li have been measured for incident neutron energies between 4 and 5.25 MeV at approximately 250 keV intervals. A pulsed proton beam, approximately 0.8 ns burst width, from the Ohio University tandem accelerator incident on a tritium gas cell provided the source of neutrons. The ^{6}Li scattering sample was enriched to 96% ^{6}Li, while the ^{7}Li sample was normal lithium having 92.6% ^{7}Li. Both metallic samples were encased in thin aluminum cans. Measurements were made at nine equally spaced laboratory angles between 20° and 160°, using time-of-flight methods. The neutron detector was a 5 cm thick by 18 cm diameter NE 224 scintillator coupled to an RCA 4522 photomultiplier tube and was located 3.6 meters from the scatterer.

In the case of scattering from ^{7}Li, it was possible at some angles to resolve neutrons inelastically scattered to the 0.478 MeV level in ^{7}Li from the elastically scattered neutrons. Corrections for attenuation, air scattering, isotopic abundance, finite geometry and multiple scattering have been made. The results show slowly varying cross sections with little resonance structure for both ^{6}Li and ^{7}Li in this energy range.

* Work supported by U. S. ERDA.

c: Structure Studies of Light Nuclei (R. O. Lane, R. M. White and H. D. Knox)

The results for differential elastic scattering of neutrons from ^{10}B, ^{11}B, ^{6}Li and ^{7}Li will be discussed at the Lowell Conference in terms of information on nuclear structure and possible reaction mechanisms. The abstract for that paper follows:

Structure Studies of Light Nuclei $7 \leq A \leq 12$ from Elastic Scattering of Neutrons* (R. O. Lane, R. M. White and H. D. Knox)

The Ohio University tandem accelerator was employed to produce neutrons via the reaction $T(p,n)^{3}He$ in the range 4 MeV $\leq E_n \leq$ 8 MeV where only sparse scattering data exist for several of the light nuclei. Differential elastic scattering cross sections were measured in this range for ^{6}Li, ^{7}Li, ^{10}B and ^{11}B at 9 angles from 20° to 160° with time-of-flight techniques for a flight path of 3.6 m. The tritium gas cell used for the source introduced an energy spread of ± 35 keV. The detector was NE 224 liquid scintillator of 5 cm thickness and 18 cm diameter housed in a large collimator-shield rotated on air pads. Multiple scattering corrections include energy-dependence of the differential cross sections of multiple events necessary for these very light nuclei.

The coefficients B_L of Legendre polynomial expansions of the differential cross sections for ^{10}B show broad resonance behavior near $E_n \sim 4.2$ MeV and 7.5 MeV. For the 30 energies at which angular distributions were measured on ^{10}B the B_L for $L \geq 5$ were negligible.

The strong resonance structure present in the B_L for ^{11}B is much narrower and shows considerable interference effects between states. Contributions by resonant d-waves are large as would be expected in this energy region which contains the parents of the T = 1 analog states in ^{12}C of the giant dipole resonance. Angular distributions for ^{11}B were measured at 60 energies between 4 MeV and 8 MeV and again B_L for $L \geq 5$ were negligible. From R-matrix analyses of the data, properties of these states will be extracted. This yields information on particle-hole structure of ^{12}B expected in this region and affords a comparison with model calculations in the A = 12 system.

* Work supported by U. S. ERDA.

d. Polarization and Differential Scattering Cross Sections for Light Nuclei in the Energy Range $2.0 \leq E_n \leq 6.0$ MeV (H. D. Knox, R. O. Lane and R. M. White)

Development of a well-shielded detector system for simultaneous measurement of neutron polarizations and differential cross sections is nearing completion. The $^9Be(p,\vec{n})^9B$ reaction will be used as a source of polarized neutrons in these experiments. A beryllium target system, which allows a maximum of shielding to be placed between the neutron producing target and the neutron detectors has been developed.

A spin precession magnet used previously at ANL and capable of precessing neutrons up to 4.2 MeV by 180° has been obtained for use in these measurements. The magnet has since been accurately calibrated by mapping its magnetic field with a Hall probe as a function of applied current. For neutron energies above 4.2 MeV polarization measurements will be made using partial precession of the neutron spins--the magnet is capable of precessing 6 MeV neutrons by 150°.

The neutron detectors are RCA 4522 photomultiplier tubes and each will have a 4.5 in diameter by 2 inch thick NE 213 scintillator bonded to it. Unusually long delays in delivery ($\sim$ 9 months) of these scintillators, caused partially by damage in shipment has slowed progress on development of this system.

Each detector is housed in a massive neutron shield that can be used for scattering angles between 30° and 130°. These wedge-shaped shields are each constructed of approximately 1000 pounds of paraffin and 1000 pounds of lead. The detector is located inside a long lead collimator approximately 2½ inches thick which is in turn surrounded by paraffin. These shields afford excellent neutron and gamma ray shielding throughout the range of neutron energies of interest here. This consequent large reduction of background has allowed successful use of pulse shape discrimination techniques which further enhances signal-to-noise ratios. Currently work is underway to adequately shield the neutron detectors from the fringing fields of the spin precession magnet.

The completion of this system will give this laboratory a unique capability allowing the simultaneous measurement of neutron differential cross sections and polarizations in an energy range where these measurements are quite difficult and the data are sparse. The A = 10 system will first be studied via $^{9}Be(\vec{n},n)^{9}Be$ and this will be followed by studies of the isotopes of lithium and boron.

D. UNBOUND STATES IN ^{27}AL

1. Multilevel Multichannel Study of the Structure of ^{27}Al from 13 to 15 MeV Excitation Energy (G. Doukellis, R. D. Koshel, J. Rapaport)

Unbound states in ^{27}Al between 13 and 15 MeV excitation energy, have been studied by means of the $^{26}Mg(p,p)^{26}Mg$, $^{26}Mg(p,p')^{26}Mg^{*}$ (1.81 MeV state), $^{26}Mg(p,n)^{26}Al$, $^{23}Na(\alpha,\alpha)^{23}Na$ and $^{23}Na(\alpha,n)^{26}Al$ reactions. The measured excitation functions reveal 34 resonances in this energy region. The data from 13.3 to 14.1 MeV were fitted using a multilevel multichannel R-matrix formalism, with background phase shifts evolved from an optical model potential. These fits produced a set of level parameters for 16 resonances in this energy region. The levels at E_x = 13.66 and 13.72 MeV in ^{27}Al have been identified as isobaric analog states of the E_x = 6.84 and 6.91 MeV levels in ^{27}Mg. A comparison of the $^{26}Mg(p,x)$ and $^{23}Na(\alpha,x)$ excitation functions, indicates that the resonances observed between 13.6 and 14.2 MeV have isospin T = 3/2, and the resonance at E_x = 14.83 MeV, T = 1/2. In addition, evidence of isospin mixing is found for levels at E_x = 14.27 and 14.47 MeV (to be published).

RENSSELAER POLYTECHNIC INSTITUTE

A. NEUTRON CROSS SECTION MEASUREMENTS

1. Neutron Capture and Transmission Measurements on ^{101}Ru, ^{102}Ru, ^{104}Ru, ^{145}Nd and ^{149}Sm

(R. W. Hockenbury, W. Koste, R. Shaw, R. H. V. Gallucci and W. Yip)

Measurements were made from ≈20 eV to 200 keV on these isotopes using the 1.25 m capture detector at 25 m. Resonance filters were left in the neutron beam at all times to improve the time-dependent background determination. The data were corrected for impurity, sample container, deadtime and background effects. The incident flux shape was measured. The capture cross sections were self-normalized to the resonance region by using both capture and transmission data. This method was straightforward for ^{101}Ru, ^{145}Nd and ^{149}Sm. For ^{102}Ru and ^{104}Ru, this resonance analysis revealed an average radiation width (≈60 meV) much smaller than reported elsewhere. This work has been completed and the results have been sent to the National Neutron Cross Section Center. In order to normalize the keV capture data, resonance parameters were obtained for a few levels in each isotope. The capture and transmission data analyses were combined for resonances with $\Gamma_n << \Gamma_\gamma$ to give a result almost independent of the radiation width for ^{101}Ru, ^{145}Nd, and ^{149}Sm. For ^{102}Ru and ^{104}Ru much less was known in advance about their average parameters. This made a more extensive analysis necessary in order to properly normalize the keV data. By using the resonance data and theoretical fits to the keV data, a radiation width of about 60 meV was determined for both ^{102}Ru and ^{104}Ru. This value is to be compared to 275 and 97 meV reported elsewhere[1] for ^{102}Ru and ^{104}Ru, respectively.

2. Neutron Capture and Transmission Experiments on ^{95}Mo, ^{97}Mo, ^{133}Cs and ^{143}Nd

(R. W. Hockenbury, R. H. V. Gallucci and W. Yip)

Capture and transmission experiments were made on the above isotopes using the 1.25 m capture detector and a ^{10}B-NaI neutron detector at 25 and 28 m, respectively to obtain the keV capture cross sections. Some resonance parameters have been obtained, primarily to normalize the capture cross sections. Most of the data reduction is complete. The capture results will be fitted using average ℓ-wave parameters.

3. Neutron-Induced Subthreshold Fission in ^{232}Th
(R. C. Block, J. R. Valentine, and R. W. Hockenbury)
(R. E. Slovacek, E. B. Bean and D. S. Cramer)

The ^{232}Th (n,f) cross section was measured from 1 eV to 100 keV with the RINS 75-ton lead-slowing-down spectrometer at the Gaerttner Linac Laboratory and the results are shown in Fig. A1. The measurement utilized a 2.2 cm d. by 22 cm long ionization chamber coated with 233 mg of high purity ThO_2 (<25 ppb ^{235}U). The ^{232}Th (n,f) cross section from 1 eV to 1 keV is smooth and can be fitted to a 1/v cross section that equals (95 ± 30) μb at 0.0253 eV. The cross section rises to a 7 μb peak at 2 keV, falls to ≈3 μb in the 8 to 80 keV region, and then rises sharply near 100 keV. The 1/v cross section is in rough agreement with the (60 ± 20) μb and (39 ± 6) μb thermal cross section reported respectively from the USSR and Mol, but in disagreement with the 4 μb upper limit recently reported from Grenoble. The absence of structure below 1 keV results in an upper limit of ≈0.5 x 10^{-9} eV for the fission width of the positive energy Th s-wave resonances. The peak at 2 keV is too weak to account for the 1/v low energy fission, and this peak can be interpreted as p-wave subthreshold fission or as a complex admixture of a class II state and a vibrational state. Similar arguments can be invoked to explain the ≈3 μb cross section at higher energies. The absence of structure below 1 keV and the weakness of the peak at 2 keV is interpreted as evidence for an s-wave subthreshold fission level below the binding energy. The lack of observation of s-wave subthreshold fission resonances below ≈100 keV is interpreted as a separation of over 3.1 MeV between the bottoms of well I and II.

4. ^{238}U (n,f) Measurements Below 100 keV*
(R. E. Slovacek, D. S. Cramer, E. B. Bean, R. W. Hockenbury, R. C. Block and J. R. Valentine)

The ^{238}U (n,f) cross section has been measured from 3 eV to ≈100 keV with the RINS 75-ton lead slowing down spectrometer at the Gaerttner Laboratory, and the results are shown in Fig. A2. Four fission ionization chambers containing a total of ≈0.8 gm of ^{238}U (4.1 ppm ^{235}U) were used for the measurements. The fission widths of the 6.67, 20.9, and the 26.8 eV resonances were measured as 10±1, (58±9), and (12±2) nanoelectronvolts respectively. By combining these fission results and published resonance parameters, the ^{238}U thermal fission cross section was determined to be 2.7±0.3μb. The resonance fission integral from 0.4 eV to 30 keV was determined to be (1.33 ± 0.15) mb.

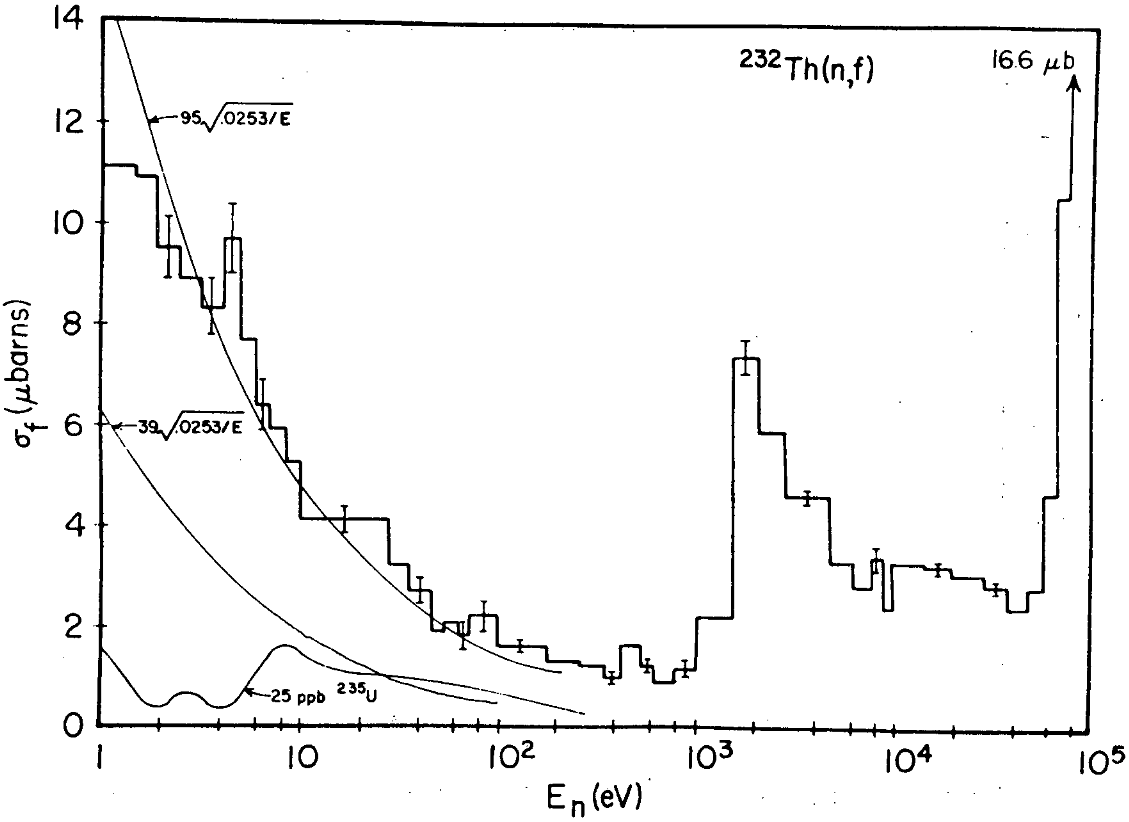

Figure A1. ^{232}Th fission cross section.

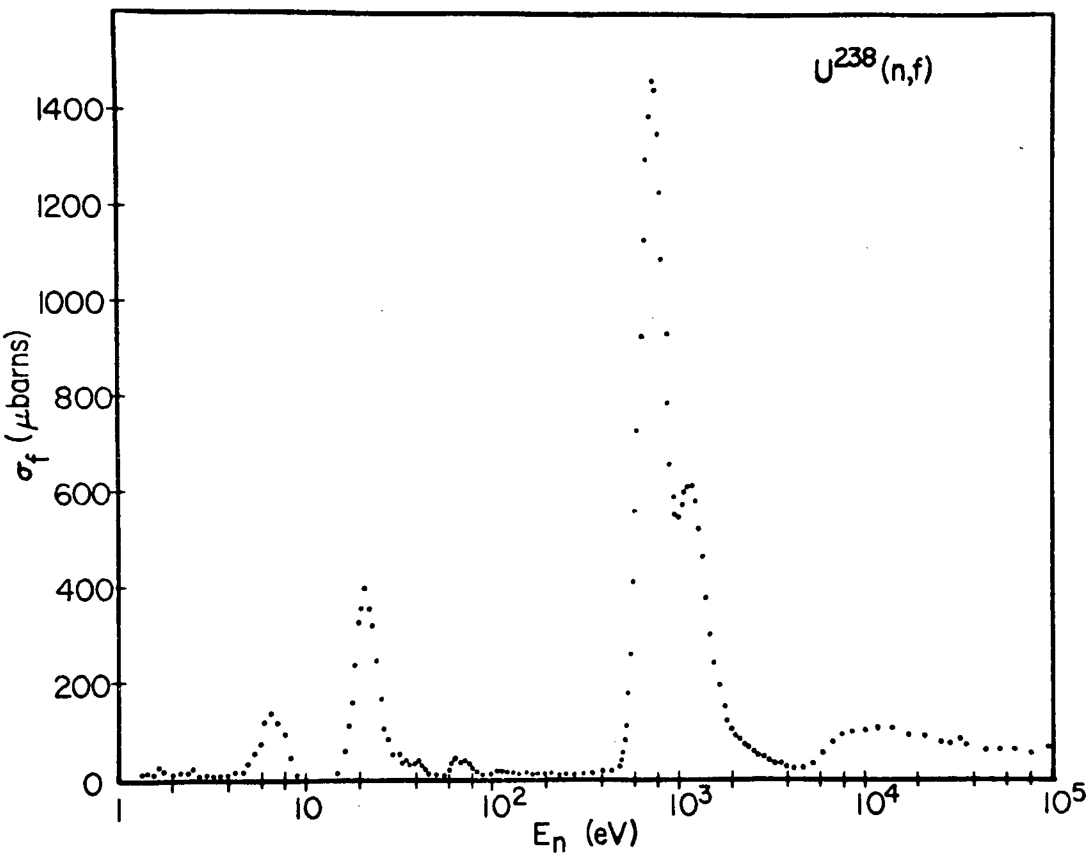

Figure A2. ^{238}U fission cross section.

5. The Neutron Total Cross Section of Sodium Near Minima
(R. C. Block, R. H. Brown,* B. L. Quan, and J. J. Weiss)

The neutron total cross section of sodium near the resonance-potential interference minima have been completed. The filtered-beam technique was used for these Na thick sample transmission measurements. A Na filter 62.2-cm or 93.3-cm thick was placed in a collimated neutron beam and a 31.1-cm-thick Na sample was cycled in and out of the beam. The experimental configuration is shown in Fig. A3. The thick filter resulted in a filtered beam containing mainly neutrons with energies near the deep minima.

The results for the total cross sections at the five deepest minima below approximately 3 MeV are listed in Table I and plotted in Figures A4 to A8, along with the values from ENDF/B-IV. The agreement is excellent in Table I between the RPI and ENDF/B-IV cross section magnitudes at the minima.

Although the magnitudes of the cross sections for all of the five deepest minima are in good agreement with ENDF/B-IV, the shape of the 297 keV minimum is in serious disagreement. The results plotted in Fig. 2 show that the RPI data result in a significantly wider minimum than ENDF/B-IV. For the application to the LMFBR with a thick layer of Na above the core, a wider minimum results in a significantly greater penetration of neutrons near 297 keV through the Na layer and into the top region of the reactor vessel. Since the cross section at the 297 minimum is much smaller than the cross section at the other minima, and since the LMFBR flux is very high near this minimum, we would expect the RPI data to predict a much higher flux of neutrons reaching the upper portion of the reactor vessel than would be predicted by the ENDF/B-IV data.

The shapes of the RPI minima are in better agreement with ENDF/B-IV for the higher energy minima plotted in Figures A5 to A8.

*Now at Nuclear Medicine Branch, Veteran's Hospital, Davis Park, Rhode Island

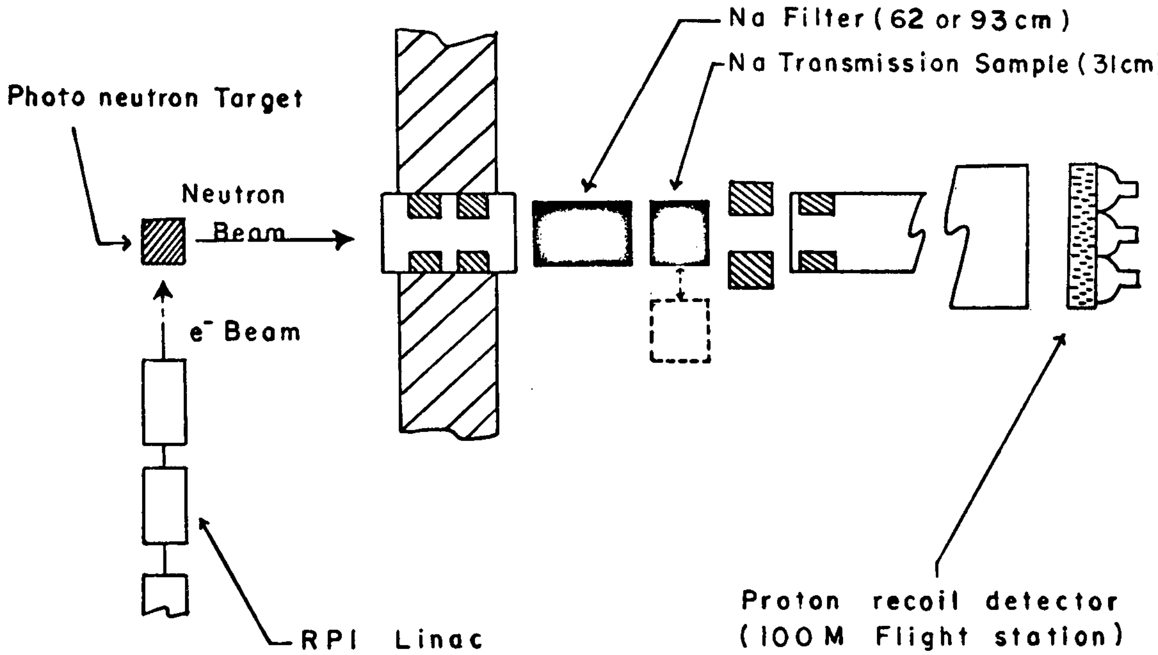

Figure A3. Experimental layout for the Na filtered-beam transmission experiment. The Na filter and Na transmission sample were approximately 10 meters from the photoneutron target.

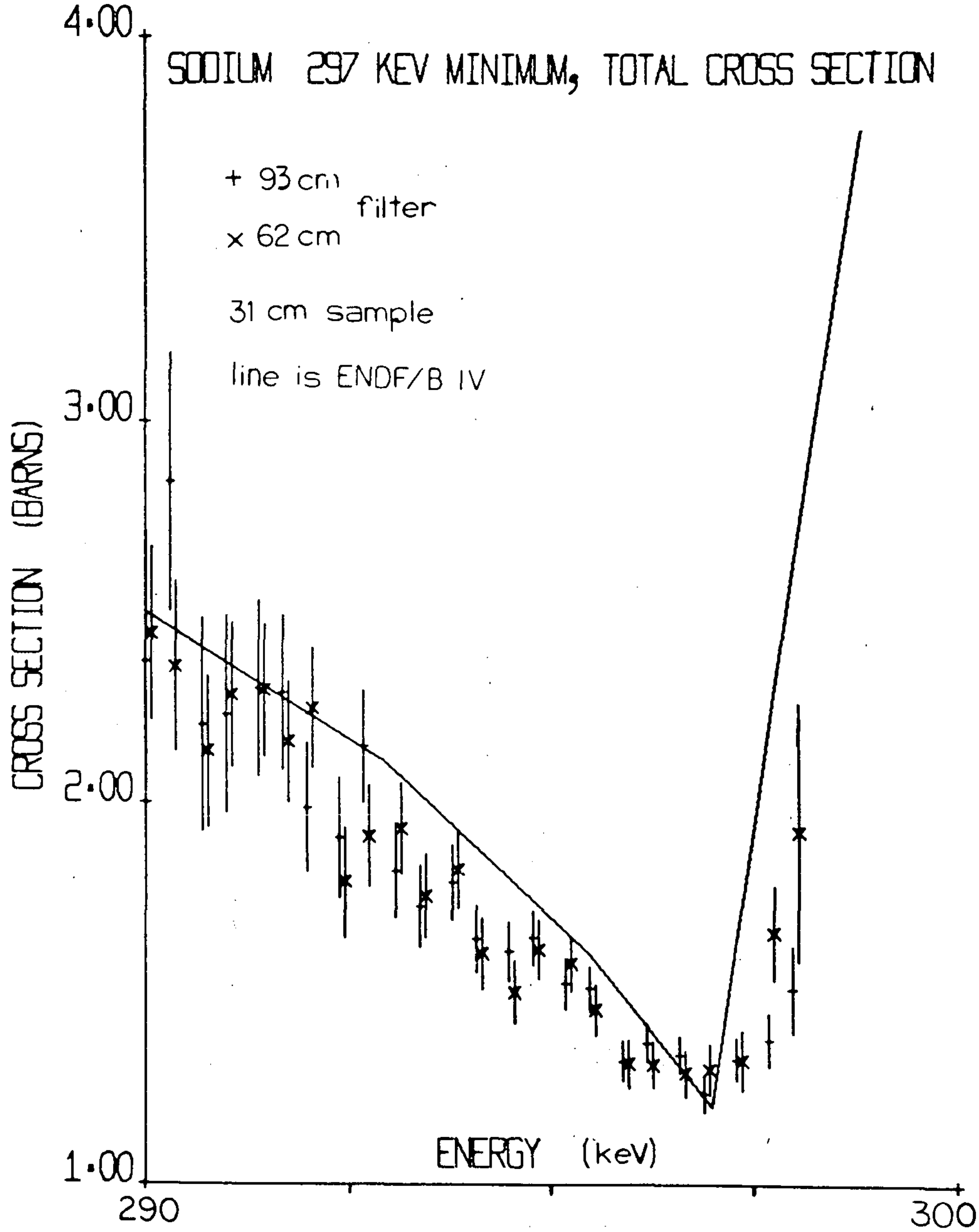

Figure A4. The neutron total cross section of Na at the 297 keV minimum.

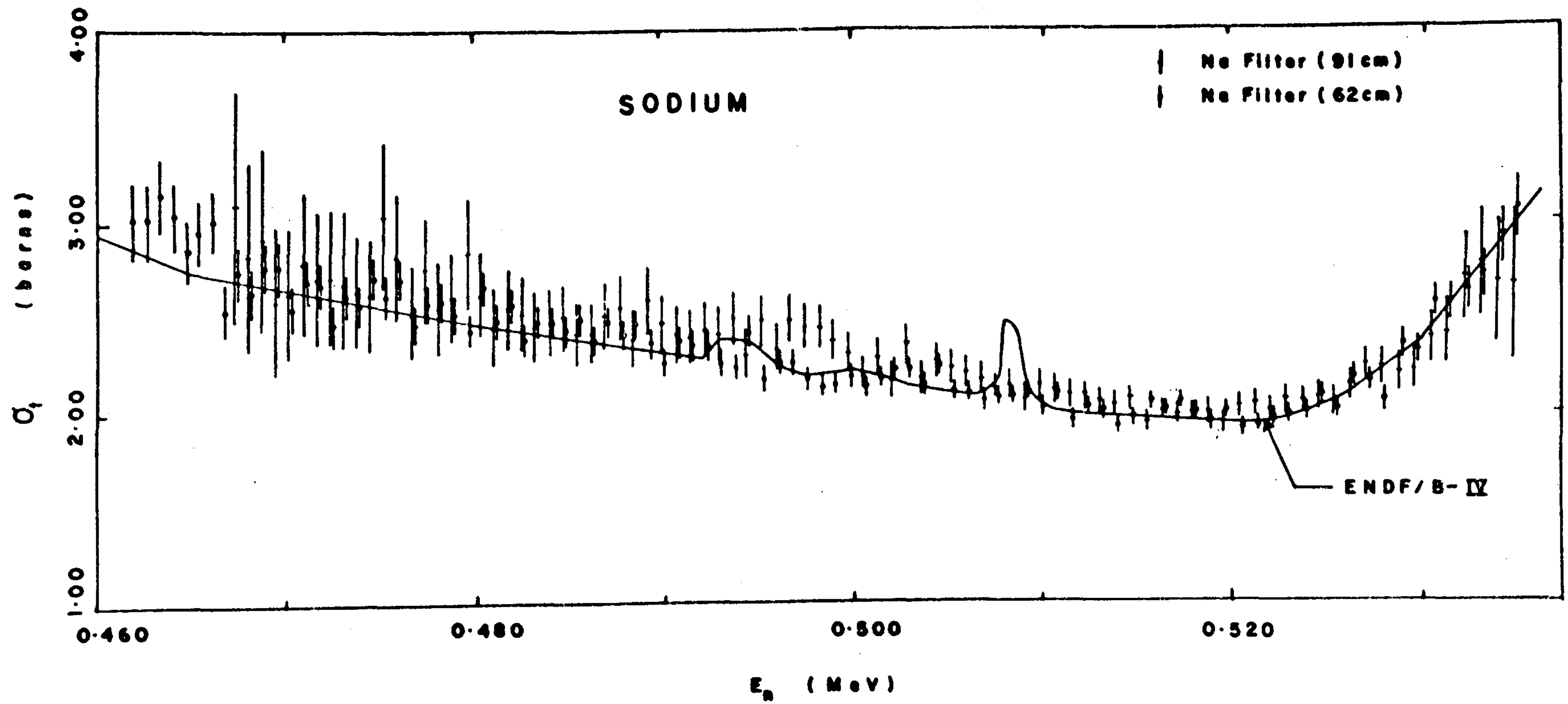

Fig. A5 The neutron total cross section of Na at the 521 KeV minimum.

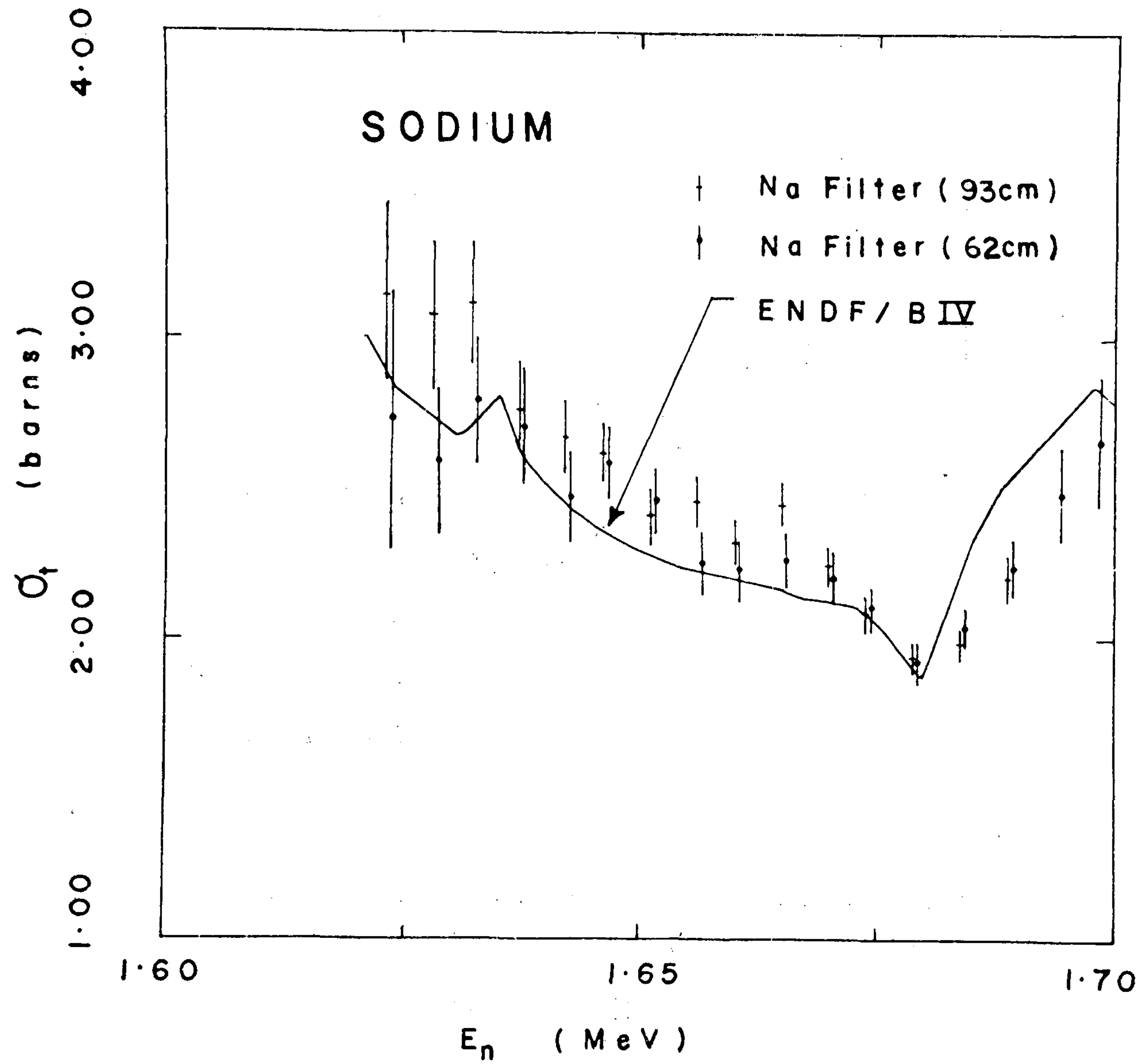

Figure A6. The neutron total cross section of Na at the 1.680 MeV minimum.

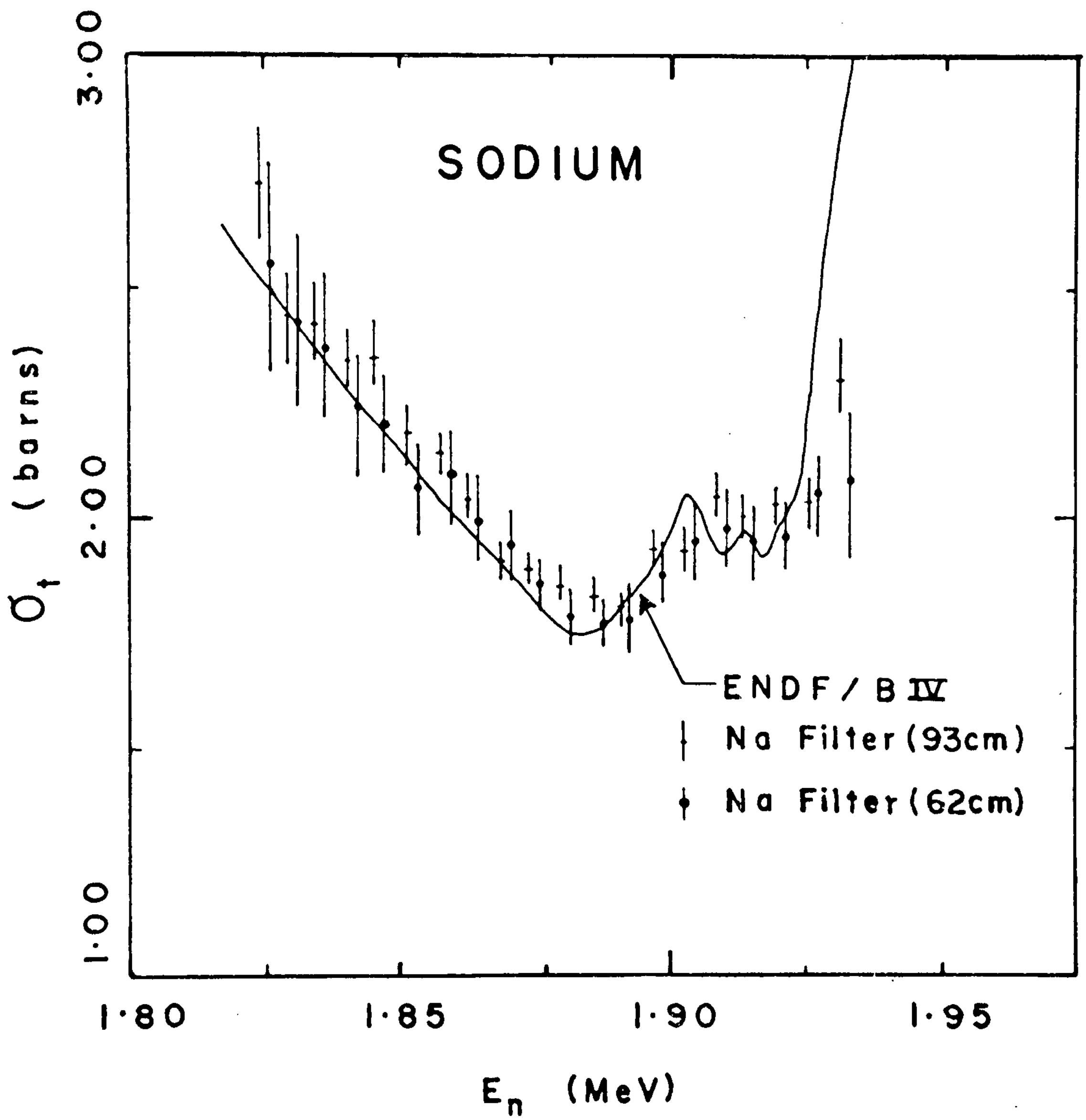

Figure A7. The neutron total cross section of Na at the 1.885 MeV minimum.

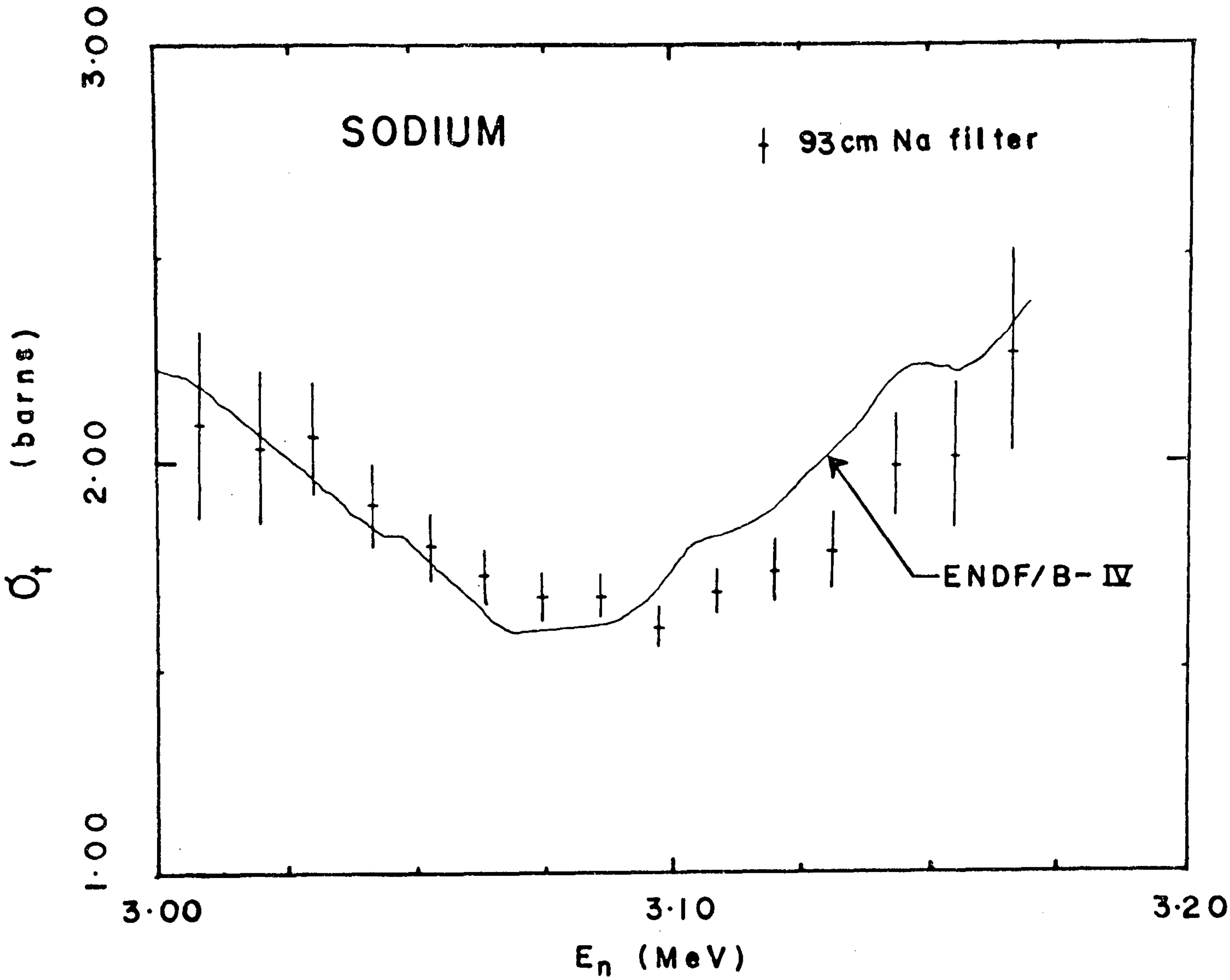

Figure A8. The neutron total cross section of Na at the 3.075 MeV minimum.

Table I

Energy at Minimum (MeV)	Total Cross Section at Minimum (barns)	
	RPI	ENDF/B-IV
0.297 ± 0.002	1.25 ± 0.05	1.20
0.521 ± 0.003	1.94 ± 0.04	1.96
1.680 ± 0.011	1.88 ± 0.05	1.86
1.885 ± 0.012	1.75 ± 0.05	1.72
3.075 ± 0.020	1.63 ± 0.05	1.58

6. The Measurement of the ^{238}U (n,γ) Cross Section with An Fe-Filtered Neutron Beam
(B. L. Quan, R. H. Pendt and R. C. Block (RPI)

The ^{238}U (n,γ) measurement was carried out at the Gaerttner LINAC Laboratory using a highly enriched sample of ^{238}U, the 1.25-m-dia. capture detector, the $^{10}B_4C$-NaI neutron flux detector, and a 20-cm-thick Fe filter in the neutron beam. The $^{238}U(n,\gamma)$ cross section was determined relative to the $^{10}B(n;\alpha, \gamma)$ cross section and to saturated capture at the 6.7 eV resonance in ^{238}U. The results for six energy regions below 200 keV are listed in Table II and are plotted in Fig. A9 along with the evaluated ENDF/B-IV data. E_L and E_U are the lower and upper energies of each band and E is the energy of the arithmetic mean of the flux within the band. The cross section errors are standard deviations resulting from counting statistics (0.8% to 4.6%), background uncertainty (0.2% to 5%) and an overall normalization error of ≈3%. This normalization error is dominated by the relative uncertainty in the capture detector efficiency at 6.7 eV; it represents the limiting error for this type of measurement.

The ENDF/B-IV data fluctuate equally above and below ≈100 keV, and the agreement here is reasonable. Above ≈100 keV the evaluated data are consistently larger, and consideration should be given toward lowering the evaluated data in this region.

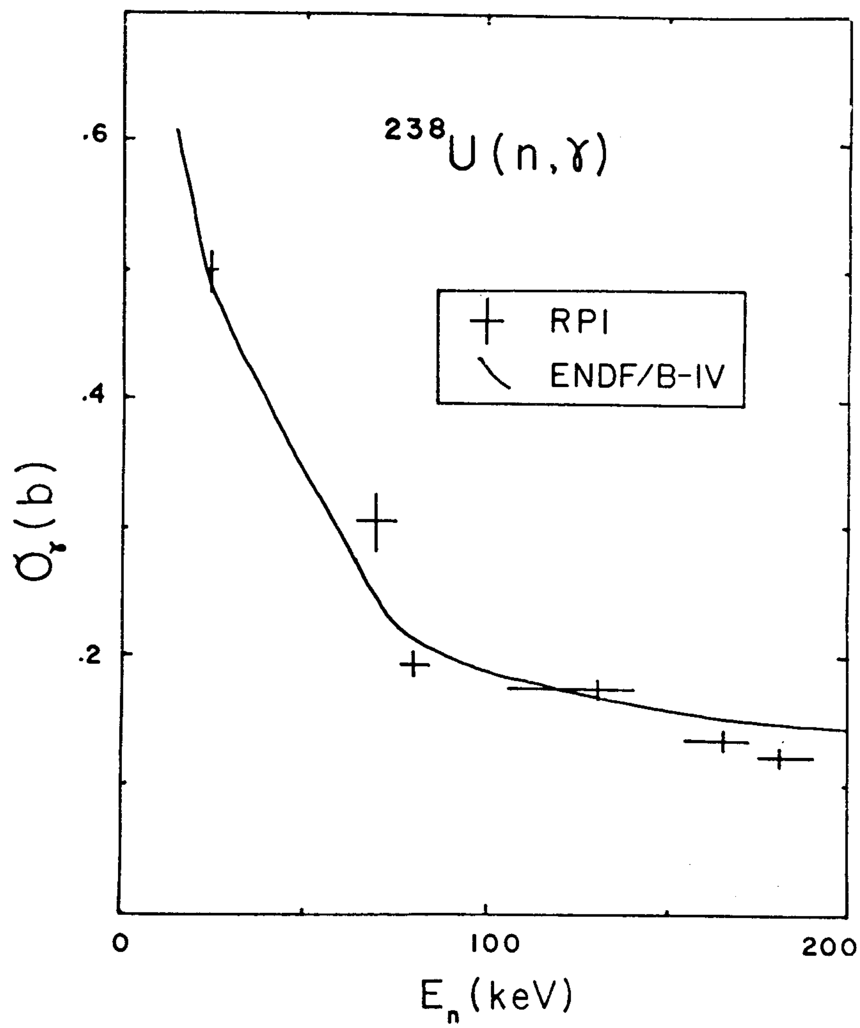

Figure A9. ^{238}U capture cross section.

Table II

Fe-Filtered Beam ^{238}U (n, γ) Cross Section

E_L (keV)	E_U (keV)	$\hat{E}$ (keV)	σ_γ (mb) RPI	σ_γ (mb) ENDF/B-IV*
23.6	26.0	24.3	499 ± 15	488
64.5	75.7	69.8	304 ± 22	247
76.5	84.9	80.3	193 ± 10	315
106.7	141.7	131.0	174 ± 7	169
155.3	173.1	165.9	134 ± 8	152
175.6	190.9	181.4	121 ± 7	147

7. Temperature-Dependent Self-Indication Measurements in ^{238}U **

(K. Kobayashi, J. Lonsdale, S. Petrossi, L. Der Gurahian, D. Harris, and R. C. Block)

A series of ^{238}U self-indication measurements were undertaken with the 1.25-meter diameter capture detector to shed light upon the resonance parameters of the low energy ^{238}U resonance parameters, particularly those resonances which contribute most strongly to the heavily self-shielded resonance integral in thermal reactor lattices. Measurements have been completed with the shielding (transmission) samples at room temperature and at 78°K and the apparatus is being prepared for ≈1000°K. The data extend from approximately a few eV to 3000 eV, and the raw data are being reduced to yields (captures per incident neutron).

A program RPIFIT is being written to analyze these yields in terms of ENDF/B resonance parameters and to determine many-level resonance parameters from the combined set of measurements at different temperatures and sample thicknesses.

*Determined at $\hat{E}$.

** Supported by the Electric Power Research Institute

B. INTEGRAL CROSS SECTION CALCULATIONS AND THEORY

1. Sensitivity of Uranium Spectra to Inelastic Matrix Perturbation (Ansar Parvez and Martin Becker)

Substantial discrepancies exist between measured and calculated spectra in depleted uranium.[1-5] These discrepancies have persisted through all ENDF/B files. Recent interactive graphic investigation[6] has indicated how the total inelastic cross-section may be modified to bring measurement and calculation into better agreement. While the modified inelastic cross-section thus obtained was able to remove high energy spectral discrepancies very readily, greater difficulty was experienced in removing low-energy discrepancies while using only the total inelastic cross-section. In addition, recent experimental results indicated that low level partial cross-sections might be higher than previously thought.[9] These results are opposite to what is required at low energies if only the total cross-sections are varied. This investigation was designed to vary the inelastic matrix to determine what types of plausible modifications could resolve low energy discrepancies.

To facilitate this investigation, the capability for interactive graphics modification was extended to handle a variety of matrix changes. (Previously,[6] it was possible to make changes only in the individual matrix elements). Interactively, the analyst specifies the types of changes he wishes to make. For example, changes can be made according to

a) ranges of source energies
b) ranges of sink energies
c) specific energy changes

At low energies, inelastic scattering is composed of a small number of discrete inelastic levels (e.g. 45 keV, 148 keV). The initial attempt at data adjustment concentrated on preferential low energy changes in individual levels, such as the 148 keV level, as a means of resolving the low energy discrepancy. It appeared to be very difficult to resolve the low energy discrepancies with plausible changes to discrete levels at low energies.

The effort then shifted toward modification of the inelastic matrix at high (above 2 MeV) energies. The objective of the interactive variation was to reduce the energy transfer to low energies while maintaining the type of total high energy cross-section obtained previously.[6] Particular emphasis was on achieving a substantial reduction of scattering to below 300 keV.

Table 1 indicates a sampling from a specific cross-section matrix modification that has been considered. It has been found that the type of modification most likely to explain the discrepancies observed would indeed involve a) total inelastic cross-section essentially as in Reference 6 at high energy, b) strong reduction (relative to ENDF/B-IV) of energy transfer from above 1 MeV to below 300 keV and c) moderate additional changes to obtain detailed agreement. To verify the conclusions based on interactive computations with approximate continuous slowing down theory (CSDT), the modified matrix of Table 1 was utilized in DTF-IV transport analysis[7] of the experiment. Results were essentially the same at energies of interest as with CSDT.

An analogous study has been performed recently, leading to analogous conclusions.[8] That study, this one, and recent differential measurements[9] appear to be consistent. While the interactive adjustment study reported here does not lead to a unique new data set, it does lead to a recommendation that evaluations for new ENDF/B files for uranium emphasize reductions in transfers from the MeV range to low energies. In this regard, it should be noted that, relative to integral experiment comparison, there is little practical difference between reducing total inelastic cross-section above 1 MeV keeping total cross-section constant, and maintaining the inelastic cross-section essentially constant by increasing the low level partial cross-section to compensate for the previously obtained reduction in total inelastic cross-section.

In summary, the capability for utilizing interactive graphics computing for direct data adjustment has been extended to facilitate studies of inelastic matrices, and has been applied to identify the type of data modification appearing most likely to resolve experiment-theory discrepancies. While this type of investigation does not yield a unique new data set, it does lead to a recommendation that evaluations for new ENDF/B files for uranium emphasize reductions in transfers from the MeV range to low energies.

TABLE I

SAMPLE MODIFIED INELASTIC MATRIX ELEMENTS (barns)*

	Group 13 1.73-1.53 Mev		Group 14 1.53-1.35 Mev		Group 15 1.35-1.19 Mev		Group 16 1.19-1.05 Mev	
	ENDF/B-IV	RPI	ENDF/B-IV	RPI	ENDF/B-IV	RPI	ENDF/B-IV	RPI
$\sigma_{i\rightarrow i+9}$	0.198	0.107	0.256	0.150	0.258	0.151	0.009	0.005
$\sigma_{i\rightarrow i+10}$	0.163	0.088	0.383	0.224	0.187	0.109	0.037	0.022
$\sigma_{i\rightarrow i+11}$	0.202	0.109	0.112	0.066	0.152	0.089	0.057	0.033
$\sigma_{i\rightarrow i+12}$	0.075	0.040	0.089	0.052	0.118	0.069	0.069	0.040
$\sigma_{i\rightarrow i+13}$	0.079	0.043	0.074	0.043	0.087	0.051	0.076	0.045
$\sigma_{i\rightarrow i+14}$	0.057	0.031	0.057	0.033	0.070	0.041	0.135	0.079
$\sigma_{i\rightarrow +15}$	0.041	0.022	0.034	0.020	0.088	0.052	0.061	0.036
$\sigma_{i\rightarrow +16}$	0.030	0.016	0.058	0.034	0.027	0.015	0.042	0.025

*Except for selected groups widths are equal to 1/8th of a lethargy unit.

References

1. N. N. Kaushal, B. K. Malaviya, M. Becker, E. T. Burns and E. R. Gaerttner, "Measurement and Analysis of Fast Neutron Spectra," Nucl. Sci. Eng. 49, 330 (1972).

2. M. Becker and N. N. Kaushal, "An Assessment of ENDF/B-III Data for Uranium-238 Based on Integral Spectrum Measurement," Nucl. Sci. Eng., 56, 307 (1975).

3. H. Bluhm, G. Fieg and H. Werle, "Evaluation of ^{238}U Neutron Cross-Section from Spectral Measurements," Nucl. Sci. Eng. 54, 300 (1974)

4. M. Becker and N. N. Kaushal, "An Assessment of Proposed $(\gamma,\gamma n')$ Data Based on Measured and Calculated Neutron Spectra in Uranium-235," Nucl. Sci. Eng., 53, 487 (1974).

5. R. Paviohi Corcuera, "Evaluation of Neutron Inelastic Scattering Cross Sections of Uranium-238 from Neutron Spectrum Measurements in Fast Media," Nucl. Sci. Eng., 58, 278 (1975).

6. A. Parvez and M. Becker, "Direct Data Adjustment for ^{238}U by Interactive Graphic Computing," Trans. Am. Nucl. Soc., 22, 717 (1975).

7. K. D. Lathrop, "DTF-IV, A FORTRAN-IV Program for Solving the Multi-group Transport Equations with Anisotropic Scattering," LA-3373, Los Alamos Scientific Laboratory (1965).

8. T. Choong and E. Kujawski, "The Importance of the ^{238}U Inelastic Transfer Matrix for Fast Reactor Analysis," General Electric Company Internal Memorandum, private communication, 1976.

9. P. Guenther, D. Havel, A. Smith, "Fast Neutron Excitation of the Ground State Rotational Band of ^{238}U, ANL-NDM-16, September 1975.

C. THERMAL HYDRAULICS STUDIES

1. Two-Phase Flow Phenomena in Nuclear Reactors
(R. T. Lahey)

An extensive research program is underway to: (1) develop accurate and reliable two-phase flow instrumentation, (2) develop an in-depth understanding of phase separation and distribution phenomena in nuclear reactor geometrics, and, (3) investigate transient parallel channel effects during hypothetical nuclear reactor accidents.

The data, analysis and instrumentation developed should make a significant contribution to the understanding of nuclear reactor performance and safety.

TRIANGLE UNIVERSITIES NUCLEAR LABORATORY

A. INTRODUCTION

This report to the ERDA Nuclear Data Committee is a summary of research at TUNL in areas of particular emphasis by ERDA at the present time. It has generally been excerpted from the TUNL annual progress report dated 31 December 1975, but where additional data are now available appropriate sections have been revised to reflect the new work. Those interested in other aspects of research being carried out at TUNL are referred to the annual report whose table of contents is attached as appendix 1.

B. NEUTRON AND FISSION PHYSICS

1. Fast Neutron Differential Cross Sections (F.O. Purser, C.R. Gould, P.W. Lisowski, C.E. Nelson, L.W. Seagondollar, P. Von Behren, H.H. Hogue, G. Glendinning, E.G. Bilpuch, H.W. Newson)

a. Experimental

The TUNL fast neutron time of flight facility has now been operational for approximately two years. An HVEC chopper/buncher system installed on the TUNL F.N. tandem provides a beam burst length on target of 1.5 to 2.5 nanoseconds for deuterons and 1 to 2 nanoseconds for protons. Our program thus far has utilized the $D(d,n)^3He$ reaction as the primary neutron source. The neutron target area beam line was constructed of all metal or ceramic components and is maintained in an ultra clean high vacuum state to hold to a minimum any hydrocarbon and/or silicate contamination of potential background producing surfaces. In addition beam transport solutions permit little or no beam interception in the target room except at the target gas cell itself. With these precautions, our primary neutron spectra are unusually free from extraneous neutron and gamma ray backgrounds and allow us to work with confidence with the $D(d,n)^3He$ reaction well above the onset of the D-D breakup reactions. The Q value difference between the breakup neutrons and the monoenergetic $D(d,n)^3He$ group produces an energy span of approximately 7 MeV over which, in the absence of any substantial competing backgrounds, we can make inelastic scattering measurements up to about 15 MeV incident neutron energy. A primary source spectrum at E_n=11 MeV is shown in Fig. 1.

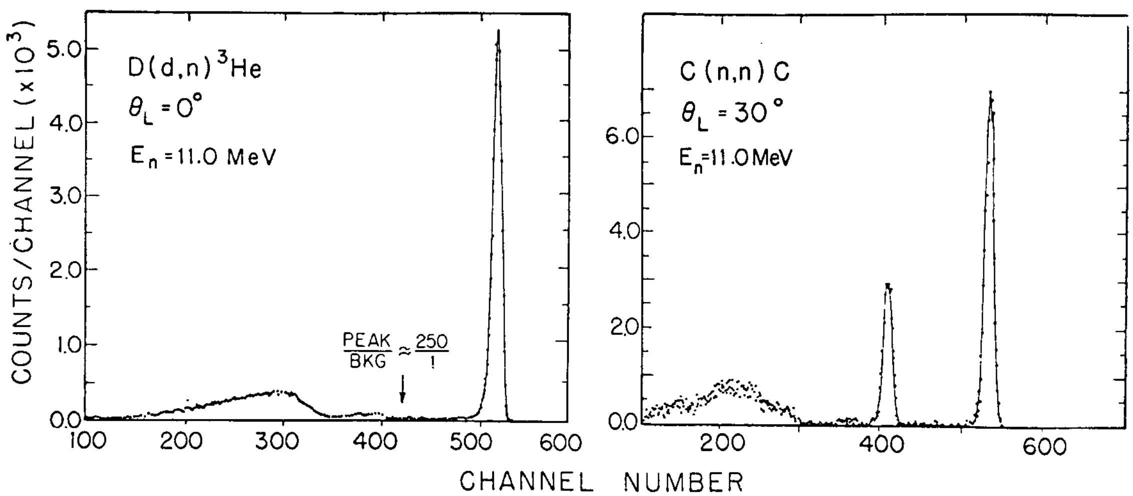

Figure A9. ^{238}U capture cross section.

The main neutron detector consists of an NE-218 liquid scintillator coupled to a bi-alkali photo multiplier and housed in a massive neutron shield which contains 6000 lb. of Cu and 10,000 lb. of a paraffin Li_2CO_3 mixture. The neutrons are collimated by a computer optimized, precision machined double truncated cone. The angular carriage for the detector is mounted on an elevated iron track which is coplanar to ±0.030" over the entire angular range of -20° to +165° for reaction studies and +25° to 165° for scattering experiments. In the present configuration the maximum flight path is 4 meters.

For scattering experiments, the incident neutron flux is monitored by a second time of flight detector mounted out of the scattering plane at a distance of two meters. For both detectors constant fraction timing and wide dynamic range n,γ pulse shape discrimination are utilized. The relative efficiency of the main detector has been determined for a neutron energy range from 2 to 15 MeV using well determined absolute differential cross sections for the $D(d,n)^3He$ reaction. Conversion of measured yields to absolute cross sections is performed using the measured relative efficiency and the results of an auxiliary (n,p) scattering experiment.

b. CTR Measurements

The principal thrust of the TUNL neutron time of flight program is to provide accurate elastic and inelastic neutron scattering cross sections for neutron energies from 9-15 MeV in support of the national CTR development effort. For the past year, approximately 25% of the total available accelerator time at TUNL has been devoted to this program. A neutron data group of 10 members has been formed with half this number working full time on the program. For the other members, data taking, analysis and support of the neutron effort is a major (or 50%) obligation on their time.

CTR related studies undertaken during the present report period are detailed below.

(1) Natural Carbon (USNDC-6, USNDC-CTR-1, Sec. 5)

Analysis of these data was completed during this period. The measurements consisted of 15 angular distributions of at least 28 points taken at 5° increments except in the vicinity of diffraction minima which were defined in 2.5° steps. The elastic and inelastic (Q = -4.439 MeV) data span the energy range from 9.0 to 15.0 MeV. Relative uncertainties in the measured cross sections are typically 2-3% and normalization uncertainties in converting to absolute cross sections range from 3 to 5%. Where available, small angle ($\theta_L < 15°$) data have been added to the data set to obtain well determined total elastic

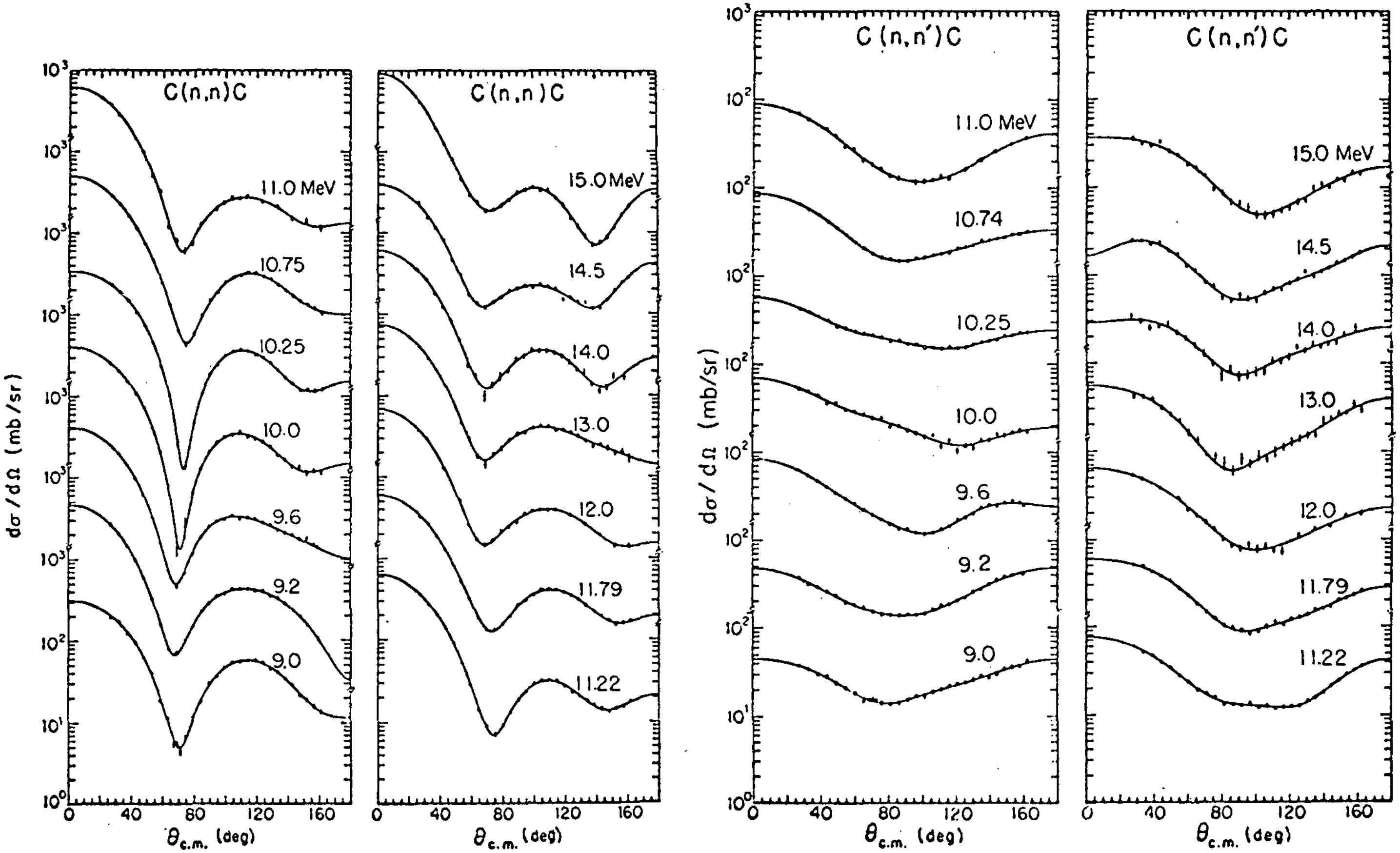
C(n,n)C
11.0 MeV
10.75
10.25
10.0
9.6
9.2
9.0
C(n,n)C
15.0 MeV
14.5
14.0
13.0
12.0
11.79
11.22
C(n,n')C
11.0 MeV
10.74
10.25
10.0
9.6
9.2
9.0
C(n,n')C
15.0 MeV
14.5
14.0
13.0
12.0
11.79
11.22
dσ/dΩ (mb/sr)
θc.m. (deg)

Fig. 2

scattering cross sections. The data will shortly be available in the CSISRS data library at NNSC.

(2) Beryllium 9 (USNDC-CTR-1, Sec. 4)

Elastic and inelastic (Q = -2.43 MeV) scattering cross sections have been measured for 9 incident neutron energies from 7.0 to 15.0 MeV in 1.0 MeV steps. The scattering sample used was a 3/4" diameter, 1" high pure ^{9}Be cylinder. Data were taken at 5° increments for the angular range from 25° to 165°. The data were corrected for the finite size and anisotropy of the primary neutron source, attenuation of the incident and scattered neutron flux density, multiple scattering, and for the differences in neutron fluence for the beryllium sample and the polyethylene normalization sample by Monte Carlo simulation. Typical relative uncertainties in the elastic cross sections are 2-4% and the normalization uncertainties range from 3-5%. The data are available in the CSISRS data library at NNSC.

(3) Lithium 6 (USNDC-CTR-1, Sec. 2)

Six elastic and inelastic (Q = -2.18) cross section angular distributions have been measured at 1 MeV intervals for the neutron energy range from 7.5 to 14.0 MeV. The scattering sample used consisted of 3.3 gm of 95% enriched ^{6}Li canned in thin walled aluminum. Sample dimensions were 3/4" diameter x 1.0" in length. Scattering from a blank nearly identical aluminum can was used to correct the measured spectra for aluminum contributions. The data are undergoing preliminary analysis at this time to correct for finite geometry, attenuation and multiple scattering effects. Final results must be corrected for the 4.9% admixture of ^{7}Li in the scattering sample. (Below.)

(4) Lithium 7 (USNDC-CTR-1, Sec. 3)

Using a 99.99% ^{7}Li sample canned simmilarly to the ^{6}Li above we began data accumulation for this isotope in December 1975. To date, seven complete angular distributions have been measured for $7.0 \leq E_n \leq 13.0$ MeV. With our present equipment neutrons from the first excited state (Q = -.478 MeV) are non separable from elastic scattering events; however, total elastic scattering cross sections may be derived using (n,γ) results from ORNL.[1] Angular distributions of neutrons leaving ^{7}Li in the second excited state (Q = -4.63 MeV) are included. These data will be extended to 15.0 MeV.

[1] J.K. Dickens, T.A. Love, and G.L. Morgan, ORNL-TM-4538

(5) (n,γ) Measurements

Design and construction of a massive (7500 lb.) copper, lead, tungsten and polyethylene shield and collimater for neutron induced gamma ray experiments is complete. The shield is designed to utilize either a 50 cc Ge(Li) detector or a 4" x 7" NaI(Tℓ) with a 9" x 9" NaI(Tℓ) anti-coincidence annulus.

The first experiment utilized the NaI(Tℓ) detector and was designed to observe the E2 strength in ^{41}Ca. The fore-aft asymmetry $R = (Y_{55} - Y_{125})/Y_{55} + Y_{125})$ was measured at neutron energies of 8, 10 and 12 MeV. Preliminary results are similar to previous measurements at 14 MeV[2] with typical values of R being = -0.08 ± 0.05. The negative value is expected from effective charge considerations, proton capture asymmetries being typically positive. The relatively small value of R compared to proton capture results is consistent with the suggestion of Ref. 2 that the forward peaking observed in (p,γ) experiments is due mainly to direct capture amplitudes. A thorough survey of the angular distributions over the region of the giant dipole and isoscalar giant quadrupole resonances is planned.

(6) Small Angle Measurements

The collimator and associated equipment obtained on loan from the Ballistics Research Laboratory, Edgewood Arsenal, Maryland have been adapted to the TUNL neutron time of flight area. This equipment permits neutron scattering cross section measurements for $1\text{-}1/2° < \theta_L < 15°$. Measurements for natural carbon and ^{9}Be have been completed and are incorporated into the data sets above.

(7) Efficiency Measurements

During this report period the relative efficiency of the main neutron detector was rechecked using very accurately determined measurements of the D(d,n)^{3}He angular distribution at 12.3 MeV. These data by Drosg[3] and Jarmie[4] permitted a considerable reduction in

---

[2] E.E. Arthur, D.M. Drake and I. Halpern, Phys. Rev. Lett. 35, 914(1975)

[3] M. Drosg and D.M. Drake, LASL Internal Report, LA-5732-MS 1974

[4] N. Jarmie, private communication

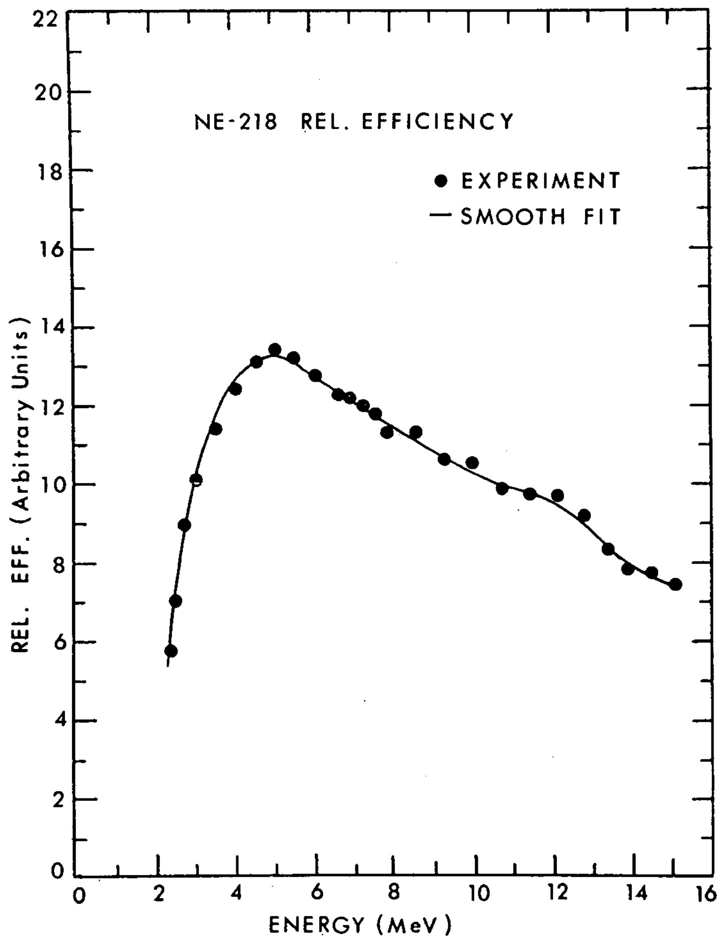
NE-218 REL. EFFICIENCY
● EXPERIMENT
— SMOOTH FIT
REL. EFF. (Arbitrary Units)
ENERGY (MeV)
0
2
4
6
8
10
12
14
16
18
20
22

Fig. 3

the statistical error assignment in our data attributable to the relative efficiency determination. The measured energy dependence is in good agreement with an efficiency calculation performed at Oak Ridge for our detector.[5] The relative efficiency curve for $2.0 < E_n < 15.0$ MeV is shown in Figure 3.

c. Theoretical Analysis of Neutron Data

The elastic and inelastic scattering data for ^{9}Be and C have been analyzed via spherical optical model (SOM) and coupled channel (CC) calculations. The nucleus ^{9}Be is known to have a strongly deformed prolate charge distribution but the spherical optical model appears to give a good description of the elastic scattering data as can be seen in Fig. 4. This shows SOM fits to neutron elastic scattering data from ^{9}Be for energies from 9 to 15 MeV. The parameters for these fits are listed in Table I. The SOM parameters for ^{9}Be are not exactly the same as those one would expect to obtain from a consideration of the parameters for proton elastic scattering data.[1] This presumably reflects the fact that (compared to an incoming proton) an incoming neutron will interact less strongly with the weakly bound last neutron in Be. The SOM parameters clearly mask the effects of the deformed core in ^{9}Be, and a more appropriate description of the neutron scattering process should explicitly include the coupling between the ground state of ^{9}Be and the $5/2^-$ state at 2.43 MeV, this state being the first excited state of the ground state rotational band. The results of such a CC calculation are shown in Fig. 5, where the parameters used in the code JUPITOR-2 are again shown in Table I. The deformation parameter extracted from this CC analysis is similar to that found in similar analyses of proton inelastic scattering data.[1] As recently discussed by Madsen _et al._,[2] the deformation parameters extracted from proton inelastic scattering, neutron inelastic scattering and Coulomb excitation data will not necessarily be identical. In the case of ^{9}Be, however, the differences appear too small to be experimentally observable. The CC fits are excellent nonetheless.

Optical model analyses of nucleon scattering from C at low energies have not been very successful in the past due to the presence

---

[5] G.L. Morgan, private communication

[1] H.J. Votava _et al._, Nucl. Phys. A204 (1973) 529

[2] V.A. Madsen _et al._, Phys. Rev. Letters 34 (1975) 1398

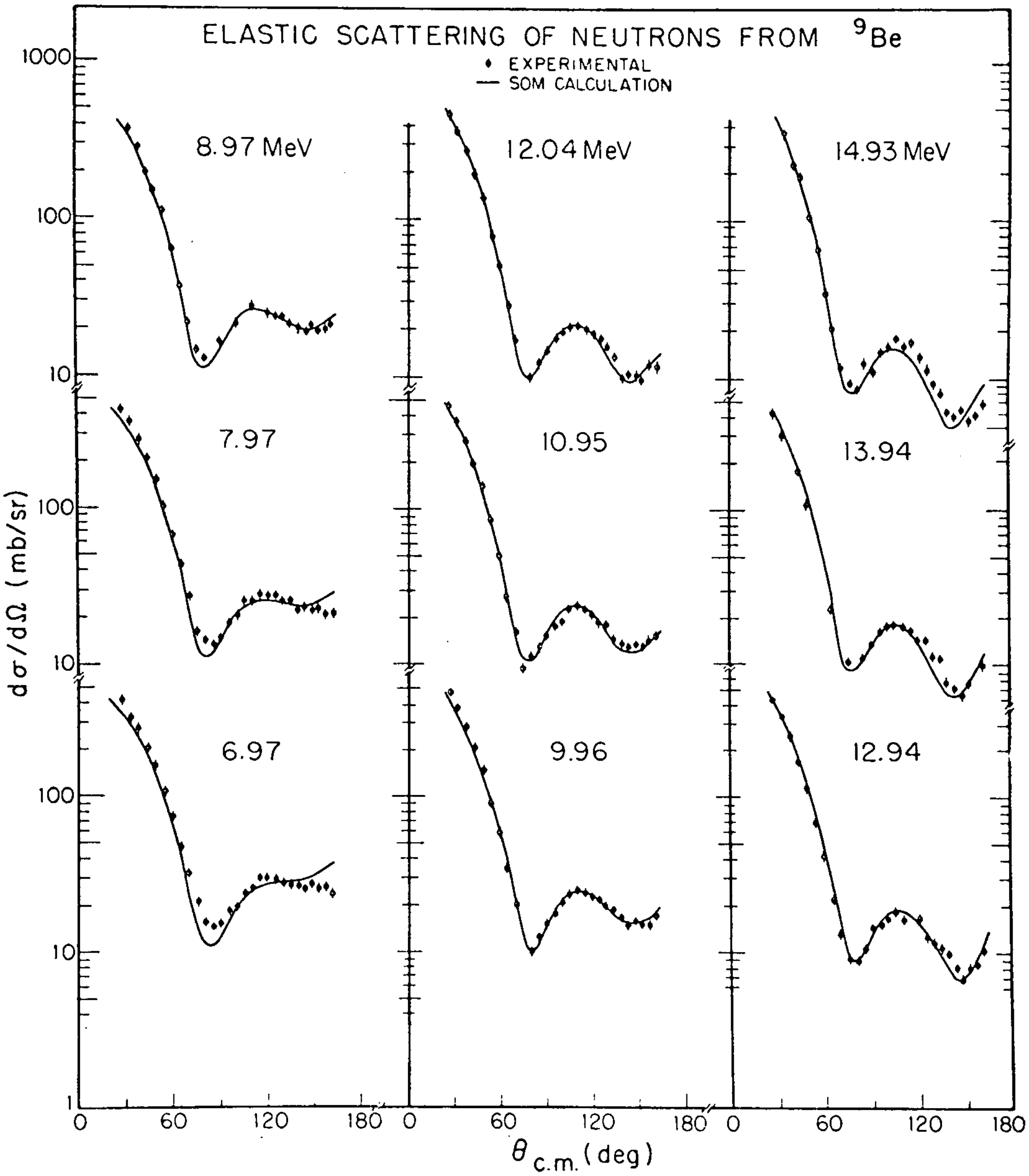

ELASTIC SCATTERING OF NEUTRONS FROM ^{9}Be
EXPERIMENTAL
SOM CALCULATION
8.97 MeV
12.04 MeV
14.93 MeV
7.97
10.95
13.94
6.97
9.96
12.94
dσ/dΩ (mb/sr)
1000
100
10
1
0
60
120
180
θ c.m. (deg)

Fig. 4

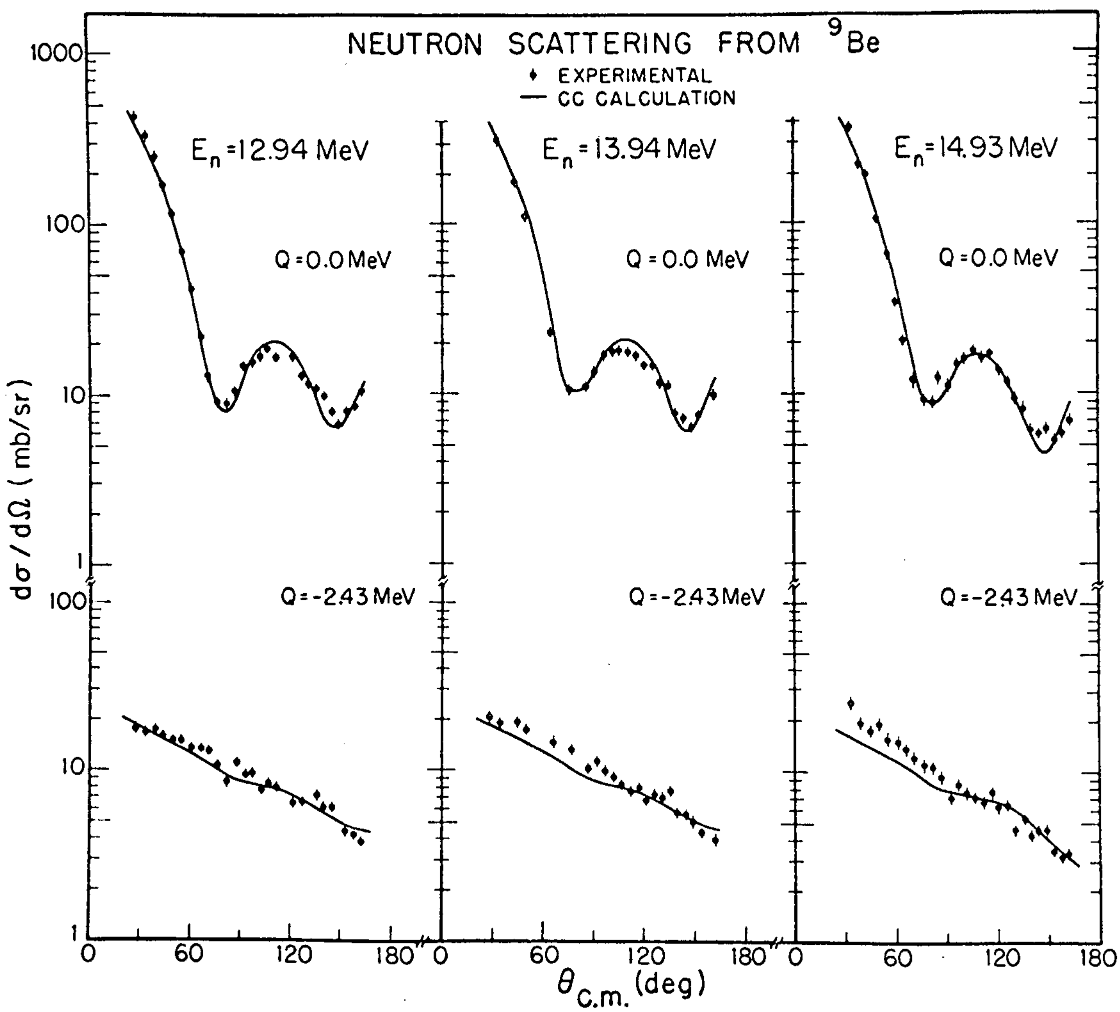
NEUTRON SCATTERING FROM ^{9}Be
EXPERIMENTAL
CC CALCULATION
E_n=12.94 MeV
E_n=13.94 MeV
E_n=14.93 MeV
Q=0.0 MeV
Q=0.0 MeV
Q=0.0 MeV
Q=-2.43 MeV
Q=-2.43 MeV
Q=-2.43 MeV
dσ/dΩ (mb/sr)
1000
100
10
1
100
10
1
0
60
120
180
$\theta_{c.m.}$ (deg)

Fig. 5

of pronounced resonances in the compound nuclear system at the excitation energies of interest. For neutrons of energies 9 to 15 MeV however, total neutron cross section data indicate the resonances in ^{13}C are not strong in the energy range 9 to 15 MeV and our SOM and CC fits to the elastic and inelastic scattering data are reasonably good, CC fits to neutron scattering data at 12-14 MeV are shown in Fig. 6. The parameters used in this case are listed in Table I and are similar to a set used by Grin et al.[3] in an analysis of 14 MeV neutron elastic and inelastic scattering data. In contrast to the CC fits to Be scattering data, the deformation parameter for C is negative, implying an oblate nuclear matter distribution.

TABLE I

SUMMARY OF PARAMETER VALUES

Analysis	Geometric Parameters (F)						Strength Param. (MeV)			Deformation
	r_R	a_R	r_I	a_I	r_{so}	a_{so}	V_R	W_s	V_{so}	β
^{9}Be, SOM	1.47	0.39	1.21	0.42	1.24	0.35	42.4 - 0.5E	1.0 + 0.37E	4.9	
^{9}Be, CC	1.17	0.54	1.21	0.20	1.20	0.31	53.9 - 0.8E	-0.2 + .54E	4.9	+1.06
^{12}C, CC	1.25	0.35	1.25	0.20	1.25	0.35	58.0 - 0.9E	0.28E	5.0	-0.64

2. Resolved Neutron Total Cross Sections and Intermediate Structure (J. Clement, B.-H. Choi, W.F.E. Pineo, M. Divadeenam,* H.W. Newson)

A paper entitled "Intermediate Structure in the $^{28}Si + n$ Reaction: R-Matrix interpretation of Experimental Data" is being submitted to Annals of Physics as Part Xf(i) of our series "s- and p-wave Neutron Spectroscopy". The abstract follows:

"A multi-level R-matrix analysis of Si neutron cross section data measured at NBS has been performed up to about 4.5 MeV neutron energy. Only a small fraction of the p-wave s.p. strength is observed while the identified f-wave strength is located around 1.7 MeV neutron energy. Both p- and f-wave resonance structure around 1 MeV and 1.7 MeV respectively is interpreted in

[3] G.A. Grin et al., Phys. Letters 25B (1967) 387

* Brookhaven National Laboratory, Upton, New York

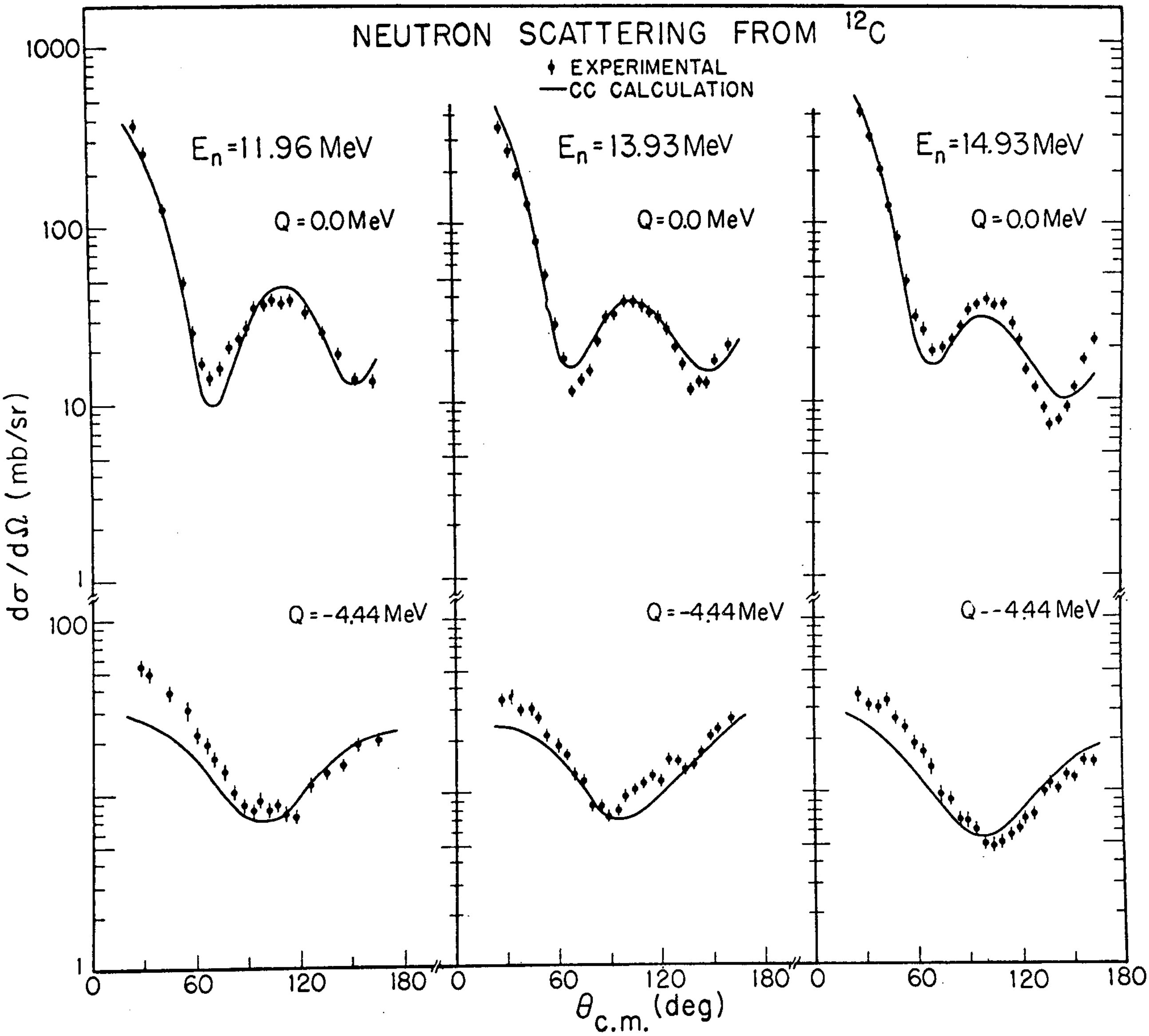

NEUTRON SCATTERING FROM ^{12}C
EXPERIMENTAL
CC CALCULATION
E_n=11.96 MeV
E_n=13.93 MeV
E_n=14.93 MeV
Q=0.0 MeV
Q=-4.44 MeV
$d\sigma/d\Omega$ (mb/sr)
$\theta_{c.m.}$ (deg)
1000
100
10
1
0
60
120
180

Fig. 6

terms of doorway state effects. Besides the well known 180 keV, strong, $1/2^+$ resonance, the s-wave resonance structure is of moderate strength, while the d-wave assignments are not unambiguous. A possible correlation between neutron and gamma decay channels and the connection between the states observed in (n,n), (d,p), (n,γ) and (γ,n) channels is discussed. A core-particle doorway interpretation for s,p and f-waves is presented in the following paper."

3. Theoretical Investigation of Neutron Cross Section Measurements (M. Divadeenam, B.-H. Choi, W.P. Beres,** S. Ramavataram,*** B. Castel,**** D. Haldeman,**** R.Y. Cusson, H.W. Newson)

A paper entitled "Structure of Doorway States in the ^{40}Ca + n Reaction" is published in Z. Physik, 274, 276 (1975). The abstract follows:

"A model including 2p-1h and collective states in ^{41}Ca is used to investigate the intermediate structure resonances seen in the n + ^{40}Ca reaction. With potential well parameters determined by a calculation of the bound states it is found that most of the s-wave strength can be accounted for by the inclusion of one main doorway state component."

^{89}Y + n doorway paper has been accepted for publication in Annals of Physics. The abstract follows:

"The resonance structure observed in the ^{89}Y(n,n)^{89}Y total cross section measurements in the range of 0.3 to 1.2 MeV incident energy was investigated using the generalized R-matrix theory of nuclear reactions and the doorway interpretation of intermediate structure. The energies and wave functions of the doorway resonances were calculated in a 2-particle and 3p-1h basis of the shell-model. The model space and the parameters of the model calculation chosen were consistent with other shell

** Wayne State University, Detroit, Michigan

*** Universite de Laval, Quebec, Michigan

**** Queen's University, Kingston, Ontario, Canada model calculations in the mass-90 region. Several strong p-wave doorways with $J=0^+$, 1^+ and 2^+ were predicted by the model in the energy range studied. The escape widths and the spreading widths for these states were evaluated using the model wave functions and the R-matrix formalism. The calculated energy dependence of the total cross section shows that the predicted doorways line up in energy with the observed anomalies with similar strength. More significantly, the underlying p-wave gross structure representing a grand average is of very similar shape in both theory and experiment. In comparison, the s- and d-wave doorways are shown to contribute less significantly to the observed structure."

The abstract of a paper entitled "Neutron and Gamma Widths of A $J^\pi = 3/2^-$ Doorway State in ^{29}Si", submitted to Phys. Rev. Letters, is given below.

"The recent experimental evidence for a $J=3/2^-$ doorway state common to the $^{28}Si + n$ and $^{29}Si + \gamma$ channels near 750 keV is found to be supported by a doorway type calculation, which reproduces neutron and gamma widths, as well as the $p_{3/2}$ low-lying spectroscopic strength."

Part Xf(ii) of the series on s- and p-wave neutron spectroscopy is ready for submission to Annals of Physics. The abstract follows:

"A core-particle calculation developed to describe the low-lying yield information on the structure of ^{29}Si is extended above neutron threshold energy to yield information on the structure of doorway states detected by the $^{28}Si + n$ reaction. The recent experimental evidence for a $J=3/2^-$ doorway state common to the $^{28}Si + n$ and the $^{29}Si + \gamma$ channels is supported by the calculation which also reproduces correctly the magnitudes of the neutron escape widths and the El radiative strengths."

4. A Selectively Excited And Distorted (SEXDD) Liquid Drop Model (H.W. Newson)

Inactive.

5. Charged Particle Fission (F.O. Purser, D. H.Epperson, H.W. Schmitt, E.G. Bilpuch, H.W. Newson)

The experimental study of fission fragment mass and kinetic energy distributions has been extended during the current report period. More than 100 complete mass/kinetic energy measurements have now been accumulated for proton induced fission of ^{236}U, ^{235}U and ^{234}U. The proton energy range extends from E_p = 6.25 MeV, well below second chance threshold, to E_p = 30 MeV.

The measurements have been carried out using the method of Schmitt, Neiler and Walter[1] in which the kinetic energy of correlated fission fragment pairs are determined by two surface barrier detectors. The detectors were calibrated first against a known ^{252}Cf source and subsequently against deduced calibration energies for a fission spectrum produced by $^{238}U(p,f)$ at E_p = 11.0 and 12.0 MeV. At the higher energies (above 10 MeV) approximately 10^6 counts were accumulated for each mass/kinetic energy measurement.

After transformation (as in reference 1) the data are obtained in a two dimensional array of fragment mass vs total kinetic energy where the mass in this case is the pre-neutron emission mass. Utilizing measured fission cross sections and an updated version of the code used by Boyce et al.[2] to unfold contributions of sequential fission channels, the individual data points in this array will be tracked as a function of the excitation energy of the fissioning nucleus. By this means, mass and kinetic energy data for the fissioning nucleus ^{236}Np can be obtained for excitation energies ranging from subthreshold to approximately 27 MeV, which corresponds to the onset of fourth chance fission in the $^{236}U(p,xnf)$ reaction. Data of this character will provide a means of testing proposed models of the fission process.[3]

Data accumulation for this project is complete and analysis is in progress.

---

[1] H.W. Schmitt, J.H. Neiler and F.J. Walter, Phys. Rev. 141, 1146 (1966)

[2] J.R. Boyce, et al., Phys. Rev. C10, 231 (1974)

[3] D. Kolb, R.Y. Cusson and H.W. Schmitt, Phys. Rev. C10, 1529 (1974) and references therein.

C. CHARGED PARTICLE REACTIONS

1. ^{6}Li Reactions with p,d and ^{3}He Ions (C.R. Gould, J.M. Joyce*, L.W. Seagondollar)

These studies form part of a continuing series of measurements of absolute cross sections in support of fusion reactor research into advanced fuel systems. In the d-^{6}Li system there are 80 possible reactions which can potentially release energy via charged particles and a knowledge of the cross sections for these reactions is clearly important in assessing the reactivity of such fuels. We have completed investigations of the $^{6}Li(p,^{3}He)^{4}He$ reaction in the energy range 3 to 12 MeV and have also studied the $(d,^{4}He)$ and (d,p) reactions on ^{6}Li in the energy range 2.25 to 7.5 MeV. Our results for the deuteron induced reaction cross sections agree well with the data of McIenahan and Segel[1] and were summarized in a contribution to the Washington conference on Nuclear Cross Sections and Technology (NBS Special Publication 425, p. 697). The abstract of this paper appears below:

> "Investigations of proton, deuteron and helium induced reactions on ^{6}Li are of importance in connection with the advantages of fusion reactor cycles involving only charged particles. The cross section data for many of these reactions are incomplete and poorly known. We report measurements of the absolute cross sections of the reactions $^{6}Li(p,p)$, $^{6}Li(p,^{3}He)$ at E_p = 3-12 MeV, $^{6}Li(d,p)$, $^{6}Li(d,\alpha)$ at E_d=2.25-6 MeV and $^{6}Li(^{3}He,p)$ at E = 3-6 MeV. Our data are combined with available information in the literature to determine reaction rate parameters as a function of the temperature of the reacting nuclei."

Our work on the highly exothermic reaction $^{6}Li(^{3}He,p)^{8}Be$ in the energy range 3 to 6 MeV has been completed and accepted for publication in Nuclear Science and Engineering. Due to a normalization error our early work on this reaction indicated the cross sections to be much lower than the only other known absolute values.[2] However, this discrepancy has now been resolved and we find our measurements in good

---

* East Carolina University, Greenville, North Carolina

1 C.R. McLenahan and R.E. Segel, Phys. Rev. C11 (1975) 370

2 J.P. Schiffer et al., Phys. Rev. 104 (1956) 1064

agreement with those of Ref. [2]. Our total cross section results are shown in Fig. 7. The points labelled "Three Body Break Up" are an estimate of the continuum cross section $^6Li(^3He,p)2\alpha$ and the other points show the cross sections for production of ^8Be in its ground and first excited states respectively. Data from reference 2 and reference 3 are shown for comparison. The abstract for the Nuclear Science and Engineering paper appears below.

> "Many reactions involving ^6Li are of interest in studies of the performance of charged particle fusion reactor systems. We report measurements of the absolute cross sections for the $^6Li(^3He,p)^8Be$ reaction from 3 to 6 MeV and include the first estimates of the absolute magnitude of the three body continuum cross section $^6Li(^3He,p)2\alpha$. The cross sections below 1 MeV are calculated from an s-wave Gamow extrapolation and are used to extract the Maxwell averaged reaction rate for the $^6Li(^3He,p)^8Be$ reaction leading to the ground and first excited states of ^8Be."

2. Thick Target Neutron Spectra and Yields (C.E. Nelson,* F.O. Purser, P. Von Behren)

The requirements for an intense source of neutrons for cancer therapy are now fairly well established.[1,2] They are: (1) in order to give the required dose rate a source strength of 4×10^{11} neutrons/(sec-sr) is needed; (2) to give the required depth dose characteristics an average neutron energy of at least 10 MeV is needed; and (3) the source should be cheap and simple enough so that it can be used in a hospital environment.

Clinical trials are presently underway in this country with neutron beams that meet the first two criteria. However, these centers use high energy cyclotrons dedicated primarily to physics research, none of which is located in a hospital environment.

---

[3] N.R. Fletcher et al., Nucl. Phys. 70 (1965) 471

* Supported by National Cancer Institute Research Fellowship No. 1 F22 CA00332-01

[1] F.T. Brenna, Radiological Clinics of North America 1 (1969) 365

[2] H.H. Barschall, Intense Sources of High Energy Neutrons, Conf. on Nuclear Structure Study with Neutrons, Budapest, Hungary, 1972

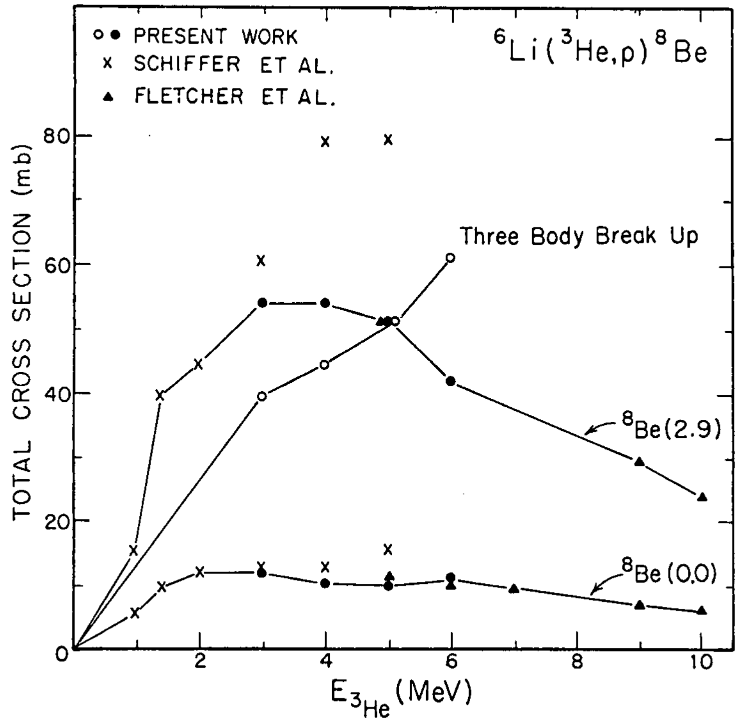

○ ● PRESENT WORK
× SCHIFFER ET AL.
▲ FLETCHER ET AL.
$^6Li(^3He,p)^8Be$
Three Body Break Up
$^8Be(2.9)$
$^8Be(0.0)$
TOTAL CROSS SECTION (mb)
$E_{^3He}$ (MeV)
0
20
40
60
80
2
4
6
8
10

Fig. 7

Present efforts to develop a hospital-based neutron source are concentrated on the DT generator[3]. This machine uses the $^3H(d,n)^4He$ reaction at several hundred keV to obtain an intense monoenergetic source of 14 MeV neutrons. Such a generator is attractive because a clinical unit presumably could be constructed that would be relatively inexpensive to purchase and operate. Presently, however, there is no target capable of producing D-T neutrons with sufficient intensity and lifetime to be employed practically in radiation therapy. Such a system also involves keeping a radioactive tritium target in a hospital environment.

A possible alternative to the D-T generator as a hospital-based neutron source is a small medical cyclotron. These machines have the capability to accelerate deuterons to 8.3 MeV, protons to 14.8 MeV and ^3He ions to 20.3 MeV. At the present time, there are two such cyclotrons installed in hospitals in the United States, both of which are used for the production of short-lived isotopes.

The d + Be reaction for deuteron energies in excess of 20 MeV is known to be suitable for neutron therapy because of its high yield and penetration. At E_d = 8.3 MeV, however, it is unacceptable for practical radiation therapy because of its relatively poor penetration (average neutron energy = 3.6 MeV).[4] The d + d reaction is one possible alternative to the d + Be reaction. Recent calculations have suggested that a deuterium gas target and the 8.3 MeV deuteron beam would increase the average neutron energy to 7.5 MeV.[5]

The large positive Q-value (approx. 15 MeV) of the $^7Li(d,n)^7Be$ reaction suggests a substantial increase in the average neutron energy. However, the few measurements on the lithium metal target

---

3 C.A. Kelsey, Current Status of DT targets for Cancer Therapy, Medical Physics, 2 (1975) 185

4 C.E. Nelson, F.T. Kuchnir and L.S. Skaggs, Initial Measurements on the Neutron Beam at the FMI Therapy Facility, presented at the Seventeenth Annual Meeting of the AAPM, San Antonio, Texas, Aug. 3-Aug. 7, 1975

5 H. Schraube et al., Second Symposium on Neutron Dosimetry in Biology and Medicine, Munich, Sept. 1974, Vol. II, p. 979

are conflicting, yielding average neutron energies from 1.5 to 7.5 MeV.[1,2,3]

The neutron time-of-flight facility at the Triangle Universities Nuclear Laboratory is excellently suited for the neutron spectral measurements.[4] A thick lithium target (99.4% ^{7}Li) is presently under construction to be used to determine the neutron energy spectra and yields for the reactions d + ^{7}Li at E_d = 8.3 MeV and p + ^{7}Li at E_p = 14.8 MeV, at several angles. A slight modification to the target will allow it to be filled with deuterium gas at high pressure so that the thick target spectra and yields can be measured at E_d = 8.3 MeV for the d + d reaction. Similar measurements will be made at the higher energies available under Cyclo-Graaff operation.

An accurate knowledge of the energy sensitivity of the neutron detector is critical to both the neutron spectral measurements and to the yield measurements. Thus considerable effort has been expended to date determining the relative efficiency of the neutron detector. The relative efficiency of the main detector has recently been measured from E_n = 14 MeV to E_n = 2.5 MeV by normalizing an angular distribution of the d(d,n)^{3}He reaction measured at 12.3 MeV deuteron energy to an accurate charged particle experiment which measured the d(d,^{3}He)n cross section. This was done at a neutron bias level of several hundred keV (1/10 ^{137}Cs). In order to extend the efficiency curve to lower energies, and also normalize the efficiency to the hydrogen scattering cross section, the elastic scattering cross section of hydrogen was measured at E_n = 7.5 MeV for laboratory angles from 35° to 72°, corresponding to scattered neutron energies of 5 MeV to .7 MeV. In contrast to the previous measurements, which efficiencies were either unknown as zero below E_n = 2 MeV, our efficiency is known to reasonable accuracy from E_n = .7 MeV to E_n = 14.0 MeV. This should provide much more precise spectral measurements and yields, and therefore average neutron energies, and thus remove some of the discrepancies quoted earlier.

---

[1] A. Pinkerton, et al., Radiology 96 (1970) 131

[2] F.M. Edwards, et al., Medical Physics 1 (1974) 317

[3] A.N. Caland et al., private communication

[4] H.W. Newson, et al., N.I.M. 122 (1974) 99

The above program should lead to an accurate knowledge of the spectra and average energies available to a small medical cyclotron operating as a fast neutron source for cancer therapy.

3. Continuation of The Development of a PIXEA System for Trace Analyses (R.D. Willis, W. Gutknecht,* R. Shaw,* R.L. Walter)

Utilizing 3-MeV proton beams, a Proton-Induced X-ray Emission Analysis system has been developed in the 4-MeV Van de Graaff laboratory. Partial support for studying the applicability of the method was received from EPA and the National Institute for Environmental Health Sciences. A major report on the technique is being written presently and will include an overview of about 4000 runs. Main concentration has been placed upon calibration, sensitivity and analysis of samples from the following categories: environmental, medical, biological, geochemical, marine life, and biochemical. Numerous useful applications appear worthwhile to pursue. Reports on our work in 1974 appeared in Anal. Chem. 46 (1974) 440, Anal. Chem. 46 (1974) 843, Anal. Biochem. 57 (1974) 618 and Proc. of Applications of Small Accelerators (1974 Conference). Papers have been submitted to Geochimica et Cosmochemica Acta, Nature, and another to Anal. Chem. A continuing cooperation in energy-related studies with NIEHS will be arranged in the near future.

Further progress has been slow but steady because of a de-emphasis on this program. A final 300 page report for the U.S.E.P.A. is 98% completed which is a great relief as the approach was to make the report suitable for a wide audience. The report, entitled "The Development of a Proton-Induced X-Ray Emission System for Multielemental Analyses of Environmental, Biological, Clinical and Geological Specimens:, covers a brief history of PIXEA, its uses, its competitiveness, a summary of standard analytical methods, and future improvements one can expect. The manuscript has been written so that it would make a good technical reference book, and currently a publisher is being sought. Related papers have appeared in Analyt. Chem. 46, pg. 440; 46, pg. 843; 47 pg. 1727; in Analyt. Lett. 5(12), pg. 943; in Analyt. Biochem. 57, pg. 618; in Applications of Small Accelerators, pg. 189; and in Radiation and Environmental Biophysics, 12, pg. 175. Reports (in press) will soon appear in Environmental Health Perspectives, X-Ray Spectrometry, and Advances in X-Ray Spectrometry. The review chapter entitled "Particle-Induced X-Ray Emission Analysis-PIXEA" has been written for Practical Spectroscopy Series, Vol. III, ed. by L.S. Birks and H.K. Herglotz by two of us (R.L.W. and R.D.W.). Numerous talks have been given to responsive audiences. The direction this program will follow in the

* Department of Chemistry, Duke University

future has not been decided. Until now, the program has been developmental and commitments were kept minimal. Only a small fraction of the available time on the 4 MeV Van de Graaff has been involved and the use then was light, i.e., low beams ($< 2\mu A$) at a low potential (< 3 MV). The possible continuation of the collaboration with the National Institute for Environmental Health Studies in energy-related research is under discussion.

D. DEVELOPMENT

1. Improved Beam Energy Resolution for The Tandem Accelerator

(E.G. Bilpuch, M.E. Bleck, D.A. Outlaw, W.K. Wells, F.O. Purser, T.B. Clegg, J.E. Cairns,* R.L. Rummel, H.W. Newson)

An improved energy stabilization system for the TUNL Cyclo-Graaff accelerator has been under development for the past nine months. This technique involves high voltage modulation of the terminal charge exchange stripper in addition to the normal corona discharge regulation. The additional control loop has no inherent frequency response limitation such as the finite ion drift time associated with the corona regulator. This is accomplished by transmitting the signal to the terminal via an intensity modulated light beam. The fast channel is designed to remove the high frequency fluctuations in machine energy due to corona oscillation so that the gain of the corona channel may be increased, resulting in better low frequency regulation. In order to free the normal running schedule from disruption during system development, the fast channel stabilizer and its associated corona regulator exist independently from the Varian corona control system currently in use.

Briefly, the system configuration is as follows. An error signal proportional to the machine energy fluctuations is derived from the current intercepted by a pair of control slits downstream from an analyzing magnet. This error signal drives both the corona regulator and the new fast channel stabilizer. In order to insure that all of the frequency information is retained in this signal, a matched pair of fast, low noise, slit current preamplifiers were designed and constructed. These preamplifiers have a logarithmic gain characteristic which renders the error signal insensitive to beam intensity fluctuations. A voltage-to-current amplifier driving a light emitting diode encodes the error signal in a light beam which shines through a port at the low energy end of the machine. A phototube in the terminal converts the light signal back to a voltage signal which drives the high voltage terminal amplifier.

---

* McMaster University, Hamilton, Ontario, Canada

This amplifier employs fast, high gain Y634 ceramic planar triodes to insure reliability in the high pressure environment of the tandem Van de Graaff terminal. The terminal amplifier is capacitatively coupled to the stripper and is capable of 6 KV peak-to-peak output swings.

Several system test runs have been completed and the preliminary results are encouraging. The fast fluctuations in the error signal are reduced essentially to the noise level and the fast components in the terminal ripple are substantially reduced. Under these conditions, the width of the beam energy resolution function necessary to fit a 300 eV natural width, $5/2^+$ resonance in $^{54}Fe(p,p)$ was approximately 1 keV. By applying the neutral beam target correction system described by Dzubay *et al.*,[1,2] the width of the resolution function was reduced to 550 eV.

The design goal of the system is a resolution function width of 100 to 300 eV. Development work is continuing along several lines in an effort to achieve this goal. First there is evidence that the corona regulation by itself has not been optimized and a study seems to indicate that the operating point for the corona tube has not been properly chosen. Another possibility involves using the 90-90 magnet system, with its greater analyzing power, in front of the control slits on the assumption that residual energy fluctuations are being obscured by the preamplifier noise. Finally, it appears that position instabilities in the neutral beam may be causing false correction signals to be applied to the target, degrading the resolution. It may be possible to eliminate these fluctuations by installing a steerer feed-back loop that centers the beam on the 90-90 magnet object slits. Such a system was developed for the corona-fast channel analyzing magnet and works very well. Prospects seem good for realizing the system design goals within the next year by correcting one or more of these problems.

APPENDIX 1

ANNUAL REPORT TUNL XIV

TABLE OF CONTENTS

Major portions of earlier TUNL reports (TUNL I - TUNL XIII) are contained in the reports of USNDC or its predecessor, the AEC Nuclear Cross Sections Advisory Committee.

YALE UNIVERSITY

A. FAST NEUTRON STUDIES (F. W. K. Firk, J. E. Bond and H. L. Schultz)

1. Polarization of Neutrons in n-^{4}He Elastic Scattering Between 1.5 and 6 MeV

We have completed measurements of the asymmetries of polarized neutrons elastically scattered from ^{4}He at five angles and as continuous functions of energy between 1.5 and 6 MeV.[1] The "point" analyzing powers are listed in Tables 1 and 2. An R-function analysis of n-^{4}He data, including both the above absolute measurements of the analyzing power and a precision measurement of the total cross section,[2] is now being carried out at energies up to 15 MeV.

2. Differential Cross Section for the Reaction ^{6}Li(n,n)^{6}Li in the MeV-region

Preliminary measurements of the differential cross section for neutrons elastically scattered from ^{6}Li have been made. The neutrons were detected at six angles between 90° and 150° at energies ranging from 1 to 5 MeV. These measurements are needed to improve upon the R-matrix analysis of our earlier polarization data.[3]

B. POLARIZATION OF PHOTONEUTRONS

1. Polarization of Photoneutrons from Liquid Deuterium (L. Drooks, F. W. K. Firk and H. L. Schultz)

Measurements of the polarization of photoneutrons from deuterium have been made at reaction angles of 60°, 90° and 120° throughout the proton energy range 6 to 15 MeV. Extreme care has been taken to reduce systematic uncertainties to negligible amounts. At all three angles, our measured polarizations are more negative than the predicted values of the classic calculations of the Partovi-type. Our observations are consistent with the recent results of calculations of Hadjimichael[4] that take into account contributions due to meson exchange currents.

---

[1] J.E. Bond and F.W.K. Firk, Nucl. Phys. A258 (1976) 189

[2] C.A. Goulding, P. Stoler and J.D. Seagrave, Nucl. Phys. A215 (1973) 253

[3] R.J. Holt, F.W.K. Firk, G.T. Hickey and R. Nath, Nucl. Phys. A237 (1975) 111

[4] E. Hadjimichael, Phys. Letters, 46B (1973) 147

20° (lab)				40° (lab)			
E_n (MeV)	A	Statistical Uncertainty	Systematic Uncertainty	E_n (MeV)	A	Statistical Uncertainty	Systematic Uncertainty
1.700	-0.013	0.061	0.008	1.688	-0.035	0.055	0.006
2.082	-0.110	0.030	0.003	2.083	-0.158	0.028	0.005
2.234	-0.120	0.021	0.003	2.232	-0.252	0.020	0.006
2.409	-0.173	0.016	0.003	2.412	-0.270	0.016	0.006
3.030	-0.244	0.024	0.005	3.034	-0.404	0.024	0.009
3.186	-0.250	0.037	0.006	3.198	-0.466	0.034	0.010
3.899	-0.319	0.071	0.008	3.363	-0.477	0.076	0.011
4.401	-0.303	0.067	0.009	3.938	-0.506	0.074	0.015
4.639	-0.255	0.060	0.010	4.306	-0.552	0.064	0.017
5.632	-0.295	0.061	0.011	4.686	-0.562	0.050	0.019
				5.659	-0.534	0.071	0.020

Table 1

60° (lab)				80° (lab)			
E_n (MeV)	A	Statistical Uncertainty	Systematic Uncertainty	E_n (MeV)	A	Statistical Uncertainty	Systematic Uncertainty
1.704	-0.029	0.104	0.011	1.701	+0.593	0.211	0.048
2.083	-0.151	0.044	0.004	2.091	+0.188	0.046	0.013
2.245	-0.146	0.023	0.004	2.254	+0.109	0.029	0.009
2.417	-0.279	0.015	0.007	2.422	+0.098	0.019	0.007
3.037	-0.495	0.017	0.010	3.032	-0.137	0.021	0.004
3.208	-0.461	0.024	0.011	3.217	-0.124	0.035	0.004
3.373	-0.509	0.056	0.012	3.378	-0.175	0.074	0.004
3.916	-0.618	0.053	0.017	3.930	-0.307	0.055	0.008
4.290	-0.713	0.047	0.021	4.282	-0.495	0.058	0.013
4.597	-0.767	0.045	0.022	4.585	-0.503	0.059	0.015
4.874	-0.692	0.046	0.023	4.869	-0.540	0.066	0.018
5.152	-0.776	0.049	0.025	5.140	-0.528	0.072	0.020
5.449	-0.711	0.055	0.027	5.443	-0.592	0.086	0.022
5.718	-0.837	0.090	0.029	5.724	-0.663	0.137	0.024

Table 2

UNIVERSITY OF WASHINGTON

A. DELAYED NEUTRON SPECTRA

1. Fast Neutron - Induced Fission
(G.W. Eccleston and G.L. Woodruff)

The near-equilibrium energy spectra of the delayed neutrons associated with fast-neutron-induced fission of ^{232}Th, ^{233}U, ^{235}U, ^{238}U and ^{239}Pu have been measured at the University of Washington Nuclear Physics Laboratory. The neutron source, produced from the $^9Be(p,n)^9B$ thick target reaction with 10 MeV protons, approximates a prompt fission spectrum.[1] Data were collected in a repetitive sequence consisting of a 1.0-sec irradiation, 0.1-sec delay and a 1.0-sec counting period. Electrostatic deflection of the proton beam produced an on/off ratio greater than 10^5. A two parameter proton-recoil spectrometry system[2] was used to discriminate gamma rays.

The delayed neutron spectrum (DNS) for ^{235}U is shown in Figure A-1. Spectra from the other isotopes are not shown, but, in general they have peaks at the same locations (but with variations in peak magnitudes) and are similar in overall shape. The equilibrium ^{235}U DNS reported by Sloan and Woodruff,[2] by Fieg,[3] and by Saphier[4] are included in Figure A-1 with all the results normalized between 80-1200 keV. The Saphier[5] spectrum is a 54 energy group set constructed using 21 fission product isotope spectra produced in fast fission and measured by Shalev.[6,7] The equilibrium spectrum of Fieg, produced by thermal fission, and of Saphier were calculated from results of varying time cycles. The Sloan-Woodruff measurement is from thermal fission and like the Eccleston-Woodruff data represents a directly measured near-equilibrium spectrum.

The DNS in Figure A-1 are in reasonable agreement at the higher energies but there are significant differences below 200 keV. Possible explanations for the differences between the spectra that have been considered are:

---

1 E. Tochilin and G.D. Kohler, Health Physics, Vol. 1 (1958).
2 W. Robert Sloan and Gene L. Woodruff, Nucl. Sci. Eng. 55, 28 (1974).
3 G. Fieg, J. Nucl. Energy 26, 585 (1972).
Saphier, Ilberg, Shalev and Yiftah, Trans. Am. Nucl. Soc. 22, 671 (1975).
4 D. Saphier, private communication, Jan. 1976.
5 S. Shalev and G. Rudstam, Phys. Rev. Letters 28, 687 (1972).
6 S. Shalev and J. Cuttler, Nucl. Sci. Eng. 51, 52 (1973).

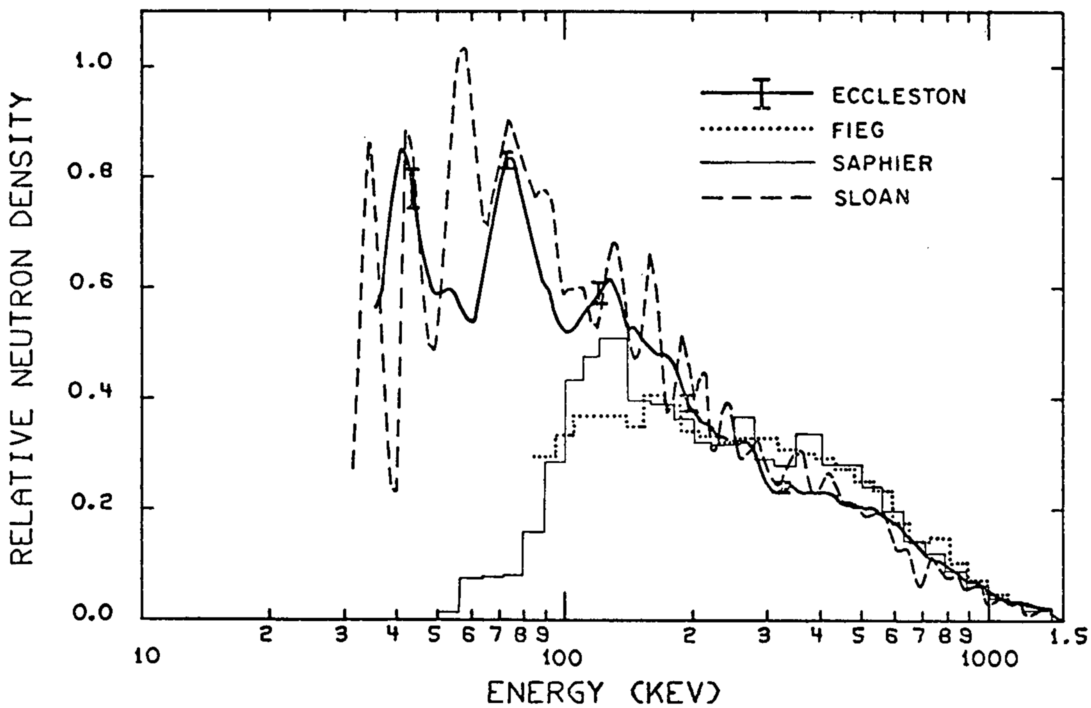

FIGURE A- 1. NEAR-EQUILIBRIUM ^{235}U DELAYED NEUTRON SPECTRA

1) Normalization Criteria - Varying the lower limit of the normalization interval from 80 to 200 keV does not appreciably affect the comparisons.

2) Room Return - Room return might be expected to bias results by producing softer spectra. The Sloan-Woodruff data were collected in a relatively confined area surrounded by a large borated paraffin shield whereas, in the experiment reported here the detector was 140 cm from the nearest surface. It is difficult to explain how a reproducible peak structure can be produced by room return, particularly in widely differing experimental configurations as were the two softest spectra in Figure A-1.

3) Gamma Ray Bias - Gamma discrimination is especially important in the low energy portion of DNS because the gamma/neutron ratio is relatively unfavorable. The bias can go in either direction, i.e., insufficient discrimination of gammas will produce a softer spectrum, while excessive discrimination can eliminate low energy neutrons producing a harder spectrum.

4) On/Off Ratio - Superpositions of a calculated prompt spectrum with a measured delayed spectrum indicate no significant bias below 1.5 MeV results from ratios in excess of 10^4.

5) Lead Shield Bias - Bias effects have shown[7] to be small for lead shields up to 5 cm in thickness. The thicker shield used in our measurement (7.8 cm), compared to the 5 cm Sloan shield, suggests that some broadening in resolution resulted in addition to a slight shift (1-2 percent) in peak locations toward lower energies.

6) Finite Detector Size Effects - Detectors are subject to a variety of effects that can bias data due to their finite size such as wall and end effects and field effects. The Sloan-Woodruff data shown in Figure A-1 is corrected for these effects and the maximum correction made was less than five percent. The corrections have not been made in the present case.

7) Source Spectrum Variations - The spectrum of source neutrons in the data of Figure A-1 varied from thermal to fast (prompt spectra). Comparison of our results with the Sloan-Woodruff data suggests that differences in peak magnitudes may be due to variations in precursor yields between thermal and fast fission. Overall shape changes large enough to account for the significant differences in the spectra are unlikely to be caused by differences between the source spectra.

8) Cycle Parameters - The Fieg and Saphier equilibrium spectra have been unfolded from several measurements each consisting of different cycle parameters (irradiation, delay and counting times). The unfolding explains the apparent differences in resolution, which is, in fact, comparable in all of the experiments. It does not explain the spectra differences which are at issue because our longer cycles have shown a significant low energy component.

---

7 G. Fieg, M. Lalovic and G. Woodruff, Nucl. Sci. Eng. 58, 260 (1975).

In summary, there remain unresolved differences in the low energy portion of DNS. Peaks below 100 keV have now been reproduced by Sloan and Woodruff,[8] Chulick, et al.,[9] Chrysochoides, et al.,[10] Shalev,[11] and in the data reported here. Their existence appears to be reasonably well confirmed.

---

[8] W. Robert Sloan and Gene L. Woodruff, Nucl. Sci. Eng. 55, 28 (1974).
[9] Chulick, Reeder, Bemis and Eichler, Nucl. Phys. A168, 250 (1971).
[10] Chrysoshoides, Anouss, Mitsonias and Perricos, J. Nucl. Energy 25, (1971).
[11] S. Shalev, TNSD-R/421, Technion-Israel Institute of Technology, Haifa, Israel (1971).

B. FOURIER TRANSFORM FILTERING OF PROTON-RECOIL

1. Analytical Results
(W.R. Sloan and G.L. Woodruff)

Proton-recoil data are widely used in measurements of neutron spectra over the energy intervals 1 keV-2 MeV (proportional counters) and 1 MeV-20 MeV (liquid scintillation detectors). The spectra are sometimes of intrinsic value or they may be of interest as tests of cross sections. The fact that proton-recoil data must be differentiated, either directly or by use of response functions, means that statistical quality is even more important than for experimental data in general.

We have analyzed the variance reduction and the bias that result from the use of Fourier Transform frequency filters with proton recoil data. The analysis shows that with a careful selection of filters, variance reduction of from about 3 to 20 cm be achieved without introducing significant bias.

The improvement in the standard deviation that is attainable with a frequency filter of the type,

$$G(W) = \begin{cases} 1, & W < W_c \\ \exp(-(W-W_c)^2/W_R^2), & W \geq W_c \end{cases}$$

where W = the Fourier transform variable
W_R = roll-off parameter
W_c = cut-off frequency

is illustrated in Figure B-1 for three different slope-taking-intervals (STI). The curves in Figure B-1 represent signal analysis while the data points are results from numerical simulation tests. The latter are,

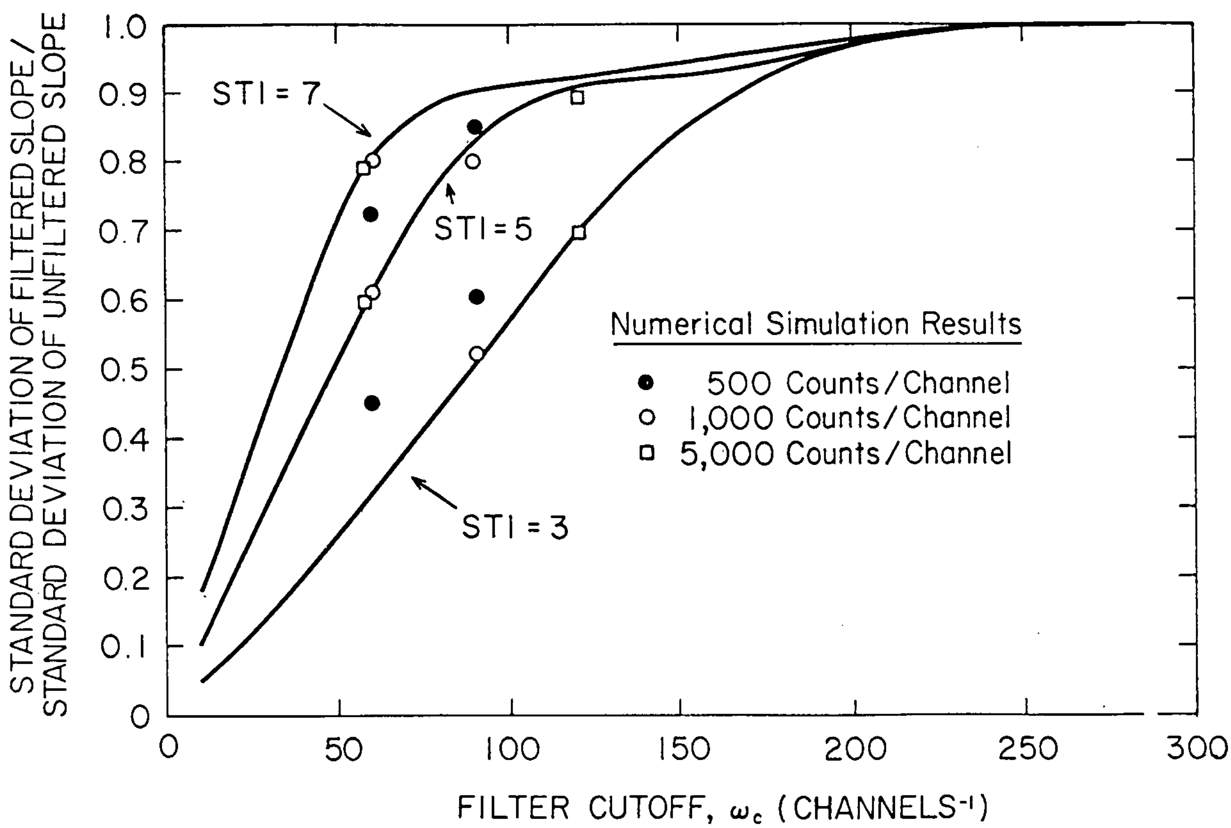
STANDARD DEVIATION OF FILTERED SLOPE/
STANDARD DEVIATION OF UNFILTERED SLOPE
1.0
0.9
0.8
0.7
0.6
0.5
0.4
0.3
0.2
0.1
0
STI = 7
STI = 5
STI = 3
Numerical Simulation Results
500 Counts/Channel
1,000 Counts/Channel
5,000 Counts/Channel
0
50
100
150
200
250
300
FILTER CUTOFF, ω_c (CHANNELS^{-1})

FIGURE B-1.

of course, stochastic in nature and contain their own uncertainties. The results show that the improvement is less for larger values of STI because such cases already include a greater amount of smoothing, i.e., filtering. Reducing the cut-off frequency eliminates more and more statistical fluctuations and all the curves extropolate to zero. Unfortunately all the signal has also been eliminated with a zero frequency cut-off and one must also consider the bias.

The bias has been defined as the change in the full-width-at-half-maximum (FWHM) of a Gaussian peak after filtering and differentiation. Other definitions, such as integrated peak areas, are less sensitive so that the proposed definition is conservative. The bias is shown in Figure B-2 for a slope-taking-interval of three channels. These results show that no bias is introduced until the filter cut-off frequency is reduced to a "break-point frequency" which depends on the resolution of the system.

The analysis shows that the optimal choice of filters to be used depends on both the STI and the resolution of the system. Table B-1 gives the break-point frequencies for typical values of interest and the resulting reduction in standard deviation. As noted above the bias definition used is conservative. Other choices will permit the use of lower cut-off frequencies with corresponding further reductions in standard deviation.

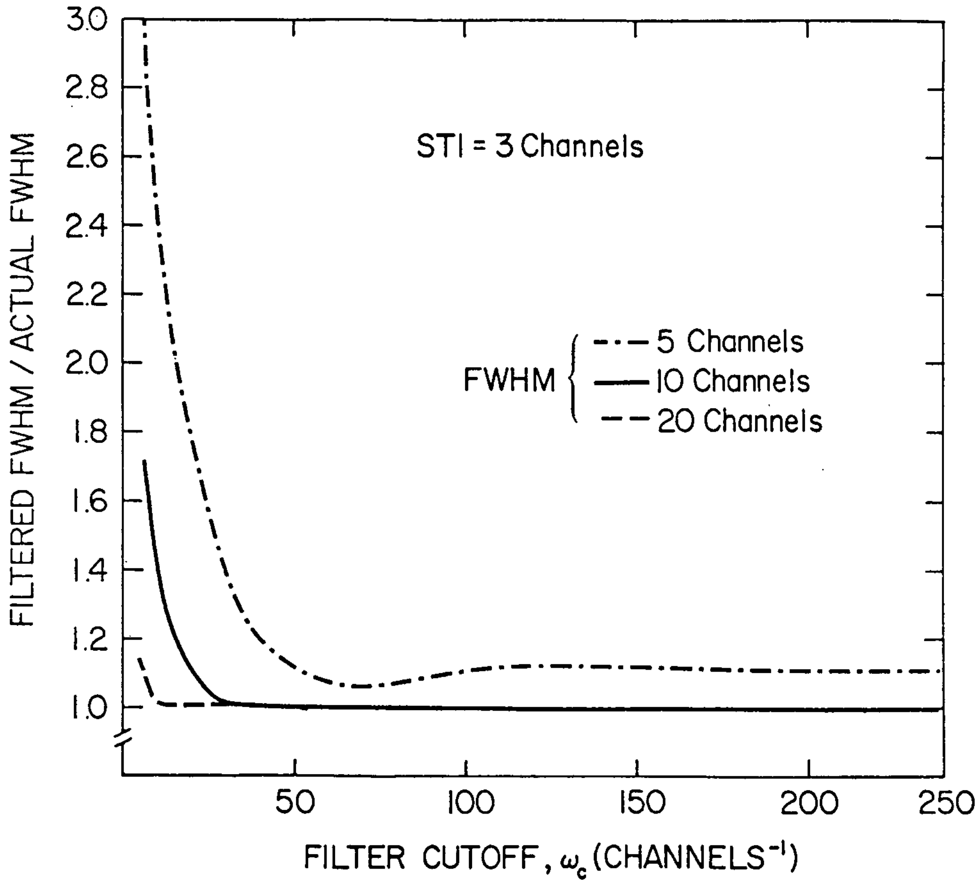
STI = 3 Channels
FWHM
5 Channels
10 Channels
20 Channels
FILTERED FWHM / ACTUAL FWHM
3.0
2.8
2.6
2.4
2.2
2.0
1.8
1.6
1.4
1.2
1.0
50
100
150
200
250
FILTER CUTOFF, ω_c (CHANNELS^{-1})

FIGURE B-2

TABLE B-1

Break Point Frequencies

STI (Channels)	FWHM (Channels)	BREAK POINT FREQUENCY (Channels^{-1})	$\frac{\sigma \text{ FILTERED}^{a}}{\sigma \text{ UNFILTERED}}$
7	5	40	0.6
7	10	20	0.32
7	20	10	0.18
5	5	50	0.52
5	10	25	0.26
5	20	12.5	0.13
3	5	50	0.26
3	10	25	0.12
3	20	12.5	0.06

[a] From Figure B-1